

High Consequence Pathogens – Refinement of Aerosol Models of Disease

The thesis is submitted in partial fulfilment of the requirements for the award of the degree of Doctor of Philosophy by Publication of the University of Portsmouth.

Graham Jonathan HATCH

Public Health England
Manor Farm Road, Porton
Salisbury SP4 0JG

Supervisor
Professor Graham Mills
University of Portsmouth

School of Pharmacy and Biomedical Science
Faculty of Science
University of Portsmouth
January 2020



Declaration

Whilst registered as a candidate for the above degree, I have not been registered for any other research award. The results and conclusions embodied in this thesis are the work of the named candidate and have not been submitted for any other academic award.

Graham HATCH

January 2020

Acknowledgements

I would like to say a huge thank you to anybody that has played even a small part in my career over the last twenty seven years. The portfolio of papers that have contributed to this thesis recognise a whole host of friends and colleagues that I have had the pleasure of working with; I thank you all.

I would like to thank my supervisor at the University of Portsmouth, Professor Graham Mills. My unofficial supervisor at PHE, Dr Allen Roberts, has been an excellent source of motivation and encouragement for a considerable part of career, thank you so much. Not forgetting Ben Walsh, thank you for helping me both fund this endeavour and giving me the time to complete it.

I'd like to dedicate this to my late wife Kim, you will be forever in our hearts. I am always thankful for our wonderful children Joshua and Amy. Guys, thank you for putting up with me and making us proud.

Abbreviations

ABES	Automated bioaerosol exposure system
ACDP	Advisory Committee on Dangerous Pathogens
AIT	Association of Inhalation Toxicologists
APS	Aerodynamic particle sizer
ASPA	Animal Scientific Procedures Act
ATCSA	Anti-Terrorism Crime and Security Act
AVA	Anthrax vaccine adsorbed
AVP	Anthrax vaccine precipitated
BARDA	Biomedical Advanced Research and Development Authority
BCG	Bacillus Calmette-Guerin
BEI	Biodefense and Emerging Infections Research Resources Repository
CCTV	Closed-circuit television
CDC	Centers for Disease Control and Prevention
CFI	Ciprofloxacin for inhalation
CFU	Colony forming units
CL	Containment level
CT	Computer tomography
COSHH	Control of Substances Hazardous to Health
Dstl	Defence Science Technology Laboratory
EU	European Union
FDA	Federal Drug Administration
FFI	Flexible film isolator
GLP	Good Laboratory Practice
HEPA	High Efficiency Particulate Air filter
HG	Hazard Group
HHS	Health and Human Services
HM	Her Majesty's
HO	Home Office
HSE	Health and Safety Executive
IFN	Interferon

MSC	Microbiological safety cabinet
MHRA	Medicines and Healthcare Products Regulatory Agency
MRE	Medical Research Establishment
MRI	Magnetic resonance imaging
MVA	Modified vaccinia Ankara
NaCTSO	National Counterterrorism Security Office
NCTC	National collection of Type Cultures
NHP	Non-human primate
NHS	National Health Service
NIAID	National Institute of Allergy and Infectious Diseases
NIH	National Institute of Health
OECD	Organisation for Economic Co-operation and Development
PET	Positive emissions tomography
PHE	Public Health England
SAPO	Specified Animal Pathogens Order
SCID	Severe combined immunodeficient
SF	Spray Factor
TB	Tuberculosis
UK	United Kingdom
US	United States of America
USAMRIID	United States Army Medical Research Institute of Infectious Disease
WHO	World Health Organisation

Preface

This thesis follows a career working with high consequence pathogens and the development of *in vivo* models of disease. I started as laboratory technician working with cell cultures and the production of viral antigens. However, it is when I moved to the tuberculosis (TB) research department that my interest in animal models took hold. It is here that I developed knowledge in the practical delivery of aerosols and the development of animal models to test vaccines, prophylaxis and interventions against disease. Whilst working in the TB department I completed a MSc. in Medical Microbiology at the University of Surrey with a thesis entitled 'Oral delivery of a gelatin based BCG formulation to combat *Mycobacterium bovis* infection in a guinea pig model'. I moved to a US contracts team of scientists where I brought my expertise to develop animal models for a range of potential biothreat agents and play a key role in projects that at their peak employed 40+ staff with funding of over \$59M. In this highly regulated environment, I led the modernisation and refinement of the organisations aerosol delivery systems, managed projects and successfully delivered on the research aims. This wealth of experience has placed me in the unique position of being able to lead the research and service delivery teams working at the maximum levels of containment for human and animal pathogens.

Abstract

The natural route of human infection with many bacterial and viral diseases is via inhalation of droplet nuclei. Therefore, the production of bioaerosols in a controlled laboratory environment is deemed the most relevant route of infection for animal models. These models can be used to study, in a more natural context, the disease pathogenesis, or preclinical evaluation of the protective efficacy of vaccines or therapeutics against the challenge agent. Critical to the success of these animal models is the ability of the pathogenic microorganism to survive the stresses incurred whilst being generated and suspended as an aerosol. The ability of the pathogen to infect is dependent on aerosol droplet size, number of inhaled organisms and infectious dose. A well-characterised aerosol exposure system is critical for preclinical testing and pathogenesis studies. This thesis contains work, in the form of published papers, with a range of pathogens and animal models. These are the culmination of differing strategies to develop, characterise and qualify aerosol exposure systems at high containment, and the performance of preclinical testing and pathogenesis studies. The strategies employed have been instrumental in the approval of a new vaccine for smallpox, post-exposure treatment regimens of anthrax and other diseases in the biodefence arena, and pre-clinical evaluation of vaccines against tuberculosis.

Table of Contents

Title Page.....	i
Declaration.....	ii
Acknowledgements.....	iii
Abbreviations.....	iv
Preface.....	vi
Abstract.....	vii
Table of Contents.....	viii
1. Commentary.....	1
1.1. High containment.....	1
1.1.1. High containment facilities.....	3
1.2. Regulatory Framework and the use of animals in research.....	5
1.2.1. The Animals (Scientific Procedures) Act 1986.....	5
1.2.2. Good Laboratory Practice (GLP).....	6
1.2.3. The “Animal Rule”.....	8
1.3. Aerosol delivery systems, biocontainment and animal model refinement.....	9
1.3.1. The history of aerosol delivery at Porton - the Henderson apparatus.....	10
1.3.2. Design evolution of aerosol, biocontainment and animal model systems ..	12
1.3.3. Qualification of the aerosol delivery system.....	22
1.4. Case Studies.....	25
1.4.1. <i>Mycobacterium tuberculosis</i>	25
1.4.2. <i>Yersinia pestis</i>	27
1.4.3. <i>Burkholderia pseudomallei</i>	30
1.4.4. <i>Coxiella burnetii</i>	33

1.4.5. <i>Bacillus anthracis</i>	34
1.4.6. Monkeypox.....	37
1.5. The future	40
1.6. Concluding comments.....	40
2. References to the Commentary.....	42
3. Timeline of key activities, presentations and publications.....	56
4. Academic contributions by Graham Jonathan HATCH	58
5. Metrics, contributions and original versions of the presented body of work.....	61
6. Ethics Form UPR16.....	211

1. Commentary

1.1. High containment

In the United Kingdom (UK) the use of biological agents is controlled by primary legislation; the Health and Safety at Work Act, 1974 and the Animal Health Act, 1981. Supporting these are secondary regulations and approved codes of practice; the Control of Substances Hazardous to Health Regulations (COSHH) (HSE, 2013b), Management of Health and Safety at Work Regulations, 1999, Genetically Modified Organisms (Contained Use) Regulations (HSE, 2014), and Specified Animal Pathogens Order (SAPO), 2008. In addition, The Advisory Committee on Dangerous Pathogens (ACDP) issues guidelines (HSE, 2018, HSE, 2015, HSE, 2013a) for working with pathogens to support the primary legislation.

Human pathogens are categorised in the published, Approved List of Biological Agents (HSE, 2013a). Micro-organisms are classified into four hazard groups based on their pathogenicity, risk to laboratory workers, transmissibility to the community, and whether effective prophylaxis is available (HSE, 2013a) (Table 1). The hazard group of the pathogen determines the laboratory containment level that must be used. The example pathogens highlighted in bold in Table 1 are the pathogens that have been used in work described in this commentary.

Table 1 Definition of ACDP Hazard Groups.

ACDP hazard group	Definition	Examples
1	An organism that is most unlikely to cause human disease.	<i>Staphylococcus epidermidis</i>
2	An organism that may cause human disease and which may be a hazard to laboratory workers but is unlikely to spread to the community. Laboratory exposure rarely produces infection and effective prophylaxis or treatment is usually available	Influenza A Newcastle disease virus
3	An organism that may cause severe human disease and presents a serious hazard to laboratory workers. It may present a risk of spread to the community but there is usually effective prophylaxis or treatment available.	<i>Bacillus anthracis</i> <i>Mycobacterium tuberculosis</i> <i>Yersinia pestis</i> <i>Burkholderia pseudomallei</i> <i>Coxiella burnetii</i> Monkeypox virus
4	An organism that causes severe human disease and is a serious hazard to laboratory workers. It may present a high risk of spread to the community and there is usually no effective prophylaxis or treatment.	Ebola virus Crimean-Congo haemorrhagic fever virus

The Specified Animal Pathogens Order classifies animal pathogens according to potential harm to susceptible animal species, the potential for the disease to spread from the laboratory and the subsequent economic impact if a release occurred (Defra, 2015). Some micro-organisms are classified under both ACDP and SAPO schemes *e.g.* *Bacillus anthracis* - ACDP hazard group 3, SAPO hazard group 3

High consequence pathogens are those that are classified in the UK as belonging to ACDP hazard groups 3 or 4. Infections caused by these pathogens frequently require co-ordination at a national level *e.g.* the two cases of Monkeypox virus infection in the UK in 2018 which was managed as an enhanced incident in Public Health England (PHE) (Vaughan et al., 2018).

1.1.1. High containment facilities

The requirements for the building, safe operation and maintenance of high containment facilities in the UK are based on the guidance and regulations of COSHH, ADCP and SAPO, and are reviewed in Table 2. Additionally, there are obligations relating to biosecurity under the Anti-Terrorism Crime and Security Act 2001 (ATCSA), which are implemented by the National Counter-Terrorism Security Office (NaCTSO). PHE also complies with United States (US) Federal Select Agent Program.

The advanced level of engineering, associated management systems, training and emergency systems required to meet these containment specifications result in high building, operation and maintenance costs for these facilities.

Table 2 Review of facility requirements for ACDP, COSHH and SAPO guidelines

Containment measure	Containment Level		
	2	3	4
Workplace separated from other activities	No	Yes	Yes
Input and extract air filtered through HEPA	No	Single extract only	Single supply, double extract
Access restricted to authorised personnel only	Yes	Yes, and via airlock where RA dictates	Yes, and via airlock
Sealable for fumigation	No	Yes	Yes
Negative pressure cascade	No	Yes	Yes, specified for SAPO (-50 to -75 Pa)
Efficient vector control e.g. rodents and insects	No, unless animal containment	No, unless animal containment. Yes, if SAPO	Yes
Surfaces impervious to water and easy to clean, resistant to decontamination agents	Yes, bench	Yes, bench, walls and floor	Yes, bench, walls, floor and ceiling
Safe storage of biological agent	Yes, secured for Schedule 5 pathogens	Yes, secured for Schedule 5 pathogens	Yes, secured.
Observation window or alternative	No	Yes	Yes
Laboratory has own equipment	No	Yes, as far as reasonably practicable	Yes
Infected material and animals in containment	Yes, where aerosol	Yes, where aerosol	Yes
Incinerator	Accessible	Accessible	On-site
Effluent treatment plant	No	Yes, where RA dictates	Yes
Shower on exit	No	No, except where RA dictates	Yes, for SAPO
Autoclave	Yes, in the building	Yes, within suite	Yes, within suite, must be double-ended and interlocked doors
Protective clothing, gloves	Yes	Yes	Yes, complete change including footwear

1.2. Regulatory Framework and the use of animals in research

1.2.1. The Animals (Scientific Procedures) Act 1986

The Cruelty to Animals Act 1876 was the first UK law to regulate animal experimentation. It stood for 110 years until in 1986, The Animals (Scientific Procedures) Act (ASPA) was passed. The Act implements the requirements of European Union (EU) directive 2010/63 governing the rules in relation to the care and use of animals in research to minimise the severity experienced by animals and to safeguard welfare.

ASPA controls regulated procedures (defined as a procedure which may have the effect of causing the animal pain, suffering, distress or lasting harm) performed on protected animals (defined as any living vertebrate, other than man, and any living cephalopod), and does this by licencing on three levels; the person, the project, and the place.

- **Personal Licence:** The licence permits an individual to carry out specified procedures on detailed animals. All procedures must be part of a programme of work authorised in a project licence.
- **Project Licence:** A Project Licence is granted to a single, named individual. The holder group must possess the appropriate level of authority to manage the project. A Project Licence authorises the holder, to perform specific regulated procedures on specific animals at a specific place or places. The programme must be detailed and justified. There must be no alternative methods available, and the licence holder must demonstrate that the benefits clearly outweigh the likely impact on the animals' well-being.
- **Establishment Licence:** An Establishment Licence is granted to an individual responsible for institutional compliance at a place where regulated animal procedures are conducted. Every individual area is listed together with the species and type of use.

ASPA is administered by the Secretary of State at the Home Office, who principally takes advice from a network of Home Office Inspectors. Inspectors have access to all facilities and can visit regularly, usually unannounced. They carry out detailed inspections and

provide advice on all matters relating to animal work and licencing thus ensuring high standards of compliance to the law and animal welfare are maintained.

The system of regulation aims to ensure compliance to the 3Rs

- Replacement: wherever possible, a scientifically satisfactory method not entailing the use of protected animals must be used instead of a regulated procedure.
- Reduction: that whenever a programme of work involving the use of protected animals is carried out the number used must be reduced to the minimum without compromising the programmes' objectives
- Refinement: the breeding, accommodation and care of protected animals and the methods used in regulated procedures applied to them must be refined to eliminate, or reduce to the minimum any possible pain, suffering, distress or lasting harm to those animals.

1.2.2. Good Laboratory Practice (GLP)

Good Laboratory Practice is defined in the Organisation for Economic Co-operation and Development (OECD) Principles as “a quality system concerned with the organisational process and the conditions under which non-clinical health and environmental safety studies are planned, performed, monitored, recorded, archived and reported.” (WHO, 2009).

The US Federal Drug Administration (FDA) has rules for GLP in 21CFR58. Preclinical trials on animals in the US use these rules prior to clinical research in humans. Research in the US not conducted under these restrictions or research done outside US not conducted according to the OECD Guidelines (or FDA rules) might be inadmissible in support of a New Drug Application in the US.

GLP is a managerial quality control system covering the process and the conditions under which non-clinical studies are planned, performed, monitored, recorded, reported and retained.

The Principles of GLP include:

- Organization and Personnel
 - Management-Responsibilities
 - Study Director-Responsibilities
 - Principal Investigator-Responsibilities
 - Study Personnel-Responsibilities
- Quality assurance program
- Facilities
 - Test System Facilities
 - Facilities for Test and Reference Items
 - Archive facilities
 - Waste disposal
- Equipment, Reagents and Materials
- Test systems
 - Physical/Chemical
 - Biological
- Test & Reference items
 - Receipt, handling, sampling and storage
 - Characterisation
- Standard operating procedures
- Performance of Study
 - Content of Study Plan
 - Conduct of Study
- Reporting of results
 - Content of Final Report
- Storage and retention of records and material

It is important to differentiate between the formal, regulatory use of the term GLP and the general application of “good laboratory practices” in scientific investigations.

PHE Porton, is a member of the UK GLP Compliance Programme that has been inspected by the Medicine and Healthcare Regulatory Agency (MHRA) and issued with a Statement of GLP Compliance.

1.2.3. The “Animal Rule”

The use of animal models is sometimes criticised and are held up to unrealistic expectation, the term “model” implies that they are not intended to fully replicate human-pathogen interaction but rather provide an insight; their limitations include (National Research Council, 2011) :

- The lack of sufficient human data of the natural history of the disease;
- Interspecies and intraspecies variability and the constraints imposed by working in biocontainment facilities; and
- For some diseases, animal models have been shown to be unreliable surrogates for, or predictors of, efficacy and safety, as indicated by experience with product development and clinical trials.

In the US regulations commonly known as the “Animal Rule” (21 CFR 314.600-650 for drugs; 21 CFR 601.90-95 for biologics) allow for the approval of products when human efficacy trials are not feasible. Its intended use is to protect public health and national security through the reduction/prevention of serious or life-threatening conditions caused by exposure to toxic chemical, biological, radiological, or nuclear substances. Its guidance

To be considered for marketing approval under the Animal Rule, a product must meet the following 4 requirements (FDA, 2015) designed to alleviate criticism of animal models:

- There is a reasonably well-understood pathophysiological mechanism of the toxicity of the substance and its prevention or substantial reduction by the product;

- The effect is demonstrated in more than one animal species expected to react with a response predictive for humans, unless the effect is demonstrated in a single animal species that represents a sufficiently well-characterized animal model for predicting the response in humans;
- The animal study endpoint is clearly related to the desired benefit in humans, generally the enhancement of survival or prevention of major morbidity; and
- The data or information on the kinetics and pharmacodynamics of the product or other relevant data or information, in animals and humans, allows selection of an effective dose in humans.

It may appear that FDA approval of countermeasures may only be of benefit to US citizens, but this is not the case; investment the US government makes in this area is beneficial to other nations. Data generated through such may allow an improved evidence base for clinicians to manage public health emergencies, particularly in the event of a deliberate release. The animal models established are potentially also available for other drug and vaccine developers to use to assess the efficacy of their candidate countermeasures. FDA approval via the 'Animal Rule' allows countermeasures against priority pathogens to be purchased for the US government Strategic National Stockpile (SNS). Through the relationship between the UK and US governments, the SNS has been deployed in the UK in the recent cases of anthrax caused by *B. anthracis* contaminated heroin in injecting drug users.

1.3. Aerosol delivery systems, biocontainment and animal model refinement

The ACDP guidelines give very clear guidance on how the laboratory should operate but these only apply to work involving standard microbiology methods. Aerosol infection of animals with high consequence pathogens is non-standard and thus requires further robust risk assessment and may need additional regulatory approval. In addition, perhaps conflicting Quality and Home Office guidelines must be adhered to. The development of systems for both aerosol exposure and the subsequent housing of infected animals has evolved with changing regulations and has necessitated many discussions with the regulatory inspectors, subsequent design and testing of systems and equipment.

1.3.1. The history of aerosol delivery at Porton - the Henderson apparatus

The Porton Down site has gone through many organizational changes since its initial development in the 1940s. One of the Centre's primary roles has been to conduct fundamental research for the testing and development of new vaccines and to coordinate responses to emerging diseases. Aerosol models have always been a key part.

An apparatus for the study of airborne infection was described by Henderson (1952). The apparatus was designed over several years to study the survival of bacteria suspended in the atmosphere, and the effect of such clouds of pathogenic bacteria on experimental animals.

This equipment, later known as the Henderson apparatus, has evolved over time. A mobile unit was developed in the 1960s and is pictured in Figure 1 (Druett, 1969).

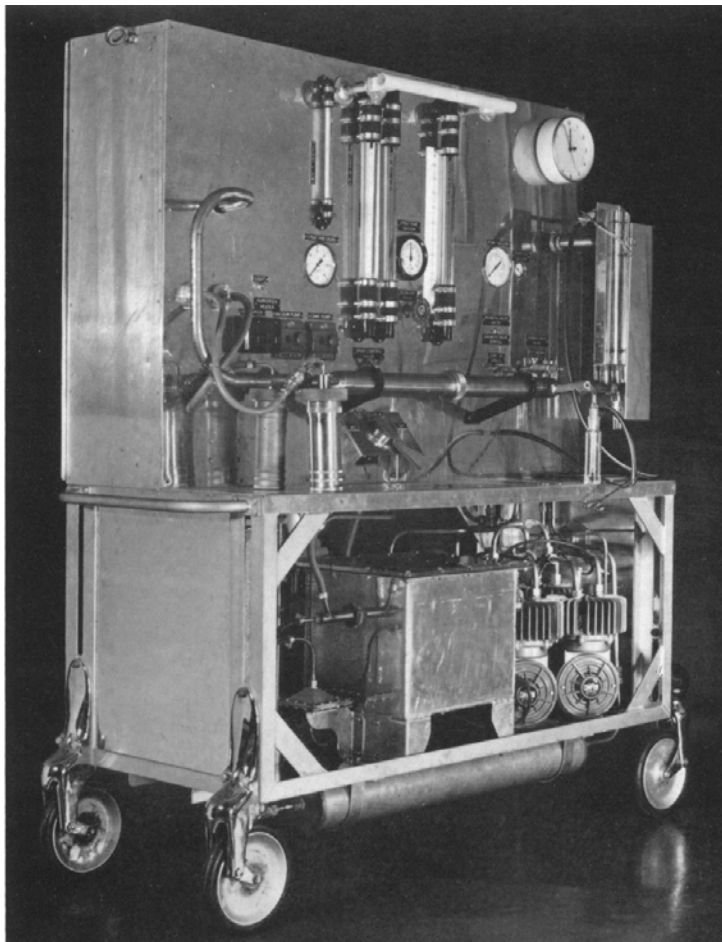


Figure 1 - A mobile Henderson Apparatus

The key components in the design of the mobile Henderson Apparatus were:

- Airflow management
 - A series of compressors, vacuum pumps, valves and critical orifices to provide controllable airflow and pressure regime.
- Humidification
 - Provision of a humidifier and drier in which airflow can be mixed to create the desired aerosol conditions.
- Nebuliser
 - Collision nebuliser
- Spray tube
 - Enables the mix of generated aerosol and conditioned air
- Animal exposure tube
 - Presentation of the aerosol to the animal
- Aerosol sampling
 - Typically, a liquid impinger

At this time there was no containment associated with the device apart from the use of personal respirators. However, with changing workplace safety regulations and the necessity for primary containment of the aerosol hazards the Henderson apparatus evolved further. Firstly, the equipment for controlling air flow and relative humidity was separated from the aerosol generating equipment, which was placed in a biosafety cabinet. This necessitated a separation between the spray tube and the animal exposure tube. It is with this configuration of equipment, named the contained Henderson apparatus that I commenced my career.

1.3.2. Design evolution of aerosol, biocontainment and animal model systems

The development of animal model systems at PHE can be categorised into three main areas; the aerosol delivery system, biocontainment, and clinical parameter assessment. Throughout the evolution of our aerosol delivery systems there has been a desire to maintain the core components of the original Henderson apparatus, thus maintaining comparison with previous data. A timeline of this work is presented in Section 3.

1.3.2.1. Evolution of the aerosol delivery system

The success of inhalation studies using laboratory animals is a difficult challenge. The inhaled dose of an agent is one of the key factors to explain the response in the test subject (Dorato and Wolff, 1991). Four factors that impact on dose include 1) respiratory function of the test subject, 2) aerosol concentration, which is further complicated when studies use biological agents, 3) duration of the exposure, and 4) retention of the inhaled aerosol (Cheng and Moss, 1997).

In its simplest form the dose can be expressed as

$$D = Caero \times MV \times texp (\times f)$$

Where D = dose, $Caero$ = concentration of agent in circulating aerosol, MV = respiratory minute volume or the volume of air inhaled in one minute, $texp$ = time or duration of the exposure, f = aerosol deposition fraction as determined by animal species, depth of respiration and particle characteristics. The above equation assumes that the aerosol concentration and respiratory function are constant throughout the aerosol challenge (Hartings and Roy, 2004)

There is often confusion when comparing results from different laboratories as dose can represent different things to different groups. The Association of Inhalation Toxicologists (AIT) Working Party recommended that delivered dose and deposited dose be adopted as standardised terminology (Alexander et al., 2008). The delivered dose is the amount of agent inhaled by or presented to the animal, and the deposited dose is the amount of agent deposited or retained in the lungs. What is most important is clarity

over what is meant by dose when presenting data. Some laboratories will apply an estimate of the deposition fraction typically 10–40% depending on the particle size and species (Alexander et al., 2008, Phillips, 2017). Our own estimate on the deposition fraction of *B. anthracis* in mice were calculated by culling animals immediately following aerosol challenge, removing the lung tissue, homogenising and enumerating the number of viable *B. anthracis* bacilli deposited. Approximately 20% of the presented dose was retained in the lung (Hatch et al., 2007, Hatch et al., 2009a).

The transition of my research from *Mycobacterium bovis* and *M. tuberculosis* to biodefence agents required a different approach to the assessment of dose. Experiments with *Mycobacterium spp.* used an empirically derived aerosol dose based upon the relationship of experimental observation of lesions on the surface of the lung following exposure to an aerosol generated from differing concentrations of *Mycobacterium spp.*. Suspensions of 1.0E+06 and 1.0E+07 CFU/mL resulted in an average of 10 and 100 lesions, respectively, on the surface of the lung 4 weeks after challenge. It was assumed that 1 lung lesion formed from 1 CFU. The term “lung lesion-forming unit” (LFU) was used to describe the deposited or retained dose (Williams et al., 2000).

Where possible, the aerosol concentration within the animal exposure chamber is best determined during the exposure rather than relying on historic data, to ensure any variations in aerosol generation efficiency are detected. Impaction, filtration, and impingement are three common sampling techniques used to separate and collect the bioaerosol. Two different types of liquid impinger, designed to operate over the respirable particle size range, were used over the course of the described studies, a SKC BioSampler (SKC Inc, PA, US) and the AGI-30 (Ace Glass, NJ, US). Two versions of the AGI-30 were trialled operating at 6 and 12.5 L/min, the BioSampler operated at 12.5 L/min. In our hands, there was no statistical differences in the collection efficacy of the three liquid impingers (data not presented).

Enumeration of the impinger samples taken from the exposure tube enabled a measurement of the number of viable organisms, in the circulating aerosol, to which an

animal was exposed. The next question to answer to estimate dose is the respiration rate of the animal. Although small animal plethysmography is available it is normal, for practical reasons, to estimate the volume of air inhaled. Allometric equations from empirical data between the relationship between body weight and respiratory volume provide an estimate of the volume inhaled in one minute i.e. minute volume (MV).

$$MV \text{ (mL)} = 2.1 \times (\text{Body weight in g})^{0.75} \quad (\text{Guyton, 1947})$$

$$MV \text{ (L)} = 0.499 \times (\text{Body weight in Kg})^{0.809} \quad (\text{Bide et al., 2000})$$

The total of volume inhaled i.e. accumulated volume (AV) can be calculated by multiplying the MV and the duration or time of exposure (*texp*).

$$AV = MV \times texp$$

Predictive equations to estimate respiration will not capture animal to animal variation. The anaesthetic, individual metabolism, respiratory effects caused by the agent under investigation, or individual response to stress during exposure can all effect respiratory function, and for larger animals a potentially wide deviation from the predictive estimate (Hartings and Roy, 2004).

The introduction of real-time plethysmography was critical to the development of our NHP models and minimising animal to animal variation of dose resulting from respiratory function. A head-out plethysmography chamber combined with BioSystemXA software (Buxco, UK) was installed. Pressure change, as the anaesthetised NHP's abdomen expands and contracts are measured to derive respiration rate, tidal volume and accumulated volume. By limiting the aerosol exposure to a set accumulated volume of aerosol rather than the more usual timed exposure, we could considerably reduce the challenge dose variability between animals.

Improved small animal restraint was incorporated into the aerosol system. Historically a box-type device was used in which the animal was held in place by neck restraint with the animal's nose introduced into the exposure tube through a latex diaphragm. By its

nature this system could impair natural respiration. An improved tube design with an open caged head section was incorporated in which the animal had no tight restraint. The design benefitted animal welfare and handling, had less adverse effect on natural respiratory function, and could be sealed in the exposure tube aiding the control of air flow and pressure.

Particle size is key to the successful delivery of an agent to the lung. Deposition is principally by inertial impaction, sedimentation, and diffusion. Large particles ($> 6 \mu\text{m}$) are mainly deposited in the upper airway; small particles ($< 2 \mu\text{m}$) are mainly deposited in the alveolar region (Darquenne, 2012). It is widely known that the region of the respiratory tract in which an agent is deposited can have an influence on both the infectious dose and the course of disease (Thomas et al., 2012). We have also shown this in our studies with Influenza A virus in cynomolgus macaques (Marriott et al., 2016). Intra-nasal challenge led to an infection that was confined to the nasal cavity. In contrast, a lower aerosol challenge dose produced an infection throughout the respiratory tract which was more aligned to the kinetics of infection displayed in human Influenza A virus infections.

The Collison nebuliser was first described in the 1930s, it was modified by Druett to accommodate the use of smaller volumes; this Druett, MRE (Medical Research Establishment) design was described by May (1973), and has been the mainstay for aerosol studies at Porton since this time. The nebuliser uses compressed air to atomise a liquid; the produced droplets have a wide particle size distribution, the vast majority are recirculated to the fluid with only the smaller particles exiting the device (May, 1973). The output of nebuliser is in the respirable range with a typical mean diameter of $2 \mu\text{m}$ (range $0.5\text{--}7 \mu\text{m}$)(Lever et al., 2000).

To reconstruct the size profile for each challenge run an Aerodynamic Particle Sizer (APS) spectrometer, model 3321 (TSI Inc., MN, US) was installed to provide accurate count and size distributions for particles with aerodynamic diameters from 0.5 to $20 \mu\text{m}$. The high concentration aerosols needed for our animal challenge models required dilution prior to measurement. The Model 3302A Diluter (TSI Inc., MN, US) was installed for a

calibrated dilution ratio of 100:1 at a total flowrate of 5L/min. Commercial versions of both a 3-jet and 6-jet versions of the modified MRE-type Collison nebuliser (BGI Inc, Waltham US) were investigated for use in the early development of the aerosol delivery system. Data showed that both versions of the nebuliser produced an aerosol in the desired respirable range, typically with a Mass Median Aerodynamic Diameter (MMAD) in the range of 1.5-2.0 μm , and a Geometric Standard Deviation (GSD) of approximately 1.8-2.0. The ability to use either a 3-jet or 6-jet Collison nebuliser gave greater flexibility over the dose.

From 2006 there was an expansion of the use of aerosol models in PHE. The manufacturing expertise of the Henderson apparatus was lost to PHE, so a critical examination of requirements was undertaken. Hartings and Roy (2004) described an automated bioaerosol exposure system (ABES); a microprocessor-driven inhalation platform providing data acquisition and control, with the inhalation chambers historically used at USAMRIID adapted from the Henderson apparatus (Henderson, 1952). A version of the ABES was manufactured and purchased from Biaera Technologies, MD, USA.

The Biaera system with AeroMP® Interface Module provided control and data acquisition of the airflow, humidity and pressure control supplied to the Collison nebuliser, impinger, spray and exposure tube previously described. In addition, the control software enabled integration of the APS and diluter into a single control and data management system. The combined systems were labelled the AeroMP-Henderson apparatus and provided much greater control and quality assurance to aerosol generation and delivery than was previously available. All air flow rates and pressures could be monitored by calibrated devices and alarmed throughout the aerosol delivery process. The real-time monitoring enabled potential issues to be immediately corrected, thus both increasing the quality assurance of the aerosol challenge process but also increasing animal welfare.

1.3.2.2. Evolution of biocontainment for aerosol studies and animal housing

The contained Henderson apparatus enclosed the aerosol generation equipment within primary containment. However, the animal exposure was performed on a downdraft table still requiring the operator to use respiratory protective equipment. Post-exposure animals were housed within open cages in the Containment Level 3 (CL3) laboratory. In recent years one of the key requirements when using high consequence pathogens is the principle of primary containment.

Animals cannot be housed in traditional class III microbiological safety cabinet (MSC). The high air-change rate and noise are incompatible with Home Office regulations. The solution was to design Flexible Film Isolators (FFI) to house the animals. These non-standard devices enabled an equivalent operator protection factor to an MSC whilst meeting animal housing requirements. The first generation of FFI looked like a traditional MSC glove-box but were ergonomically poor. A half-suit design of FFI (Figure 2) was quickly adopted and has become the mainstay of housing small animals infected with high consequence pathogens.



Figure 2 – Small Animal Flexible Film Isolator; shown with guinea pig caging

In addition to the animal housing, a FFI was designed to enclose the aerosol delivery apparatus with the existing Henderson control system (Figure 3).



Figure 3 - An aerosol challenge isolator with the original mobile Henderson control

The introduction of the Biaera system with AeroMP® software interface enabled user control from within the FFI and provided (Figure 4).



Figure 4 - A challenge isolator with the AeroMP-Henderson system. Insert displays the operator controlling the aerosol delivery from inside the isolator

The development of a large animal system followed. Non-human primates (NHP) and rabbits cannot be readily housed within a FFI. A directional flow containment booth was

developed to offer primary containment (Figure 5). Animals are housed in Home Office compliant cages and conditions behind a Perspex panel. Air is directed from the room through weighted dampers in the panel and extracted to the rear through HEPA filters. A face velocity of a least 0.7 m/s is maintained when accessing animals through doors within the Perspex barrier thus maintaining operator protection.



Figure 5 - A large animal directional flow containment system; pictured with NHP cages

Large animal aerosol exposure is performed on a downdraft table whilst operators wear respiratory protective equipment (Figure 6). Rabbits are exposed via a traditional exposure tube; their snouts placed through a latex diaphragm into the aerosol flow. Non-human primates required a different set-up. A canine anaesthesia mask was modified to allow a flow through system that could be held on the animals' face forming a seal. A head-out plethysmography chamber (Buxco, UK) was used to monitor the respiration of each sedated NHP throughout the aerosol challenge.



Figure 6 - AeroMP-Henderson NHP exposure system; Head-out plethysmography chamber and exposure mask

The flexible bio-containment solutions that we have developed have been critical to the success of the animal models described in this submission but also provide ready solutions to emerging health problems. This has been evidenced by the swift transition of the directional flow containment booths to house ferrets for our pre-clinical evaluation of vaccines and therapeutics against SARS-CoV-2.

1.3.2.3. Animal model refinement - assessment of clinical parameters

To make the best use of the animals, improve the models and collect data on key clinical parameters, we have invested in several new technologies for both in-life and ex vivo analyses. These include implantable telemetry, clinical chemistry and haematology analysers, CCTV for remote welfare assessment, radiography, and the ability to use CT and PET-CT scanners.

Implantable telemetry allows for the safe, continuous monitoring and recording of a wide range of physiological parameters in conscious, freely moving experimental

animals. These data can help in the understanding of pathogenesis, may provide information to identify appropriate humane endpoints before progression to severe disease, and in post exposure treatment models provide the indicator to begin treatment. Considerable effort and expense were required for the installation of this technology ranging from the design of caging systems to eliminate radio frequency interference, development of the surgical skills and qualification of the system. The original implants, D70-PCT (Data Sciences International (DSI), US) transmitted on a radio frequency requiring animals to be singly housed. An upgraded digital system with L11 implants (DSI, US) was later installed which allowed NHPs to be group housed providing both an improvement in animal welfare and better data integrity. The implants measured body temperature, activity, heart rate, blood pressure and ECG. The conventional method for measuring respiratory rate via implantable telemetry is via a pressure sensor implanted into the pleural cavity via the serosal layer of the oesophagus. We demonstrated that respiration rate can be derived from a blood pressure signal reducing complexity of required surgery (Hatch et al., 2008a).

Developed for our TB programme but recently of great value to our Covid-19 response is the ability for in-life CT scanning of NHPs. A considerable effort was required to enable this programme; from consultation with the HSE, design and testing (including crash tests) of a battery powered mobile FFI testing, and reassurance to the scanner providers. The solution, displayed in Figure 7, enables us to remove anaesthetised animals infected with HG3 agents such as *M. tuberculosis* or SARS-CoV-2 for the facility, obtain in-life scan, and return to the facility.

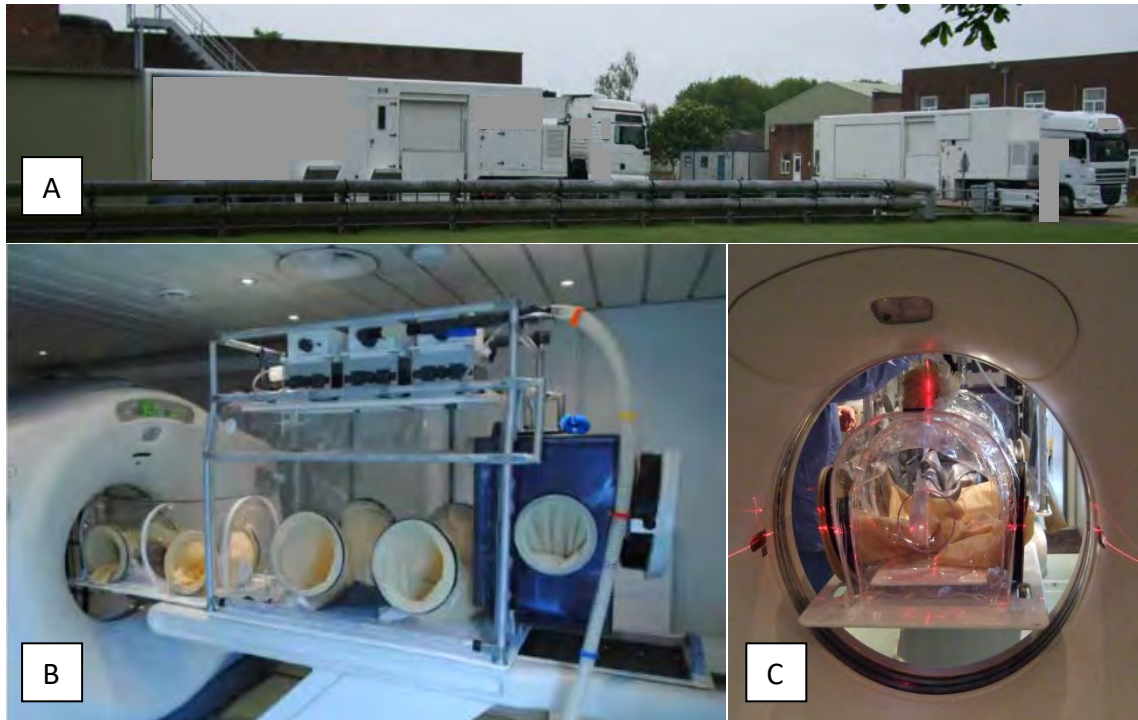


Figure 7 – Panel A depicts the mobile scanner outside our facility. Panel B displays the mobile FFI inside the scanning truck, and Panel C shows the FFI extension being inserted into the scanner.

1.3.3. Qualification of the aerosol delivery system

During aerosol model development and prior to the use of animals, the system parameters for each agent should be investigated and a standard aerosol protocol established. The use of agent specific parameters ensures that the presented dose can be controlled and that run to run variation is minimised. The spray factor (SF) can be used as a fundamental indicator to measure and assess the performance of the aerosol system over time. The SF is a unit-less ratio of the aerosol concentration to the starting concentration in the nebuliser. It is a function of the nebuliser, agent and system flow and describes the dilution that is to be expected during an aerosol experiment using a specific agent and aerosol system. If all components of the aerosol system are operating correctly the SF should be in the same range each time (Barnewall et al., 2012).

$$SF = \frac{C_{aero}}{C_{neb}} = \frac{\{C_{imp} \times V_{imp}\}}{\{Q_{imp} \times t_{exp}\} C_{neb}}$$

Where SF = spray factor, $Caero$ = concentration of agent in the circulating aerosol, $Cneb$ = concentration of agent in the nebuliser, $Cimp$ = concentration of agent in the impinger sample, $Vimp$ = volume of collection fluid in the impinger, $Qimp$ = sample flow rate of the impinger, $texp$ = time or duration of the aerosol exposure.

The effect of relative humidity (RH) on the survival bacteria and viruses in an aerosol is a well-established although complicated relationship e.g. even bacteria with the same structural classification vary in their response to RH (Tang, 2009). For each agent the SF between low (50% RH) and high humidity (90%) was assessed. In our system RH had little effect on the viability of challenge agent due the short time in which the agent was in an aerosol between nebuliser and animal or impinger. However, in the configuration required to challenge NHPs a humidity of over 85% RH did result in a lower SF, likely due to greater losses due to impaction in the longer and less straight tubing required to deliver the aerosol to the animal. For consistency humidity was controlled at $65\pm 5\%$ RH.

The dose presented to each animal is easily controlled by the nebuliser output and the concentration of agent within. This relationship must be examined and should be linear over the desired dose range, equating to a consistent SF. Figure 8 presents data from *B. anthracis*. The following calculations can be used to determine the necessary concentration of agent in the nebuliser in order to achieve a desired presented dose (PD) where the SF is known for a given agent.

$$C_{neb} = \frac{PD}{AV \times SF}$$

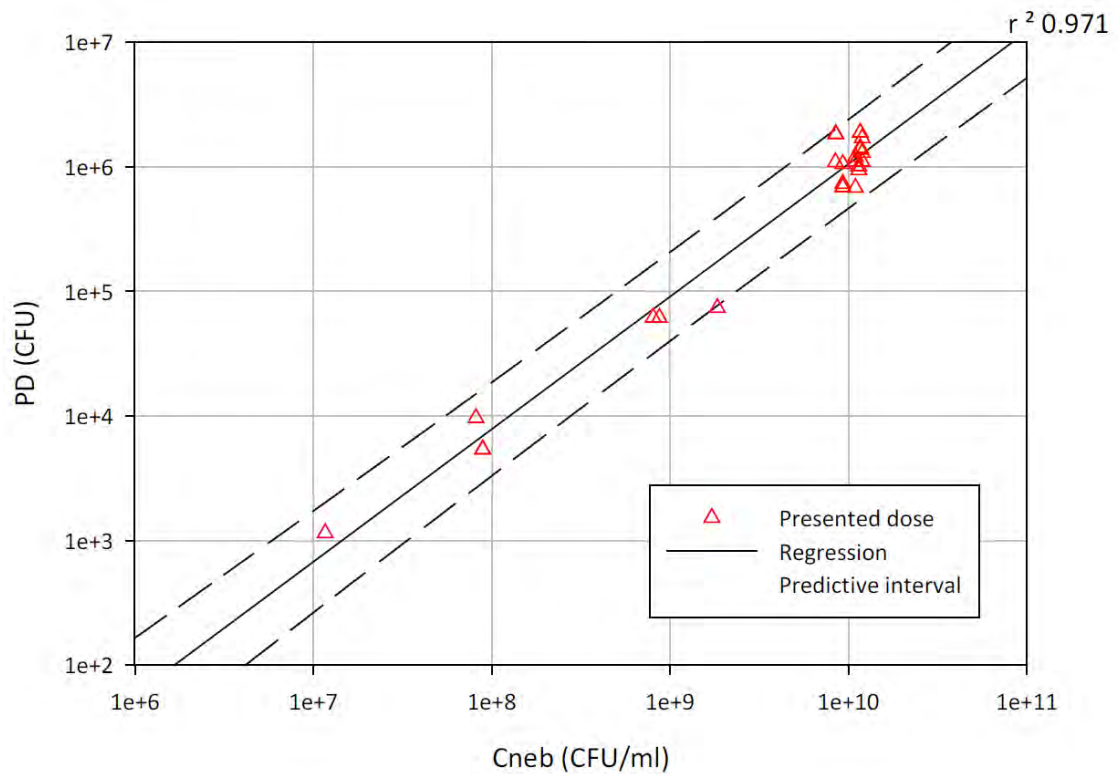


Figure 8 – Linear relationship between concentration of *B. anthracis* in the nebuliser and presented dose to a mouse.

The aerosol delivery capability was a critical component in our animal studies. I initiated installation and operational qualification of the described AeroMP-Henderson apparatus and plethysmography system to the principles of GLP. The system, including both hardware and software components completed installation, operational and performance qualification. The refined aerosol delivery systems enabled PHE to continue to safely deliver a highly accurate and controllable dose of aerosolised biological agents to a variety of species. The equipment was unconditionally released for beneficial use.

1.4. Case Studies

1.4.1. *Mycobacterium tuberculosis*

Mycobacterium tuberculosis the causative agent of tuberculosis is one of the leading reasons of death from a single infectious agent worldwide. The WHO reported 1.5 million people died from TB in 2018 (including 251 000 people with HIV). Worldwide an estimated 10 million people fell ill with TB. Multidrug-resistant TB (MDR-TB) remains a public health crisis and a health security threat with nearly 500 000 new cases resistant to the first-line drug, rifampicin (WHO, 2020).

The current vaccine, Bacillus Calmette–Guérin (BCG), is only partially effective with efficacy ranging globally from 0% to 80% (Fine, 1995). Most infections do not have symptoms, in which case it is known as latent tuberculosis. The symptoms of active TB are a chronic cough with blood-containing mucus, fever, night sweats, and weight loss. TB is spread from person to person through aerosol transmission when people with pulmonary infection cough, sneeze or spit. The WHO estimates one-quarter of the world's population has latent TB. 5-15% of those with latent infections will eventually develop active TB, immune-compromised people are most at risk.

PHE Porton, has been continuously conducting research into TB, and contributing to pre-clinical testing of vaccines in animal models from the late 1990s. From 1999 to 2005 I was employed in this research, specifically in the development and subsequent use of inhalational animal models of TB.

M. tuberculosis is exposed to different environmental conditions during disease, including intracellular growth in macrophages, extracellular growth in cavitory lesions and survival in anoxic granulomas (Danneburg 1994). Bacon et al. (2004) described the growth of *M. tuberculosis* H37Rv in a chemostat culture system under reduced oxygen tension. Using the guinea pig aerosol challenge model, we established that bacteria grown in a low-oxygen environment displayed a phenotype that was more infectious than aerobically grown cells. The infectivity assay was described in Williams et al. (2005c) and assessed the ability of a strain or phenotype to establish hematogenous spread from the lung to the spleen. Micro-array analysis highlighted 77 genes expressed

at higher levels in low oxygen which may contribute to increased virulence. Potential vaccine candidates were identified by examination of genes that were up- or down-regulated in conditions that *M. tuberculosis* might encounter e.g. low oxygen or carbon starvation. Formulated as DNA vaccines a selection of candidates was evaluated in the guinea pig model (Vipond et al., 2006b, Vipond et al., 2006a) and provided protection against inhaled *M. tuberculosis*.

As part of the EU TB Vaccine cluster funded by the EU Fifth Framework programme we contributed our guinea pig model to evaluate novel vaccines against tuberculosis with a view to provide promising candidates for clinical evaluation. This EU collaboration could provide comparative evaluations on vaccines that had previously demonstrated efficacy in animal models. Survival was used as the principal read-out of protection with additional data gathered from histopathology and mycobacterial count in the lung and spleen. Williams et al. (2005b), Williams et al. (2005a), Olsen et al. (2004), Agger et al. (2006) and Martin et al. (2006) describe this successful period of collaborations and pre-clinical evaluation in which the aerosol guinea pig model of tuberculosis was key.

Throughout my period in the TB research programme development of the aerosol and biocontainment continued. Containment systems for housing animals evolved; infected small animals were housed in FFIs and directional flow containment booths developed for NHPs. Chemostat cultures of *M. tuberculosis* were produced and aliquots frozen to provide a consistent challenge stock. Whilst this approach has obvious advantages it was noted that the freeze/thaw cycle had an adverse effect on the ability of *M. tuberculosis* to survive the forces of the aerosol generation process (Clark et al., 2011). Procedural controls were utilised to negate this effect.

An aerosol NHP model of tuberculosis was developed in rhesus and cynomolgus macaques. Systems for the safe delivery of the aerosol to the snout of the NHP were developed, replacing the traditional small animal exposure tube with a modified canine anaesthesia mask that allowed flow through of the aerosol and monitoring of the relative pressure. A head out plethysmography chamber enabled the real-time monitoring of NHP respiration and enabled a more accurate dose to be delivered across

the groups by limiting exposure to the aerosol to an accumulated volume rather than time. Routine in-life imaging in the form of radiography was established to refine clinical assessment of disease progression. Sharpe et al. (2009) describe the macaque model and the use of magnetic resonance imaging (MRI) and stereology to determine post-mortem lung lesion volume. These studies highlighted the power of imaging technologies in a disease such as tuberculosis. We have invested considerable effort to incorporate in-life imaging of macaques by CT and recently PET-CT scans to fulfil our 3Rs obligation and thus reduce animal numbers and refine the clinical assessment of disease progression.

The animal models that I helped establish and refine continue to contribute to the worldwide effort in pre-clinical evaluation of improved vaccines against TB. There currently 14 TB vaccine candidates in clinical trials, seven are based on subunits (mycobacterial fusion protein(s) in new adjuvant formulations and recombinant live-attenuated or replication-deficient virus-vectored), and seven consist on whole-cell mycobacteria (based on inactivated/extracts of mycobacteria and on live attenuated mycobacteria)(Martin et al., 2020). Many of these vaccine candidates, or their precursors, have been successfully screened in our guinea pig or NHP TB challenge models.

1.4.2. *Yersinia pestis*

Yersinia pestis is a gram-negative bacterium and is the causative agent of plague. Plague is primarily a disease of small mammals which is transmitted between animals via their fleas, and can cause zoonotic disease by aerosol transmission or indirectly via arthropod vectors. Historically there have been human pandemics. Throughout history, there have been human pandemics, the greatest being during the Middle Ages where at least 25% of the population was killed (Prentice and Rahalison, 2007). Plague remains endemic in several areas worldwide, including China, central and southern Africa, and areas of Asia and South America (Williamson, 2009). Humans are extremely susceptible to plague with a route dependent aetiology. Pneumonic plague, caused by inhalation of droplets containing *Y. pestis*, has a fatality rate nearing 100% if treatment is not rapidly administered.

Killed whole cell vaccines for plague have been available for over one hundred years but there is no evidence that they provide protection against primary pneumonic plague (Williamson, 2009). Antibiotics such as streptomycin, chloramphenicol, tetracycline and newer options gentamicin and doxycycline have been used for the treatment of plague. Although *Y. pestis* has been shown to accept plasmids containing antibiotic resistant genes, it is very rare in nature (Butler, 2013). The high fatality rate of pneumonic plague combined with the potential to acquire antibiotic resistance makes *Y. pestis* a potential bioterrorist threat, and the production of a vaccine to protect against pneumonic plague is required.

A robust and reproducible model of pneumonic plague was developed, in both BALB/c and Hsd:NIHS mice, with *Y. pestis* CO92 strain (biovar Orientalis, NR641) supplied by the Biodefence and Emerging Infections (BEI) Research Repository (US). Master and working stocks were prepared and characterised included microscopic staining (Wayson's), colony morphology and purity checks, Congo red uptake on Congo red agar, multiple loci (5 target) PCR, 16S rRNA sequencing, and VNTR for genetic integrity checks. Preparation of Inoculum. A standardised protocol for the preparation of *Y. pestis* for aerosol challenge was developed. Briefly, a vial from the working stock was thawed and streaked onto Tryptic Soy Agar (TSA) and incubated at 26°C for 54 hours. Following successful subculture and purity check, the streak plate was used to seed Tryptic Soy Broth (TSB) and was incubated with orbital agitation at 26°C for 18 hours. Fresh TSB was added, and broths further incubated until an optical density of over 3 was measured at 600nm wavelength (within approximately 3h). A four-target real time PCR was developed to confirm the presence of all three plasmids and the *pgm* virulence locus, to ensure genetic integrity and stability of the *Y. pestis* prior to use in each aerosol challenge study. A sample taken after the 18h TSB culture was analysed for the presence of genes; HmsF (chromosomal *pgm* locus), F1 (pMT1), Pst (pPCP1), and VAg (pCD1).

Early developments of the aerosol challenge protocols were presented at the American Society of Microbiology (ASM), Biodefense and Emerging Diseases Research Meeting, Baltimore, US (Hatch et al., 2008b). In our system the median lethal dose (MLD) of *Y. pestis* in BALB/c mice was determined to be 5.0E+03 CFU (presented dose) with a time

to death of approximately 3-4 days following aerosol challenge. The aerosol systems used in these studies spanned the previously described refinement of the aerosol system, from the contained Henderson apparatus to the AeroMP-Henderson. At each change bridging studies were required to ensure equivalence. The desire to maintain the core components i.e. the Collison nebuliser, spray and exposure tubes and standardised conditions of 65% RH ensured the ease of transition.

It has been shown that both humoral and cellular immunity are required for complete plague immunity (Anderson et al., 1997, Levy et al., 2011, Motin et al., 1994); however, antibodies against two natural virulence proteins F1 and V are associated with protection during a natural infection and have been shown to be protective in mouse models of pneumonic plague when given as recombinant proteins (Motin et al., 1994, Hill et al., 2006, Fellows et al., 2010). These (rF1 and rV) are the major constituents of new subunit plague vaccines (Williamson et al., 1997, Heath et al., 1998, Jones et al., 2000, Quenee et al., 2011). With our characterised aerosol challenge model passive transfer studies in BALB/c mice showed a correlation between human IgG ELISA titre (to either rF1 or rV) and the mean time to death following aerosol challenge. However, it did not show the protection reported by Fellows et al. (2010). We next developed a model of pneumonic plague in Hsd:NIHS mice. Keeping all aerosol system and bacteria cultures parameter consistent there was no statistical difference between the susceptibility of either strain of mouse to an aerosolised challenge with *Y. pestis*, with equivalent MLD and time to death.

The development of a pneumonic plague mouse models in BALB/c and Hsd:NIHS mice, and their subsequent use to test the *Y. pestis* subunit vaccine containing rF1 and rV by the passive transfer of unfractionated serum and plasma from immunised cynomolgus macaques and humans was described in Graham et al. (2014). This model of pneumonic plague and its use in passive transfer studies (using antibodies isolated from vaccinated individuals) may provide a tool to measure a correlate of protection against pneumonic plague and assist in the licensure of a new plague vaccine.

1.4.3. *Burkholderia pseudomallei*

Burkholderia pseudomallei, the aetiological agent of melioidosis, causes a serious and often fatal disease in humans and animals (Titball et al., 2008). It is a soil-dwelling bacterium found in tropical and subtropical regions worldwide, and predominate in Southeast Asia and Northern Australia. Humans generally become infected through contact with polluted water; the bacteria entering the body through wounds, inhalation, or ingestion. *B. mallei*, the causative agent of Glanders (a disease that occurs primarily in horses, mules and donkeys) has been used as a biological weapon by several nations throughout recent history. Although *B. pseudomallei* has never been used as a biological weapon it is of concern. *B. pseudomallei* is resistant to many antibiotics, there is no licensed vaccine (Wiersinga et al., 2006), it is readily available in the environment, and can be aerosolised and transmitted by inhalation.

Melioidosis results in approximately 89,000 deaths per annum, with diabetes a major risk factor (Wiersinga et al., 2006). Treatment for melioidosis involves an intensive intravenous antibiotic infusion (10-14 days) followed by 3-6 months of oral antibiotic therapy (Pitman et al., 2015). Given the long treatment regimen and inherent antibiotic resistance there is a desire for new medical countermeasures. The low natural occurrence of melioidosis makes traditional clinical trials difficult. We were awarded NIAID task order, N01-AI-30062, to develop and characterise both mouse and NHP aerosol infection models with a view to test the efficacy of medical countermeasures.

A variety of mouse models of *B. pseudomallei* have been published with a range of bacterial strains, mouse species, and challenge routes (Lever et al., 2009, Conejero et al., 2011, Thomas et al., 2012, West et al., 2012, Lafontaine et al., 2013, Titball et al., 2008, Massey et al., 2014). BALB/c mice appear to more sensitive to *B. pseudomallei* and are suitable to model acute infection, C57BL6 mice appear to better model a more chronic infection (Leakey et al., 1998, Hoppe et al., 1999, Tan et al., 2008, Liu et al., 2002). We first sought to characterise the aerosol dose of and subsequent disease in BALB/c mice challenged with *B. pseudomallei* strain NCTC 13392.

B. pseudomallei strain NCTC 13392 was originally isolated from a septicaemic, diabetic patient with fatal melioidosis, in Khon Kaen, Thailand in 1996. The Mahidol University (Sirijad Hospital and Mahidol-Oxford Research Unit) assignment number was K96263. We obtained stocks from the NCTC and produced working and master banks. The use of this strain provides a cautionary tale on the quality assurance of challenge agents. It was not until after several years into our use of this strain in our work that sequencing demonstrated that the isolate differed from published genome of K96243. Subsequent investigation identified that although NCTC 13392 was received from the same laboratory in Thailand at the same time as K96243, it was unexpectedly a different strain (Sahl et al., 2013). Colony morphology variant sequences from our working stocks were reported by Vipond et al. (2013) and were deposited in the DNA Data Bank of Japan, ERX272106 (<https://trace.ddbj.nig.ac.jp/DRAsearch/experiment?acc=ERX272106>), which matched that reported by Sahl et al. (2013).

Early experiments defined the required aerosol conditions (challenge stock growth conditions, relative humidity, sampling medium, challenge dose) for a lethal infection in BALB/c mice. I presented posters detailing this work at ASM Aerobiology in Biodefense IV, Richmond, MD (Hatch et al., 2011a), ASM Biodefense and Emerging Diseases Research Meeting Baltimore, MD (Hatch et al., 2010a) and the associated ASM *Burkholderia spp.* Workshop Baltimore, MD (Hatch et al., 2010b). Aerosol challenge stock was generated in Luria Bertani Broth (LBB) incubated at 37°C, orbital shaking at 175 rpm seeded from an overnight streak plate of NCTC 13392 on Luria Bertani Agar (LBA). Various harvest times were assessed early in the development of the aerosol model parameters ranging from a 4h mid-log, through 18h late-log to early stationary phase, and 24h stationary phase cultures. The spray factor of 4h and 18h cultures were respectively 10-fold and 5-fold lower than that of the stationary phase culture, indicating its greater resistant to the stress of the aerosolisation and sampling processes.

The aerosol dose of *B. pseudomallei* (NCTC 13392) had a profound effect on the course of disease (Funnell et al., 2019). Initial studies focused on an acute disease and were designed with an endpoint at 14 days post-challenge. A presented dose of 3.0E+04 CFU induced an acute lethal disease. However, it became evident that surviving animals had

a disease burden and subsequent studies were lengthened to 30 days post-challenge. A presented dose of $1.1E+02$ CFU produced some clinical signs that appeared resolved but returned from day 5 onwards increasing slowly over the next 25 days. BALB/c mice exposed to $7.7E+01$ CFU initially had mild clinical signs, which cleared and then returned from day 20 post-challenge, mimicking a chronic infection with bacteria found in multiple sites and abscesses, like that observed in human chronic disease (White, 2003). The described model could be used to evaluate vaccines and therapeutics in both acute and chronic forms of infection.

The development of the NHP model was presented at the World Melioidosis Conference, Townsville, Australia (Hatch, 2013) and required a series of studies to assess the aerosolised dose of *B. pseudomallei* NCTC 13392 in cynomolgus and rhesus macaques. Post-challenge data was gathered via continuous telemetry, monitoring core parameters including temperature, respiration rate, blood pressure and activity. Animals were observed and health scores taken throughout the study. Blood was sampled for bacteriology, immunology and haematology analysis every three days. Upon necropsy, tissues were processed to paraffin blocks, sectioned at 3-5 μm , and stained with haematoxylin and eosin and examined microscopically.

Rhesus macaques were more susceptible to aerosol challenge than cynomolgus macaques; in fact, we could not establish a disease in cynomolgus macaques following a high presented dose of $4.0E+04$ CFU. This finding was in line with other researcher's observations (personal communication). Rhesus macaques were chosen to test the efficacy of post-exposure treatment with oral delivery of co-trimoxazole following aerosol challenge with *B. pseudomallei*.

Twelve Rhesus macaques were successfully challenged with an aerosol of *B. pseudomallei* (NCTC 13392) with a mean presented dose mean of $2.9E+04$ CFU. In summary, in the rhesus macaque post-exposure prophylaxis with co-trimoxazole conferred significant protection against a lethal aerosol exposure to *B. pseudomallei* (NCTC 13392). The characteristics of the disease resembled acute human melioidosis with a rapid onset of clinical signs; pneumonia, fever 24-48 hours post-challenge,

dyspnoea 3-5 days post-challenge, leukocytosis 2-3 days post-challenge, high C-Reactive protein 2 days post-challenge and death 3-6 days post-challenge.

1.4.4. *Coxiella burnetii*

Coxiella burnetii is a Gram-negative intracellular bacterium and the etiological agent of Q fever. Q fever is a zoonotic disease that typically presents a self-limiting febrile disease but can progress to an atypical pneumonia, which can result in a life-threatening acute respiratory distress syndrome. *C. burnetii* can also cause a severe, and sometimes life-threatening, chronic form of disease characterized by endocarditis or hepatitis (Brouqui et al., 1993). Q fever is found throughout the world, with the exception of New Zealand (Hilbink et al., 1993). *C. burnetii* has historically been developed as a biological weapon (Madariaga et al., 2003). It is stable in the environment, virulent, and is classed as a category B pathogen and bioterrorism agent by the CDC.

A vaccine is available and licensed in Australia. Q-VAX® is a purified suspension of formalin-inactivated, *C. burnetii* prepared from the Phase I Henzerling strain of the organism grown in the yolk sacs of embryonated eggs. It has been given to “at-risk” workers (e.g. abattoir). Prior to immunisation, all potential vaccinees must be screened and have a serum antibody estimation and a skin test reported. If Q-VAX® is administered to those who are sensitised to Q fever antigens, serious hypersensitivity reactions can occur.

Recovery from acute disease usually occurs within 2 weeks, or less following treatment with oral doxycycline. Delays in, or incorrect, diagnosis of Q fever often result in ineffective or inappropriate antibiotic treatment (Fournier et al., 1998). The chronic form of the disease is treated with a combination of doxycycline and chloroquine. Treatment periods are extensive from 18 months to 4 years (Raoult et al., 1999). Doxycycline-resistant strains have been observed in patients (Rouli et al., 2012).

We developed and characterised a murine model of Q-fever and used it to assess the post-exposure efficacy of a liposome encapsulated ciprofloxacin. Studies are described in Norville et al. (2014). The model developed in A/J mice was non-lethal, so five

parameters were used to assess the disease; weight loss, clinical signs, organ weight (lung and spleen), bacterial burden and histopathology. Following aerosol challenge with axenically grown *C. burnetii* Nine Mile, A/J mice displayed clinical signs of disease from days 4-5 post-challenge. Clinical signs resolved within 14 days of infection which is similar to the acute disease observed in humans. Formulations of liposome-encapsulated ciprofloxacin had previously been reported to improve antibiotic efficacy in *Francisella tularensis*, *Mycobacterium avium*, and *Streptococcus pneumoniae* in animal models (Oh et al., 1995, Conley et al., 1997, Ellbogen et al., 2003, Wong et al., 2003). We demonstrated that ciprofloxacin for inhalation (CFI), a liposome-encapsulated ciprofloxacin, allows effective pulmonary delivery, and showed significant improvements over doxycycline. In these development studies CFI was administered by intranasal inoculation. To better replicate the delivery that would be used in a human regimen, aerosol inoculation was investigated. The large volumes of material required by the Collison nebuliser made it unsuitable. Two alternative nebulisers were trialled; the LC Sprint star (Pari Medical Ltd, UK), compressed air driven producing particles of 3.5 µm MMAD, and the Aerogen Pro (Aerogen, Ireland), vibrating plate producing particles of 3 µm MMAD. The LC Sprint star was successfully combined with our animal exposure system and proven as a delivery method to mice.

1.4.5. *Bacillus anthracis*

Bacillus anthracis is a Gram-positive, spore-forming bacterium that causes anthrax, a severe infectious disease of both animals and humans. An anthrax vaccine is available for humans deemed to be at high-risk of contracting anthrax; cell-free filtrates of the attenuated, non-capsulated Sterne strain of *B. anthracis* are licensed in both the UK and US for human use (Turnbull, 1991). The UK vaccine is made by alum-precipitation of antigen from *in vitro* Sterne cultures and is termed anthrax vaccine precipitated (AVP), to distinguish it from anthrax vaccine adsorbed (AVA) which is licensed for use in the US. Human infection is rare and usually occurs with low lethality via the cutaneous or gastrointestinal route. Human inhalational anthrax has a high mortality rate of 45-80% (Holty et al., 2006) with death occurring within days of exposure without subsequent treatment.

B. anthracis spores are highly resistant to extremes of temperature and humidity, and to treatment with chemical disinfectants; spores can remain viable for long periods in soil, and have been recovered from contaminated soil and animal remains after many decades (Wilson and Russell, 1964). These properties have led to anthrax being successfully developed as an effective biological weapon (Jernigan et al., 2002); anthrax weaponisation has been achieved by at least five national bioweapons programs: in the UK, Japan, the US, Russia and Iraq.

An NIH-FDA Antibiotic Working Group recommended five antibiotics to be tested for prophylactic efficacy against inhalational anthrax, to increase therapeutic options and to address the needs of special populations e.g. children and pregnant women. The HHS Public Health Emergency Medical Countermeasures Enterprise (PHEMCE) emphasised the needs of these special populations; however, these drugs required approval for use in the general population before seeking extended label indications for special populations.

We were awarded two NIAID task orders; to test the efficacy of antibiotics in both a small animal and NHP models. The development of our mouse model spanned the refinement of our aerosol and containment systems. *B. anthracis* AMES (BEI resources NR-3838) was grown on solid medium over 21 days prior to harvesting and concentration by centrifugation. A median lethal dose was established in BALB/c mice. However, both the volume and quality of spores required for the large programme of work required we developed a small fed-batch fermenter production method. Using the source material, *B. anthracis* AMES (BEI resources NR-3838) we produced a fully characterised (real-time PCR, scanning electron microscopy, spore capsule staining (using malachite green stain) and demonstrating gamma bacteriophage and penicillin sensitivity) high titre spore stock to meet our development and testing needs. Due to security issues around the nature of this work, this methodology is not publicly available; however, the virulence of the resulting spore stock was presented at the American Society of Microbiology, Biodefense and Emerging Diseases Research Meeting, Baltimore (Hatch et al., 2009).

The recommended antibiotic (ciprofloxacin) against *B. anthracis* is based upon empirical treatments for sepsis, as there are no clinical studies of the treatment of anthrax in humans (Inglesby et al., 1999). The CDC updated their guidelines on treatment of post-exposure inhalational anthrax, to include doxycycline and levofloxacin as well as ciprofloxacin (Hendricks et al., 2014). Ciprofloxacin has been investigated in many animal models of inhalational infection, ranging from mice, guinea pigs and rabbits (Altboum et al., 2002, Steward et al., 2004, Peterson et al., 2010) through to marmoset and rhesus macaques (Friedlander et al., 1993, Nelson et al., 2011, Fritz et al., 1995) and it has proved effective. To combat potential antibiotic resistance, continued research into the efficacy of different antibiotics or indeed different combinations of antibiotics is important. In addition, treatment with ciprofloxacin alone during the Amerithrax incident was seen to fail to protect 5 out of 11 individuals against inhalational anthrax. It is speculated that this failure was due to continued action of toxin in the absence of viable organisms (Twenhafel, 2010). A combination of antibiotics (e.g. bactericidal agents with protein synthesis inhibitors) may be more effective.

Human inhalational anthrax has an incredibly rapid disease course, with death occurring within a few days of exposure without treatment. Following aerosol exposure to an inhaled dose $\sim 1.2E+06$ CFU *B. anthracis* (equating to 20 LD₅₀) BALB/c mice will succumb to infection within 2-3 days. In Hatch et al. (2014) we describe our small animal model and the evaluation of levofloxacin, amoxicillin and co-amoxiclav which conferred significant protection ($p < 0.001$) from inhalational anthrax, whereas azithromycin and clarithromycin failed to protect. Two of these drugs, amoxicillin and co-amoxiclav, were selected for further evaluation.

To support medical countermeasures against inhalational anthrax the FDA guidance recommended the use of an appropriate macaque model (FDA, 2002) and subsequent guidance and publications support the use of the African green, rhesus or cynomolgus macaque (FDA, 2015, Friedlander et al., 1993, Fritz et al., 1995, Vasconcelos et al., 2003, Twenhafel et al., 2007). We developed a cynomolgus model of inhalational anthrax for efficacy testing of post-exposure therapeutics. The pivotal studies in NHPs were required by the US to be conducted to GLP. Whilst not strictly within the remit of UK

regulatory GLP we gained approval from the MHRA to claim compliance. This necessitated a huge amount of equipment, system and assay, characterisation and validation. The model was used to successfully evaluate the post-exposure efficacy of amoxicillin and co-amoxiclav in terms of animal survival, bacterial burden, and time course of progression of diseases (including disease manifestations e.g. pathologic features and immune status). These data supported NIAID in their aim to increase the options for post-exposure prophylaxis indication for inhalational anthrax.

The approach to prophylaxis and treatment of inhalation anthrax could be compromised by the release of *B. anthracis* carrying antibiotic resistance genes. Naturally occurring strains resistant to currently useful antibiotics have been reported (Altboum et al., 2002, Heine et al., 2007). In our BALB/c model, Negus et al. (2015) assessed the prophylactic and therapeutic potential of the poly- λ -D-glutamic acid (PDGA). This enzyme selectively removes the capsule from the surface of vegetative *B. anthracis* cell and prevented the emergence of signs of disease and death following a lethal inhalational dose of *B. anthracis*.

1.4.6. Monkeypox

Variola virus, the aetiological agent of smallpox, is highly contagious and causes disease with a high mortality rate (Chapman et al., 2010). Endemic smallpox was eradicated through a successful global immunization campaign by the World Health Organization (WHO) more than 30 years ago (Jacobs et al., 2009), with the final natural case of smallpox recorded in Somalia in 1977 (WHO, 2001). Since the eradication, vaccination against this pathogen has been discontinued, and so much of the world's population currently lacks protective immunity (von Krempelhuber et al., 2010). Consequently, the use of variola virus as a biological weapon poses a current major public health threat. Other orthopoxviruses, for example, monkeypox, cowpox virus and a variety of vaccinia virus-like viruses (Bhanuprakash et al., 2010, Glatz et al., 2010, Rimoin et al., 2010, Trindade et al., 2007) can spread to humans by zoonotic infection and therefore also threaten public well-being.

The testing of new medical countermeasures against orthopoxviruses is a prime example of why the “Animal Rule” was developed. In the past, macaques were used in studies employing both variola virus and monkeypox virus in order to model the ordinary disease presentation of smallpox infection in people (Chapman et al., 2010). Since working with variola virus is both unethical and impossible given the obvious risks of reintroducing an eradicated disease, monkeypox virus infection in macaques has now become an acceptable surrogate model for human smallpox disease (Zaucha et al., 2001, Cann et al., 2012), provided an appropriate dose and route of challenge (Chapman et al., 2010).

A number of challenge routes have been described for macaques; subcutaneous (Nagata et al., 2014), intravenous (Earl et al., 2008, Earl et al., 2004, Buchman et al., 2010), intrabronchial (Stittelaar et al., 2005) and intratracheal (Goff et al., 2011). Fenner et al. (1988) stated the natural route of infection for smallpox in man is through close contact with an infected person via the oropharynx or nasopharynx. A deliberate release of an aerosol of smallpox or monkeypox would permit rapid dispersion across a large area. We sought to develop an aerosol challenge model of monkeypox in cynomolgus macaques.

What little is known about susceptibility of cynomolgus macaques to monkeypox is based on animals sourced from other parts of the world than those from our breeding colony. It is understood that the susceptibility of a species to various agents can vary considerably, even with the same species, within a geographical sub-population. A stepwise approach was taken to first verify that we could repeat the results from an intravenous challenge. We sought to determine a dose of monkeypox that would produce a reproducible model of natural disease for us to fully characterise the model, compared with Smallpox in man, and eventually use it to assess protection.

The data generated in our studies detailing clinical observations, viral loads, immune responses and pathological changes (Tree et al., 2015) supported and expanded on previous work using this infection model (Zaucha et al., 2001). The model displayed similarities to the clinical presentation of smallpox in humans (Fenner et al., 1988). Our

studies were reviewed by the US government and we were granted approval to use aerosolised monkeypox infection in cynomolgus macaques as a model for studying human pox infections utilising the FDA Animal Rule.

The traditional smallpox vaccines used to eradicate smallpox are based on replicating vaccinia virus. Although highly efficacious, there are associated side effects ranging from mild and self-limiting to severe and life-threatening (Metzger and Mordmueller, 2007). Second generation smallpox vaccines (e.g. ACAM2000) produced in cell cultures from the Lister-Elstree or New York City Board of Health vaccinia virus strains are cleaner and appear as effective as the earlier vaccines. However, there are still contra-indications and it is estimated that 25% of the population would be at risk of developing complications (Kemper et al., 2002). Third-generation modified vaccinia Ankara (MVA) vaccines have been shown to be comparatively safe with none of the complications of first- and second-generation smallpox vaccines, especially for those with contra-indications e.g. immune-compromised or atopic dermatitis (Kennedy and Greenberg, 2009, Earl et al., 2004).

IMVAMUNE® is a third-generation, MVA derived, vaccine manufactured by Bavarian-Nordic (Martinsried, Germany). It has been supported through to licensure by the US Government, the National Institute of Allergy and Infectious Diseases (NIAID) for animal studies and subsequently the Biomedical Advanced Research and Development Authority (BARDA) clinical trials. The pivotal study in this programme of work assessed the protective efficacy of either one or two (prime-boost; administered 28 days apart) doses of IMVAMUNE® against an aerosol monkeypox virus challenge, protective efficacy was evaluated against the second-generation vaccine ACAM2000 (Hatch et al., 2013a). We showed that the use of a prime-boost regime of IMVAMUNE® provided complete protection from subsequent challenge with monkeypox.

We played an essential part in providing evidence supporting the licensure an MVA derived vaccine against smallpox and monkeypox (Hatch et al., 2013a, Tree et al., 2015, Tree et al., 2016). JYNNEOS™ was approved by the US Food and Drug Administration (FDA) in September 2019 for the prevention of smallpox and monkeypox in adults. It is

the only FDA-approved non-replicating smallpox and monkeypox vaccine and the only approved monkeypox vaccine in the world. The vaccine is marketed under the brand names IMVANEX® and IMVAMUNE® in the EU and Canada. Recent cases of monkeypox virus infection in the UK have used IMVANEX® as part of the national response, and it is now used to vaccinate 'at risk' staff at PHE.

1.5. The future

The expertise I have gained, and the systems developed in the refinement of aerosol animal models at high containment continues to be of importance to the PHE goal of protecting human health. A large programme of TB vaccine research and testing continues, as does research into countermeasures against emerging pathogens and potential biowarfare agents. The skills and systems are easily transferrable in the event of a required response to a national demand or research objectives.

PHE is committed to building a high containment *in vivo* facility when it relocates its headquarters and two scientific centres, Porton and Colindale to a new campus at Harlow on the former GlaxoSmithKline New Frontiers Science Park. The new build facility at PHE Harlow will contain a suited *in vivo* facility capable of handling animals up to ACDP and SAPO Containment Levels 4. This will be a first in the UK and I am the PHE Senior User advising the Science Hub programme on high containment *in vivo* facilities. Transition to PHE Harlow is key for my department. The expertise and knowledge I have gained working in the development of aerosol models and the challenges around handling high consequence pathogens will prove vital in the process.

1.6. Concluding comments

This thesis has brought together my published papers, which involve the development and use of animal models of a range of pathogens mostly from ACDP hazard group 3. The work follows a career that has grown from research technician, through study management, to leadership of research and service delivery.

The improvements in aerosol delivery technology, containment strategies and clinical data gathering have all fed into the principles of reduction, refinement and replacement

embedded in animal research. The technological and procedural advances introduced during my career have positively impacted the way high containment animal studies are performed at PHE Porton. We have increased the reproducibility of delivered aerosol doses thus enabling reduction of the number of test animals required. Studies have been refined by telemetry, advanced CCTV, veterinary blood analysers, radiographs and imaging capabilities to both improve euthanasia endpoints, reduce numbers, and make best use of the animals.

The strategies employed have been instrumental in the pre-clinical evaluation of vaccines against tuberculosis, the approval of a new vaccine for smallpox, and post-exposure treatment regimens of anthrax and other diseases in the biodefence arena.

The last year has seen our in vivo facility largely dedicated to the evaluation of vaccines and therapeutics against SARS-CoV-2. The flexible high containment facilities, knowledge and skilled staff have enabled PHE to rapidly develop NHP, ferret and hamster models of Covid-19 and assist in the UK and worldwide effort to rapidly assess the efficacy of new vaccines and therapeutics.

2. References to the Commentary

- AGGER, E. M., ROSENKRANDS, I., OLSEN, A. W., HATCH, G., WILLIAMS, A., KRITSCH, C., LINGNAU, K., VON GABAIN, A., ANDERSEN, C. S., KORSHOLM, K. S. & ANDERSEN, P. 2006. Protective immunity to tuberculosis with Ag85B-ESAT-6 in a synthetic cationic adjuvant system IC31. *Vaccine*, 24, 5452-60.
- ALEXANDER, D. J., COLLINS, C. J., COOMBS, D. W., GILKISON, I. S., HARDY, C. J., HEALEY, G., KARANTABIAS, G., JOHNSON, N., KARLSSON, A., KILGOUR, J. D. & MCDONALD, P. 2008. Association of Inhalation Toxicologists (AIT) working party recommendation for standard delivered dose calculation and expression in non-clinical aerosol inhalation toxicology studies with pharmaceuticals. *Inhal Toxicol*, 20, 1179-89.
- ALTBOUM, Z., GOZES, Y., BARNEA, A., PASS, A., WHITE, M. & KOBILER, D. 2002. Postexposure prophylaxis against anthrax: evaluation of various treatment regimens in intranasally infected guinea pigs. *Infect Immun*, 70, 6231-41.
- ANDERSON, G. W., JR., WORSHAM, P. L., BOLT, C. R., ANDREWS, G. P., WELKOS, S. L., FRIEDLANDER, A. M. & BURANS, J. P. 1997. Protection of mice from fatal bubonic and pneumonic plague by passive immunization with monoclonal antibodies against the F1 protein of *Yersinia pestis*. *Am J Trop Med Hyg*, 56, 471-3.
- BACON, J., JAMES, B. W., WERNISCH, L., WILLIAMS, A., MORLEY, K. A., HATCH, G. J., MANGAN, J. A., HINDS, J., STOKER, N. G., BUTCHER, P. D. & MARSH, P. D. 2004. The influence of reduced oxygen availability on pathogenicity and gene expression in *Mycobacterium tuberculosis*. *Tuberculosis (Edinb)*, 84, 205-17.
- BARNEWALL, R. E., FISHER, D. A., ROBERTSON, A. B., VALES, P. A., KNOSTMAN, K. A. & BIGGER, J. E. 2012. Inhalational monkeypox virus infection in cynomolgus macaques. *Front Cell Infect Microbiol*, 2, 117.
- BHANUPRAKASH, V., VENKATESAN, G., BALAMURUGAN, V., HOSAMANI, M., YOGISHARADHYA, R., GANDHALE, P., REDDY, K. V., DAMLE, A. S., KHER, H. N., CHANDEL, B. S., CHAUHAN, H. C. & SINGH, R. K. 2010. Zoonotic infections of buffalopox in India. *Zoonoses Public Health*, 57, e149-55.
- BIDE, R. W., ARMOUR, S. J. & YEE, E. 2000. Allometric respiration/body mass data for animals to be used for estimates of inhalation toxicity to young adult humans. *J Appl Toxicol*, 20, 273-90.
- BROUQUI, P., DUPONT, H. T., DRANCOURT, M., BERLAND, Y., ETIENNE, J., LEPONT, C., GOLDSTEIN, F., MASSIP, P., MICOUD, M., BERTRAND, A. & ET AL. 1993. Chronic

- Q fever. Ninety-two cases from France, including 27 cases without endocarditis. *Arch Intern Med*, 153, 642-8.
- BUCHMAN, G. W., COHEN, M. E., XIAO, Y., RICHARDSON-HARMAN, N., SILVERA, P., DETOLLA, L. J., DAVIS, H. L., EISENBERG, R. J., COHEN, G. H. & ISAACS, S. N. 2010. A protein-based smallpox vaccine protects non-human primates from a lethal monkeypox virus challenge. *Vaccine*, 28, 6627-36.
- BUTLER, T. 2013. Plague gives surprises in the first decade of the 21st century in the United States and worldwide. *Am J Trop Med Hyg*, 89, 788-93.
- CANN, J. A., JAHRLING, P. B., HENSLEY, L. E. & WAHL-JENSEN, V. 2012. Comparative pathology of smallpox and monkeypox in man and macaques. *J Comp Pathol*.
- CHAMBERS, M. A., WILLIAMS, A., HATCH, G., GAVIER-WIDEN, D., HALL, G., HUYGEN, K., LOWRIE, D., MARSH, P. D. & HEWINSON, R. G. 2002. Vaccination of guinea pigs with DNA encoding the mycobacterial antigen MPB83 influences pulmonary pathology but not hematogenous spread following aerogenic infection with *Mycobacterium bovis*. *Infect Immun*, 70, 2159-65.
- CHAMBERS, M. A., WRIGHT, D. C., BRISKER, J., WILLIAMS, A., HATCH, G., GAVIER-WIDEN, D., HALL, G., MARSH, P. D. & GLYN HEWINSON, R. 2004. A single dose of killed *Mycobacterium bovis* BCG in a novel class of adjuvant (Novasome) protects guinea pigs from lethal tuberculosis. *Vaccine*, 22, 1063-71.
- CHAPMAN, J. L., NICHOLS, D. K., MARTINEZ, M. J. & RAYMOND, J. W. 2010. Animal models of orthopoxvirus infection. *Vet Pathol*, 47, 852-70.
- CHENG, Y. & MOSS, O. 1997. Inhalation exposure systems. In: MCELLAN, R. O. & HENDERSON, R. E. (eds.) *Inhalation toxicology*. New York: Pergamon.
- CLARK, S. O., HALL, Y., KELLY, D. L., HATCH, G. J. & WILLIAMS, A. 2011. Survival of *Mycobacterium tuberculosis* during experimental aerosolization and implications for aerosol challenge models. *J Appl Microbiol*, 111, 350-9.
- CONEJERO, L., PATEL, N., DE REYNAL, M., OBERDORF, S., PRIOR, J., FELGNER, P. L., TITBALL, R. W., SALGUERO, F. J. & BANCROFT, G. J. 2011. Low-dose exposure of C57BL/6 mice to *Burkholderia pseudomallei* mimics chronic human melioidosis. *Am J Pathol*, 179, 270-80.
- CONLEY, J., YANG, H., WILSON, T., BLASETTI, K., DI NINNO, V., SCHNELL, G. & WONG, J. P. 1997. Aerosol delivery of liposome-encapsulated ciprofloxacin: aerosol characterization and efficacy against *Francisella tularensis* infection in mice. *Antimicrob Agents Chemother*, 41, 1288-92.

- COUNCIL, N. R. 2011. *Animal models for assessing countermeasures to bioterrorism agents*, Washington, DC, The National Academies Press.
- DARQUENNE, C. 2012. Aerosol deposition in health and disease. *J Aerosol Med Pulm Drug Deliv*, 25, 140-7.
- DEFRA 2015. Animal Pathogens: Guidance on Control. Retrieved from https://assets.publishing.service.gov.uk/government/uploads/system/uploads/attachment_data/file/400360/animal-pathogens-guidance-controls.pdf.
- DORATO, M. A. & WOLFF, R. K. 1991. Inhalation exposure technology, dosimetry, and regulatory issues. *Toxicol Pathol*, 19, 373-83.
- DRUETT, H. A. 1969. A mobile form of the Henderson apparatus. *J Hyg (Lond)*, 67, 437-48.
- EARL, P. L., AMERICO, J. L., WYATT, L. S., ELLER, L. A., WHITBECK, J. C., COHEN, G. H., EISENBERG, R. J., HARTMANN, C. J., JACKSON, D. L., KULESH, D. A., MARTINEZ, M. J., MILLER, D. M., MUCKER, E. M., SHAMBLIN, J. D., ZWIERS, S. H., HUGGINS, J. W., JAHRLING, P. B. & MOSS, B. 2004. Immunogenicity of a highly attenuated MVA smallpox vaccine and protection against monkeypox. *Nature*, 428, 182-5.
- EARL, P. L., AMERICO, J. L., WYATT, L. S., ESPENSHADE, O., BASSLER, J., GONG, K., LIN, S., PETERS, E., RHODES, L., JR., SPANO, Y. E., SILVERA, P. M. & MOSS, B. 2008. Rapid protection in a monkeypox model by a single injection of a replication-deficient vaccinia virus. *Proc Natl Acad Sci U S A*, 105, 10889-94.
- ELLBOGEN, M. H., OLSEN, K. M., GENTRY-NIELSEN, M. J. & PREHEIM, L. C. 2003. Efficacy of liposome-encapsulated ciprofloxacin compared with ciprofloxacin and ceftriaxone in a rat model of pneumococcal pneumonia. *J Antimicrob Chemother*, 51, 83-91.
- FDA 2002. New drug and biologics and drug products; evidence needed to demonstrate effectiveness of new drugs when human efficacy studies are not ethical or feasible. *Federal Register (31/-5/02) 67 (105); 21 CFR parts 314 and 601*.
- FDA 2015. Product development under the Animal Rule. Guidance for industry. Retrieved from <https://www.fda.gov/media/88625/download>.
- FELLOWS, P., ADAMOVIČ, J., HARTINGS, J., SHERWOOD, R., MEGA, W., BRASEL, T., BARR, E., HOLLAND, L., LIN, W., ROM, A., BLACKWELDER, W., PRICE, J., MORRIS, S., SNOW, D. & HART, M. K. 2010. Protection in mice passively immunized with serum from cynomolgus macaques and humans vaccinated with recombinant plague vaccine (rF1V). *Vaccine*, 28, 7748-56.

- FENNER, F., HENDERSON, D. A., ARITA, I., JEZEK, Z. & LADNYI, I. D. 1988. *The epidemiology of smallpox, p 169–208, in Smallpox and its eradication, WHO, Geneva, Switzerland., .*
- FINE, P. E. 1995. Variation in protection by BCG: implications of and for heterologous immunity. *Lancet*, 346, 1339-45.
- FOURNIER, P. E., MARRIE, T. J. & RAOULT, D. 1998. Diagnosis of Q fever. *J Clin Microbiol*, 36, 1823-34.
- FRIEDLANDER, A. M., WELKOS, S. L., PITT, M. L., EZZELL, J. W., WORSHAM, P. L., ROSE, K. J., IVINS, B. E., LOWE, J. R., HOWE, G. B., MIKESELL, P. & ET AL. 1993. Postexposure prophylaxis against experimental inhalation anthrax. *J Infect Dis*, 167, 1239-43.
- FRITZ, D. L., JAAX, N. K., LAWRENCE, W. B., DAVIS, K. J., PITT, M. L., EZZELL, J. W. & FRIEDLANDER, A. M. 1995. Pathology of experimental inhalation anthrax in the rhesus monkey. *Lab Invest*, 73, 691-702.
- FUNNELL, S. G. P., TREE, J. A., HATCH, G. J., BATE, S. R., HALL, G., PEARSON, G., RAYNER, E. L., ROBERTS, A. D. G. & VIPOND, J. 2019. Dose-dependant acute or subacute disease caused by *Burkholderia pseudomallei* strain NCTC 13392 in a BALB/c aerosol model of infection. *J Appl Microbiol*, 127, 1224-1235.
- GLATZ, M., RICHTER, S., GINTER-HANSELMAYER, G., ABERER, W. & MULLEGGER, R. R. 2010. Human cowpox in a veterinary student. *Lancet Infect Dis*, 10, 288.
- GOFF, A. J., CHAPMAN, J., FOSTER, C., WLAZLOWSKI, C., SHAMBLIN, J., LIN, K., KREISELMEIER, N., MUCKER, E., PARAGAS, J., LAWLER, J. & HENSLEY, L. 2011. A novel respiratory model of infection with monkeypox virus in cynomolgus macaques. *J Virol*, 85, 4898-909.
- GRAHAM, V. A., HATCH, G. J., BEWLEY, K. R., STEEDS, K., LANSLEY, A., BATE, S. R. & FUNNELL, S. G. 2014. Efficacy of primate humoral passive transfer in a murine model of pneumonic plague is mouse strain-dependent. *J Immunol Res*, 2014, 807564.
- GUYTON, A. C. 1947. Measurement of the respiratory volumes of laboratory animals. *Am J Physiol*, 150, 70-7.
- HAMASUR, B., HAILE, M., PAWLOWSKI, A., SCHRODER, U., WILLIAMS, A., HATCH, G., HALL, G., MARSH, P., KALLENIOUS, G. & SVENSON, S. B. 2003. *Mycobacterium tuberculosis* arabinomannan-protein conjugates protect against tuberculosis. *Vaccine*, 21, 4081-93.

- HARTINGS, J. M. & ROY, C. J. 2004. The automated bioaerosol exposure system: preclinical platform development and a respiratory dosimetry application with nonhuman primates. *J Pharmacol Toxicol Methods*, 49, 39-55.
- HATCH, G. J. 2013. Characterisation of the natural history of inhalational melioidosis in cynomolgus and rhesus macaques. *World Melioidosis Conference*. Townsville, Aus.
- HATCH, G. J., BATE, S., FRETWELL, R., FUNNELL, S. G., VIPOND, J. & ROBERTS, A. D. 2011a. Experimental respiratory *Burkholderia pseudomallei* infection in BALB/c mice. *ASM Aerobiology in Biodefense IV*. Richmond, MD, US.
- HATCH, G. J., BATE, S., FRETWELL, R., VIPOND, J., FUNNELL, S. G. & ROBERTS, A. D. 2011b. Efficacy testing of orally administered antibiotics against an inhalational *Bacillus anthracis* infection in BALB/c mice. *ASM Biodefense and Emerging Diseases Research Meeting*. Washington, MD, US.
- HATCH, G. J., BATE, S. R., CROOK, A., JONES, N., FUNNELL, S. G. & VIPOND, J. 2014. Efficacy testing of orally administered antibiotics against an inhalational *Bacillus anthracis* infection in BALB/c mice. *Journal of Infectious Diseases and Therapy*, 02, 1000175.
- HATCH, G. J., DENNIS, M., PEARCE, P. C., NAYLOR, I. & FUNNELL, S. G. 2008a. Derived respiration rate offers a refinement in the surgical procedure necessary for radio-telemetry. *NC3Rs Refinement and Use of Chronic Implants in Animal Research*. London, UK.
- HATCH, G. J., FRETWELL, R., BATE, S., FUNNELL, S. G. & ROBERTS, A. D. 2010a. Assessment of the effect of different growth phases and both spray and collection medium on aerosol survival of *Burkholderia pseudomallei*. *ASM Biodefense and Emerging Diseases Research Meeting*. Baltimore, MD, US.
- HATCH, G. J., FUNNELL, S. G., BATE, S., FRETWELL, R. & ROBERTS, A. D. 2010b. Development of *Burkholderia pseudomallei* aerosolisation challenge method for infection model development. *ASM Biodefense and Emerging Diseases Research Meeting - Burkholderia spp. Workshop* Baltimore, MD, US.
- HATCH, G. J., GRAHAM, V. A., BEWLEY, K. R., TREE, J. A., DENNIS, M., TAYLOR, I., FUNNELL, S. G., BATE, S. R., STEEDS, K., TIPTON, T., BEAN, T., HUDSON, L., ATKINSON, D. J., MCLUCKIE, G., CHARLWOOD, M., ROBERTS, A. D. & VIPOND, J. 2013a. Assessment of the protective effect of Imvamune and Acam2000 vaccines against aerosolized monkeypox virus in cynomolgus macaques. *J Virol*, 87, 7805-15.

- HATCH, G. J., HOPKINS, D. L., ATKINSON, A., THOMAS, S., FINNEY, M., BEWLEY, K. R., ROBERTS, A. D. & FUNNELL, S. G. 2008b. Performance of the Henderson apparatus to produce defined aerosols using multiple species of micro-organisms. *ASM Biodefense and Emerging Diseases Research Meeting*. Baltimore, MD, US.
- HATCH, G. J., HOPKINS, D. L., FRETWELL, R., BATE, S., FUNNELL, S. G. & ROBERTS, A. D. 2009a. Assessment of the virulence in BALB/c mice of bioreactor produced anthrax spores stocks, delivered by the aerosol route. *ASM Biodefense and Emerging Diseases Research Meeting*. Baltimore, MD, US.
- HATCH, G. J., HOPKINS, D. L., FUNNELL, S. G. & ROBERTS, A. D. 2007. Increasing the efficacy of the Henderson apparatus to deliver a lethal aerosol dose of *Bacillus anthracis* to BALB/c mice. *ASM Aerobiology in Biodefense II*. Rocky Gap, MD, US.
- HATCH, G. J., KANE, J., BATE, S., TONKS, K., TSANG, C., FRETWELL, R., FUNNELL, S. G., VIPOND, J. & ROBERTS, A. D. 2013b. Characterisation of inhalational infection with *Burkholderia pseudomallei* in BALB/c mice. *World Melioidosis Conference*. Townsville, Aus.
- HATCH, G. J., SCOTT, A. E., BATE, S., PRIOR, J. L., ATKINS, T. & VIPOND, J. 2013c. Evaluation of the protective efficacy of heat killed cell *Burkholderia spp.* preparations in mice against inhalational challenge with *B. pseudomallei*. *World Melioidosis Conference*. Townsville, Aus.
- HATCH, G. J., VIPOND, J., FUNNELL, S. G., BEWLEY, K. R., HOPKINS, D. L. & ROBERTS, A. D. 2009b. Assessment of the dose response of aerosolised monkeypox in cynomolgus macaques *ASM Aerobiology in Biodefense III*. Rocky Gap, MD, US.
- HEATH, D. G., ANDERSON, G. W., JR., MAURO, J. M., WELKOS, S. L., ANDREWS, G. P., ADAMOVIČZ, J. & FRIEDLANDER, A. M. 1998. Protection against experimental bubonic and pneumonic plague by a recombinant capsular F1-V antigen fusion protein vaccine. *Vaccine*, 16, 1131-7.
- HEINE, H. S., BASSETT, J., MILLER, L., HARTINGS, J. M., IVINS, B. E., PITT, M. L., FRITZ, D., NORRIS, S. L. & BYRNE, W. R. 2007. Determination of antibiotic efficacy against *Bacillus anthracis* in a mouse aerosol challenge model. *Antimicrob Agents Chemother*, 51, 1373-9.
- HENDERSON, D. W. 1952. An apparatus for the study of airborne infection. *J Hyg (Lond)*, 50, 53-68.
- HENDRICKS, K. A., WRIGHT, M. E., SHADOMY, S. V., BRADLEY, J. S., MORROW, M. G., PAVIA, A. T., RUBINSTEIN, E., HOLTY, J. E., MESSONNIER, N. E., SMITH, T. L., PESIK, N., TREADWELL, T. A., BOWER, W. A. & WORKGROUP ON ANTHRAX CLINICAL, G.

2014. Centers for disease control and prevention expert panel meetings on prevention and treatment of anthrax in adults. *Emerg Infect Dis*, 20.
- HILBINK, F., PENROSE, M., KOVACOVA, E. & KAZAR, J. 1993. Q fever is absent from New Zealand. *Int J Epidemiol*, 22, 945-9.
- HILL, J., EYLES, J. E., ELVIN, S. J., HEALEY, G. D., LUKASZEWSKI, R. A. & TITBALL, R. W. 2006. Administration of antibody to the lung protects mice against pneumonic plague. *Infect Immun*, 74, 3068-70.
- HOLTY, J. E., BRAVATA, D. M., LIU, H., OLSHEN, R. A., MCDONALD, K. M. & OWENS, D. K. 2006. Systematic review: a century of inhalational anthrax cases from 1900 to 2005. *Ann Intern Med*, 144, 270-80.
- HOPPE, I., BRENNEKE, B., ROHDE, M., KREFT, A., HAUSSLER, S., REGANZEROWSKI, A. & STEINMETZ, I. 1999. Characterization of a murine model of melioidosis: comparison of different strains of mice. *Infect Immun*, 67, 2891-900.
- HSE 2013a. The Approved List of Biological Agents, Third edition. Retrieved from <http://www.hse.gov.uk/pubns/misc208.pdf>.
- HSE 2013b. Control of Substances Hazardous to Health Regulations 2002 (as amended). ISBN 978 0 7176 6582 2.
- HSE 2014. The Genetically Modified Organisms (Contained Use) Regulations. Retrieved from <http://www.hse.gov.uk/pubns/priced/l29.pdf>.
- HSE 2015. Guidance for licence holders on the containment and control of specified animal pathogens. retrieved from <http://www.hse.gov.uk/pubns/priced/hsg280.pdf>.
- HSE 2018. The management and operation of microbiological containment laboratories. Retrieved from <http://www.hse.gov.uk/biosafety/management-containment-labs.pdf>.
- INGLESBY, T. V., HENDERSON, D. A., BARTLETT, J. G., ASCHER, M. S., EITZEN, E., FRIEDLANDER, A. M., HAUER, J., MCDONALD, J., OSTERHOLM, M. T., O'TOOLE, T., PARKER, G., PERL, T. M., RUSSELL, P. K. & TONAT, K. 1999. Anthrax as a biological weapon: medical and public health management. Working Group on Civilian Biodefense. *JAMA*, 281, 1735-45.
- JACOBS, B. L., LANGLAND, J. O., KIBLER, K. V., DENZLER, K. L., WHITE, S. D., HOLECHEK, S. A., WONG, S., HUYNH, T. & BASKIN, C. R. 2009. Vaccinia virus vaccines: past, present and future. *Antiviral Res*, 84, 1-13.

- JERNIGAN, D. B., RAGHUNATHAN, P. L., BELL, B. P., BRECHNER, R., BRESNITZ, E. A., BUTLER, J. C., CETRON, M., COHEN, M., DOYLE, T., FISCHER, M., GREENE, C., GRIFFITH, K. S., GUARNER, J., HADLER, J. L., HAYSLETT, J. A., MEYER, R., PETERSEN, L. R., PHILLIPS, M., PINNER, R., POPOVIC, T., QUINN, C. P., REEFHUIS, J., REISSMAN, D., ROSENSTEIN, N., SCHUCHAT, A., SHIEH, W. J., SIEGAL, L., SWERDLOW, D. L., TENOVER, F. C., TRAEGER, M., WARD, J. W., WEISFUSE, I., WIERSMA, S., YESKEY, K., ZAKI, S., ASHFORD, D. A., PERKINS, B. A., OSTROFF, S., HUGHES, J., FLEMING, D., KOPLAN, J. P., GERBERDING, J. L. & NATIONAL ANTHRAX EPIDEMIOLOGIC INVESTIGATION, T. 2002. Investigation of bioterrorism-related anthrax, United States, 2001: epidemiologic findings. *Emerg Infect Dis*, 8, 1019-28.
- JONES, S. M., DAY, F., STAGG, A. J. & WILLIAMSON, E. D. 2000. Protection conferred by a fully recombinant sub-unit vaccine against *Yersinia pestis* in male and female mice of four inbred strains. *Vaccine*, 19, 358-66.
- KEMPER, A. R., DAVIS, M. M. & FREED, G. L. 2002. Expected adverse events in a mass smallpox vaccination campaign. *Eff Clin Pract*, 5, 84-90.
- KENNEDY, J. S. & GREENBERG, R. N. 2009. IMVAMUNE: modified vaccinia Ankara strain as an attenuated smallpox vaccine. *Expert Rev Vaccines*, 8, 13-24.
- LAFONTAINE, E. R., ZIMMERMAN, S. M., SHAFFER, T. L., MICHEL, F., GAO, X. & HOGAN, R. J. 2013. Use of a safe, reproducible, and rapid aerosol delivery method to study infection by *Burkholderia pseudomallei* and *Burkholderia mallei* in mice. *PLoS One*, 8, e76804.
- LEAKEY, A. K., ULETT, G. C. & HIRST, R. G. 1998. BALB/c and C57Bl/6 mice infected with virulent *Burkholderia pseudomallei* provide contrasting animal models for the acute and chronic forms of human melioidosis. *Microb Pathog*, 24, 269-75.
- LEVER, M. S., NELSON, M., STAGG, A. J., BEEDHAM, R. J. & SIMPSON, A. J. 2009. Experimental acute respiratory *Burkholderia pseudomallei* infection in BALB/c mice. *Int J Exp Pathol*, 90, 16-25.
- LEVER, M. S., WILLIAMS, A. & BENNETT, A. M. 2000. Survival of mycobacterial species in aerosols generated from artificial saliva. *Lett Appl Microbiol*, 31, 238-41.
- LEVY, Y., FLASHNER, Y., TIDHAR, A., ZAUBERMAN, A., AFTALION, M., LAZAR, S., GUR, D., SHAFFERMAN, A. & MAMROUD, E. 2011. T cells play an essential role in anti-F1 mediated rapid protection against bubonic plague. *Vaccine*, 29, 6866-73.
- LIU, B., KOO, G. C., YAP, E. H., CHUA, K. L. & GAN, Y. H. 2002. Model of differential susceptibility to mucosal *Burkholderia pseudomallei* infection. *Infect Immun*, 70, 504-11.

- MADARIAGA, M. G., REZAI, K., TRENHOLME, G. M. & WEINSTEIN, R. A. 2003. Q fever: a biological weapon in your backyard. *Lancet Infect Dis*, 3, 709-21.
- MARRIOTT, A. C., DENNIS, M., KANE, J. A., GOOCH, K. E., HATCH, G., SHARPE, S., PREVOSTO, C., LEEMING, G., ZEKENG, E. G., STAPLES, K. J., HALL, G., RYAN, K. A., BATE, S., MOYO, N., WHITTAKER, C. J., HALLIS, B., SILMAN, N. J., LALVANI, A., WILKINSON, T. M., HISCOX, J. A., STEWART, J. P. & CARROLL, M. W. 2016. Influenza A virus challenge models in cynomolgus macaques using the authentic inhaled aerosol and intra-nasal routes of infection. *PLoS One*, 11, e0157887.
- MARTIN, C., AGUILO, N., MARINOVA, D. & GONZALO-ASENSIO, J. 2020. Update on TB Vaccine Pipeline. 10, 2632.
- MARTIN, C., WILLIAMS, A., HERNANDEZ-PANDO, R., CARDONA, P. J., GORMLEY, E., BORDAT, Y., SOTO, C. Y., CLARK, S. O., HATCH, G. J., AGUILAR, D., AUSINA, V. & GICQUEL, B. 2006. The live *Mycobacterium tuberculosis* phoP mutant strain is more attenuated than BCG and confers protective immunity against tuberculosis in mice and guinea pigs. *Vaccine*, 24, 3408-19.
- MASSEY, S., YEAGER, L. A., BLUMENTRITT, C. A., VIJAYAKUMAR, S., SBRANA, E., PETERSON, J. W., BRASEL, T., LEDUC, J. W., ENDSLEY, J. J. & TORRES, A. G. 2014. Comparative *Burkholderia pseudomallei* natural history virulence studies using an aerosol murine model of infection. *Sci Rep*, 4, 4305.
- MAY, K. R. 1973. The Collison nebulizer: Description, performance and application. *Aerosol Science*, 4, 235-243.
- METZGER, W. & MORDMUELLER, B. G. 2007. Vaccines for preventing smallpox. *Cochrane Database Syst Rev*, CD004913.
- MOTIN, V. L., NAKAJIMA, R., SMIRNOV, G. B. & BRUBAKER, R. R. 1994. Passive immunity to yersiniae mediated by anti-recombinant V antigen and protein A-V antigen fusion peptide. *Infect Immun*, 62, 4192-201.
- MOVAHEDZADEH, F., WILLIAMS, A., CLARK, S., HATCH, G., SMITH, D., TEN BOKUM, A., PARISH, T., BACON, J. & STOKER, N. 2008. Construction of a severely attenuated mutant of *Mycobacterium tuberculosis* for reducing risk to laboratory workers. *Tuberculosis (Edinb)*, 88, 375-81.
- NAGATA, N., SAIJO, M., KATAOKA, M., AMI, Y., SUZAKI, Y., SATO, Y., IWATA-YOSHIKAWA, N., OGATA, M., KURANE, I., MORIKAWA, S., SATA, T. & HASEGAWA, H. 2014. Pathogenesis of fulminant monkeypox with bacterial sepsis after experimental infection with West African monkeypox virus in a cynomolgus monkey. *Int J Clin Exp Pathol*, 7, 4359-70.

- NEGUS, D., VIPOND, J., HATCH, G. J., RAYNER, E. L. & TAYLOR, P. W. 2015. Parenteral administration of capsule depolymerase EnvD prevents lethal inhalation anthrax infection. *Antimicrob Agents Chemother*, 59, 7687-92.
- NELSON, M., STAGG, A. J., STEVENS, D. J., BROWN, M. A., PEARCE, P. C., SIMPSON, A. J. & LEVER, M. S. 2011. Post-exposure therapy of inhalational anthrax in the common marmoset. *Int J Antimicrob Agents*, 38, 60-4.
- NORVILLE, I. H., HATCH, G. J., BEWLEY, K. R., ATKINSON, D. J., HAMBLIN, K. A., BLANCHARD, J. D., ARMSTRONG, S. J., PITMAN, J. K., RAYNER, E., HALL, G., VIPOND, J. & ATKINS, T. P. 2014. Efficacy of liposome-encapsulated ciprofloxacin in a murine model of Q fever. *Antimicrob Agents Chemother*, 58, 5510-8.
- OH, Y. K., NIX, D. E. & STRAUBINGER, R. M. 1995. Formulation and efficacy of liposome-encapsulated antibiotics for therapy of intracellular *Mycobacterium avium* infection. *Antimicrob Agents Chemother*, 39, 2104-11.
- OLSEN, A. W., WILLIAMS, A., OKKELS, L. M., HATCH, G. & ANDERSEN, P. 2004. Protective effect of a tuberculosis subunit vaccine based on a fusion of antigen 85B and ESAT-6 in the aerosol guinea pig model. *Infect Immun*, 72, 6148-50.
- PETERSON, J. W., MOEN, S. T., HEALY, D., PAWLIK, J. E., TAORMINA, J., HARDCASTLE, J., THOMAS, J. M., LAWRENCE, W. S., PONCE, C., CHATUEV, B. M., GNADE, B. T., FOLTZ, S. M., AGAR, S. L., SHA, J., KLIMPEL, G. R., KIRTLEY, M. L., EAVES-PYLES, T. & CHOPRA, A. K. 2010. Protection afforded by fluoroquinolones in animal models of respiratory infections with *Bacillus anthracis*, *Yersinia pestis*, and *Francisella tularensis*. *Open Microbiol J*, 4, 34-46.
- PHILLIPS, J. E. 2017. Inhaled efficacious dose translation from rodent to human: A retrospective analysis of clinical standards for respiratory diseases. *Pharmacol Ther*, 178, 141-147.
- PITMAN, M. C., LUCK, T., MARSHALL, C. S., ANSTEY, N. M., WARD, L. & CURRIE, B. J. 2015. Intravenous therapy duration and outcomes in melioidosis: a new treatment paradigm. *PLoS Negl Trop Dis*, 9, e0003586.
- PRENTICE, M. B. & RAHALISON, L. 2007. Plague. *Lancet*, 369, 1196-207.
- QUENEE, L. E., CILETTI, N. A., ELLI, D., HERMANAS, T. M. & SCHNEEWIND, O. 2011. Prevention of pneumonic plague in mice, rats, guinea pigs and non-human primates with clinical grade rV10, rV10-2 or F1-V vaccines. *Vaccine*, 29, 6572-83.
- RAOULT, D., HOUPIKIAN, P., TISSOT DUPONT, H., RISS, J. M., ARDITI-DJIANE, J. & BROUQUI, P. 1999. Treatment of Q fever endocarditis: comparison of 2 regimens

containing doxycycline and ofloxacin or hydroxychloroquine. *Arch Intern Med*, 159, 167-73.

- RIMOIN, A. W., MULEMBAKANI, P. M., JOHNSTON, S. C., LLOYD SMITH, J. O., KISALU, N. K., KINKELA, T. L., BLUMBERG, S., THOMASSEN, H. A., PIKE, B. L., FAIR, J. N., WOLFE, N. D., SHONGO, R. L., GRAHAM, B. S., FORMENTY, P., OKITOLONDA, E., HENSLEY, L. E., MEYER, H., WRIGHT, L. L. & MUYEMBE, J. J. 2010. Major increase in human monkeypox incidence 30 years after smallpox vaccination campaigns cease in the Democratic Republic of Congo. *Proc Natl Acad Sci U S A*, 107, 16262-7.
- ROULI, L., ROLAIN, J. M., EL FILALI, A., ROBERT, C. & RAOULT, D. 2012. Genome sequence of *Coxiella burnetii* 109, a doxycycline-resistant clinical isolate. *J Bacteriol*, 194, 6939.
- SAHL, J. W., STONE, J. K., CARL GELHAUS, H., WARREN, R. L., FUNNELL, S. G., KEIM, P. & TUANYOK, A. 2013. Genome sequence of *Burkholderia pseudomallei* NCTC 13392. *Genome Announcements*, Vol. 1
- SHARPE, S. A., ESCHELBACH, E., BASARABA, R. J., GLEESON, F., HALL, G. A., MCINTYRE, A., WILLIAMS, A., KRAFT, S. L., CLARK, S., GOOCH, K., HATCH, G., ORME, I. M., MARSH, P. D. & DENNIS, M. J. 2009. Determination of lesion volume by MRI and stereology in a macaque model of tuberculosis. *Tuberculosis (Edinb)*, 89, 405-16.
- STEWARD, J., LEVER, M. S., SIMPSON, A. J., SEFTON, A. M. & BROOKS, T. J. 2004. Post-exposure prophylaxis of systemic anthrax in mice and treatment with fluoroquinolones. *J Antimicrob Chemother*, 54, 95-9.
- STITTELAAR, K. J., VAN AMERONGEN, G., KONDOVA, I., KUIKEN, T., VAN LAVIEREN, R. F., PISTOOR, F. H., NIESTERS, H. G., VAN DOORNUM, G., VAN DER ZEIJST, B. A., MATEO, L., CHAPLIN, P. J. & OSTERHAUS, A. D. 2005. Modified vaccinia virus Ankara protects macaques against respiratory challenge with monkeypox virus. *J Virol*, 79, 7845-51.
- TAN, G. Y., LIU, Y., SIVALINGAM, S. P., SIM, S. H., WANG, D., PAUCOD, J. C., GAUTHIER, Y. & OOI, E. E. 2008. *Burkholderia pseudomallei* aerosol infection results in differential inflammatory responses in BALB/c and C57Bl/6 mice. *J Med Microbiol*, 57, 508-15.
- TANG, J. W. 2009. The effect of environmental parameters on the survival of airborne infectious agents. *J R Soc Interface*, 6 Suppl 6, S737-46.
- THOMAS, R. J., DAVIES, C., NUNEZ, A., HIBBS, S., EASTAUGH, L., HARDING, S., JORDAN, J., BARNES, K., OYSTON, P. & ELEY, S. 2012. Particle-size dependent effects in the

- BALB/c murine model of inhalational melioidosis. *Front Cell Infect Microbiol*, 2, 101.
- TITBALL, R. W., RUSSELL, P., CUCCUI, J., EASTON, A., HAQUE, A., ATKINS, T., SARKAR-TYSON, M., HARLEY, V., WREN, B. & BANCROFT, G. J. 2008. *Burkholderia pseudomallei*: animal models of infection. *Trans R Soc Trop Med Hyg*, 102 Suppl 1, S111-6.
- TREE, J. A., HALL, G., PEARSON, G., RAYNER, E., GRAHAM, V. A., STEEDS, K., BEWLEY, K. R., HATCH, G. J., DENNIS, M., TAYLOR, I., ROBERTS, A. D., FUNNELL, S. G. & VIPOND, J. 2015. Sequence of pathogenic events in cynomolgus macaques infected with aerosolized monkeypox virus. *J Virol*, 89, 4335-44.
- TREE, J. A., HALL, G., REES, P., VIPOND, J., FUNNELL, S. G. & ROBERTS, A. D. 2016. Repeated high-dose (5×10^8 TCID₅₀) toxicity study of a third generation smallpox vaccine (IMVAMUNE) in New Zealand white rabbits. *Hum Vaccin Immunother*, 12, 1795-801.
- TRINDADE, G. S., EMERSON, G. L., CARROLL, D. S., KROON, E. G. & DAMON, I. K. 2007. Brazilian vaccinia viruses and their origins. *Emerg Infect Dis*, 13, 965-72.
- TURNBULL, P. C. 1991. Anthrax vaccines: past, present and future. *Vaccine*, 9, 533-9.
- TWENHAFEL, N. A. 2010. Pathology of inhalational anthrax animal models. *Vet Pathol*, 47, 819-30.
- TWENHAFEL, N. A., LEFFEL, E. & PITT, M. L. 2007. Pathology of inhalational anthrax infection in the african green monkey. *Vet Pathol*, 44, 716-21.
- VASCONCELOS, D., BARNEWALL, R., BABIN, M., HUNT, R., ESTEP, J., NIELSEN, C., CARNES, R. & CARNEY, J. 2003. Pathology of inhalation anthrax in cynomolgus monkeys (*Macaca fascicularis*). *Lab Invest*, 83, 1201-9.
- VAUGHAN, A., AARONS, E., ASTBURY, J., BALASEGARAM, S., BEADSWORTH, M., BECK, C. R., CHAND, M., O'CONNOR, C., DUNNING, J., GHEBREHEWET, S., HARPER, N., HOWLETT-SHIPLEY, R., IHEKWEAZU, C., JACOBS, M., KAINDAMA, L., KATWA, P., KHOO, S., LAMB, L., MAWDSLEY, S., MORGAN, D., PALMER, R., PHIN, N., RUSSELL, K., SAID, B., SIMPSON, A., VIVANCOS, R., WADE, M., WALSH, A. & WILBURN, J. 2018. Two cases of monkeypox imported to the United Kingdom, September 2018. *Euro Surveill*, 23.
- VIPOND, J., CLARK, S. O., HATCH, G. J., VIPOND, R., MARIE AGGER, E., TREE, J. A., WILLIAMS, A. & MARSH, P. D. 2006a. Re-formulation of selected DNA vaccine candidates and their evaluation as protein vaccines using a guinea pig aerosol infection model of tuberculosis. *Tuberculosis (Edinb)*, 86, 218-24.

- VIPOND, J., HATCH, G. J., LANSLEY, A., BATE, S., FUNNELL, S. G. & SHUTTLEWORTH, H. 2012. Assessment of the post-exposure prophylactic efficacy of orally administered levofloxacin in a *Bacillus anthracis* aerosol infection model. *ASM Biodefense*. Washington, MD, US.
- VIPOND, J., KANE, J., HATCH, G., MCCORRISON, J., NIERMAN, W. C. & LOSADA, L. 2013. Sequence determination of *Burkholderia pseudomallei* Strain NCTC 13392 colony morphology variants. *Genome Announc*, 1.
- VIPOND, J., VIPOND, R., ALLEN-VERCOE, E., CLARK, S. O., HATCH, G. J., GOOCH, K. E., BACON, J., HAMPSHIRE, T., SHUTTLEWORTH, H., MINTON, N. P., BLAKE, K., WILLIAMS, A. & MARSH, P. D. 2006b. Selection of novel TB vaccine candidates and their evaluation as DNA vaccines against aerosol challenge. *Vaccine*, 24, 6340-50.
- VON KREMPELHUBER, A., VOLLMAR, J., POKORNY, R., RAPP, P., WULFF, N., PETZOLD, B., HANDLEY, A., MATEO, L., SIERSBOL, H., KOLLARITSCH, H. & CHAPLIN, P. 2010. A randomized, double-blind, dose-finding Phase II study to evaluate immunogenicity and safety of the third generation smallpox vaccine candidate IMVAMUNE. *Vaccine*, 28, 1209-16.
- WEST, T. E., MYERS, N. D., LIGGITT, H. D. & SKERRETT, S. J. 2012. Murine pulmonary infection and inflammation induced by inhalation of *Burkholderia pseudomallei*. *Int J Exp Pathol*, 93, 421-8.
- WHITE, N. J. 2003. Melioidosis. *Lancet*, 361, 1715-22.
- WHO 2001. Smallpox. *Weekly Epidemiological Record*, 76, 337-344.
- WHO 2009. Handbook: Good Laboratory Practice (2nd Edition). ISBN 978 92 4 154755 0.
- WHO 2020. Global Tuberculosis Report 2020. Geneva: Licence: CC BY-NC-SA 3.0 IGO.
- WIERSINGA, W. J., VAN DER POLL, T., WHITE, N. J., DAY, N. P. & PEACOCK, S. J. 2006. Melioidosis: insights into the pathogenicity of *Burkholderia pseudomallei*. *Nat Rev Microbiol*, 4, 272-82.
- WILLIAMS, A., DAVIES, A., MARSH, P. D., CHAMBERS, M. A. & HEWINSON, R. G. 2000. Comparison of the protective efficacy of bacille calmette-Guerin vaccination against aerosol challenge with *Mycobacterium tuberculosis* and *Mycobacterium bovis*. *Clin Infect Dis*, 30 Suppl 3, S299-301.

- WILLIAMS, A., GOONETILLEKE, N. P., MCSHANE, H., CLARK, S. O., HATCH, G., GILBERT, S. C. & HILL, A. V. 2005a. Boosting with poxviruses enhances *Mycobacterium bovis* BCG efficacy against tuberculosis in guinea pigs. *Infect Immun*, 73, 3814-6.
- WILLIAMS, A., HATCH, G. J., CLARK, S. O., GOOCH, K. E., HATCH, K. A., HALL, G. A., HUYGEN, K., OTTENHOFF, T. H., FRANKEN, K. L., ANDERSEN, P., DOHERTY, T. M., KAUFMANN, S. H., GRODE, L., SEILER, P., MARTIN, C., GICQUEL, B., COLE, S. T., BRODIN, P., PYM, A. S., DALEMANS, W., COHEN, J., LOBET, Y., GOONETILLEKE, N., MCSHANE, H., HILL, A., PARISH, T., SMITH, D., STOKER, N. G., LOWRIE, D. B., KALLENIOUS, G., SVENSON, S., PAWLOWSKI, A., BLAKE, K. & MARSH, P. D. 2005b. Evaluation of vaccines in the EU TB Vaccine Cluster using a guinea pig aerosol infection model of tuberculosis. *Tuberculosis (Edinb)*, 85, 29-38.
- WILLIAMS, A., JAMES, B. W., BACON, J., HATCH, K. A., HATCH, G. J., HALL, G. A. & MARSH, P. D. 2005c. An assay to compare the infectivity of *Mycobacterium tuberculosis* isolates based on aerosol infection of guinea pigs and assessment of bacteriology. *Tuberculosis (Edinb)*, 85, 177-84.
- WILLIAMSON, E. D. 2009. Plague. *Vaccine*, 27 Suppl 4, D56-60.
- WILLIAMSON, E. D., ELEY, S. M., STAGG, A. J., GREEN, M., RUSSELL, P. & TITBALL, R. W. 1997. A sub-unit vaccine elicits IgG in serum, spleen cell cultures and bronchial washings and protects immunized animals against pneumonic plague. *Vaccine*, 15, 1079-84.
- WILSON, J. B. & RUSSELL, K. E. 1964. Isolation of *Bacillus anthracis* from soil stored 60 years. *J Bacteriol*, 87, 237-8.
- WONG, J. P., YANG, H., BLASETTI, K. L., SCHNELL, G., CONLEY, J. & SCHOFIELD, L. N. 2003. Liposome delivery of ciprofloxacin against intracellular *Francisella tularensis* infection. *J Control Release*, 92, 265-73.
- ZAUCHA, G. M., JAHRLING, P. B., GEISBERT, T. W., SWEARENGEN, J. R. & HENSLEY, L. 2001. The pathology of experimental aerosolized monkeypox virus infection in cynomolgus monkeys (*Macaca fascicularis*). *Lab Invest*, 81, 1581-600.

3. Timeline of key activities, presentations and publications

	Key developments: 1) Aerosol 2) Biocontainment 3) Clinical	Presentations	Agent	Publications
2001				
2002				Chambers et al. (2002)
2003				Hamasur et al. (2003)
2004				Bacon et al. (2004) Chambers et al. (2004) Olsen et al. (2004)
2005	NHP challenge mask NHP plethysmography Ex-vivo MRI lung scans NHP directional flow containment system		<i>M. bovis</i> – guinea pig <i>M. tuberculosis</i> – guinea pig and mouse <i>M. tuberculosis</i> - NHP	Williams et al. (2005a) Williams et al. (2005b) Williams et al. (2005c)
2006	Small animal procedures isolator Improved mouse restraint 6-jet Collison nebuliser Aerosol sampling via impinger		<i>B. anthracis</i> – mouse <i>B. anthracis</i> – NHP	Agger et al. (2006) Martin et al. (2006) Vipond et al. (2006a) Vipond et al. (2006b)
2007	Biaera AeroMP-Henderson Large animal CL3 facility Improved NHP plethysmography Implantable telemetry for NHPs	Hatch et al. (2007)	<i>Y. pestis</i> – mouse Monkeypox - NHP	
2008	Haematology and Clinical Chemistry analyser Aerodynamic Particle Sizer (APS)	Hatch et al. (2008b) Hatch et al. (2008a)		Movahedzadeh et al. (2008)
2009		Hatch et al. (2009b) Hatch et al. (2009a)		Sharpe et al. (2009)

Key developments:	Presentations	Agent	Publications
2010	Hatch et al. (2010a) Hatch et al. (2010b)		
2011	Hatch et al. (2011a) Hatch et al. (2011b)		Clark et al. (2011)
2012	Completion of Aerosol systems GLP validation Vipond et al. (2012)		
2013	Digital Telemetry system including GLP validation CT scanning or NHPs Hatch et al. (2013b) Hatch (2013) Hatch et al. (2013c)		Hatch et al. (2013a) Vipond et al. (2013)
2014	Design of procedures of systems for aerosol challenge of rabbits at high containment		Hatch et al. (2014) Graham et al. (2014) Norville et al. (2014)
2015	Design of procedures of systems for aerosol challenge of ferrets at high containment		Tree et al. (2015) Negus et al. (2015)
2016			Marriott et al. (2016)
2017			
2018	PET-CT for NHPs		
2019			Funnell et al. (2019)
2020			

4. Academic contributions by Graham Jonathan HATCH

Articles are listed in chronological order. Contributions that are part of this submission are listed in **bold**.

CHAMBERS, M. A., WILLIAMS, A., HATCH, G., GAVIER-WIDEN, D., HALL, G., HUYGEN, K., LOWRIE, D., MARSH, P. D. & HEWINSON, R. G. 2002. Vaccination of guinea pigs with DNA encoding the mycobacterial antigen MPB83 influences pulmonary pathology but not hematogenous spread following aerogenic infection with *Mycobacterium bovis*. *Infect Immun*, 70, 2159-65.

HAMASUR, B., HAILE, M., PAWLOWSKI, A., SCHRODER, U., WILLIAMS, A., HATCH, G., HALL, G., MARSH, P., KALLENIOUS, G. & SVENSON, S. B. 2003. *Mycobacterium tuberculosis* arabinomannan-protein conjugates protect against tuberculosis. *Vaccine*, 21, 4081-93.

BACON, J., JAMES, B. W., WERNISCH, L., WILLIAMS, A., MORLEY, K. A., HATCH, G. J., MANGAN, J. A., HINDS, J., STOKER, N. G., BUTCHER, P. D. & MARSH, P. D. 2004. The influence of reduced oxygen availability on pathogenicity and gene expression in *Mycobacterium tuberculosis*. *Tuberculosis (Edinb)*, 84, 205-17.

CHAMBERS, M. A., WRIGHT, D. C., BRISKER, J., WILLIAMS, A., HATCH, G., GAVIER-WIDEN, D., HALL, G., MARSH, P. D. & GLYN HEWINSON, R. 2004. A single dose of killed *Mycobacterium bovis* BCG in a novel class of adjuvant (Novasome) protects guinea pigs from lethal tuberculosis. *Vaccine*, 22, 1063-71.

OLSEN, A. W., WILLIAMS, A., OKKELS, L. M., HATCH, G. & ANDERSEN, P. 2004. Protective effect of a tuberculosis subunit vaccine based on a fusion of antigen 85B and ESAT-6 in the aerosol guinea pig model. *Infect Immun*, 72, 6148-50.

WILLIAMS, A., GOONETILLEKE, N. P., MCSHANE, H., CLARK, S. O., HATCH, G., GILBERT, S. C. & HILL, A. V. 2005a. Boosting with poxviruses enhances *Mycobacterium bovis* BCG efficacy against tuberculosis in guinea pigs. *Infect Immun*, 73, 3814-6.

WILLIAMS, A., HATCH, G. J., CLARK, S. O., GOOCH, K. E., HATCH, K. A., HALL, G. A., HUYGEN, K., OTTENHOFF, T. H., FRANKEN, K. L., ANDERSEN, P., DOHERTY, T. M., KAUFMANN, S. H., GRODE, L., SEILER, P., MARTIN, C., GICQUEL, B., COLE, S. T., BRODIN, P., PYM, A. S., DALEMANS, W., COHEN, J., LOBET, Y., GOONETILLEKE, N., MCSHANE, H., HILL, A., PARISH, T., SMITH, D., STOKER, N. G., LOWRIE, D. B., KALLENIOUS, G., SVENSON, S., PAWLOWSKI, A., BLAKE, K. & MARSH, P. D. 2005b. Evaluation of vaccines in the EU TB Vaccine Cluster using a guinea pig aerosol infection model of tuberculosis. *Tuberculosis (Edinb)*, 85, 29-38.

- WILLIAMS, A., JAMES, B. W., BACON, J., HATCH, K. A., HATCH, G. J., HALL, G. A. & MARSH, P. D. 2005c. An assay to compare the infectivity of *Mycobacterium tuberculosis* isolates based on aerosol infection of guinea pigs and assessment of bacteriology. *Tuberculosis (Edinb)*, 85, 177-84.
- AGGER, E. M., ROSENKRANDS, I., OLSEN, A. W., HATCH, G., WILLIAMS, A., KRITSCH, C., LINGNAU, K., VON GABAIN, A., ANDERSEN, C. S., KORSHOLM, K. S. & ANDERSEN, P. 2006. Protective immunity to tuberculosis with Ag85B-ESAT-6 in a synthetic cationic adjuvant system IC31. *Vaccine*, 24, 5452-60.
- MARTIN, C., WILLIAMS, A., HERNANDEZ-PANDO, R., CARDONA, P. J., GORMLEY, E., BORDAT, Y., SOTO, C. Y., CLARK, S. O., HATCH, G. J., AGUILAR, D., AUSINA, V. & GICQUEL, B. 2006. The live *Mycobacterium tuberculosis* phoP mutant strain is more attenuated than BCG and confers protective immunity against tuberculosis in mice and guinea pigs. *Vaccine*, 24, 3408-19.
- VIPOND, J., CLARK, S. O., HATCH, G. J., VIPOND, R., MARIE AGGER, E., TREE, J. A., WILLIAMS, A. & MARSH, P. D. 2006a. Re-formulation of selected DNA vaccine candidates and their evaluation as protein vaccines using a guinea pig aerosol infection model of tuberculosis. *Tuberculosis (Edinb)*, 86, 218-24.
- VIPOND, J., VIPOND, R., ALLEN-VERCOE, E., CLARK, S. O., HATCH, G. J., GOOCH, K. E., BACON, J., HAMPSHIRE, T., SHUTTLEWORTH, H., MINTON, N. P., BLAKE, K., WILLIAMS, A. & MARSH, P. D. 2006b. Selection of novel TB vaccine candidates and their evaluation as DNA vaccines against aerosol challenge. *Vaccine*, 24, 6340-50.
- MOVAHEDZADEH, F., WILLIAMS, A., CLARK, S., HATCH, G., SMITH, D., TEN BOKUM, A., PARISH, T., BACON, J. & STOKER, N. 2008. Construction of a severely attenuated mutant of *Mycobacterium tuberculosis* for reducing risk to laboratory workers. *Tuberculosis (Edinb)*, 88, 375-81.
- SHARPE, S. A., ESCHELBACH, E., BASARABA, R. J., GLEESON, F., HALL, G. A., MCINTYRE, A., WILLIAMS, A., KRAFT, S. L., CLARK, S., GOOCH, K., HATCH, G., ORME, I. M., MARSH, P. D. & DENNIS, M. J. 2009. Determination of lesion volume by MRI and stereology in a macaque model of tuberculosis. *Tuberculosis (Edinb)*, 89, 405-16.
- CLARK, S. O., HALL, Y., KELLY, D. L., HATCH, G. J. & WILLIAMS, A. 2011. Survival of *Mycobacterium tuberculosis* during experimental aerosolization and implications for aerosol challenge models. *J Appl Microbiol*, 111, 350-9.
- HATCH, G. J., GRAHAM, V. A., BEWLEY, K. R., TREE, J. A., DENNIS, M., TAYLOR, I., FUNNELL, S. G., BATE, S. R., STEEDS, K., TIPTON, T., BEAN, T., HUDSON, L., ATKINSON, D. J., MCLUCKIE, G., CHARLWOOD, M., ROBERTS, A. D. & VIPOND,

J. 2013a. Assessment of the protective effect of Imvamune and Acam2000 vaccines against aerosolized monkeypox virus in cynomolgus macaques. *J Virol*, 87, 7805-15.

VIPOND, J., KANE, J., HATCH, G., MCCORRISON, J., NIERMAN, W. C. & LOSADA, L. 2013. Sequence determination of *Burkholderia pseudomallei* Strain NCTC 13392 colony morphology variants. *Genome Announc*, 1.

GRAHAM, V. A., HATCH, G. J., BEWLEY, K. R., STEEDS, K., LANSLEY, A., BATE, S. R. & FUNNELL, S. G. 2014. Efficacy of primate humoral passive transfer in a murine model of pneumonic plague is mouse strain-dependent. *J Immunol Res*, 2014, 807564.

HATCH, G. J., BATE, S. R., CROOK, A., JONES, N., FUNNELL, S. G. & VIPOND, J. 2014. Efficacy testing of orally administered antibiotics against an inhalational *Bacillus anthracis* infection in BALB/c mice. *Journal of Infectious Diseases and Therapy*, 02, 1000175.

NORVILLE, I. H., HATCH, G. J., BEWLEY, K. R., ATKINSON, D. J., HAMBLIN, K. A., BLANCHARD, J. D., ARMSTRONG, S. J., PITMAN, J. K., RAYNER, E., HALL, G., VIPOND, J. & ATKINS, T. P. 2014. Efficacy of liposome-encapsulated ciprofloxacin in a murine model of Q fever. *Antimicrob Agents Chemother*, 58, 5510-8.

NEGUS, D., VIPOND, J., HATCH, G. J., RAYNER, E. L. & TAYLOR, P. W. 2015. Parenteral administration of capsule depolymerase EnvD prevents lethal inhalation anthrax infection. *Antimicrob Agents Chemother*, 59, 7687-92.

TREE, J. A., HALL, G., PEARSON, G., RAYNER, E., GRAHAM, V. A., STEEDS, K., BEWLEY, K. R., HATCH, G. J., DENNIS, M., TAYLOR, I., ROBERTS, A. D., FUNNELL, S. G. & VIPOND, J. 2015. Sequence of pathogenic events in cynomolgus macaques infected with aerosolized monkeypox virus. *J Virol*, 89, 4335-44.

MARRIOTT, A. C., DENNIS, M., KANE, J. A., GOOCH, K. E., HATCH, G., SHARPE, S., PREVOSTO, C., LEEMING, G., ZEKENG, E. G., STAPLES, K. J., HALL, G., RYAN, K. A., BATE, S., MOYO, N., WHITTAKER, C. J., HALLIS, B., SILMAN, N. J., LALVANI, A., WILKINSON, T. M., HISCOX, J. A., STEWART, J. P. & CARROLL, M. W. 2016. Influenza A virus challenge models in cynomolgus macaques using the authentic inhaled aerosol and intra-nasal routes of infection. *PLoS One*, 11, e0157887.

FUNNELL, S. G. P., TREE, J. A., HATCH, G. J., BATE, S. R., HALL, G., PEARSON, G., RAYNER, E. L., ROBERTS, A. D. G. & VIPOND, J. 2019. Dose-dependant acute or subacute disease caused by *Burkholderia pseudomallei* strain NCTC 13392 in a BALB/c aerosol model of infection. *J Appl Microbiol*, 127, 1224-1235.

5. Metrics, contributions and original versions of the presented body of work

Metrics, contributions and original versions of the publications submitted in the support of this PhD by publication are listed in chronological order.

Original article

WILLIAMS, A., HATCH, G. J., CLARK, S. O., GOOCH, K. E., HATCH, K. A., HALL, G. A., HUYGEN, K., OTTENHOFF, T. H., FRANKEN, K. L., ANDERSEN, P., DOHERTY, T. M., KAUFMANN, S. H., GRODE, L., SEILER, P., MARTIN, C., GICQUEL, B., COLE, S. T., BRODIN, P., PYM, A. S., DALEMANS, W., COHEN, J., LOBET, Y., GOONETILLEKE, N., MCSHANE, H., HILL, A., PARISH, T., SMITH, D., STOKER, N. G., LOWRIE, D. B., KALLENIOUS, G., SVENSON, S., PAWLOWSKI, A., BLAKE, K. & MARSH, P. D. 2005b. Evaluation of vaccines in the EU TB Vaccine Cluster using a guinea pig aerosol infection model of tuberculosis. *Tuberculosis (Edinb)*, 85, 29-38.

Impact factor: 1.960

Contributions by HATCH, G. J.

Home Office – Personal Licence and Deputy Project Licence holder

Animal procedures – Aerosol challenge, necropsy

Study management – Liaison and co-ordination with sponsors and in vivo team, scheduling, reporting

Microbiological experimental work and data analysis

Manuscript review

Citation metrics

Google Scholar: 182 citations



Evaluation of vaccines in the EU TB Vaccine Cluster using a guinea pig aerosol infection model of tuberculosis [☆]

Ann Williams^{a,*}, Graham J. Hatch^a, Simon O. Clark^a, Karen E. Gooch^a, Kim A. Hatch^a, Graham A. Hall^a, Kris Huygen^b, Tom H.M. Ottenhoff^c, Kees L.M.C. Franken^c, Peter Andersen^d, T. Mark Doherty^d, Stefan H.E. Kaufmann^e, Leander Grode^e, Peter Seiler^e, Carlos Martin^f, Brigitte Gicquel^g, Stewart T. Cole^h, Priscille Brodin^h, Alexander S. Pymⁱ, Wilfried Dalemans^j, Joe Cohen^j, Yves Lobet^j, Nilu Goonetilleke^k, Helen McShane^k, Adrian Hill^k, Tanya Parish^l, Debbie Smith^m, Neil G. Stokerⁿ, Douglas B. Lowrie^o, Gunilla Källenius^p, Stefan Svenson^p, Andrzej Pawlowski^p, Karen Blake^a, Philip D. Marsh^a

^aHealth Protection Agency, Porton Down, Salisbury SP4 0JG, UK

^bMycobacterial Immunology, Pasteur Institute of Brussels, 642 Engelandstraat, B1180 Brussels, Belgium

^cDepartment of Immunohematology and Blood Transfusion, Leiden University Medical Center, Albinusdreef 2, 2333 ZA Leiden, The Netherlands

^dDepartment for Infectious Disease Immunology, Statens Serum Institute, Artillerivej 5, Copenhagen 2300s, Denmark

^eDepartment of Immunology, Schumannstrasse 21/22, D-10117 Berlin, Germany

^fDept. Microbiología, Grupo de Genética de Micobacterias, Medicina Preventiva y Salud Pública Facultad de Medicina, Universidad de Zaragoza, C/Domingo Miral sn, 50009 Zaragoza, Spain

^gUnité de Génétique Mycobactérienne, Institut Pasteur 25-28, rue du Dr. Roux, 75724 Paris Cedex 15, France

^hUnité de Génétique Moléculaire Bactérienne, Institut Pasteur 25-28, rue du Dr. Roux, 75724 Paris Cedex 15, France

ⁱLiverpool School of Tropical Medicine, Pembroke Place, Liverpool L3 5QA, UK

^jGlaxoSmithKline Biologicals, 89, rue de l'Institut, B-1330 Rixensart, Belgium

^kNuffield Department of Clinical Medicine, Oxford University, John Radcliffe Hospital, Oxford, OX3 9DU, UK

^lCentre for Infectious Disease, Barts and the London, London, UK

^mImmunology Unit, Department of Infectious and Tropical Diseases, LSHTM, Keppel Street, London WC1E 7HT, UK

[☆] This work was funded by the European Community (QKL2-CT1999-01093) and the Department of Health, UK.

*Corresponding author. Tel.: +44 1980 612813; fax: +44 1980 612731.

E-mail addresses: ann.williams@camr.org.uk, ann.rawkins@hpa.org.uk (A. Williams).

^aDepartment of Pathology and Infectious Diseases, Royal Veterinary College, Royal College Street, London NW1 0TU, UK

^bNational Institute for Medical Research, The Ridgeway, Mill Hill, London NW7 1AA, UK

^cSwedish Institute for Infectious Disease Control and the Karolinska Institutet, S-171 82 Solna, Sweden

Accepted 17 September 2004

KEYWORDS

Vaccine;
Tuberculosis;
Guinea pig;
Aerosol

Summary The TB Vaccine Cluster project funded by the EU Fifth Framework programme aims to provide novel vaccines against tuberculosis that are suitable for evaluation in humans. This paper describes the studies of the protective efficacy of vaccines in a guinea pig aerosol-infection model of primary tuberculosis. The objective was to conduct comparative evaluations of vaccines that had previously demonstrated efficacy in other animal models. Groups of 6 guinea pigs were immunized with vaccines provided by the relevant EU Vaccine Cluster partners. Survival over 17 or 26 weeks was used as the principal measure of vaccine efficacy following aerosol challenge with H37Rv. Counts of mycobacteria in lungs and spleens, and histopathological changes in the lungs, were also used to provide evidence of protection.

A total of 24 vaccines were evaluated in 4 experiments each of a different design. A heterologous prime-boost strategy of DNA and MVA, each expressing Ag85A and a fusion protein of ESAT-6 and Ag85B in adjuvant, protected the guinea pigs to the same extent as BCG. Genetically modified BCG vaccines and boosted BCG strategies also protected guinea pigs to the same extent as BCG but not statistically significantly better. A relatively high aerosol-challenge dose and evaluation over a protracted time post-challenge allowed superior protection over BCG to be demonstrated by BCG boosted with MVA and fowl pox vectors expressing Ag85A.

© 2004 Elsevier Ltd. All rights reserved.

Introduction

Tuberculosis (TB) kills in excess of 2 million people every year and the global epidemic is increasing. The current and only TB vaccine, *Mycobacterium bovis* bacille Calmette–Guérin (BCG), has been applied world-wide for several decades but possesses many drawbacks,¹ including variable efficacy in humans, an inability to protect against re-activation or re-infection, and pathogenicity in the immunocompromised host. Thus, there have been concerted efforts towards the discovery and development of a vaccine to replace BCG. Publication of the complete *M. tuberculosis* genome² and developments in both laboratory and 'in silico' methods of screening large numbers of proteins for immunogenicity has now accelerated the process of antigen discovery. In addition to the growing number of potential antigens, novel adjuvants and delivery systems are continually being developed.

The TB Vaccine Cluster project funded by the European Union Fifth Framework programme aimed to develop novel vaccines against tuberculosis that would be superior to BCG and suitable for evaluation in humans. This included a step-wise evalua-

tion of new candidate vaccines in mice, guinea pigs and non-human primates. Mouse studies enabled the initial selection of promising candidates by measuring the immunogenicity and protection against virulent challenge, and these candidates were then evaluated using the more discriminative aerosol-infection guinea pig model. Criteria for the selection of candidates for evaluation in the guinea pig model included evidence of immunogenicity and protective efficacy equivalent to or better than BCG in mouse and in some cases guinea pig models. The programme provided an opportunity to directly compare, within a single experiment, a number of vaccine candidates which had previously been demonstrated to be efficacious when evaluated separately. Here, we report the results of these comparative studies.

Materials and methods

Vaccines

The vaccines evaluated in the studies are listed in Table 1. The source of each vaccine is given and,

Table 1 Details, and sources of vaccines evaluated in the EU studies.

Vaccine	Short name	Source and references
Experiment 1		
Heterologous prime-boost of DNA and MVA both expressing Ag85A	DNA prime MVA/Ag85A boost	Prof. A.V.S. Hill, ¹⁴ Oxford, UK
Ag85B/ESAT-6 fusion protein (Hybrid 1) in DDA/MPL [®]	Hybrid 1 in DDA/MPL [®]	Prof. P. Andersen, SSI, Copenhagen, Denmark ⁷
Hybrid 1 protein in ASO2 adjuvant	Hybrid 1 in ASO2	Prof. P. Andersen, GSK (Rixensart, Belgium) for adjuvant
Plasmid DNA-encoding Hsp65 (CMV4.65)	Hsp65 DNA	Prof. D. Lowrie, ¹⁵ NIMR, London, UK
Arabinomannan (AM)—Mycobacterial protein Ag85B conjugate in L3 adjuvant	AM–Ag85B conjugate in L3	Prof. S.B. Svenson, SMI, Stockholm and SLU, Uppsala, Sweden ^{16–18}
Experiment 2		
Ag85A recombinant protein in ASO2 adjuvant	rAg85A protein in ASO2	Prof THM Ottenhof, ¹⁹ Leiden, The Netherlands; GSK for adjuvant
Fowlpox-Ag85A and MVA-Ag85A prime-boost	Fowlpox/Ag85A–MVA/Ag85A	Prof. A.V.S. Hill
Ag85A DNA in vaxfectin	Ag85A DNA in vaxfectin	Dr. K. Huygen, ²⁰ Brussels, Belgium
Ag85A DNA in vaxfectin with rAg85A protein in ASO2 boost	Ag85A DNA in vaxfectin, rAg85A in ASO2 boost	Dr. K. Huygen
Hybrid 1 protein in DDA/MPL [®] +trehalose dibehenate (TDB)	Hybrid 1 protein in DDA/MPL [®] /TDB	Prof. P. Andersen
Hybrid 1 protein in DDA/MPL [®] , sub-cutaneous prime, boosted orally with Hybrid 1 in TDB	Hybrid 1 protein, oral boost	Prof. P. Andersen
Hybrid 1–AM conjugate in L3	Hybrid 1–AM in L3	Prof. S.B. Svenson and Prof. P. Andersen
Experiment 3		
<i>M. tuberculosis trpD</i> ⁻ mutant	<i>M. tuberculosis trpD</i> ⁻ mutant	Prof. N.G. Stoker, ^{21,22} London, UK
rBCG-expressing listeriolysin (Hly)	rBCG-Hly	Prof. S.H.E. Kaufmann, MPIIB, Berlin, Germany ²³
BCG Pasteur::RD1-2F9	rBCG-RD1	Prof. S. Cole, ⁸ IP, Paris, France
BCG Danish 1331, prime+boost with hybrid 1 in DDA/MPL [®]	BCG+hybrid 1 in DDA/MPL [®]	Prof. P. Andersen
BCG Danish 1331 prime+boost with MVA expressing Ag85A	BCG+MVA/Ag85A	Prof. A.V.S. Hill
BCG Danish 1331+BCG Danish 1331	BCG+BCG	SSI, Copenhagen, Denmark
Experiment 4		
<i>M. tuberculosis phoP</i> ⁻ mutant	<i>M. tuberculosis phoP</i> ⁻ mutant	Prof. B. Gicquel Paris, France; Prof. C Martin, Zaragoza, Spain ^{9,24}
PstS3–Ag85A DNA prime–BCG Danish 1331 boost	PstS3–Ag85A DNA–BCG	Dr. K. Huygen
<i>M. microti</i> OV254::RD1-2F9	<i>M. microti</i> -RD1	Prof. S. Cole ¹⁰
BCG Danish 1331+MVA/85A+FP/85A	BCG+MVA/85A+FP/85A	Prof. A.V.S. Hill ¹¹
r Δ <i>ureC</i> BCG expressing Hly	r <i>ureC</i> BCG expressing Hly	Prof. S.H.E. Kaufmann
AM-Tetanus toxoid, conjugate in L3 adjuvant	Tetanus toxoid-AM+L3	Prof. S.B. Svenson

where relevant, supporting background information is referenced. Four experiments were conducted and the candidates are listed in experiment groups. The grouping of the candidates in each experiment reflects the aim to compare similar types of vaccine e.g. sub-units or live attenuated, although it was not always possible to design the experiment where one type of vaccine was tested exclusively. A selection process was established in which vaccines had to satisfy criteria that would show a potential for the vaccine to be effective against challenge with virulent *M. tuberculosis*. These criteria included immunogenicity and/or protection in mice or guinea pigs.

The candidates in Experiments 1 and 2 were selected in order to compare sub-unit vaccines in different delivery systems and were predominantly based on two antigens, antigen 85A (Ag85A) and a fusion protein between antigen 85B and ESAT-6 (referred to throughout as 'Hybrid 1'). A number of different delivery systems were used, including recombinant or native protein in various adjuvants, recombinant pox viruses and plasmid DNA. Combinations of delivery systems and routes of administration of the antigen were also tested.

The candidates in Experiments 3 and 4 were predominantly live attenuated vaccines. This included targeted mutants of *M. tuberculosis* and genetic modifications of BCG; for these, an additional requirement for selection was the demonstration of attenuation in immunocompetent and/or immunocompromised mice. Also included in these studies were vaccine candidates given in addition to conventional BCG vaccination.

Immunization

The immunization schedules for each candidate were specified by the provider of the vaccines and are briefly described in Table 2. The vaccines were supplied as prepared formulations wherever possible and, for those vaccines that required formulation immediately prior to inoculation, detailed instructions were provided and followed.

Female Dunkin-Hartley guinea pigs (weighing between 250 and 300 g, and free of infection) were obtained from a commercial supplier (David Hall, Burton-on-Trent, UK). Groups of 6 guinea pigs were used to evaluate the efficacy of each candidate vaccine compared with BCG and saline controls. Individual animals were identified using sub-cutaneously implanted microchips (PLEXX BV, The Netherlands). Animals were vaccinated as appropriate and then allowed to rest for at least 6 weeks prior to aerosol challenge with *M. tuberculosis*.

Rationale for challenge doses

In Experiment 1, the intention was to infect the animals with a relatively low dose (10–50 cfu) aerosol challenge since this is within the range of doses conventionally used in guinea pig models of tuberculosis. In Experiments 2–4 the challenge dose was increased with the intention to make the model more stringent and thus discriminate vaccine candidates that had already been proven to be efficacious in previous studies.

Aerosol challenge with *M. tuberculosis*

Aerosol challenge was performed using a contained Henderson apparatus as previously described.^{3,4} Fine particle aerosols of *M. tuberculosis* H37Rv, with a mean diameter of 2 µm, (diameter range, 0.5–7 µm)⁵ were generated using a Collison nebulizer and delivered directly to the animal snout. The aerosol was generated from a saline suspension containing 5×10^6 organisms per ml in order to obtain an estimated retained, inhaled dose of approximately 10–50 colony forming units (cfu)/lung, (Experiment 1) or from a suspension containing 5×10^7 or 1×10^8 cfu/ml in order to deliver 500 or 1000 cfu to the lungs (Experiments 2–4). The Henderson apparatus allows controlled delivery of aerosols to the animals and the reproducibility of the system and relationship between inhaled cfu and the concentration of organisms in the nebulizer have been described previously.^{3,6}

Measurement of protective efficacy

Animals were monitored regularly for weight changes as indicators of disease, and were killed humanely at 17 weeks (Experiments 1–3) or 26 weeks (Experiment 4) post-challenge or at the humane endpoint (20% loss of maximal body weight). Protection was primarily assessed by comparing the overall survival time of the vaccinated groups of animals with the control groups (BCG and un-vaccinated) over the period of the experiment. Animals killed at the humane endpoint were considered to have died due to infection for the purposes of analysing survival. The vaccine was considered to have offered protection if the survival time of the group was equivalent to or significantly longer than that of the BCG control group, and was significantly longer than the saline control group.

The extent of pulmonary disease and disseminated infection as measured by total lung consolidation and by comparison of lung and spleen

Table 2 Vaccination schedules for all the experiments.

Vaccine	Vaccination schedule	
	Quantity, volume, route and number of inoculations	Vaccine-challenge interval* (weeks)
Experiment 1		
DNA prime MVA/Ag85A boost	2 × 200 µg DNA i.m., 2 × 10 ⁷ p.f.u. MVA, i.d., 2 weeks apart	6
Hybrid 1 in DDA/MPL [®]	3 × 20 µg, s.c. 3 weeks apart	6
Hybrid 1 in ASO2	3 × 20 µg, s.c. 3 weeks apart	6
Hsp65 DNA	3 × 100 µg, i.m. 3 weeks apart	6
AM-Ag85B conjugate in L3	15 µg carbohydrate, 10 µg protein per dose, given s.c. once then i.n. 3 weeks later.	6
Experiment 2		
rAg85A protein in ASO2	3 × 20 µg, s.c., 3 weeks apart	6
Fowlpox/Ag85A-MVA/Ag85A	FP, followed by MVA, FP, MVA, all given i.d. at 10 ⁷ p.f.u., 2 weeks apart	6
Ag85A DNA in vaxfectin	3 × 100 µg DNA i.m., 3 weeks apart	6
Ag85A DNA in vaxfectin, rAg85A in ASO2 boost	2 × 100 µg DNA, i.m., 1 × 20 µg s.c., protein, 3 weeks apart	6
Hybrid 1 protein in DDA/MPL [®] / TDB	3 × 20 µg s.c., 3 weeks apart	6
Hybrid 1 protein, oral boost	1 × 20 µg s.c., 2 × 20 µg oral, 3 weeks apart	6
Hybrid 1-AM in L3	15 µg carbohydrate, 10 µg protein per dose given s.c. once and x2 i.n., 3 weeks apart	6
Experiment 3		
<i>M. tuberculosis</i> trpD ⁻ mutant	5 × 10 ⁴ cfu s.c. 12 weeks pre-challenge, animals housed at ACDP containment level 3.	12
rBCG-Hly	5 × 10 ⁴ cfu s.c. 12 weeks pre-challenge	12
rBCG-RD1 region	5 × 10 ⁴ cfu s.c. 12 weeks pre-challenge	12
BCG+Hybrid 1 in DDA/MPL [®]	5 × 10 ⁴ cfu s.c. BCG (1331), 20 µg protein 4 weeks later	8
BCG+MVA/Ag85A	5 × 10 ⁴ cfu s.c. BCG (1331), 10 ⁷ p.f.u. MVA/85A 4 weeks later	8
BCG+BCG	5 × 10 ⁴ cfu s.c. BCG (1331) x2, 4 weeks apart	8
Experiment 4		
PstS3-Ag85A DNA-BCG	2 × 100 µg DNA i.m., 2 weeks apart, 5 × 10 ⁴ cfu s.c. BCG (1331) 4 weeks later.	10
<i>M. microti</i> -RD1	5 × 10 ⁴ cfu s.c. 10 weeks pre-challenge, animals housed at ACDP containment level 3.	10
BCG+MVA/85A+FP/85A	5 × 10 ⁴ cfu s.c. BCG (1331), 10 ⁷ p.f.u. MVA/85A 4 weeks later, 10 ⁷ p.f.u. FP9/85A, 2 weeks later.	6
rΔ ureC BCG expressing Hly	5 × 10 ⁴ cfu s.c. 10 weeks pre-challenge	10
Tetanus toxoid-AM+L3	1 × 100 µl s.c., 2 × 50 µl i.n., 3 weeks apart	8

s.c. = sub-cutaneous, i.n. = intranasal, p.f.u. = plaque forming units, i.m. = intramuscular, i.d. = intradermal.
* = interval between administration of final inoculation of vaccine and aerosol challenge.

cfu were also used to compare the vaccinated animals with the control groups. A significant reduction in any of these parameters in the vaccinated animals when compared with the control groups was considered as a protective effect of the vaccine.

Agar infusion of lungs

To improve the accuracy of image analysis techniques to measure consolidation, a controlled inflation of lungs was performed. An agar infusion technique was used in order to maintain the ability

to culture lung lobes for viable *M. tuberculosis*. Guinea pigs were killed by intraperitoneal injection of pentobarbitone (Euthatal) and sterile molten agar (2%) was injected into the lungs via an incision in the trachea (exposed in the neck) whilst the thorax was still intact. The trachea was then clamped and the lungs were dissected once the agar had set. Three lung lobes (right caudal, right middle and accessory lobes) were removed and fixed in 10% neutral-buffered formaldehyde. These were cut at the widest organ diameter, ensuring each lobe was sectioned at the same position for every animal, embedded in paraffin wax blocks and 5 µm sections cut on to glass slides. Each lung section was stained with Haematoxylin & Eosin (H&E) for objective measurement of consolidation by image analysis. The remaining lung lobes were aseptically removed for bacteriology (cfu counts).

Image analysis of lung sections

An image of each H&E-stained section of agar-infused lung was captured using Image Analysis equipment (Zeiss Axio Cam digital camera connected to a Zoom Micro-NIKKOR 55 mm 1:2.8 photo lens using a MicroCam C-mount converter 0.65 × to Nikon F-bayonet) and Axio-Vision 2.0.5 software and archived using the Image Access 3.10 software. Analysis of the images was undertaken using the Zeiss KS300 3.0 software. A software programme was written to assess the area of consolidation of each lobe objectively. This measured the area of each lung lobe and the area of consolidation, and thus calculated the percentage area of consolidation. Mean percentages of consolidation per animal (3 lobes per animal) and per vaccine group were determined.

Bacterial counts in organs

Tissues were homogenized in 10 ml (lungs) or 5 ml (spleens) of sterile distilled water using a rotating blade macerator system. Viable counts were performed on the macerate by preparing decimal dilutions in sterile deionized water and plating 100 µl aliquots onto Middlebrook 7H11+OADC agar. Plates were incubated at 37 °C for 3 weeks before counting the number of *M. tuberculosis* colonies (cfu).

Statistical analyses

Statistical analyses were performed using Minitab (version 13.32). The ability of vaccines to prolong

survival was compared with controls using Kaplan–Meier survival estimates with right censoring only. A Log Rank distribution analysis was used to identify statistical significance between control groups and individual test vaccine groups. The cfu and consolidation data were analysed by ANOVA, using Fishers pairwise comparisons to compare mean values of the vaccine groups with either the saline or BCG control groups.

Results

A summary of the results of all the experiments is shown in Table 3.

Experiment 1

A Kaplan–Meier plot of the survival data for Experiment 1 is shown in Fig. 1. Over the 17 week period of the study, several of the animals in the saline control and test vaccine groups became ill and were killed at the humane end-point. Two of the vaccine candidates, the DNA/MVA-Ag85A prime-boost candidate and Hybrid 1 in DDA/MPL³⁶⁷ prolonged survival significantly ($p = 0.03$ and 0.025 , respectively) longer than the saline control and equivalent to the BCG control (Fig. 1). None of the vaccines showed improved survival over the BCG control.

All of the vaccines reduced numbers of viable *M. tuberculosis* (cfu) in the spleens but no significant protection was observed in the lungs (Table 3). The group of animals vaccinated with the DNA/MVA-Ag85A prime-boost candidate also had a significantly lower mean percentage lung consolidation than the saline controls (Table 3).

Experiment 2

The challenge dose in Experiments 2 was approximately 100-fold higher than Experiment 1 and as a result, the time taken for severe disease to develop in the unvaccinated controls was reduced and by the end of the 17 week period of the experiment, none of the animals in this group had survived. In contrast, all of the BCG-vaccinated animals survived to the end of the experiment. However, none of the vaccines tested in Experiment 2 showed a statistically significant improved survival over the saline control although Hybrid 1 (s.c. prime, oral boost) significantly reduced CFU in spleens (Table 3).

Table 3 Summary of the results of all the vaccine evaluations indicating whether each candidate demonstrated a statistically significant effect compared with control groups.

Vaccine	Significant protection as demonstrated by:			
	Prolonged survival	Reduced cfu in lungs	Reduced cfu in spleens	% lung consolidation
Experiment 1				
DNA prime MVA/Ag85A boost	✓	x	✓	✓
Hybrid 1 in DDA/MPL [®]	✓	x	✓	x
Hybrid 1 in ASO2 adjuvant	x	x	✓	x
Hsp65 DNA	x	x	✓	x
AM-Ag85B conjugate in L3	x	x	✓	x
BCG control	✓	✓	✓	✓
Experiment 2				
rAg85A protein in ASO2	x	x	x	NT
Fowlpox/Ag85A-MVA/Ag85A prime-boost	x	x	x	NT
Ag85A DNA in vaxfectin	x	x	x	NT
Ag85A DNA in vaxfectin boosted with rAg85A protein in S2	x	x	x	NT
Hybrid 1 protein in DDA/MPL [®]	x	x	x	NT
Hybrid 1 protein, sub-cutaneous prime, oral boost	x	x	✓	NT
Hybrid 1-arabinomannan conjugate in L3	x	x	x	NT
BCG control	✓	✓	✓	NT
Experiment 3				
<i>M. tuberculosis</i> <i>trpD</i> ⁻ mutant	x	x	x	NT
rBCG-Hly	✓	✓	✓	✓
rBCG-RD1 region	✓	✓	✓	✓
BCG+Hybrid 1 in DDA/MPL [®]	✓	✓	✓	✓
BCG+MVA/Ag85A	✓	✓	✓	✓
BCG+BCG	✓	✓	✓	✓
BCG control	✓	✓	✓	✓
Experiment 4				
PstS3-Ag85ADNA-BCG	✓	✓	✓	✓
<i>M. microti</i> -RD1 region	✓	✓	✓	✓
BCG+MVA/85A+FP/85A	✓	✓	✓	✓
rΔ <i>ureC</i> BCG expressing Hly	✓	✓	✓	✓
Tetanus toxoid-arabinomannan+L3	x	x	x	x
BCG control	✓	✓	✓	✓

✓ = significantly better protection than the saline control ($p = <0.05$).
 ✓✓ = significantly better protection than the BCG control ($p = <0.05$).
 x = no protection.
 NT = not tested.

Experiments 3 and 4

Animals in Experiment 3 were challenged with approximately 1000 cfu *M. tuberculosis* by aerosol and the resulting disease in the unvaccinated guinea pigs was similar to that observed in Experiment 2 i.e. there were no survivors at the end of the 17 week post-challenge period. The vaccines based on BCG (rBCG-Hly, rBCG-RD1,⁸

BCG+Hybrid1, BCG+MVA/85A, BCG+BCG) all prolonged survival significantly longer than the saline control but over the 17 weeks post-challenge period, it was not possible to discriminate between these vaccines and the BCG control. Similarly, the vaccines that prolonged survival also significantly reduced both cfus in organs and lung pathology but did not show a statistically significant improvement over the BCG control group (Table 3).

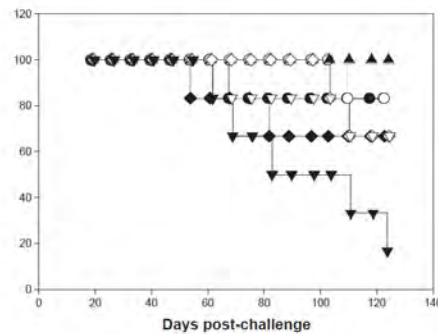


Figure 1 Survival of vaccinated guinea pigs following aerosol infection with *M. tuberculosis*. Experiment 1, guinea pigs given low-dose aerosol challenge with H37Rv and monitored for 124 days. Vaccine groups: ● DNA+MVA/85A, ○ Hyb1 in DDA/MPL[®], △ Hyb1 in ASO2, □ DNA-Hsp65, Protein-AM conjugate, ▲ BCG control, ▼ Saline control.

The vaccines in Experiment 4 were mostly live attenuated and the study design was changed compared with Experiment 3 with an aim to identify any vaccines with improved efficacy over BCG. Vaccinated animals were challenged with a high aerosol dose (approx. 500 cfu) and were followed for up to 26 weeks post-challenge. Over this period, all of the animals in the unvaccinated control group succumbed to infection and between weeks 17 and 26 post-challenge, four of the animals in the BCG control group were killed at the humane end-point. The results of the group vaccinated with the *M. tuberculosis* phoP mutant will be reported elsewhere.⁹ Three of the vaccines, Pst53-Ag85A DNA+BCG, *M. microti*-RD1¹⁰ and *rΔ ureC* BCG-Hly prolonged survival compared with the unvaccinated controls but the statistical analysis of the survival data did not indicate a significant improvement over the BCG control. In the group vaccinated with BCG boosted by MVA and Fowlpox vectors expressing Ag85A¹¹ there were no deaths over the experiment period. Analysis of survival times showed that this group had significantly prolonged survival compared with the BCG controls ($p = 0.018$).

Discussion

The aim of these studies was to screen a number of potential TB candidate vaccines in a stringent guinea pig aerosol infection model of primary

tuberculosis. A total of 24 candidates were tested and several of these demonstrated a protective efficacy equivalent to the current BCG vaccine, which was included in all experiments as a positive control. The ability of the test vaccine to prevent severe illness was used as the primary indicator of protective efficacy and this was measured by an analysis of survival over the period of the experiment. Two sub-unit vaccines, a heterologous prime-boost strategy of DNA and MVA each expressing Ag85A and a fusion protein consisting of ESAT-6 and Ag85B (Hybrid 1),⁷ protected the guinea pigs to the same extent as BCG by prolonging survival following low-dose aerosol challenge as compared with the unvaccinated controls. Against a high-dose aerosol challenge, eight vaccine candidates gave a level of protection equivalent to the BCG control. These were either genetically modified non-pathogenic mycobacteria, or were prime-boost strategies involving vaccines that were given in addition to conventional BCG (Danish 1331). The genetically modified strains were: rBCG expressing listeriolysin, BCG Pasteur::RD1-2F9,⁸ *M. microti* OV254::RD1-2F9¹⁰ and *rΔ ureC* BCG expressing listeriolysin. The prime-boost strategies were: BCG followed by Hybrid 1 in DDA/MPL[®], BCG followed by MVA expressing Ag85A, BCG followed by BCG and DNA encoding both Pst5-3 and Ag85A followed by BCG. All of the candidates that demonstrated a protective efficacy equivalent to the BCG control would be considered as having the potential to be taken forward for further improvement and evaluation in other test systems such as non-human primates or animal models of post-primary disease. Other factors such as previous data obtained in different animal models will influence the decision to progress vaccines into potentially expensive further trials and it will also be important to establish that key experimental results in animal models are reproducible.

Ideally, the outcome of a programme of work to identify a vaccine that could replace or improve upon BCG would be a demonstration in animal models that the new vaccine candidate had significantly better protective efficacy than BCG. In the guinea pig model this has been demonstrated by an ability of the candidate vaccine to prevent replication of *M. tuberculosis* in the lungs to a significantly greater extent than the BCG control.¹² BCG vaccination will protect guinea pigs against low-dose challenge with *M. tuberculosis* such that they survive for one or two years post challenge¹³ and there are thus practical difficulties in demonstrating that a candidate vaccine can significantly improve upon this. In this study we employed a strategy of using a high-dose challenge in order to

make the test system more stringent. Over a period of 17 weeks (Experiment 3), it was not possible to identify differences in the test vaccines versus BCG but when the period of study was extended to 26 weeks, the BCG-vaccinated animals had begun to be overwhelmed by the higher challenge dose. In contrast, animals vaccinated with BCG boosted with MVA and fowlpox vectors expressing Ag85A¹¹ significantly prolonged survival of the animals compared with the BCG control.

The high challenge doses used in these experiments resulted in a disease model that was much more severe than that conventionally used to evaluate the protective efficacy of TB vaccines. However, since the aim of these studies was to discriminate vaccine candidates which had already been proven to be effective in other test models, it was important that the system should be stringent. It was apparent from these studies that the high challenge dose is best applied to vaccines that are based on or are similar to BCG (i.e. live attenuated). For some of the vaccines, the system was probably too stringent and a failure to offer protection equivalent to BCG in the high-dose model should not indicate that the vaccine is ineffective but rather that it should be re-evaluated in a low-dose challenge system over a prolonged post-challenge period.

The 4 experiments reported here were each of a different design, with challenge doses and length of post-challenge period being the main variables. Thus the protective efficacy of a vaccine candidate can be compared only with the other vaccines in that experiment and in relation to the positive and negative controls. The changes to the experimental design were influenced strongly by the main objective of these studies which was to discriminate between the vaccine candidates and to identify the most promising of all those tested within a programme that was limited by both time and budget. Thus, some of the vaccines may have performed better (or worse) when tested in a different study protocol. As an example, it is possible that some of the vaccines in Experiment 3 could have demonstrated a superior protective efficacy to BCG if the post-challenge period had been extended from 17 to 26 weeks. It is important that the design of future TB vaccine evaluations in guinea pigs takes into account the potential for variability in vaccine potency which can be caused by differences in experimental schedules. It is also necessary to ensure that there is comparability with previous studies conducted within the EC programme and with similar vaccine evaluation programmes conducted elsewhere.

Enumeration of viable *M. tuberculosis* (cfu) in the lungs and spleens of all animals in these studies revealed that the cfu in animals that had been killed at the humane end-point were significantly higher than cfu in animals that survived to the end of the experiment. This is perhaps not surprising but the practical outcome was a large spread in the cfu values within vaccine groups comprised of both killed and surviving animals. Thus, because in these studies survival was the principal read out of vaccine efficacy, cfu in organs was not always an informative measure of vaccine efficacy.

In conclusion, the vaccine evaluation studies reported here represent an objective evaluation of a number of TB vaccine candidates which allowed the identification of several promising vaccine strategies to take forward to future development and evaluation and thus progression to human clinical trials. An EC Sixth Framework-funded programme of work which began in 2004 will provide a means of such progression, and the evaluations in guinea pigs will remain in this programme as an important stage in the pre-clinical development of potential vaccines.

Acknowledgements

This work was funded by the European Community (QLK2-CT1999-01093) and the Department of Health (UK). The views expressed in this publication are those of the authors and not necessarily those of the funding bodies. All the providers of the vaccines, as listed in Table 1 are gratefully acknowledged, as are members of the TB Cluster Steering Committee, namely Prof. Brigitte Gicquel, Prof. Douglas Young, Prof. Stefan H.E. Kaufmann, Prof. THM Ottenhoff, Dr. Jelle Thole, Dr. Carlos Martin, Dr. Jean-Jacques Fournie and Prof. Peter Andersen. The staff in the Biological Investigations Group at HPA Porton Down are sincerely thanked for their technical support.

References

1. Andersen P. TB vaccines: progress and problems. *Trends Immunol* 2001;**22**:160–8.
2. Cole ST, Brosch R, Parkhill J, Garnier T, Churcher C, Harris D, Gordon SV, Eiglmeier K, Gas S, Barry CE, 3rd., Tekaia F, et al. Deciphering the biology of *Mycobacterium tuberculosis* from the complete genome sequence. *Nature* 1998;**393**:537–44.
3. Williams A, Davies A, Marsh PD, Chambers MA, Hewinson RG. Comparison of the protective efficacy of Bacille Calmette–Guerin vaccination against aerosol challenge with *Mycobacterium tuberculosis* and *Mycobacterium bovis*. *Clin Infect Dis* 2000;**30**(Suppl 3):S299–301.

4. Chambers MA, Williams A, Gavier-Widen D, Whelan A, Hall G, Marsh PD, Bloom BR, Jacobs WR, Hewinson RG. Identification of a *Mycobacterium bovis* BCG auxotrophic mutant that protects guinea pigs against *M. bovis* and hematogenous spread of *Mycobacterium tuberculosis* without sensitization to tuberculin. *Infect Immun* 2000;68:7094-9.
5. Lever MS, Williams A, Bennett AM. Survival of mycobacterial species in aerosols generated from artificial saliva. *Lett Appl Microbiol* 2000;31:238-41.
6. Chambers M, Williams A, Gavier-Widen D, Whelan A, Hughes C, Hall G, Lever M, Marsh P, Hewinson R. A guinea pig model of low-dose *Mycobacterium bovis* aerogenic infection. *Vet Microbiol* 2001;80:213-26.
7. Olsen AW, Williams A, Okkels LM, Hatch GJ, Andersen P. Evaluation of a tuberculosis subunit vaccine based on a fusion of Ag85B and ESAT-6 in the aerosol guinea pig model. *Infect Immun* 2004, in press.
8. Pym AS, Brodin P, Majlessi L, Brosch R, Demangel C, Williams A, Griffiths KE, Marchal G, Leclerc C, Cole ST. Recombinant BCG exporting ESAT-6 confers enhanced protection against tuberculosis. *Nat Med* 2003;9:533-9.
9. Martin C, Williams A, Hernandez-Pando R, Cardona PJ, Gormley E, Bordat Y, Soto CY, Clark SO, Hatch GJ, Aguilar D, Ausina V, Gicquel B. The highly attenuated *Mycobacterium tuberculosis* phoP confers superior protection against tuberculosis when compared to *Mycobacterium bovis* BCG. *Nat Med*, submitted for publication.
10. Brodin P, Majlessi L, Brosch R, Smith D, Bancroft G, Clark S, Williams A, Leclerc C, Cole ST. Enhanced protection against extrapulmonary tuberculosis with an attenuated live *Mycobacterium microti* vaccine inducing T-cell immunity against RD1 antigens. *J Infect Dis* 2004;190:115-22.
11. Williams A, Goonetilleke NP, McShane H, Clark SO, Hatch GJ, Gilbert SC, Hill AVS. Boosting with poxviruses enhances BCG efficacy against tuberculosis in guinea-pigs. *Infect Immun*, submitted for publication.
12. Horwitz MA, Harth G, Dillon BJ, Mastesa-Galic S. Recombinant bacillus calmette-guérin (BCG) vaccines expressing the *Mycobacterium tuberculosis* 30-kDa major secretory protein induce greater protective immunity against tuberculosis than conventional BCG vaccines in a highly susceptible animal model. *Proc Natl Acad Sci USA* 2000;97:13853-8.
13. Wiegand EH, McMurray DN, Grover AA, Harding GE, Smith DW. Host-parasite relationships in experimental airborne tuberculosis. 3. Relevance of microbial enumeration to acquired resistance in guinea pigs. *Am Rev Respir Dis* 1970;102:422-9.
14. McShane H, Behboudi S, Goonetilleke N, Brookes R, Hill AV. Protective immunity against *Mycobacterium tuberculosis* induced by dendritic cells pulsed with both CD8(+) and CD4(+) T-cell epitopes from antigen 85A. *Infect Immun* 2002;70:1623-6.
15. Lowrie DB, Tascon RE, Bonato VL, Lima VM, Faccioli LH, Stavropoulos E, Colston MJ, Hewinson RG, Moelling K, Silva CL. Therapy of tuberculosis in mice by DNA vaccination. *Nature* 1999;400:269-71.
16. Hamasur B, Källenius G, Svenson S. Synthesis and immunologic characterization of *Mycobacterium tuberculosis* lipoarabinomannan specific oligosaccharide-protein conjugates. *Vaccine* 1999;17:2853-61.
17. Hamasur B, Haile M, Pawlowski A, Schröder U, Williams A, Hatch G, Hall G, Marsh P, Källenius G, Svenson S. *Mycobacterium tuberculosis* arabinomannan-protein conjugates protect against tuberculosis. *Vaccine* 2003;21:4081-93.
18. Haile M, Hamasur B, Jaxmar T, Gavier-Widen D, Chambers MA, Sanchez B, Schröder U, Källenius G, Svenson SB, Pawlowski A. Heat killed BCG and arabinomannan-protein conjugates in Eurocine L3adjuvant as nasal booster vaccines against tuberculosis. *Tuberculosis* 2004.
19. Tanghe A, D'Souza S, Rosseels V, Denis O, Ottenhoff TH, Dalemans W, Wheeler C, Huygen K. Improved immunogenicity and protective efficacy of a tuberculosis DNA vaccine encoding Ag85 by protein boosting. *Infect Immun* 2001;69:3041-7.
20. D'Souza S, Rosseels V, Denis O, Tanghe A, De Smet N, Jurion F, Palfliet K, Castiglioni N, Vanonckelen A, Wheeler C, Huygen K. Improved tuberculosis DNA vaccines by formulation in cationic lipids. *Infect Immun* 2002;70:3681-8.
21. Smith D, Parish T, Stoker N, Bancroft G. Characterization of auxotrophic mutants of *Mycobacterium tuberculosis* and their potential as vaccine candidates. *Infect Immun* 2001;69:1142-50.
22. Parish T, Gordhan B, McAdam R, Duncan K, Mizrahi V, Stoker N. Production of mutants in amino acid biosynthesis genes of *Mycobacterium tuberculosis* by homologous recombination. *Microbiology* 1999;145:3497-503.
23. Hess J, Miko D, Catic A, Lehmsiek V, Russell DG, Kaufmann SHE. *Mycobacterium bovis* Bacille Calmette-Guérin strains secreting listeriolysin of *Listeria monocytogenes*. *Proc Natl Acad Sci USA* 1998;95:5299-304.
24. Perez E, Samper S, Bordas Y, Guillhot C, Gicquel B, Martin C. An essential role for phoP in *Mycobacterium tuberculosis* virulence. *Mol Microbiol* 2001;41:179-87.

Available online at www.sciencedirect.com



Original article

WILLIAMS, A., JAMES, B. W., BACON, J., HATCH, K. A., HATCH, G. J., HALL, G. A. & MARSH, P. D. 2005c. An assay to compare the infectivity of *Mycobacterium tuberculosis* isolates based on aerosol infection of guinea pigs and assessment of bacteriology. *Tuberculosis (Edinb)*, 85, 177-84.

Impact factor: 1.960

Contributions by HATCH, G. J.

Home Office – Personal Licence and Deputy Project Licence holder

Animal procedures – Aerosol challenge, necropsy

Study management – Liaison and co-ordination with histology and in vivo facility, scheduling, reporting

Microbiological experimental work and data analysis

Manuscript review

Citation metrics

Google Scholar: 29 citations



An assay to compare the infectivity of *Mycobacterium tuberculosis* isolates based on aerosol infection of guinea pigs and assessment of bacteriology [☆]

Ann Williams^{*}, Brian W. James, Joanna Bacon, Kim A. Hatch, Graham J. Hatch, Graham A. Hall, Philip D. Marsh

Health Protection Agency Porton Down, Salisbury, Wiltshire, SP4 0JG, UK

Accepted 7 October 2004

KEYWORDS

Aerosol;
Guinea pig;
Infectivity;
Iron;
Oxygen

Summary The aim of this study was to establish an assay to compare *Mycobacterium tuberculosis* strains, and cells grown under different growth conditions, in terms of their ability to cause a lung infection and disseminate to the spleen.

M. tuberculosis strains H37Rv, Erdman, South Indian (TMC120, SI) and H37Rv cells grown aerobically or under low oxygen/iron limitation in a chemostat were assayed for infectivity. Groups of 8 animals were challenged with 3 different doses of each strain. Lung and spleen bacteriology was assessed at 16 days post-infection for all strains. Bacteriology and lung pathology at day 56 was studied for H37Rv, Erdman and SI.

Strains H37Rv and Erdman had a statistically significantly higher pathogenic potential than SI and this was confirmed by analysis of lung pathology performed at 8 weeks post-infection, although the Erdman strain caused more extensive caseation without calcification and little encapsulation.

The model could discriminate between cells grown under different growth conditions; low-oxygen/iron-limited cells had a significantly higher infectivity than those grown aerobically.

This study presents a quick and reliable method for comparing with statistical confidence, the pathogenic potential of *M. tuberculosis* strains and the impact of in vitro growth conditions on the infectivity of *M. tuberculosis* in vivo.

© 2004 Elsevier Ltd. All rights reserved.

[☆]This work was supported by the Department of Health, UK.

^{*}Corresponding author. Tel.: +1980 612813; fax: +1980 612763.

E-mail addresses: ann.williams@camr.org.uk, ann.rawkins@hpa.org.uk (A. Williams).

Introduction

Tuberculosis (TB) is recognized as a major cause of human mortality. A resurgence in the number of TB cases in the late 1980s and early 1990s promoted renewed efforts to develop more effective control and preventative strategies.¹ Of particular concern to public health was the emergence of drug-resistant strains, the increased susceptibility of HIV-infected individuals and the prevalence of infection in developing countries.

Significant progress has been made in mycobacterial research over the past decade in terms of both immunology and the development of techniques to study the physiology and genetics of the organism and its interaction with the host.²⁻⁴ Relevant stimuli such as oxygen and iron availability are important environmental cues for changes in microbial gene expression, which will play a key role in regulating the pathogenicity of *Mycobacterium tuberculosis*.⁵⁻¹¹ In order to understand more about the processes by which *M. tuberculosis* causes disease, the organism needs to be studied in the laboratory under growth conditions that are relevant to the host environment. Therefore, we are using continuous culture, to investigate the influence of specific environmental stimuli on gene expression.^{5,12,13} Relevant and reliable models of infection are essential to determine the in vivo relevance of these studies, and mice, guinea pigs and rabbits have all contributed to current knowledge. Guinea pigs have been widely used because they reproduce key elements of human disease, in particular, primary pulmonary lesions that histologically resemble human tubercles together with extrapulmonary dissemination and re-seeding to lesion-free regions of the lung.¹⁴⁻¹⁷

The aim of this study was to establish a rapid and robust assay of early pulmonary infection in guinea pigs that was sufficiently discriminatory so that different strains or the same strain grown under different environmental conditions could be compared. Key considerations during the development of this assay were that it should (i) provide a reliable assessment of the infectivity of mycobacteria, and discriminate between strains/mutants of different virulence, (ii) allow robust statistical analysis of the data, and (iii) be of short duration since this will minimize suffering to the animals, and reduce cost and the burden on high containment facilities.

A study by Balasubramanian et al.¹⁸ described an assay to compare the virulence of *M. tuberculosis* clinical isolates that was based on the numbers of viable bacilli in the spleen and demonstrated that

bacterial enumeration correlated with the 'Root Index of Virulence' (RIV) score developed by Mitchison.¹⁹ The RIV is a numerical score but is based on subjective evaluations of the severity of the disease in various tissues and thus the numerical spleen assessment was deemed to be more objective and reliable. This and other studies²⁰ had demonstrated a correlation between the extent of gross disease and the ability of a strain to disseminate to the spleen but the assays were based on intramuscular infection and the evaluation was performed at 6 weeks post-challenge. Our aim was to develop a more rapid assay based on a more relevant route of infection, so we chose to evaluate whether quantification of bacilli in spleens at an early time point (16 days post-aerosol infection) could be used as a reliable measure of the infectivity of strains. This time point was chosen to coincide with the onset of extrapulmonary dissemination since the spread of *M. tuberculosis* from the lungs to the spleens of guinea pigs challenged by the aerosol route, followed by subsequent re-seeding of lungs are important features of the pulmonary disease in guinea pigs.²¹ To assist with the development and validation of the assay, an assessment of the bacterial burden and pulmonary lesion severity was conducted on animals at 8 weeks post-infection.

Materials and methods

Strains

The studies were performed with *M. tuberculosis* strains H37Rv (NCTC 7416), Erdman (ATCC 35801) and South Indian (SI) isolate TMC120 (ATCC 35811). The strains were subcultured once on Middlebrook 7H10+OADC agar and stored at -70°C as dense suspensions in sterile water.

Growth conditions

All strains were cultured on Middlebrook 7H10+OADC agar for 3 weeks at 37°C prior to aerosol challenge. Bacterial suspensions were prepared in sterile deionized water to a cell density of at least 10^8 cfu ml⁻¹.

Growth of *M. tuberculosis* under aerobic conditions

M. tuberculosis strain H37Rv (NCTC 7416) was grown to steady-state conditions in a chemostat in CAMR Mycobacterium medium (CMM), as

described previously.¹² In brief, culture was performed in a 1 litre fermentation vessel with a working volume of 500 ml. Fresh medium was added at a constant flow rate of 15 ml h⁻¹ to give a dilution rate (*D*) of 0.03 h⁻¹, which corresponds to a mean generation time of 24 h. Under aerobic conditions a dissolved air saturation of 50% at 37 °C (equivalent to a dissolved oxygen tension (DOT) of 10%) and pH 6.9 were used, as described previously.¹² Samples were collected from the culture system to monitor culture turbidity (OD₅₄₀), viability and nutrient utilization, as detailed previously.¹² Cultures were grown for 8 days (equivalent to 8 culture generations) after the turbidity stabilized before commencing steady-state sample collection.

Growth of *Mycobacterium tuberculosis* under low-oxygen/iron-limited conditions

Aerobic cultures were established in steady-state at 10% DOT level. The CMM was then modified by removing the exogenous iron source, ferric sulphate (FeSO₄·7H₂O). The culture was transferred to a new fermentation vessel, allowed to adjust to the new medium, and steady-state growth was re-established in the iron-limited environment. The turbidity of the culture was monitored daily. Low concentrations of ferric sulphate were added to the medium to encourage the culture to stabilize. Levels of iron (Fe²⁺) provided in the growth medium were 0.45 and 0.04 ppm under iron-replete and iron-limited conditions, respectively. To achieve reduced oxygen/iron-limited growth, the DOT of the culture was dropped slowly from 10% to 2%, in steps of 1% over a period of 4–5 days. The culture was then transferred to a new fermentation vessel and allowed to stabilize at 2% DOT and iron-limited conditions for 5–7 days.

Aerosol infection of guinea pigs

A decimal dilution series was prepared for each strain to obtain challenge suspensions with approximately 10⁸, 10⁷ and 10⁶ cfu ml⁻¹ (estimated by OD at λ540 nm). For each strain the suspensions were used to challenge separate groups of female Dunkin–Hartley guinea pigs (weighing between 300–350 g), free of intercurrent infection and obtained from a commercial supplier (David Hall, Burton-on-Trent, UK), for 5 min with aerosolized *M. tuberculosis*. Twelve animals were given the highest dose, 8 animals given the middle dose and 16 animals infected with the lowest dose. Aerosol particles with a diameter range of 0.5–7.0 μm, mean 2.0 μm,²² were generated and delivered

directly to the snout of the animals using a 3-jet Collison nebulizer in conjunction with a Henderson apparatus.²³ Four animals that received the highest dose were killed immediately after challenge by intraperitoneal injection of 2 ml pentobarbitone and their lungs were processed and cultured (see below) to confirm the precise retained dose.

At 16 days post-infection, 8 animals that received each dose were killed and lungs and spleens were aseptically removed and stored at –20 °C before processing to determine the number of bacteria present. Tissues were homogenized in 10 ml (lungs) or 5 ml (spleens) of sterile distilled water using a rotating blade macerator system (MSE homogenizer). Viable counts were performed on the macerate by preparing decimal dilutions in sterile deionized water and plating 100 μl aliquots onto Middlebrook 7H10+OADC agar. Plates were incubated at 37 °C for 3 weeks before counting the number of *M. tuberculosis* colonies formed.

A group of 8 animals that received the lowest dose were killed 8 weeks post-infection and samples of lung and spleen collected for bacteriology and histopathology. For each animal, the left middle and left and right cranial and the right caudal lobes were placed in one sterile container for bacteriology and the remaining lung lobes were retained for histopathology as described below. The lung and spleen tissues were processed for bacteriology as detailed above.

Histopathology

Lung tissue was fixed in 10% (v/v) normal buffered formalin. Samples of tissue were removed by sagittal section through the middle of two lung lobes and processed to paraffin wax. Sections (5 μm) were stained with haematoxylin and eosin for routine evaluation, by the van Gieson method to aid detection of encapsulated lesions and with Alizarin Red to detect calcified lesions. The nature and severity of the microscopic lesions was evaluated subjectively and scored by a board-certified pathologist; evaluations were blinded. Lung lobes were assigned a score as follows: no abnormality = 0; small, well-demarcated lesions and <20% consolidation = 1; medium-sized lesions and 20–33% consolidation = 2; moderately large lesions and 33–50% consolidation = 3; large lesions and 50–80% consolidation = 4; and extensive granulomatous pneumonia and >80% consolidation = 5. A mean consolidation score per lobe was calculated for each group. The number of foci of caseation, the number of calcified lesions and the number of encapsulated lesions was recorded and a mean

score per lobe was calculated for each group. The extent to which lesions were infiltrated by lymphocytes was scored subjectively between 0 and 4 and a mean score per lobe was calculated for each group. Lung lobes that did not contain lesions were not scored for lymphocyte infiltration.

Statistical analysis

Multiple regression and analysis of variance was used to test the dose responses for significant differences. Regression analysis was performed using Minitab (v13.1).

Results

Comparison of strains

Bacterial load in organs at day 16 post-challenge

The guinea pigs challenged with strains H37Rv, Erdman and SI developed pulmonary tuberculosis with bacterial replication in the lung after aerosol challenge (Table 1) and extrapulmonary dissemination to the spleen within 16 days post-infection. Challenge doses between 100 and 10,000 were used to ensure that cells of the SI isolate would disseminate to the spleen by day 16. An additional experiment was conducted with lower doses of H37Rv in order to evaluate the assay over a wider dose-range that included a more natural low dose. The data for H37Rv in Fig. 1 is that of the lower dose study where groups of animals were challenged with either 33, 330 or 3300 bacilli (retained dose in the lung).

For each strain there was a log-log linear relationship over the dose range \log_{10} 1.0–5.0 between the number of bacilli in the spleen at day 16 and the challenged dose delivered to the lung at day 0 (Fig. 1). The spleens of animals infected with strains Erdman or H37Rv contained consistently higher bacterial counts, at least nine-fold at each dose, than in animals infected with SI (Fig. 1).

Multiple regression and analysis of variance, using the *F*-distribution at the 5% significance level, was used to compare the dose-responses of the three strains in the spleens. The dose-response of strain H37Rv over the lower dose range was not significantly different to that over a higher dose range (data not shown) indicating that the assay was valid over a wide dose range.

The log-transformed spleen data for the three strains gave a dose-response consisting of three separate and parallel lines. The dose-responses for the H37Rv and Erdman strains were not significantly different to each other, but both were significantly different to the SI isolate. Regression analysis was used to calculate an infectivity index for each strain. The infectivity index was defined as the challenge dose required (i.e. dose delivered to the lung at day 0) to cause a disseminated infection with 1000 colony-forming bacilli in the spleen at 16 days post-infection. The infectivity index for H37Rv was 114 cfu, for Erdman 173 cfu and for SI 5279 cfu.

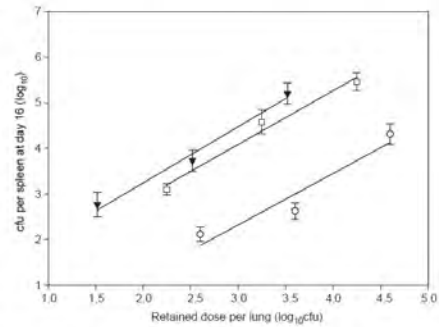


Figure 1 Relationship between the number of bacilli in the spleen at 16 days post-infection and the dose delivered to the lungs by aerosol at day 0 (retained dose) for *M. tuberculosis* strains H37Rv (▼), Erdman (□) and South Indian isolate TMC120 (○). All values represent the mean determination for at least 8 animals \pm standard error.

Table 1 Comparison of day 16 and 56 lung and spleen bacteriology following guinea pig infection with strains H37Rv, Erdman and South Indian isolate TMC120

Strain	Lung		Spleen	
	\log_{10} cfu day 16	\log_{10} cfu day 56	\log_{10} cfu day 16	\log_{10} cfu day 56
H37Rv	5.98 (0.07)	5.72 (0.46)	2.84 (0.26)	5.06 (0.39)
Erdman	6.48 (0.05)	6.25 (0.17)	3.10 (0.12)	6.25 (0.18)
South Indian	5.29 (0.16)	3.66 (0.22)	2.12 (0.15)	2.99 (0.32)

All values represent the mean determination for 8 animals \pm standard error.

Thus a significantly ($p = <0.05$) higher challenge dose was required for SI.

Bacterial load in organs at day 56 post-challenge

In order to determine whether the infectivity indices predicted the behaviour of the three strains during the later stages of infection, bacteriology was performed on animals challenged with similar doses and killed at day 56 post-infection. The animals challenged with H37Rv and Erdman received approximately 200 cfu and animals given SI received approximately 500 cfu. Animals challenged with H37Rv and Erdman contained significantly higher numbers of viable bacteria in the lungs than the SI isolate despite having received a lower initial challenge dose (Table 1, $p = 0.002$ and <0.001 , respectively). Whereas numbers of *M. tuberculosis* in the lungs of H37Rv and Erdman remained unchanged between day 16 and 56, the bacterial load in the lungs of SI infected animals had declined 40-fold, this was a statistically significant decrease ($p = <0.001$) indicating a greater control of the pulmonary infection in these animals. In all three strains the numbers of *M. tuberculosis* in the spleens had increased by day 56 relative to day 16; however, the most significant increase in cfu was observed in the spleens of Erdman challenged animals.

Lung histopathology

Lungs of guinea pigs at 8 weeks post-challenge with strain H37Rv contained discrete lesions comprising foci of consolidation by macrophages and lymphocytes (Fig. 2B) or foci where alveolar walls were thickened by macrophages and lymphocytes. Mature lesions, presumed to be primary lesions, frequently were encapsulated by fibrous tissue and were caseated or calcified in the centre. These could be distinguished from the smaller, non-encapsulated lesions that were neither caseated

nor calcified and were assumed to be secondary lesions. Animals challenged with SI contained primary and secondary lesions of a similar nature

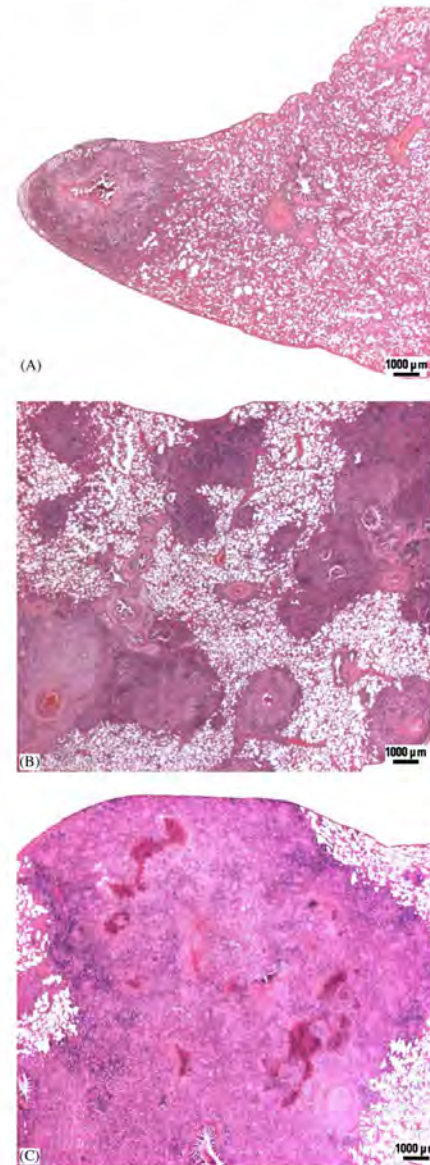


Figure 2 Representative photomicrographs of lesions in lungs of guinea pigs at 8 weeks after aerosol challenge with *M. tuberculosis*; (A) South Indian isolate, TMC120 (B) strain H37Rv and (C) strain Erdman. Panel A illustrates a discrete granuloma that is encapsulated, caseated and mineralized—a typical lesion associated with the South Indian isolate. Panel B illustrates granulomas that are well defined and some are encapsulated and caseated; these lesions were typically associated with the H37Rv strain. Panel C illustrates extensive granulomatous consolidation with numerous foci of caseation and absence of encapsulation and mineralization; a lesion typically associated with the Erdman strain. (haematoxylin and eosin, bar = 1000 µm).

Table 2 Comparison of subjective mean lesion scores (range) in lungs of guinea pigs that had received an aerosol challenge with *M. tuberculosis* strain H37Rv, strain Erdman or South Indian strain TMC120 (SI)^a

Lesion	H37Rv	Strain Erdman	SI
Mean consolidation scores per lobe	2.9 (2-5)	3.3 (1-5)	1.2 (0-2)
Mean number of foci of caseation per lobe	3.0 (0-8)	11.5 (0-30)	1.8 (0-5)
Mean number of foci of calcification per lobe	2.1 (0-5)	1.3 (0-5)	1.9 (0-5)
Mean number of encapsulated lesions per lobe	3.1 (0-9)	1.1 (0-4)	2.1 (0-6)

^aSee text for scoring criteria.

to those seen with H37Rv (Fig. 2A). In contrast, lesions of a different nature were detected in lungs of guinea pigs infected with strain Erdman. Discrete, focal lesions were numerous in some lungs and frequently were either confluent or too numerous to count. The primary and secondary lesions were not distinctively different; extensive granulomatous pneumonia was recorded and foci of caseation were frequently numerous and extensive (Fig. 2C).

Blind scoring of lesions detected differences in the nature and severity of the pathology in guinea pigs challenged with the three strains (Table 2). Mean consolidation scores were similar in animals infected with either strain H37Rv or Erdman but were lower in animals infected with the SI strain ($p < 0.001$). The mean number of foci of caseation, foci of calcification and encapsulated lesions was similar in animals infected with strain H37Rv or the SI strain, whereas animals infected with strain Erdman had a significantly higher number of foci of caseation than both H37Rv ($p = 0.006$) and SI ($p = 0.003$) infected animals.

Infectivity of *M. tuberculosis* grown under different environmental conditions

The guinea pigs challenged with *M. tuberculosis* grown in a low-oxygen/iron-limited environment developed pulmonary tuberculosis with bacterial replication in the lungs over 16 days following aerosol challenge. There was a log-log linear relationship over the dose range \log_{10} 1.0-5.0 between the number of bacilli in the spleen at day 16 and the challenge dose delivered to the lung at day 0 (Fig. 3). The infectivity index of *M. tuberculosis* grown under low oxygen/iron-limited was 23 cfu compared with 219 cfu for cells grown aerobically. Thus, a lower dose of the cells cultured

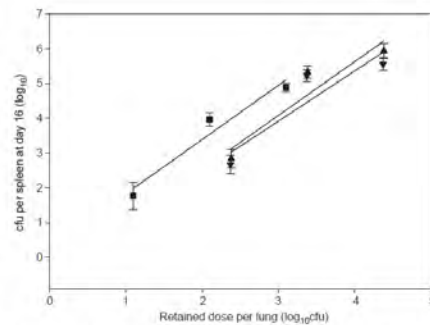


Figure 3 Relationship between the number of bacilli in the spleen at 16 days post-infection and dose delivered to the lungs by aerosol at day 0 (retained dose). *M. tuberculosis* H37Rv aerobic/iron replete, replicate chemostat cultures (\blacktriangledown & \blacktriangle), and H37Rv low-oxygen/iron-limited chemostat culture (\blacksquare). All values represent the mean determination for at least 8 animals \pm standard error.

in a combined low-oxygen/iron-limited environment was required to cause disseminated infection than cells grown in an aerobic/iron-replete environment, thereby indicating a greater infectivity of *M. tuberculosis* grown in a low oxygen/iron-limited environment.

Discussion

This study describes a rapid assay for comparing the pathogenic potential of different strains of *M. tuberculosis* based on assessment of bacteriology in the spleen at 16 days post-infection. Using this assay it was possible to differentiate between strains Erdman, H37Rv and SI. The assay was designed so that robust statistical comparisons

between the strains were possible. The effects of variations between samples due to the differences in inhaled doses were shown to be minimal (in separate studies comparing dose-responses — data not shown). The statistical comparisons of the dose-response slopes identified differences between the strains in terms of their ability to establish infection in the lung and disseminate to the spleen. An infectivity index was also calculated as a measure of each strain's ability to cause a disseminated infection. The assay demonstrated that both H37Rv and Erdman were markedly more able to establish a disseminated infection than the SI isolate. This is consistent with previous studies, which have demonstrated that isolates from South India were generally less virulent based on post-mortem scores, spleen culture and mortality.^{18,20}

It was also possible to use this assay to identify a change in the pathogenic potential of H37Rv caused by growth under altered environmental conditions. Growth of *M. tuberculosis* under low-oxygen/iron-limited conditions resulted in an increase in its infectivity and ability to disseminate to the spleen in the guinea pig. Cells grown under low-oxygen (0.2%DOT) but iron-replete conditions have also been shown to have an increased infectivity.⁵ This suggests that important physiological changes had occurred in vitro that had an effect on the pathogenesis of *M. tuberculosis* in vivo and indicates that the specific stimuli tested in vitro have direct relevance in vivo. We are using microarray analysis to determine the mechanisms that are employed by *M. tuberculosis* to adapt to specific environmental conditions and give rise to the physiological changes we have observed.⁵ We envisage that the infectivity assay will also play a particularly important role in the characterization of mutants, which have been disrupted in genes identified as potentially important virulence factors.

In this study, infectivity has been related to the ability of a strain to establish a haematogenous infection. Extrapulmonary dissemination is an important stage in human infection, which is reproduced in the guinea pig model and has been used in previous studies to compare the infectivity of clinical isolates of *M. tuberculosis*.^{20,24} As well as using the airborne route of infection, the assay is valid for both high and lower, more natural doses, which are important factors when interpreting experimental data. The assay also enabled robust statistical comparisons of strains over a relatively short time period; this has significant advantages in terms of animal welfare and reduced requirements for high containment animal husbandry facilities.

Previous studies have advocated the importance of lung pathology when assessing virulence.²⁵ The results of blinded subjective description of lesions combined with blinded subjective scoring have identified a different pathogenicity for each strain. Consolidation scores, assumed to be the most useful measure of loss of functional lung tissue, indicated that strains H37Rv and Erdman were of similar pathogenicity and that both were greater than the SI strain, and this was supported by the bacteriology data at day 56. The lesions induced by strain Erdman were distinctively different from H37Rv and SI; lung lesions induced by this strain were extensively consolidated, with frequent and extensive caseation and little encapsulation of lesions, indicating a less controlled pathogenic process than that induced by strain H37Rv.

In conclusion, this study presents a short-term assay for assessing the infectivity of *M. tuberculosis* strains based on spleen bacteriology at 16 days post-infection. Both Erdman and H37Rv were significantly more pathogenic than the SI isolate TMC 120 using the assay and this was supported by pathology performed at 8 weeks post-infection. Whilst the assay provides important information to compare the initial infectivity of isolates, subtle differences in the pathogenic process in the lung may not be predicted. When used to evaluate the effects of specific environmental stimuli on the pathogenicity of *M. tuberculosis*, the assay provided a robust statistically valid read-out of pathogenic potential that could be used as a basis to progress with further studies of the effects of these stimuli on patterns of gene expression.

Acknowledgements

The authors wish to thank Dr. J Cobby, University of the West of England, Bristol, UK for statistical analysis of data and the staff of the Biological Investigations Group at HPA Porton Down for care of the animals.

This work was funded by the Department of Health UK. The views expressed in the publication are those of the authors and not necessarily those of the Department of Health UK.

References

1. Maher D, Raviglione MC. The global epidemic of tuberculosis: a World Health Organisation perspective. In: Schlossberg D, editor. *Tuberculosis and non-tuberculous mycobacterial infections*. Philadelphia: W. B. Saunders Co.; 1999. p. 104–15.

2. Pellicic V, Jackson M, Reyrat JM, Jacobs Jr. WR, Gicquel B, Guilhot C. Efficient allelic exchange and transposon mutagenesis in *Mycobacterium tuberculosis*. *Proc Natl Acad Sci USA* 1997;**94**:10955-60.
3. Cole ST, Brosch R, Parkhill J, Garnier T, Churcher C, Harris D, et al. Deciphering the biology of *Mycobacterium tuberculosis* from the complete genome sequence. *Nature* 1998;**393**:537-44.
4. Andersen P. TB vaccines: progress and problems. *Trends Immunol* 2001;**22**:160-8.
5. Bacon J, James BW, Wernisch L, Williams A, Morley KA, Hatch GJ, Mangan JA, Hinds J, Stoker NG, Butcher PD, Marsh PD. The influence of reduced oxygen availability on pathogenicity and gene expression in *Mycobacterium tuberculosis*. *Tuberculosis* 2004;**84**:205-17.
6. Wayne LG, Lin KY. Glyoxylate metabolism and adaptation of *Mycobacterium tuberculosis* to survival under anaerobic conditions. *Infect Immun* 1982;**37**:1042-9.
7. Wayne LG, Hayes LG. An in vitro model for sequential study of shutdown of *Mycobacterium tuberculosis* through two stages of nonreplicating persistence. *Infect Immun* 1996;**64**:2062-9.
8. Sherman DR, Voskuil M, Schnappinger D, Liao R, Harrell MI, Schoolnik GK. Regulation of the *Mycobacterium tuberculosis* hypoxic response gene encoding alpha-crystallin. *Proc Natl Acad Sci USA* 2001;**98**:7534-9.
9. Park HD, Guinn KM, Harrell MI, Liao R, Voskuil MI, et al. Rv3133c/dosR is a transcription factor that mediates the hypoxic response of *Mycobacterium tuberculosis*. *Mol Microbiol* 2003;**48**:833-43.
10. Ratledge C, Dover LG. Iron metabolism in pathogenic bacteria. *Annu Rev Microbiol* 2000;**54**:881-941.
11. Rodriguez GM, Rodriguez IS. Mechanisms of iron regulation in mycobacteria: role in physiology and virulence. *Mol Microbiol* 2003;**47**:1485-94.
12. James BW, Williams A, Marsh PD. The physiology and pathogenicity of *Mycobacterium tuberculosis* grown under controlled conditions in a defined medium. *J Appl Microbiol* 2000;**88**:669-77.
13. James BW, Bacon J, Hampshire T, Morley K, Marsh PD. In vitro gene expression dissected: chemostat surgery for *Mycobacterium tuberculosis*. *Comp Funct Genom* 2002;**3**:345-7.
14. Smith DW, Harding GE. Approaches to the validation of animal test systems for assay of protective potency of BCG vaccines. *J Biol Stand* 1977;**5**:131-8.
15. Smith DW, Wiegshaus EH. What animal models can teach us about the pathogenesis of tuberculosis in humans. *Rev Infect Dis* 1989;**11**(Suppl 2):S385-93.
16. Stead WW. Pathogenesis of tuberculosis: clinical and epidemiologic perspective. *Rev Infect Dis* 1989;**11**(Suppl 2):S366-8.
17. Balasubramanian V, Wiegshaus EH, Smith DW. Mycobacterial infection in guinea pigs. *Immunobiology* 1994;**191**:4-5.
18. Balasubramanian V, Guo-Zhi W, Wiegshaus E, Smith D. Virulence of *Mycobacterium tuberculosis* for guinea pigs: a quantitative modification of the assay developed by Mitchison. *Tuberc Lung Dis* 1992;**73**:268-72.
19. Mitchison DA. The virulence of tubercle bacilli from patients with pulmonary tuberculosis in India and other countries. *Bull Int Union Tuberc* 1964;**35**:287-306.
20. Prabhakar R, Venkataraman P, Vallishayee RS, Reeser P, Musa SR, et al. Virulence for guinea pigs of tubercle bacilli isolated from the sputum of participants in the BCG trial, Chingleput District, South India. *Tubercle* 1987;**68**:3-17.
21. McMurray DN. Guinea pig model of tuberculosis. In: Bloom BR, editor. *Tuberculosis: pathogenesis, protection and control*. Washington, DC: ASM Press; 1994. p. 135-47.
22. Lever MS, Williams A, Bennett AM. Survival of mycobacterial species in aerosols generated from artificial saliva. *Lett Appl Microbiol* 2000;**31**:238-41.
23. Williams A, Davies A, Marsh PD, Chambers MA, Hewinson RG. Comparison of the protective efficacy of Bacille Calmette-Guerin vaccination against aerosol challenge with *Mycobacterium tuberculosis* and *Mycobacterium bovis*. *Clin Infect Dis* 2000;**30**(Suppl 3):S299-301.
24. Bhatia AL, Mitchinson DA, Selkon JB, Somasundaram PD, Subbaiah TV. The virulence in the guinea-pig of tubercle bacilli isolated before treatment from south Indian patients with pulmonary tuberculosis. *Bull WHO* 1961;**25**:313-22.
25. Dunn PL, North RJ. Virulence ranking of some *Mycobacterium tuberculosis* and *Mycobacterium bovis* strains according to their ability to multiply in the lungs, induce lung pathology, and cause mortality in mice. *Infect Immun* 1995;**63**:3428-37.

Available online at www.sciencedirect.com



Original article

MARTIN, C., WILLIAMS, A., HERNANDEZ-PANDO, R., CARDONA, P. J., GORMLEY, E., BORDAT, Y., SOTO, C. Y., CLARK, S. O., HATCH, G. J., AGUILAR, D., AUSINA, V. & GICQUEL, B. 2006. The live *Mycobacterium tuberculosis* phoP mutant strain is more attenuated than BCG and confers protective immunity against tuberculosis in mice and guinea pigs. *Vaccine*, 24, 3408-19.

Impact factor: 3.269

Contributions by HATCH, G. J.

Home Office – Personal Licence and Deputy Project Licence holder

Animal procedures – Aerosol challenge, necropsy

Study management – Liaison and co-ordination with sponsors, histology and in vivo team, scheduling, reporting

Microbiological experimental work and data analysis

Manuscript review

Citation metrics

Google Scholar: 268 citations



The live *Mycobacterium tuberculosis* *phoP* mutant strain is more attenuated than BCG and confers protective immunity against tuberculosis in mice and guinea pigs

Carlos Martin^{a,*}, Ann Williams^b, Rogelio Hernandez-Pando^c, Pere J. Cardona^d,
Eamonn Gormley^e, Yann Bordat^f, Carlos Y. Soto^a, Simon O. Clark^b, Graham J. Hatch^b,
Diana Aguilar^c, Vicente Ausina^d, Brigitte Gicquel^f

^a Grupo de Genética de Micobacterias, Departamento de Microbiología, Facultad de Medicina, Universidad de Zaragoza, Spain

^b Health Protection Agency, Porton Down, Salisbury SP4 0JG, UK

^c Experimental Pathology Section, Department of Pathology, National Institute of Medical Sciences and Nutrition "Salvador Zubirán", Mexico City, Mexico

^d Unitat de Tuberculosi Experimental, Servicio de Microbiología, Fundació Institut per al Investigació en Ciències de la Salut "Germans Trias i Pujol", Universitat Autònoma de Barcelona, Spain

^e School of Agriculture, Food Science & Veterinary Medicine, University College Dublin, Ireland

^f Unité Génétique Mycobactérienne, Institut Pasteur Paris, France

Received 23 January 2006; received in revised form 15 February 2006; accepted 2 March 2006

Available online 15 March 2006

Abstract

The *Mycobacterium tuberculosis phoP* mutant strain SO2 has previously been shown to have reduced multiplication in mouse macrophages and in vivo using the mouse intravenous-infection model. In this study we demonstrate that the *M. tuberculosis* SO2 is highly attenuated when compared with the parental *M. tuberculosis* MT103 strain and also more attenuated than BCG in severe combined immunodeficiency disease (SCID) mice. Complementation of the *M. tuberculosis* SO2 with the wild-type *phoP* gene restored the virulence of the strain in the SCID mice, confirming that the attenuated phenotype is due to the *phoP* mutation. In Balb/c mice subcutaneously vaccinated with either *M. tuberculosis* SO2 or BCG, the proportions of CD4⁺ and CD8⁺ populations measured in the spleen were significantly higher in the *M. tuberculosis* SO2 vaccinated group. In addition, the proportion of antigen-stimulated CD4⁺/CD8⁺ cells expressing IFN- γ was significantly higher in the *M. tuberculosis* SO2 vaccinated group when compared with the BCG group. Balb/c mice subcutaneously vaccinated with the *M. tuberculosis* SO2 strain were also protected against intra-venous challenge with *M. tuberculosis* H37Rv at levels comparable to mice vaccinated with BCG, as measured by reduced bacterial counts in lung and spleens. Guinea pigs subcutaneously vaccinated with the *M. tuberculosis* SO2 strain were protected against aerosol challenge with *M. tuberculosis* H37Rv delivered at different doses. A high dose aerosol challenge of *M. tuberculosis* SO2 vaccinated guinea pigs resulted in superior levels of protection when compared with BCG vaccination, as measured by guinea pig survival and reduction in disease severity in the lung.

© 2006 Elsevier Ltd. All rights reserved.

Keywords: Tuberculosis; Attenuation; Live vaccine; BCG

* Corresponding author at: Facultad de Medicina, Universidad de Zaragoza, C/Domingo Miral sn., 50009 Zaragoza, Spain. Tel.: +34 976 761 759; fax: +34 976 761 664.

E-mail addresses: carlos@unizar.es (C. Martin), ann.rawkins@hpa.org.uk (A. Williams), rhdezpando@hotmail.com (R. Hernandez-Pando), pcardona@ns.hugtip.scs.es (P.J. Cardona), egormley@ucd.ie (E. Gormley), ybordat@pasteur.fr (Y. Bordat), cysoto@unizar.es (C.Y. Soto), simon.clark@hpa.org.uk (S.O. Clark), graham.hatch@hpa.org.uk (G.J. Hatch), aguilarleon@hotmail.com (D. Aguilar), vausina@ns.hugtip.scs.es (V. Ausina), bgicquel@pasteur.fr (B. Gicquel).

1. Introduction

Tuberculosis remains one of the leading causes of infectious disease mortality throughout the world [1]. The HIV/AIDS pandemic, the deterioration of public health infrastructures in developing countries, and the emergence of multi-drug resistance forms of tuberculosis have further contributed to the spread of the disease [2]. Given the variable protective efficacy generated by *Mycobacterium bovis* BCG (Bacillus Calmette–Guérin) vaccination against tuberculosis, there is a concerted effort worldwide to develop better vaccines that could be used to reduce the burden of tuberculosis. Rational attenuated mutants of *Mycobacterium tuberculosis* are vaccine candidates that offer some potential in this area. As an eradication strategy, the concept of mass vaccination is a relatively cost-effective alternative to expensive chemotherapy as a means to reduce the global burden of tuberculosis. The aims of the 'classical' live vaccine are to generate host responses that mimics natural infection, but without causing disease [3]. In this context, *M. bovis* BCG is the only vaccine available for the prevention of tuberculosis in humans. The live, attenuated BCG vaccine, originally derived by serial passage of a virulent strain of *M. bovis*, has been used to prevent tuberculosis since 1921. The BCG is effective against severe forms of childhood tuberculosis but appears to be of limited efficacy against adult pulmonary disease in endemic areas [4]. It is now clear that a number of BCG vaccine strains have evolved that differ from the original BCG after many years of growth passages in different laboratories. Recent genomic comparisons have made it possible to determine the precise order of genetic events and revealed the existence of *M. tuberculosis*-specific regions that have been deleted from all BCG strains as the deletion of RD1 [5]. The absence of RD1 in BCG removes immunodominant antigens such as ESAT-6, which have recently been shown to be important for protection against *M. tuberculosis* challenge in the guinea pig model [6].

In establishing a set of criteria to measure and demonstrate that a vaccine is superior to BCG the minimum requirements would be that it is at least as attenuated as BCG in stringent animal model systems, e.g. SCID mice, it would reduce tissue damage in the lungs equivalent to BCG following challenge, lower the bacterial burden and enhance survival after virulent challenge. In a concerted effort to improve on the protective efficacy afforded by BCG, several broad approaches to tuberculosis vaccine development are being pursued. One approach is to use non-viable subunit vaccines to deliver immunodominant mycobacterial antigens. Both protein and DNA vaccines induce partial protection against experimental tuberculosis infection in mice, however, their efficacy has generally been equivalent to or less than that afforded by BCG [7–9]. The second approach utilises live vaccines modified by genetic manipulation of BCG to express new antigens and/or cytokines [10]. Alternatively, attenuated strains of *M. tuberculosis* are produced by random mutagenesis or targeted deletion of known genes. Rational attenuated mutants of *M.*

tuberculosis are also potential vaccine candidates against tuberculosis. A particular advantage of this approach is that many potential immunologically important genes are conserved, unlike in BCG substrains where these are deleted [5]. The relatively recent development of sophisticated biological tools has facilitated the ability to genetically manipulate *M. tuberculosis* [11–13]. These advances, in combination with the completion of the *M. tuberculosis* genome sequence [14], have increased our understanding of the contribution of individual genes to *M. tuberculosis* virulence [15,16]. Several studies have described the development of *M. tuberculosis* auxotrophic mutant strains with different levels of attenuation and potential as vaccine candidates in animal models [17,18]. Two-component regulatory signal transduction systems (TCS) are important elements in the adaptive response of prokaryotes to a variety of environmental stimuli [19] and are also implicated in virulence regulation [20]. The *phoP* transcription factor, a component of the *M. tuberculosis* PhoP/R TCS is strongly upregulated in a clinical isolate demonstrated to be a cause of multidrug resistant tuberculosis [21]. Recently, it has been shown that *phoP* is involved in the regulation of complex mycobacterial lipids implicated in the virulence of *M. tuberculosis* [22]. In previous work, the *M. tuberculosis phoP* SO2 strain was constructed by a single gene disruption [23] and it was established that the *M. tuberculosis* SO2 exhibited impaired multiplication in vitro within mouse cultured macrophages, and in vivo in a mouse infection model. Here, we have extended these studies and demonstrate that *M. tuberculosis* SO2 strain is highly attenuated in the SCID mouse model and is effective as a vaccine against tuberculosis in mice and guinea pigs. Moreover, we show that vaccination of guinea pigs with *M. tuberculosis* SO2 is superior to BCG in conferring protection to guinea pigs against virulent *M. tuberculosis* challenge as measured by guinea pig survival and severity of lung disease.

2. Methods

2.1. Protein extraction and immunoblotting

Polyclonal antibodies against PhoP protein were obtained from rabbits that received four doses of PhoP (0.5 mg), at weeks 0, 4, 8, 12 and 16, respectively. The anti-PhoP antibodies were detected by ELISA (ZEU-Immunotec Zaragoza, Spain). Monoclonal antibodies against ESAT-6 were kindly provided by Stewart Cole [24]. Cell-free protein extracts of mycobacteria were prepared from early log-phase cultures grown on Middlebrook 7H9-ADC using standard procedures [25]. Protein extracts of *M. tuberculosis* were filtered through a 0.22 μ m pore size Millex-GP filter (Millipore, Bedford, MA). Culture filtrate was harvested from *M. tuberculosis* H37Rv grown for 5–6 weeks and filtrate proteins precipitated with 45% (w/v) ammonium sulphate. Western Blot analysis was carried out using standard procedures. Horseradish peroxidase-labelled goat anti-rabbit antibodies

(Bio-Rad Laboratories, Hercules, CA) were used as secondary antibodies.

2.2. SCID mice infection with *M. tuberculosis*

SCID mouse work was carried out under the Animal Care Committee of the Hospital Universitari “Germans Trias i Pujol” in agreement with the European Union Laws for protection of experimental animals. CB-17/cr lco SCID specific pathogen free (*spf*) mice were obtained from Charles River (Bagneux Cedex, France). For aerosol infection, mice were placed in the exposure chamber of an airborne infection apparatus (Glas-col Inc., Terre Haute, IN, USA). For aerosol infection, the nebulizer compartment was filled with 7 ml of a *M. tuberculosis* suspension to provide an approximate uptake of 20 viable bacilli within the lungs. Ten mice were used per experimental group. For intravenous infection, groups of seven mice were infected with 200 μ l PBS containing doses equivalent to 2×10^5 , 2×10^4 and 2×10^3 viable *M. bovis* BCG Pasteur and 5.4×10^6 , 5.4×10^5 and 5.4×10^4 viable *M. tuberculosis phoP* strain via a lateral tail vein. The significance in differences of survival times among treated mice was determined using the Mantel–Haenszel test. Viable counts were performed on serial dilutions of the homogenate, plated onto Middlebrook 7H11 + OADC agar and examined after 3 weeks for growth. For histological analysis, tissues were fixed in formal-buffered saline and were embedded in paraffin. Five-micrometer thickness sections were cut and sections were stained with Ziehl–Neelsen.

2.3. Determination of cellular immunity activation in Balb/c mice following *M. tuberculosis* SO2 and BCG subcutaneous vaccination

Groups of four Balb/C mice were sacrificed at days 7, 14, 21, 28, 45 and 60 post-subcutaneous vaccination with 8×10^3 cfu of *M. bovis* BCG (Phipps) or 2.5×10^3 cfu SO2. The spleens were collected and placed in 2 ml of RPMI medium and 10% fetal calf serum (GIBCO, Invitrogen Corporation) containing 0.5 mg/ml collagenase type 2 (Worthington, NJ, USA), and 2 U/ml of DNAase (GIBCO), and incubated for 1 h at 37 °C at 5% CO₂. They were then passed through a 70 μ m cell sieve (Falcon, Becton Dickinson 70 μ m Nylon 35-2350), crushed with a syringe plunger, and rinsed with medium. Cells were centrifuged, the supernatant was removed and red cells were eliminated with lysis buffer [26]. After centrifugation and washing with RPMI medium, cells were resuspended in FACS buffer (PBS 1 \times , pH 7.2, 1% BSA), and counted. Cell surface labeling was performed by incubating 10^6 cells with 100 μ l of monoclonal antibodies against CD4-FITC or CD8-FITC diluted 1:20 in PBS containing 1% BSA and 0.1% sodium azide during 20 min at 4 °C, and analyzed with a FACScan cytometer.

The *M. tuberculosis* H37Rv strain was grown in Middlebrook 7H9 medium (Difco Laboratories) supplemented with OADC (Difco Laboratories). After 1 month of culture, the

bacterial mass was separated and the culture filtrate was harvested. Culture filtrate antigens were precipitated with 45% (w/v) ammonium sulfate, washed and re-dissolved in PBS. For cell stimulation, 1×10^6 spleen cells were resuspended in 100 μ l RPMI medium per culture well and incubated with 10 μ g of *M. tuberculosis* culture filtrate antigens suspended in 100 μ l PBS for 72 h at 37 °C with 5% CO₂. Cells and culture medium were centrifuged, the supernatant was discarded and after counting and checking viability, 2.5×10^5 cells per tube were CD4⁺ or CD8⁺ cell surface labelled as described above. After washing, cells were resuspended and incubated for 20 min at 4 °C in 0.1% saponin dissolved in PBS. Intracellular IFN- γ was detected by incubating the cells for 20 min at 4 °C in the dark with 100 μ l of a 1/20 dilution of phycoerythrin (PE)-labelled monoclonal anti-IFN- γ . Cells were fixed with 100 μ l of 4% paraformaldehyde diluted in PBS. Samples were analyzed after 20 min with a FACScan cytometer. Isotype controls were Ab-FITC (1:20 dilution) + Ab-PE (1:20 dilution).

2.4. Protective efficacy of *M. tuberculosis* SO2 in Balb/c mice

All of the animals were kept under controlled conditions in the P3 High Security Laboratory of the Animal Facility at the Pasteur Institute in Paris and in agreement with the European Union directives for protection of experimental animals. Groups of Balb/c mice (seven per group) were vaccinated subcutaneously in the base of the tail with 10^7 cfu of either *M. tuberculosis phoP* strain or *M. bovis* BCG (Pasteur). At 8 weeks post-vaccination, all mice were challenged by the intra-venous route with 2.5×10^5 cfu of *M. tuberculosis* H37Rv. Mice were then sacrificed 4 weeks post-challenge. Viable counts were performed on serial dilutions of the homogenate, plated onto Middlebrook 7H11 + OADC agar and examined after 3 weeks for growth of *M. tuberculosis*. The *M. tuberculosis* H37Rv was distinguished from the *M. tuberculosis phoP* on the basis of the kanamycin resistance phenotype of the latter strain.

2.5. Protective efficacy of *M. tuberculosis* SO2 in guinea pigs

Guinea pig experimental work was conducted according to UK Laws for animal experimentation and was approved by a local ethical committee at Health Protection Agency, Porton Down, UK. Female Dunkin–Hartley guinea pigs were obtained from (UK Home Office) accredited commercial suppliers (David Hall, Burton-on-Trent, UK or Harlan Ltd, UK, Bicester, UK) and were full barrier reared.

2.6. Low dose challenge

Groups of six were vaccinated subcutaneously in the nape of the neck with 250 μ l of either; 5×10^4 cfu BCG Pasteur; 5×10^4 *M. tuberculosis* SO2; or saline. Animals were rested

for a period of 12 weeks prior to aerosol challenge using a contained Henderson apparatus as previously described [27]. Fine particle aerosols of *M. tuberculosis* H37Rv, with a mean diameter of 2 μm , (diameter range, 0.5–7 μm) were generated using a Collison nebulizer and delivered directly to the animal snout. The aerosol was generated from a water suspension containing 2×10^6 cfu/ml in order to obtain an estimated retained, inhaled dose of approximately 10–50 cfu/lung.

Protection was assessed at 4 weeks post-challenge. Animals were killed by peritoneal overdose of sodium pentobarbitone. Spleen and lung tissue (the left cranial and middle lobes, right middle lobe and right caudal lobes) were aseptically removed and placed into sterile containers. Material was stored at -20°C then processed to enumerate the number of bacteria. Tissues were homogenised in 10 ml (lung) or 5 ml (spleen) of sterile deionised water using a rotating blade macerator system (Ystral). Viable counts were performed on serial dilutions of the homogenate, plated onto Middlebrook 7H11 + OADC agar and examined after 3 weeks for growth of *M. tuberculosis*. The data was \log_{10} transformed for analysis and the numbers of viable *M. tuberculosis* in each vaccine group were compared with the saline control group by Student's *t*-test.

2.7. High dose challenge

Groups of six guinea pigs were vaccinated subcutaneously with 5×10^4 cfu of *M. tuberculosis* SO2 or BCG (Danish 1331) 10 weeks prior to aerosol challenge with *M. tuberculosis*. Aerosol challenge was performed as described above using a suspension of 5×10^7 cfu/ml in order to deliver approximately 500 cfu to the lungs. Following challenge, the animals were housed at ACDP containment level 3, were monitored regularly for weight changes and were killed humanely at 180 days post-challenge or at the humane endpoint (20% loss of maximal body weight). Post-mortem collection and processing of samples was as described above with the exception that lung consolidation was measured using image analysis on sections of formalin fixed lung tissue stained with Haematoxylin & Eosin (H&E). Animal survival was compared using Kaplan Meier survival estimates and Log Rank distribution analysis was used to identify statistically significant differences. The cfu and lesion consolidation data were analyzed by ANOVA, using Fishers pairwise comparisons to compare mean values of the groups.

3. Results

3.1. Characterization of *M. tuberculosis* *phoP*

The construction of the *M. tuberculosis* SO2 strain from a clinical isolate of *M. tuberculosis* has been described previously [23]. Evidence for the involvement of the *phoP* gene in global regulation of mycobacteria gene circuits was provided by the observation of changes in bacillus size and

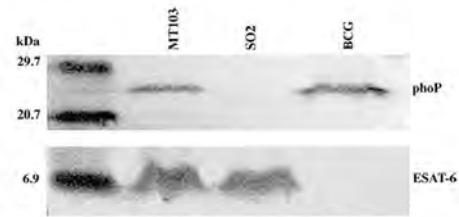


Fig. 1. Western blot analysis. Western blot image of *M. tuberculosis* MT103, *M. tuberculosis* SO2 and BCG Pasteur cell-free extracts using polyclonal antibodies raised against PhoP and ESAT-6.

coding properties of growing cells harboring the inactivated *phoP* gene. Given the key properties of secreted antigens as determinants of protective immunity against tuberculosis, we wanted to determine if the pleiotropic effects of the *phoP* mutation extended to influence synthesis of the major immunodominant antigen, ESAT-6. Western blot analysis was carried out on the *M. tuberculosis* SO2 strain, BCG and *M. tuberculosis* MT103 using antibodies raised against the PhoP protein and ESAT-6. The results clearly showed that the PhoP was expressed constitutively in the *M. tuberculosis* MT103 and BCG strains while it was completely absent in the *M. tuberculosis* SO2 strain (Fig. 1). In contrast, the levels of expression of ESAT-6 in the supernatant of cultures of the *M. tuberculosis* SO2 strain were comparable to those detected from the parental *M. tuberculosis* MT103 strain and, as expected, no ESAT-6 protein was detected in BCG (Fig. 1).

3.2. Survival of SCID mice infected with *M. tuberculosis* SO2 and BCG

The survival of immuno-compromised SCID mice was assessed following infection by the aerosol route (approximately 20 cfu) with *M. tuberculosis* MT103, *M. tuberculosis* SO2 and the *M. tuberculosis* SO2 complemented with wild-type *phoP* gene (pSO5) [23]. All mice infected with *M. tuberculosis* SO2 survived for >245 days. In contrast, all SCID mice infected with either *M. tuberculosis* MT103 or the complemented *M. tuberculosis* SO2-pSO5 were dead by 62 days post-infection, indicating restoration of virulence in the complemented strain (Fig. 2a).

The attenuation of the *M. tuberculosis* SO2 strain was also compared with BCG in SCID mice following intravenous delivery. Groups of SCID mice were inoculated with a range of doses (2×10^5 , 2×10^4 and 2×10^3 cfu) of BCG Pasteur or with *M. tuberculosis* SO2 strain (5.4×10^6 , 5.4×10^5 and 5.4×10^4 cfu) via a lateral tail vein. Histological staining of infected alveolar macrophages from a sub-group of mice sacrificed at three weeks post-infection revealed fewer acid fast bacilli in lungs of mice infected the *M. tuberculosis* SO2 strain when compared with BCG (data not shown). All mice inoculated with the highest dose of BCG (2×10^5 cfu) died after 92 days post-infection (median survival time of 89 ± 3.5

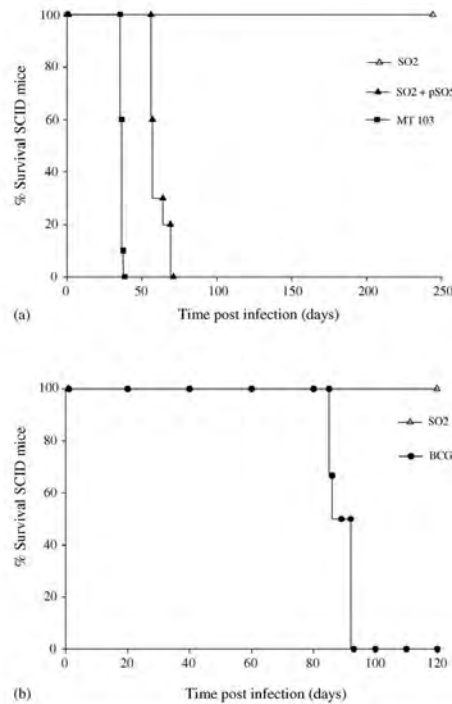


Fig. 2. Attenuation of *M. tuberculosis* SO2 in SCID mice. (a) Survival curve of SCID mice infected ($n=10$) by the aerosol route with 20 cfu of *M. tuberculosis* SO2, *M. tuberculosis* SO2 complemented with pSO5 (SO2 + pSO5) and *M. tuberculosis* MT103. Means of the survival days were, >245 days (*M. tuberculosis* SO2), 62.1 ± 5.88 (*M. tuberculosis* SO2 + pSO5) and 36.7 ± 0.67 (*M. tuberculosis* MT103). (b) Survival curves of SCID mice ($n=7$) infected by intravenous injection with 5.4×10^6 *M. tuberculosis* SO2 and 2×10^5 *M. bovis* BCG Pasteur.

days) (Fig. 2b). In contrast, all mice infected with the highest dose *M. tuberculosis* SO2 (5.4×10^6 cfu) survived after 120 days (Fig. 2b). At the time of death, the bacterial loads in the lungs of BCG infected mice with 2×10^5 cfu were at least 100-fold higher when compared with the *M. tuberculosis* SO2 infected mice with 5.4×10^6 cfu.

3.3. Quantitative CD4⁺ and CD8⁺ responses of Balb/c vaccinated mice

In order to compare cellular immunity activation induced by vaccination with *M. tuberculosis* SO2 and BCG, spleen cell suspensions from groups of at least four Balb/c mice subcutaneously vaccinated with *M. tuberculosis* SO2 and BCG Phipps were collected on days 7, 14, 30, 45 and 60 post-vaccination, and the relative proportions of CD4⁺ and

CD8⁺ cells determined by cytofluorometry (Fig. 3). Vaccination with *M. tuberculosis* SO2 induced significantly more CD4⁺ cells after 14 days of vaccination, when compared with BCG vaccination and significantly more CD8⁺ cells after 45 days. These splenocytes were stimulated with *M. tuberculosis* culture filtrate-derived whole antigens. After 3 days, the lymphocyte populations were analyzed by flow cytometry, combining antibodies specific for CD4⁺/CD8⁺ detection and intracellular synthesis of IFN- γ . Vaccination with *M. tuberculosis* SO2 induced a significantly higher proportion of CD4⁺/IFN- γ ⁺ producing cells after 45 days of vaccination when compared with BCG (Fig. 3). Apart from one time-point, the proportion of CD8⁺/IFN- γ ⁺ producing cells was consistently higher in the *M. tuberculosis* SO2 group (significantly different at day 14). Data obtained from mice immunised with the parental *M. tuberculosis* MT103 strain revealed cell populations and IFN- γ expression levels similar to that measured following *M. tuberculosis* SO2 immunisation (data not shown).

3.4. Protective immunity generated by *M. tuberculosis* SO2 in Balb/c mice

Having established that *M. tuberculosis* SO2 strain was attenuated in SCID mice, we were interested to determine whether the observed decrease in virulence conferred any protective properties to the mutant strain. We subcutaneously vaccinated Balb/c mice with either *M. tuberculosis* SO2 strain or BCG (Pasteur). At 8 weeks post-vaccination, all mice were challenged by the intra-venous route with 2.5×10^5 cfu of *M. tuberculosis* H37Rv. The mice were then sacrificed at 4 weeks post-challenge. The levels of protection were determined by evaluating the numbers of viable *M. tuberculosis* H37Rv recovered from the lungs and the spleen in both groups of mice (Fig. 4). Both vaccines conferred similar but significant levels of protection compared to the saline-treated controls ($p < 0.05$). Growth inhibition of *M. tuberculosis* H37Rv was recorded in both lungs and spleen, with reductions of approximately $1.5 \log_{10}$ and $1.3 \log_{10}$ cfu, respectively.

3.5. Protective immunity of *M. tuberculosis* SO2 in guinea pigs

The results obtained from the mouse vaccination experiments indicated that the attenuation of *M. tuberculosis* SO2 strain afforded it vaccine characteristics that were comparable with BCG Pasteur. However, it is widely recognized that guinea pigs constitute a more relevant model of human tuberculosis, with many similarities in the progression and pathology of the disease. Thus, this animal model is a more challenging system with which to evaluate vaccine efficacy. In order to investigate the protective efficacy of the *M. tuberculosis* SO2 strain, we performed experiments involving low-dose (10–50 cfu) and high-dose (500 cfu) aerosol-challenge of vaccinated animals. Groups of six guinea pigs were vac-

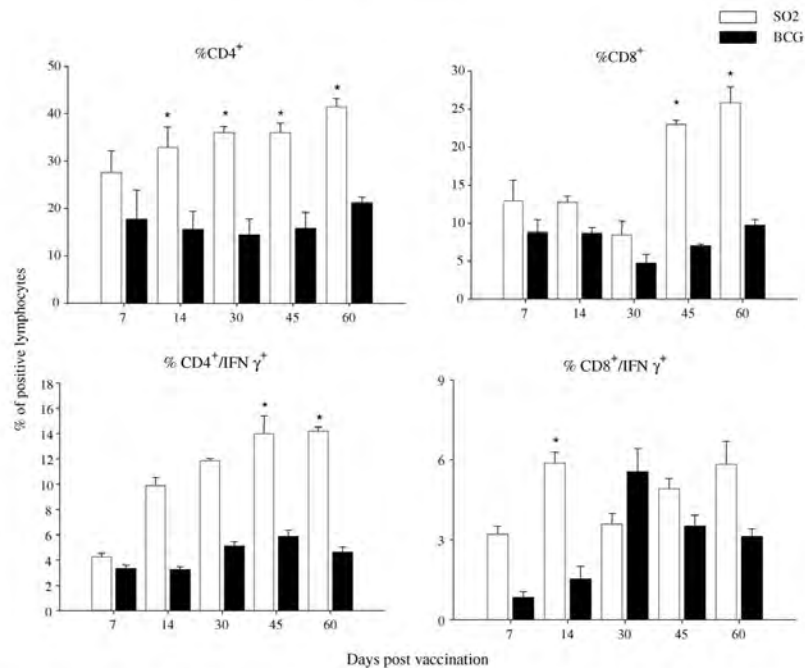


Fig. 3. Cellular immune responses in *M. tuberculosis* SO2 and BCG vaccinated mice. Balb/C mice were vaccinated by the subcutaneous route with 8×10^3 cfu of *M. bovis* BCG (Phipps) or 2.5×10^3 cfu *M. tuberculosis* SO2. The results are presented as the percentage of total CD4⁺/CD8⁺ populations in lymph nodes at time intervals after vaccination and the percentage of cells expressing IFN- γ from the total CD4⁺/CD8⁺ population after *M. tuberculosis* whole antigen stimulation. *Denotes significant statistical differences between the groups at the time points indicated ($p < 0.05$).

cinated subcutaneously with either *M. tuberculosis* SO2 or BCG. Ten weeks post-vaccination all guinea pigs were challenged with inhaled doses of *M. tuberculosis* H37Rv.

Animals receiving the low-dose challenge were sacrificed at 4 weeks and bacterial loads enumerated in lungs and spleens. Protective efficacy was determined by comparing the numbers of viable *M. tuberculosis* H37Rv recovered from the organs of guinea pigs in each treatment group. In this experiment, the reduction of cfu in lungs and spleens was significantly different between non-vaccinated control animals and those vaccinated with BCG or *M. tuberculosis* SO2 ($p = 0.005$). However, no significant difference was found between the vaccinated groups (Fig. 5).

Guinea pigs challenged with the high-dose were killed at day 180 post-challenge or at the humane end point (20% loss of maximal body weight). For the purposes of analyzing survival, animals killed at the humane end-point were considered to have died due to infection. The levels of protection were determined by comparing the survival times of guinea pigs in each treatment group. The progression of lesion development

was also studied in the vaccinated/challenged guinea pigs and compared with that observed in non-vaccinated/challenged animals. During the post-challenge phase of the experiment all of the non-vaccinated and four of the BCG vaccinated guinea pigs were euthanased at the humane end-point, prior to the last time-point (180 days) because of severe and progressive disease (Fig. 6a). In contrast, all of the guinea pigs vaccinated with the *M. tuberculosis* SO2 strain survived for the duration of the study. Guinea pigs vaccinated with the *M. tuberculosis* SO2 strain survived significantly longer than guinea pigs vaccinated with BCG ($p = 0.018$) which in turn survived significantly longer than control guinea pigs treated with saline ($p = 0.0049$). In addition, the guinea pigs vaccinated with the *M. tuberculosis* SO2 strain gained weight and did not present with any visible or clinical signs of disease.

The extent of pulmonary disease, as measured by total lung consolidation, also differed between the treatment groups. The highest level of disease progression was observed, not unexpectedly, in the non-vaccinated guinea pigs and a mean percentage consolidation of 76% was measured in this group

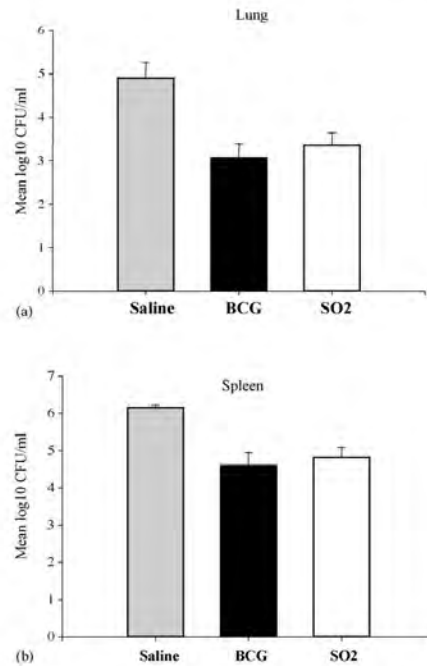


Fig. 4. Protective efficacy in vaccinated Balb/c mice. Numbers of cfus recovered from lungs (a) and spleens (b) of Balb/c mice vaccinated with *M. tuberculosis* SO2 and BCG, intravenously infected with *M. tuberculosis* H37Rv.

of animals (Fig. 6b and c). The coalescence of granulomas was also pronounced in the BCG vaccinated guinea pigs with a mean 70% consolidation measured in the lungs. In contrast, there was less consolidation (approximately 50%) in the *M. tuberculosis* SO2 vaccinated guinea pigs and this was significantly ($p < 0.05$) reduced compared with both the non-vaccinated and BCG vaccinated animals (Fig. 6c). This reduction in disease severity was also reflected in the bacterial counts from lung and spleen homogenates. In the vaccinated groups, there were differences in the levels of growth inhibition of *M. tuberculosis* H37Rv in both organs. The numbers of cfu recovered from the guinea pigs vaccinated with *M. tuberculosis* SO2 were reduced by more than 1×10^1 compared to that from guinea pigs vaccinated with BCG and this reduction was statistically significant ($p < 0.05$) in the spleen (Fig. 6d). These data demonstrated that the *M. tuberculosis* SO2 strain was superior to BCG in conferring enhanced survival to infected guinea pigs, reduction in the severity of the disease in the lung, and dissemination of infection to the spleen.

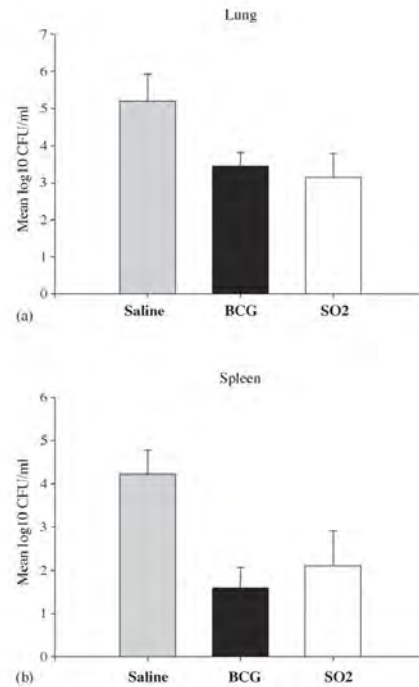


Fig. 5. Protective efficacy of *M. tuberculosis* SO2 and BCG vaccinated guinea pigs against low dose challenge with *M. tuberculosis* H37Rv. Mean log₁₀ cfu/ml counts in the lungs (a) and spleens (b) of vaccinated and saline-control guinea pigs challenged with low dose of *M. tuberculosis* H37Rv. Data represents mean cfu of all animals ($n = 6$) sacrificed after 4 weeks. Error bars indicate S.E.M.

4. Discussion

The use of vaccines to control tuberculosis in human populations has proved a formidable challenge for almost a century. The development and widespread administration of the BCG vaccine since the early 1920s was originally hailed as a major breakthrough with the promise to eradicate the world of the scourge of tuberculosis. However, the early promise was not realised and from the results of a large number of efficacy trials, it became clear that the BCG vaccine, in its existing form, was of limited use in controlling disease, particularly in adults in disease endemic areas of the developing world [4]. With a greater understanding of the virulence of *M. tuberculosis* and the patterns of immune responses that lead to the generation of protective immunity, there is renewed optimism that vaccines superior to *M. bovis* BCG can be developed. The observation that the highest levels of protection are obtained when the host is vaccinated with

live *M. bovis* BCG indicates that viability and persistence are key attributes required for a successful tuberculosis vaccine. In this study, we used the *M. tuberculosis* SO2 strain as a prototype single dose live vaccine and showed that, in addition to being more attenuated than BCG in SCID mice, it elicited high levels of protection in mice and superior protection in

guinea pigs. The *phoP* gene is part of a two component system (along with *phoR*) that shows a high degree of similarity to other two-component systems, including *phoP/phoQ*, a well described system that controls the transcription of key virulence genes in intracellular pathogens such as *Salmonella* sp. [20]. It also controls expression of many other genes not

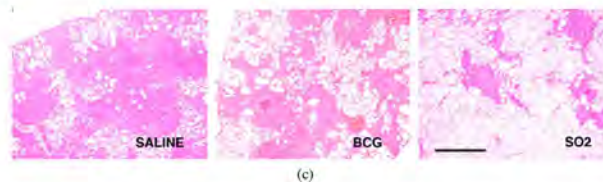
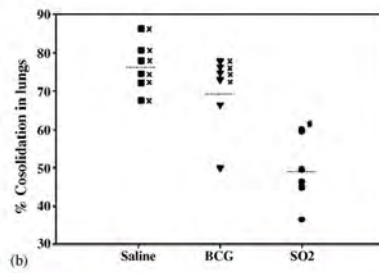
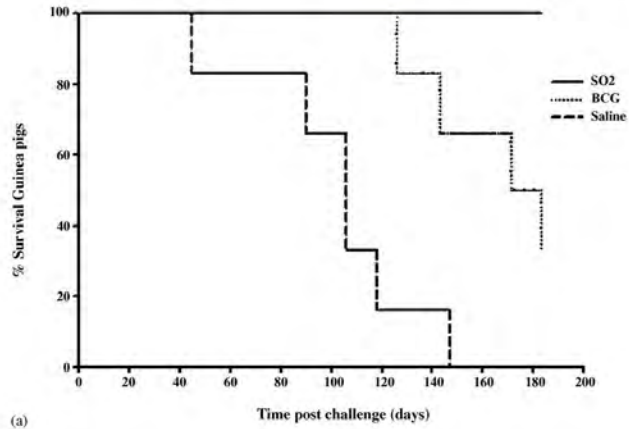


Fig. 6. Protective efficacy of *M. tuberculosis* SO2 and BCG vaccinated guinea pigs against high dose challenge with *M. tuberculosis* H37Rv. (a) Survival curve of vaccinated and non-vaccinated guinea pigs after aerosol infection with *M. tuberculosis* H37Rv. (b) The extent of pulmonary disease and disseminated infection as measured by total lung consolidation. Values for individual animals euthanased at humane end-point are indicated by an 'x'. Dashed line indicates the mean % value for the group (# in SO2 corresponds to two animals). (c) Low power magnification (30x) images of representative lung lobe sections taken from guinea pigs in each of the treatment groups. Bar represents 1 mm. (d) Mean cfu counts in the spleen and lungs of vaccinated and non-vaccinated guinea pigs.

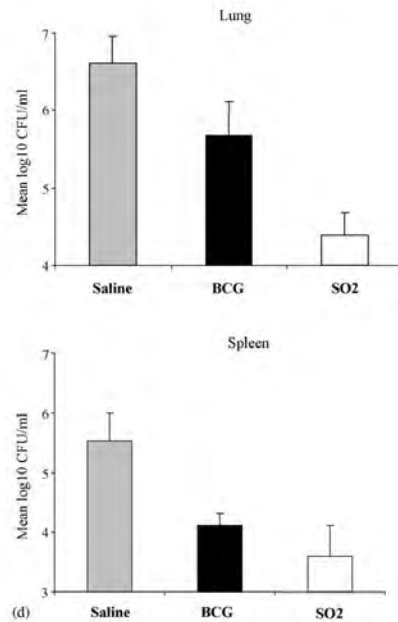


Fig. 6. (Continued).

directly involved in virulence [19]. The removal of virulence genes per se does not appear to be crucial for attenuation of *M. tuberculosis*. A pantothenate auxotrophic mutant of *M. tuberculosis*, incapable of de novo synthesis of pantothenic acid (vitamin B5), was shown to persist in SCID mice without being able to cause disease [17]. Single leucine auxotrophs are also highly attenuated and incapable of in vivo replication in SCID mice [28]. Thus, there is now a well-established proof of principle that vaccine strains based on *M. tuberculosis* can be successfully attenuated while retaining the genes that are deleted in *M. bovis* BCG.

The role of secreted antigens as determinants of protective immunity has been well described and vaccination with the major extracellular antigens does produce significant levels of protection against challenge [29]. However, subunit vaccines containing single or combinations of antigens, while capable of eliciting protective immunity, are generally not as efficient as BCG [30]. To overcome this limitation, recombinant BCG strains have been created with the aim to either overexpress immunodominant antigens (e.g. Ag-85B) that are already present in BCG [31] or by re-introducing antigen coding genes (e.g. *esat-6* [6]) from *M. tuberculosis* that have been lost in BCG. In both these examples, the levels of protection surpassed that conferred by BCG when the recombinant strains were used as vaccines in guinea pigs [31,6]. These results highlighted the important role played by secreted

antigens in eliciting protective immunity. Because of the pleiotropy associated with the *phoP* mutation, we were interested to determine whether it had any effect on synthesis of immunodominant secreted antigens. Using Western blotting, we found no significant differences on the in vitro production of ESAT6 in the *M. tuberculosis* SO2 strain compared to the parental *M. tuberculosis* MT103. However, without deleting these antigen-coding genes from the *M. tuberculosis* SO2 strain we cannot rule out that their de novo synthesis contributes to the protective efficacy of the *M. tuberculosis* SO2 vaccine in mice and guinea pigs.

The search for vaccines better than BCG was often, in the past, predicated on the notion that the loss of virulence in BCG was in itself a factor contributing to its lack of complete protective efficacy [32]. Thus, it was reasoned that new attenuated mutants of *M. tuberculosis* with reduced virulence might prove to be more effective as vaccines. However, recent work has demonstrated that natural infection with *M. tuberculosis* and vaccination with BCG do not differ in their capacity to produce protective immunity against tuberculosis [33]. This raises the questions as to whether it is possible to improve on the BCG by rational attenuation of *M. tuberculosis*. In this context, the observation that the *M. tuberculosis* SO2 strain proved to be more attenuated than BCG in the SCID mouse model, even when delivered at a 10-fold higher dose, is particularly relevant. That the attenuation was caused by the mutated *phoP* gene was proven beyond doubt by the restoration of virulence in the wt *phoP* complemented strain.

In the vaccination experiments carried out in the Balb/c mice, the levels of protection conferred by *M. tuberculosis* SO2 and BCG were similar both in the lungs and spleen up to four weeks post challenge. When we compared the relative proportions of CD4⁺ and CD8⁺ cells from the spleens of vaccinated mice, a higher percentage of both CD4⁺ and CD8⁺ cells was found in *M. tuberculosis* SO2 vaccinated mice when compared with the BCG vaccinated mice. Moreover, when these cells were stimulated with culture filtrate derived antigens, a significant higher percentage of CD4⁺/IFN- γ ⁺ was measured in *M. tuberculosis* SO2 vaccinated mice after 45 and 60 days post-vaccination. Although not significant at every time point, a similar trend was measured for CD8⁺/IFN- γ ⁺ in the *M. tuberculosis* SO2 vaccinated mice. The data suggests that vaccination with *M. tuberculosis* SO2 results in enhanced T cell activation compared with BCG vaccination, as measured by IFN- γ synthesis. As protective immunity against *M. tuberculosis* generally depends on the generation of a TH₁ type cellular immune response, characterized by secretion of IFN- γ from antigen-specific T cells, we can speculate that the relatively high levels of T cell activation induced by *M. tuberculosis* SO2 contributes to its ability to mount a potent protective response.

By using several test model systems and conditions we were able to demonstrate the relative capacity of the animal models to reveal differences in vaccine efficacy between the *M. tuberculosis* SO2 strain and the BCG. Having demonstrated equivalence of the vaccines in the mouse model, we

then undertook a strategy of comparing the vaccines in a more relevant and progressively more stringent challenge of guinea pigs. This systematic approach to vaccine comparison may represent a useful starting point for identifying the best candidate vaccines that should progress to further trials. It is generally accepted that the guinea pig is more susceptible to tuberculosis infection and may therefore be a more relevant model for this disease [30]. The guinea pig has the advantage over mice in that the pathology of the disease is closer to that seen in human tuberculosis and thus it serves as an appropriate model to test vaccine efficacy. In a recent aerosol vaccine study with a double leucine and pantothenate auxotrophic mutant of *M. tuberculosis*, protection levels equivalent to *M. bovis* BCG were generated in the lungs and spleen of vaccinated guinea pigs, with reduced dissemination of infection to the spleen induced by both vaccines, five weeks after aerosol challenge with *M. tuberculosis* [34]. In another study using recombinant BCG expressing ESAT-6, protection levels superior to *M. bovis* BCG were only observed in the spleen [6] suggesting that the improved protection was restricted to its ability to prevent dissemination of infection from the lung. In guinea pigs challenged with low dose of *M. tuberculosis* H37Rv the levels of protection conferred by vaccination with *M. tuberculosis* SO2 and BCG were similar both in the lungs and spleen up to 4 weeks post-challenge. Both vaccines gave highly efficient protection, reducing the cfu in lungs and spleens by approximately 2 logs compared with the saline control groups. However, there was no statistically significant difference between the two vaccine groups. With such a short period post-challenge, we can surmise that it would be difficult to demonstrate the superior efficacy of a novel vaccine over BCG. This is because, at this time point the cfu in the organs of the BCG-vaccinated animals are so low that the assay does not have the discriminatory power to demonstrate a significant further reduction in cfu. In other guinea pig survival studies, it has been shown that whilst BCG vaccination provides statistically significant protection compared to unvaccinated controls (or ineffective vaccines), this protection is only partial even against low-dose challenge with *M. tuberculosis*. In low-dose challenge studies, conducted over 60–80 weeks post-challenge, some BCG controls failed to protect any of the guinea pigs [35] whilst others protected a small (20–30) percentage of the animals [36,37]. In contrast, a high challenge dose can result in disease more severe than that conventionally used to evaluate the protective efficacy of TB vaccines. However, this may be required where it is necessary to discriminate between candidates that have demonstrated vaccine potential [38]. We, therefore, used a relatively high dose aerosol challenge with *M. tuberculosis* H37Rv and used a period of study up to 180 days. We did this to generate a stringent level of challenge that might demonstrate the potential protective efficacy of the *M. tuberculosis* SO2 strain and also provide a level of discrimination in comparison with BCG. In terms of survival, the animals in the BCG vaccinated group were significantly protected compared with the unvaccinated controls and demonstrated

an overall level of protection similar to that seen in other studies, despite the relatively higher challenge dose used in our study. However, we also found a statistically significant increase in the protective efficacy of the *M. tuberculosis* SO2 strain compared with BCG, as measured by several indicators including prolonged survival and the degree of lesion consolidation in the lung. This less severe form of disease may have directly lead to the prolonged survival of the *M. tuberculosis* SO2 vaccinated animals.

The inability of the BCG vaccination to provide 100% protection has been exploited to demonstrate the superior efficacy of other candidate vaccines [35,36]. Also, in a recent comparative testing of 24 tuberculosis vaccine candidates in the guinea pig model (a 3-year study funded by the EU Fifth Framework Programme) [38] two vaccine candidates, the recombinant modified vaccinia virus Ankara (MVA85A) and fowlpox vectors expressing antigen 85A used to boost guinea pigs previously vaccinated with BCG, and a single dose of *M. tuberculosis* SO2 vaccine, were found to protect better than BCG Danish 1331 as measured by animal survival. The former candidate has been tested in Phase I of human trials and the MVA85A vaccine shown to significantly boost cell-mediated immune responses in volunteers previously vaccinated with BCG [39].

The results described in our study demonstrate that *M. tuberculosis* SO2, when delivered as a single dose, is a superior vaccine to BCG by a number of criteria. It is more attenuated than BCG in SCID mice. It confers protective immunity to mice at least as good as BCG and generates more potent CMI responses. It protects guinea pigs against low dose challenge equivalent to BCG. However, against a more stringent challenge, it confers 100% survival to guinea pigs under circumstances where BCG confers 33% survival. This protection is associated with reduced severity of disease and bacterial burden. Some of the variability in levels of protection observed in the different animal model systems may be due the choice of BCG strain used in the participating laboratories. If the *M. tuberculosis* *phoP* mutant strain is to progress to clinical trials it will need to be formulated appropriately and compared with the BCG strains currently registered for use in humans. Nevertheless, the results described here may provide a rational starting point for the development of a new generation of live vaccines against tuberculosis based on inactivation of virulence pathway regulated by PhoP. It has many attributes desirable of a tuberculosis vaccine. It has a defined mutation which reduces virulence but allows persistence in the host. In addition, it has a complete repertoire of genes coding for immunodominant antigens. Unlike other vaccine candidates tested, it may potentially provide high levels of protection when delivered as a single dose. It should be possible to add additional mutations to address safety concerns associated with clinical development of a new vaccine [40]. If this can be achieved then vaccines based on *M. tuberculosis* SO2 may be likely candidates to progress to comparative vaccine efficacy trials in humans and to eventually replace BCG.

Acknowledgements

We thank Stewart Cole for advice, support and reagents, and Alberto Cebollada for the statistical analyses of data and figure preparation. This work was funded by the FP5 (QLK2-CT1999-01093) and FP6 TB-VAC Project (LSHP-CT2003-503367), MEC Spain (BIO2002-04133 and BIO2005-07949) and CONACyT Mexico (grant G36923-M).

References

- [1] WHO. Global Report Tuberculosis. Global tuberculosis control – surveillance, planning, financing. World Health Organization, Geneva, 2005. http://www.who.int/tb/publications/global_report/en/index.html.
- [2] WHO/IUATLD. Anti-Tuberculosis Drug Resistance in the World. Report no. 3: prevalence and trends. WHO/IUATLD. Global Project on Anti-Tuberculosis Drug Resistance Surveillance 1999–2002. World Health Organization and International Union Against Tuberculosis and Lung Disease, Geneva, 2004. http://www.who.int/tb/publications/who_hm.tb_2004_343/en/index.html.
- [3] Young DB. Building a better tuberculosis vaccine. *Nat Med* 2003;9(5):503–4.
- [4] Fine PE. Variation in protection by BCG: implications of and for heterologous immunity. *Lancet* 1995;346(8986):1339–45.
- [5] Behr MA. BCG—different strains, different vaccines? *Lancet Infect Dis* 2002;2(2):86–92.
- [6] Pym AS, Brodin P, Majlessi L, et al. Recombinant BCG exporting ESAT-6 confers enhanced protection against tuberculosis. *Nat Med* 2003;9(5):533–9.
- [7] Young DB. Current tuberculosis vaccine development. *Clin Infect Dis* 2000;30(Suppl. 3):S254–6.
- [8] Orme IM. Preclinical testing of new vaccines for tuberculosis: a comprehensive review. *Vaccine* 2006;24(1):2–19.
- [9] Kaufmann SH. Is the development of a new tuberculosis vaccine possible? *Nat Med* 2000;6(9):955–60.
- [10] Britton WJ, Palendira U. Improving vaccines against tuberculosis. *Immunol Cell Biol* 2003;81(1):34–45.
- [11] Pelicic V, Jackson M, Reyrat JM, Jacobs Jr WR, Gicquel B, Guilhot C. Efficient allelic exchange and transposon mutagenesis in *Mycobacterium tuberculosis*. *Proc Natl Acad Sci U S A* 1997;94(20):10961–6.
- [12] Bardarov S, Kriakov J, Carriere C, et al. Conditionally replicating mycobacteriophages: a system for transposon delivery to *Mycobacterium tuberculosis*. *Proc Natl Acad Sci U S A* 1997;94(20):10961–6.
- [13] Clark-Curtiss JE, Haydel SE. Molecular genetics of *Mycobacterium tuberculosis* pathogenesis. *Annu Rev Microbiol* 2003;57:517–49.
- [14] Cole ST, Brosch R, Parkhill J, et al. Deciphering the biology of *Mycobacterium tuberculosis* from the complete genome sequence. *Nature* 1998;393(6685):537–44.
- [15] Camacho LR, Ensergueix D, Perez E, Gicquel B, Guilhot C. Identification of a virulence gene cluster of *Mycobacterium tuberculosis* by signature-tagged transposon mutagenesis. *Mol Microbiol* 1999;34(2):257–67.
- [16] Cox JS, Chen B, McNeil M, Jacobs Jr WR. Complex lipid determines tissue-specific replication of *Mycobacterium tuberculosis* in mice. *Nature* 1999;402(6757):79–83.
- [17] Sambandamurthy VK, Wang X, Chen B, et al. A pantothenate auxotroph of *Mycobacterium tuberculosis* is highly attenuated and protects mice against tuberculosis. *Nat Med* 2002;8(10):1171–4.
- [18] Smith DA, Parish T, Stoker NG, Bancroft GJ. Characterization of auxotrophic mutants of *Mycobacterium tuberculosis* and their potential as vaccine candidates. *Infect Immun* 2001;69(2):1142–50.
- [19] Groisman EA. The pleiotropic two-component regulatory system *PhoP-PhoQ*. *J Bacteriol* 2001;183(6):1835–42.
- [20] Fields PI, Groisman EA, Heffron F. A *Salmonella* locus that controls resistance to microbicidal proteins from phagocytic cells. *Science* 1989;243(4894 Pt 1):1059–62.
- [21] Soto CY, Menendez MC, Perez E, et al. IS6110 mediates increased transcription of the *phoP* virulence gene in a multidrug-resistant clinical isolate responsible for tuberculosis outbreaks. *J Clin Microbiol* 2004;42(1):212–9.
- [22] Gonzalo Asensio J, Maia C, Ferrer NL, et al. The virulence-associated two-component *PhoP-PhoR* system controls the biosynthesis of polyketide-derived lipids in *Mycobacterium tuberculosis*. *J Biol Chem* 2006;281(3):1313–6.
- [23] Perez E, Samper S, Bordas Y, Guilhot C, Gicquel B, Martin C. An essential role for *phoP* in *Mycobacterium tuberculosis* virulence. *Mol Microbiol* 2001;41(1):179–87.
- [24] Pym AS, Brodin P, Brosch R, Huerre M, Cole ST. Loss of RD1 contributed to the attenuation of the live tuberculosis vaccines *Mycobacterium bovis* BCG and *Mycobacterium microti*. *Mol Microbiol* 2002;46(3):709–17.
- [25] Sambrook JAR, DW. Molecular cloning a laboratory manual. New York: Cold Spring Harbor Laboratory Press; 2001.
- [26] Arriaga AK, Orozco EH, Aguilar LD, Rook GA, Hernandez Pando R. Immunological and pathological comparative analysis between experimental latent tuberculous infection and progressive pulmonary tuberculosis. *Clin Exp Immunol* 2002;128(2):229–37.
- [27] Williams A, Davies A, Marsh PD, Chambers MA, Hewinson RG. Comparison of the protective efficacy of bacille Calmette-Guerin vaccination against aerosol challenge with *Mycobacterium tuberculosis* and *Mycobacterium bovis*. *Clin Infect Dis* 2000;30(Suppl 3):S299–301.
- [28] Hondalus MK, Bardarov S, Russell R, Chan J, Jacobs Jr WR, Bloom BR. Attenuation of and protection induced by a leucine auxotroph of *Mycobacterium tuberculosis*. *Infect Immun* 2000;68(5):2888–98.
- [29] Horwitz MA, Lee BW, Dillon BJ, Harth G. Protective immunity against tuberculosis induced by vaccination with major extra cellular proteins of *Mycobacterium tuberculosis*. *Proc Natl Acad Sci U S A* 1995;92(5):1530–4.
- [30] Baldwin SL, D'Souza C, Roberts AD, et al. Evaluation of new vaccines in the mouse and guinea pig model of tuberculosis. *Infect Immun* 1998;66(6):2951–9.
- [31] Horwitz MA, Harth G, Dillon BJ, Maslesa-Galic S. Recombinant bacillus Calmette-guerin (BCG) vaccines expressing the *Mycobacterium tuberculosis* 30-kDa major secretory protein induce greater protective immunity against tuberculosis than conventional BCG vaccines in a highly susceptible animal model. *Proc Natl Acad Sci U S A* 2000;97(25):13853–8.
- [32] Behr MA, Wilson MA, Gill WP, et al. Comparative genomics of BCG vaccines by whole-genome DNA microarray. *Science* 1999;284(5419):1520–3.
- [33] Mollenkopf HJ, Kursar M, Kaufmann SH. Immune response to postprimary tuberculosis in mice: *Mycobacterium tuberculosis* and *Mycobacterium bovis* bacille Calmette-Guerin induce equal protection. *J Infect Dis* 2004;190(3):588–97.
- [34] Sampson SL, Dascher CC, Sambandamurthy VK, et al. Protection elicited by a double leucine and pantothenate auxotroph of *Mycobacterium tuberculosis* in guinea pigs. *Infect Immun* 2004;72(5):3031–7.
- [35] Horwitz MA, Harth G. A new vaccine against tuberculosis affords greater survival after challenge than the current vaccine in the guinea pig model of pulmonary tuberculosis. *Infect Immun* 2003;71(4):1672–9.
- [36] Brandt L, Skeiky YA, Alderson MR, et al. The protective effect of the *Mycobacterium bovis* BCG vaccine is increased by coadministration with the *Mycobacterium tuberculosis* 72-kilodalton fusion polyprotein Mtb72F in *M. tuberculosis*-infected guinea pigs. *Infect Immun* 2004;72(11):6622–32.

- [37] Wiegshaus EH, McMurray DN, Grover AA, Harding GE, Smith DW. Host-parasite relationships in experimental airborne tuberculosis. 3. Relevance of microbial enumeration to acquired resistance in guinea pigs. *Am Rev Respir Dis* 1970;102(3):422–9.
- [38] Williams A, Hatch GJ, Clark SO, et al. Evaluation of vaccines in the EU TB Vaccine Cluster using a guinea pig aerosol infection model of tuberculosis. *Tuberculosis (Edinb)* 2005;85(1–2):29–38.
- [39] McShane H, Pathan AA, Sander CR, et al. Recombinant modified vaccinia virus Ankara expressing antigen 85A boosts BCG-primed and naturally acquired antimycobacterial immunity in humans. *Nat Med* 2004;10(11):1240–4.
- [40] Kamath AT, Fruth U, Brennan MJ, et al. New live mycobacterial vaccines: the Geneva consensus on essential steps towards clinical development. *Vaccine* 2005;23(29):3753–61.

Original article

VIPOND, J., CLARK, S. O., HATCH, G. J., VIPOND, R., MARIE AGGER, E., TREE, J. A., WILLIAMS, A. & MARSH, P. D. 2006a. Re-formulation of selected DNA vaccine candidates and their evaluation as protein vaccines using a guinea pig aerosol infection model of tuberculosis. *Tuberculosis (Edinb)*, 86, 218-24.

Impact factor: 1.960

Contributions by HATCH, G. J.

Home Office – Personal Licence and Deputy Project Licence holder

Animal procedures – In vivo experimental design, aerosol challenge, necropsy

Study management – Liaison and co-ordination with sponsors and in vivo team, scheduling, reporting

Microbiological experimental work and data analysis

Manuscript review

Citation metrics

Google Scholar: 14 citations



Re-formulation of selected DNA vaccine candidates and their evaluation as protein vaccines using a guinea pig aerosol infection model of tuberculosis

Julia Vipond^{a,*}, Simon O. Clark^a, Graham J. Hatch^a, Richard Vipond^a,
Else Marie Agger^b, Julia A. Tree^a, Ann Williams^a, Philip D. Marsh^a

^aResearch Division, Health Protection Agency, Porton Down, Salisbury SP4 0JG, UK

^bDepartment of Infectious Disease Immunology, Statens Serum Institut, Artillerivej 5-2300, Copenhagen S, Denmark

Received 23 September 2005; accepted 20 January 2006

KEYWORDS

Tuberculosis;
Vaccination;
Subunit vaccine;
Mycobacterium
tuberculosis

Summary A selection of previously identified protective *Mycobacterium tuberculosis* DNA vaccines were re-formulated as proteins and administered with a Th1-inducing adjuvant to help stimulate the relevant immune responses necessary for protection. All three candidate-vaccines conferred high levels of antigen-specific cellular and humoral responses, as indicated by lymphocyte proliferation and serum IgG levels. Protective efficacy was also assessed in comparison with the current vaccine, BCG (the 'gold-standard' against which new vaccines are tested), and a saline (negative) control. One candidate (Rv1806-1807) induced protection in the guinea pig aerosol infection model 30 days post-challenge on the basis of reducing the bacterial burden of *M. tuberculosis* in the lungs.
© 2006 Elsevier Ltd. All rights reserved.

Introduction

Mycobacterium bovis bacille Calmette–Guérin (BCG) is currently the only vaccine available against tuberculosis (TB), and has been widely used since the 1950s. Although BCG is most effective in protecting children from the disease, the protec-

tion conferred by BCG vaccination against pulmonary TB in adults can range from 0% to 80%¹ depending on the population, global location and sub-strain of BCG used. Therefore, the development of a new alternative vaccine is a high priority.

The publication of the complete genome sequence of *M. tuberculosis*, and its subsequent re-annotation, has led to the identification of 3995 predicted protein-coding genes, of which 52% have an assigned function.^{2,3} Genomics, as a tool, is

*Corresponding author. Tel.: +44 1980 612584;
fax: +44 1980 611310.

E-mail address: julia.vipond@hpa.org.uk (J. Vipond).

underpinning vaccine development by defining some of the antigens in *M. tuberculosis* that can be classed as virulence factors. This knowledge has been used to benefit the development of DNA and subunit vaccines; for instance, secreted or surface-exposed proteins are widely regarded as good candidates due to their early contact with both the innate and acquired immune defence systems. In the development of new vaccines, an understanding of the protective immune response against *M. tuberculosis* is required. The major factor of protective immunity against *M. tuberculosis* is a T-cell-mediated response characterized, in particular, by secretion of IFN γ .^{4,5} DNA vaccines stimulate both the MHC Class II restricted and MHC Class I restricted antigen presentation pathways and are therefore good candidate vaccines against TB. However, despite the advances in DNA vaccination and the proof that they are safe and well tolerated,⁶ they have been unable to provide greater protective immunity against TB in comparison with BCG, even when they have elicited both humoral and cellular immune responses.^{7,8} The major problem with DNA vaccination is thought to be the potency, with as little as nanogram doses of synthesized protein being generated from microgram doses of initial DNA.⁹ In this study we re-formulated as protein, three DNA vaccines that we have previously shown to protect guinea pigs against a low dose of *M. tuberculosis* delivered via the aerosol route (Vipond et al., unpublished results). Aerosol infection of guinea pigs with a low dose of *M. tuberculosis* results in the progression of disease that is very similar to that seen in humans.¹⁰ The guinea pig is regarded as a more stringent model and for this reason we chose to screen our candidates directly in the guinea pig aerosol infection model. The genes of interest were sub-cloned into an *Escherichia coli* expression vector with an N- and C-terminal protein tag to facilitate purification, and were formulated with a Th1-inducing adjuvant. Both the protective efficacy following challenge from *M. tuberculosis*, and the generation of antigen-specific immune responses were evaluated.

Materials and methods

Bacterial strains and media

The *E. coli* DH5 α and RosettaTM 2(DE3)pLysS strains, used for cloning and expression, respectively, were routinely propagated in Luria Bertani (LB) broth and solid medium at 37 °C.

Construction of modified expression vector

Standard molecular biology techniques were used throughout.¹¹ The pET11d expression vector (Novagen) was modified as follows to create the new expression vector pET3a. The ampicillin cassette was excised from pET11d and replaced with a kanamycin resistance cassette. The internal *Hind*III site was removed by restriction digest and a new linker was inserted containing both the N- and C-terminal 6 \times histidine tag and respective cloning sites.

Cloning, expression and purification of vaccine candidates

The genes encoding the selected vaccine candidates were amplified from *M. tuberculosis* genomic DNA by PCR and cloned into pVAX1tPA using standard molecular biology techniques (Vipond et al., unpublished results). Following sequence confirmation, the genes encoding Rv1806, Rv1807, Rv2999, Rv3000 and Rv0847 were sub-cloned into pET3a in-frame to the N-terminal His-tag using *Hind*III and *Pvu*I restriction sites. The recombinant plasmids were transformed into *E. coli* RosettaTM 2(DE3)pLysS (Novagen). Transformed cells were grown in LB medium (containing 50 μ g/ml kanamycin and 34 μ g/ml chloramphenicol) at 37 °C until optical density (OD_{600nm}) reached 0.4–0.6. Induction was performed by addition of isopropyl-D-thiogalactopyranoside (IPTG) to a final concentration of 0.5 mM for 2.5 h at 30 °C. The induced cells were then harvested at 10,000g for 20 min at 4 °C. The bacterial pellet was lysed using BugBuster[®] (Novagen) and purified by nickel-iminodiacetic acid (Ni²⁺-IDA) technology (Novagen). Briefly, the cell pellet was resuspended in 5 ml BugBuster[®] per gram of wet cell paste and 25 units Benzonase Nuclease (Novagen) per ml of BugBuster[®]. Insoluble debris was removed by centrifugation at 16,000g for 20 min and the supernatant filtered through a 0.45 μ m syringe filter prior to loading on the pre-equilibrated His.Bind column (Novagen). Purification was performed according to the manufacturer's instructions, and the eluted protein captured in five 1 ml fractions.

Protein determination

Fractions were assayed for total protein concentration and analysed by SDS-PAGE using NuPAGE[®] 4–12% bis-tris polyacrylamide gels (Invitrogen). Protein concentration was determined by the Bradford method, using the Bio-Rad protein assay kit (Bio-

Rad) and bovine serum albumin as a standard. Proteins coded by genes within an operon (Rv1806-1807 and Rv2999-3000) were pooled together at equal concentrations. Endotoxin levels were measured by the gel-clot LAL assay (Bio Whittaker).¹²

Vaccination and aerosol infection of guinea pigs

Female Dunkin-Hartley guinea pigs (David Hall, Burton-on-Trent, UK) were vaccinated with purified protein formulated in adjuvant. Briefly, 100 µg of protein was injected intramuscularly into both hind quadriceps muscles of each guinea pig in 100 µl volume of dioctadecylammonium (DDA) and trehalose dibehenate (TDB) (500 µg DDA plus 100 µg TDB) stable liposomes (SSI) (10 animals per vaccine). Ten positive control animals were inoculated subcutaneously with 5×10^4 cfu BCG Pasteur, and 10 negative control animals received saline. Protein-vaccinated animals received booster vaccinations of 200 µg protein in adjuvant after 3 and 6 weeks. Six weeks after the final vaccination, six animals per group were aerosol challenged, using a contained Henderson apparatus with *M. tuberculosis* H37Rv (NCTC 7416) to give approximately 50 cfu per animal. Protection was assessed 30 days post-challenge on the basis of cfu in the lungs and spleen as described previously.¹³ Spleen and lung tissues were aseptically removed post-mortem and homogenized in 5 ml (spleen) or 10 ml (lung) sterile distilled water. Ten-fold dilutions of these samples were performed and plated onto Middlebrook 7H11 plus OADC selective agar. Plates were incubated at 37 °C and examined after 3 weeks for growth of *M. tuberculosis*. The mean log₁₀ cfu of test vaccines were compared with the negative controls and differences analysed statistically. The remaining four animals per group were terminally anaesthetized and blood removed by cardiac puncture for PBMC isolation (see below).

IgG enzyme-linked immunosorbant assay (ELISA)

Antibody titres were measured by ELISA on individual animal sera. Briefly, 96-well microtitre plates were coated overnight with the relevant antigen at 1 µg/ml in 0.1 M carbonate coating buffer (Sigma). The sera were diluted 1:100, followed by triplicate dilutions over 7 wells. All washes and incubations were performed at room temperature. The endpoint titre was determined as the final value where OD_{450 nm} > mean blank ± 2 SEM. Sera from the saline-vaccinated animals served as controls.

Isolation of PBMC and T-cell proliferation assays

Peripheral blood mononuclear cells (PBMC) were isolated from heparinized blood samples by the Ficoll-Hypaque density gradient method. The cells were cultured at 1×10^6 cells per ml in RPMI 1640 supplemented with 2 mM glutamine, 100 U/ml penicillin, 100 µg/ml streptomycin and 10% foetal calf serum (FCS) in flat-bottom 96-well microtitre plates with either 1 or 10 µg/ml of recombinant antigen, *M. tuberculosis* purified protein derivative (SSI, Denmark) (10 µg/ml), media only or lipopolysaccharide (Sigma) (1 EU/mg) in a humidified atmosphere of 5% CO₂ at 37 °C for 6 days. Incubations with the mitogen Concanavalin-A (ConA) (Sigma) (8 µg/ml) were carried out for a period of 3 days. Lymphocyte proliferation was measured by the incorporation of [³H]thymidine (Amersham) that was added at 1.0 µCi per well for the final 6–18 h of culture. The cells were harvested using a Skatron combi cell harvester (Skatron) and the amount of incorporated radiolabel was determined in a Tri-Carb liquid scintillation analyser (Perkin-Elmer). All tests were performed in triplicate wells. The proliferative response was expressed as the stimulation index (SI), which was calculated as follows: SI = mean counts per minute (cpm) of test antigen-stimulated cultures/mean cpm of unstimulated cultures in triplicate wells. A positive response to the proteins was based on the criterion that the SI was ≥ 2.0.

Statistical analysis

Values for the mean and standard error of the mean were calculated for each cfu data set. The Student *t*-test was used to determine the significance of differences. Probability values of <0.05 were taken as significant.

Results

Construction of pET3a

Figure 1 details the modified pET vector, pET3a, showing the inserted linker with the lac promoter and terminator, restriction cloning site and N- and C-terminal 6 × His tags. The original ampicillin marker was removed by restriction digest and replaced with a kanamycin cassette and the internal *Hind*III site was also removed which enabled the efficient sub-cloning of our selected DNA vaccines into the new protein expression

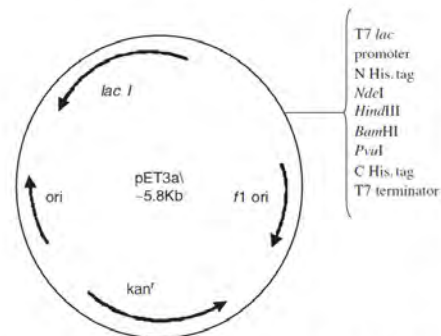


Figure 1 Schematic diagram of the modified pET vector showing the inserted linker containing the T7 promoter and terminator, restriction cloning sites and N- and C-terminal 6 × histidine tags.

vector. Selected genes (based on their protective efficacy as DNA vaccines) were sub-cloned from pVAX1tPA into pET3a and resultant clones confirmed by restriction analysis. The sequences of the genes were verified by sequencing using T7 primers and then transformed into *E. coli* Rosetta™(2) DE3 pLysS host strain for recombinant protein expression.

Expression and purification of recombinant *M. tuberculosis* proteins

The Rosetta™ 2 strains are BL21 derivatives designed to alleviate codon bias when expressing heterologous proteins in *E. coli* and were thus selected to enhance expression of the selected *M. tuberculosis* proteins. A selection of expression conditions were investigated and we found optimal conditions to be 0.5 mM final concentration IPTG at 30 °C for 2.5 h. Analysis of a sample from our induced cultures by SDS-PAGE revealed that our selected proteins were all expressed in the soluble fraction and purification could be performed using nickel-iminodiacetic acid (Ni²⁺-IDA) technology, relying on the 6 × His tags to bind the protein of interest to a column. Unbound proteins were washed away and the target protein recovered by elution. Purification was performed using pre-packaged His.Bind columns and buffer sets (Novagen) to prevent variability between different purifications. Purified, soluble proteins gave values of < 1.0 EU/mg protein as determined by the LAL endotoxin assay.

Protection against *M. tuberculosis* aerosol challenge

To evaluate any protective effect of the candidate vaccines, groups of 10 guinea pigs received three protein vaccinations formulated in DDA/TDB. Six of these animals received an aerosol challenge of *M. tuberculosis* H37Rv at week 15. Figure 2(A) and (B) shows protection in the lungs and spleens of vaccinated guinea pigs (expressed as viable *M. tuberculosis* log₁₀ cfu/ml) compared with saline and BCG. None of the candidates protected better than, or as well as, BCG but one vaccine (Rv1806-1807) gave a level of protection that was significantly better than saline ($p = 0.018$ in the lungs) and comparable with the previous results obtained following DNA vaccinations.

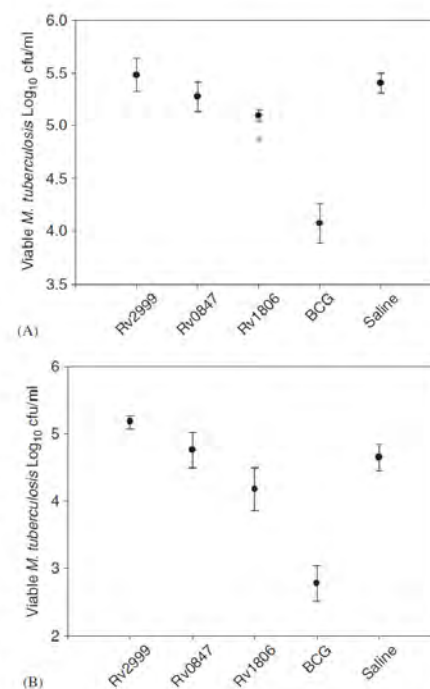


Figure 2 Protective efficacy of protein vaccines against aerosol challenge in a guinea pig model of TB. (A) Log₁₀ cfu viable bacteria in the lungs. The points indicate the mean values from 6 animals ± SEM and the asterisk indicates statistical significance compared to the saline group as determined by Student *t*-test ($p = 0.018$). (B) Viable bacteria (log₁₀ cfu) in the spleen.

Table 1 Antigen-specific PBMC proliferative responses from four individual animals, 6 weeks following final immunization.

SI of individuals animals following PBMC stimulation with respective antigens									
Animal	Rv0847			Rv1806			Rv2999		
	1 µg/ml	10 µg/ml	Saline	1 µg/ml	10 µg/ml	Saline	1 µg/ml	10 µg/ml	Saline
1	32.4	14.1	0.0	0.0	15.3	0.0	0.0	16.3	0.0
2	17.1	14.6	0.0	0.0	6.4	1.5	0.0	14.5	0.0
3	26.2	12.0	0.0	1.1	7.5	1.3	0.0	25.2	0.0
4	30.1	14.7	2.2	6.4	13.2	0.0	1.5	6.8	0.0

Cells were cultured in the presence of specific antigens (Rv0847, Rv1806-1807, Rv2999-3000) at 1 µg/ml or 10 µg/ml and saline. Results are expressed as a stimulation index (SI).

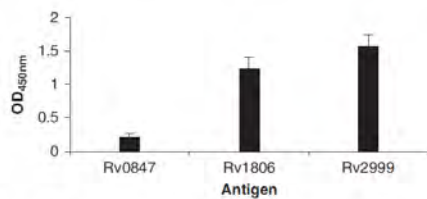


Figure 3 Antigen-specific serum IgG levels, 6 weeks following final immunization as measured by ELISA. Bars represent mean antibody levels (OD_{490nm}) from four animals at 10⁻³ sera dilutions ± 2SEM. Saline control data are not shown.

Antigen-specific cellular and humoral responses

Antigen-specific PBMC proliferative responses from individual animals were measured six weeks following the final immunization. Two concentrations of antigen were used to stimulate the cells (1 µg/ml or 10 µg/ml) (Table 1). The optimum antigen concentration for Rv0847 was 1 µg/ml whereas 10 µg/ml was the optimum for Rv1806 and Rv2999. The results are expressed as stimulation index (SI) and those >2 are considered biologically significant. All vaccinated animals demonstrated a greater proliferative response to stimulation with specific antigens compared to the control vaccine group that received saline.

ELISAs were used to test for antigen-specific serum IgG levels at 6 weeks following final immunization. All vaccine groups displayed high IgG titres (Fig. 3); however, titres for Rv1806 and Rv2999 were much higher than those with Rv0847 (endpoint titres for Rv1806 and Rv2999 were 1/72,900 compared with 1/2700 for Rv0847). This is in contrast to the SI values, which were greatest for

Rv0847 (mean = 26.45) compared with Rv1806 and Rv2999 (mean = 10.6 and 15.7, respectively). The use of a highly potent adjuvant in the vaccine formulation probably explains the high IgG titres observed.

Discussion

DNA vaccines have been found to be promising in small animal models (e.g. mice)^{7,8,14-16} but have generally been unable to transfer their protective success to larger animal models (e.g. guinea pigs and non-human primates).¹⁷⁻¹⁹ Consequently, we decided to re-formulate a selection of the protective DNA candidates identified from our previous study (Vipond et al., unpublished results), as proteins, and deliver them in a Th1-inducing adjuvant formulation. The two main issues requiring addressing for this study were the purification of protein and the selection of a suitable adjuvant.

Mycobacteria have a very high G-C content and unique codon usage, which can lead to problems for the recombinant production of some *M. tuberculosis* proteins in *E. coli*, the most commonly used host for over-expression.^{20,21} By using *E. coli* host strains that have been codon-optimized for G-C-rich organisms it can be possible to improve on poor expression yields. For this reason, we decided to use the RosettaTM 2 strain. The cells carry a chloramphenicol-resistant plasmid with the tRNA genes that decode seven rare codons (AGA, AGG, AUA, CUA, GGA, CCC, and CGG) to improve the yield of full-length proteins. In RosettaTM 2(DE3)-pLysS, the rare tRNA genes are present on the same plasmids that carry the T7 lysozyme gene. T7 lysozyme is a natural inhibitor of T7 RNA polymerase and serves to suppress activity of T7 RNA polymerase prior to induction, thus stabilizing

recombinants encoding target proteins that affect cell growth and viability. Expression of foreign proteins in *E. coli* often results in the formation of insoluble inclusion bodies; therefore, to reduce the chances of this occurring, we tested various IPTG concentrations and growth temperatures, with the optimal conditions for our proteins being a concentration of 0.5 mM IPTG and 2.5 h growth at 30 °C. Using this host strain and choice of conditions we were able to express and purify our selected proteins ready for testing in the animal model.

Immunologic control of *M. tuberculosis* infection is based on a cell-mediated response specific for mycobacterial proteins and in particular a Th1 T-cell response, but attempts at the correct protein and adjuvant combination have often been unsuccessful due to the lack of induction of cell-mediated immunity.²² Adjuvants are used because they are necessary to activate and direct the immune responses to the vaccine. The vaccine can often be poorly immunogenic and thus the need for an adjuvant that will deliver a suitable immune response is a major contributing factor to the success of any novel subunit vaccine.²³ Several types of adjuvant have been tested with respect to TB subunit vaccines, and monophosphoryl lipid A (MPL), DDA and TDB all display a degree of cellular stimulation.^{17,19,24-25} For this work, we chose to use stabilized DDA/TDB liposomes as this adjuvant has previously been found to promote the development of efficient and protective Th1 responses in the mouse model (Agger, unpublished results).

The guinea pig is regarded as a more stringent model of human TB than the mouse model and was used in our previous studies to select protective vaccines formulated as DNA. We sought to re-formulate, as protein, a selection of those DNA vaccines that were protective in the guinea pig following aerosol challenge. Although the protective efficacy relative to BCG remains the 'gold-standard' against which new vaccines are evaluated, other criteria may indicate the potential of novel vaccines to induce a protective immune response. These include antigen-specific proliferation and IFN γ secretion assays.^{26,27} Most vaccines that do not induce good levels of antigen-specific IFN γ do not induce effective immunity in animal models.²⁸ In this study, we were able to demonstrate good levels of humoral and cellular immunity to the vaccines, although the antigen-specific proliferation did not correlate with protection.

Only one of the vaccines, Rv1806-1807, was able to demonstrate a significant level of protection and this was comparable with the results obtained following DNA vaccination (a reduction in log₁₀ cfu of -0.52 and -0.83 in lungs and spleen, respec-

tively, following DNA vaccination, compared with reductions of -0.3 and -0.57, respectively, with a protein formulation in this study). We recognize that the ability of a sub-unit vaccine to reduce the bacterial burden at 30 days post-challenge is only one aspect of the potential of the vaccine to protect against TB infection in guinea pigs. This 'short-term' experimental design has been adopted in order to provide a screening system that enables us to reduce the number of promising candidates to be taken forward for further analysis. Candidate Rv1806-1807 has repeatedly demonstrated a level of protective efficacy in independent studies formulated as both DNA (Vipond et al., unpublished results) and protein in adjuvant. Further experiments evaluating other promising DNA vaccine candidates are in progress and we anticipate a final selection of two or three candidates from an original list of 47 vaccine candidates. Additional formulations and vaccination strategies, such as prime-boost, may be used to enhance the protective capacity of these final two or three most promising vaccines.

In conclusion, we were able to develop an expression vector that enabled us to efficiently sub-clone our promising DNA vaccines and optimize protein expression and purification in *E. coli*, thus leading to their re-formulation as protein vaccines. By delivering our vaccines in a Th1-inducing adjuvant we were able to demonstrate levels of humoral and cellular antigen-specific immune responses for all three candidates, and a level of protection against TB aerosol challenge in the guinea pig model for one of the candidates.

Acknowledgements

This study was funded by the Department of Health, UK. The views expressed in this publication are those of the authors and not necessarily those of the Department of Health. We acknowledge the support of the staff in the Biological Investigations Group at HPA, Porton Down and technical assistance in lymphocyte proliferation assays from Karen Gooch and Stuart Dowall.

References

1. Fine PE. Variation in protection by BCG: implications of and for heterologous immunity. *Lancet* 1995; **346**:1339-45.
2. Cole ST, Brosch R, Parkhill J, Garnier T, Churcher C, Harris D, et al. Deciphering the biology of *Mycobacterium tuberculosis* from the complete genome sequence. *Nature* 1998; **393**:537-44.

3. Camus JC, Pryor MJ, Medigue C, Cole ST. Re-annotation of the genome sequence of *Mycobacterium tuberculosis* H37Rv. *Microbiol* 2002;148:2967-73.
4. Caruso AM, Serbina N, Klein E, Triebold K, Bloom BR, Flynn JL. Mice deficient in CD4 T cells have only transiently diminished levels of IFN- γ , yet succumb to tuberculosis. *J Immunol* 1999;162:5407-16.
5. Tascon RE, Stravropoulos E, Lukacs KV, Colston MJ. Protection against *Mycobacterium tuberculosis* infection by CD8 T cells requires production of gamma interferon. *Infect Immun* 1998;66:830-4.
6. Donnelly J, Berry K, Ulmer JB. Technical and regulatory hurdles for DNA vaccines. *Int J Parasitol* 2003;33:457-67.
7. Derrick SC, Repique C, Snoy P, Yang AL, Morris S. Immunization with a DNA vaccine cocktail protects mice lacking CD4 cells against an aerogenic infection with *Mycobacterium tuberculosis*. *Infect Immun* 2004;72:1685-92.
8. Lima KM, dos Santos SA, Santos RR, Brandao IT, Rodrigues JM, Silva CL. Efficacy of DNA-hsp65 vaccination for tuberculosis varies with method of DNA introduction *in vivo*. *Vaccine* 2003;22:49-56.
9. Huygen K. Plasmid DNA vaccination. *Microbes Infect* 2005;7:932-8.
10. McMurray DN. Guinea pig model of tuberculosis. In: Bloom BR, editor. *Tuberculosis: pathogenesis, protection and control*. Washington: ASM; 1994. p. 135-47.
11. Ausebel FM. *Current protocols in molecular microbiology*. Chichester, USA: Wiley; 1992.
12. Levin J, Bang FB. The role of endotoxin in the extracellular coagulation of *Limulus* blood. *Bull Johns Hopkins Hosp* 1964;115:265-74.
13. Williams A, Davies A, Marsh PD, Chambers MA, Hewinson RG. Comparison of the protective efficacy of bacille Calmette-Guerin vaccination against aerosol challenge with *Mycobacterium tuberculosis* and *Mycobacterium bovis*. *Clin Infect Dis* 2000;30:S299-301.
14. Huygen K, Content J, Dennis O, Montgomery DL, Yawman AM, Deck RR, et al. Immunogenicity and protective efficacy of a tuberculosis DNA vaccine. *Nat Med* 1996;2:893-8.
15. Baldwin SL, D'Souza CD, Orme IM, Liu MA, Huygen K, Dennis O, et al. Immunogenicity and protective efficacy of DNA vaccines encoding secreted and non-secreted forms of *Mycobacterium tuberculosis* Ag85A. *Tuber Lung Dis* 1999;79:251-9.
16. Brandt L, Elhay M, Rosenkrands I, Lindblad EB, Andersen P. ESAT-6 subunit vaccination against *Mycobacterium tuberculosis*. *Infect Immun* 2000;68:791-5.
17. Baldwin SL, D'Souza C, Roberts AD, Kelly BP, Frank AA, Lui MA, et al. Evaluation of new vaccines in the mouse and guinea pig model of tuberculosis. *Infect Immun* 1998;66:2951-9.
18. Chambers MA, Williams A, Hatch G, Gavier-Widen D, Hall G, Huygen K, et al. Vaccination of guinea pigs with DNA encoding the mycobacterial antigen MPB83 influences pulmonary pathology but not hematogenous spread following aerogenic infection with *Mycobacterium bovis*. *Infect Immun* 2002;70:2159-65.
19. Olsen AW, Williams A, Okkels LM, Hatch G, Andersen P. Protective effect of a tuberculosis subunit vaccine based on a fusion of Antigen 85B and ESAT-6 in the aerosol guinea pig model. *Infect Immun* 2004;72:6148-50.
20. Laqueyrie A, Militzer P, Romain F, Eiglmeier K, Cole S, Marchal G. Cloning, sequencing and expression of the *apa* gene coding for the *Mycobacterium tuberculosis* 45/47-kDa secreted antigen complex. *Infect Immun* 1995;63:4003-10.
21. Oettinger T, Holm A, Mtoni IM, Andersen AB, Haslov K. Mapping of the delayed-type hypersensitivity-inducing epitope of secreted protein MPT64 from *Mycobacterium tuberculosis*. *Infect Immun* 1995;63:4613-8.
22. Flynn JL. Immunology of tuberculosis and implications in vaccine development. *Tuberculosis* 2004;84:93-101.
23. Schijns VEJC. Mechanisms of vaccine adjuvant activity: initiation and regulation of immune responses by vaccine adjuvants. *Vaccine* 2003;21:829-31.
24. Horwitz MA, Lee B-WE, Dillon BJ, Harth G. Protective immunity against tuberculosis induced by vaccination with major extracellular proteins of *Mycobacterium tuberculosis*. *Proc Natl Acad Sci* 1995;92:1530-4.
25. Hogarth PJ, Jahans KJ, Hecher R, Hewinson RG, Chambers MA. Evaluation of adjuvants for protein vaccines against tuberculosis in guinea pigs. *Vaccine* 2003;21:977-82.
26. Vordermeier HM, Chambers MA, Cockle PJ, Whelan AO, Simmons J, Hewinson RG. Correlation of ESAT-6-specific gamma interferon production with pathology in cattle following *Mycobacterium bovis* BCG vaccination against experimental bovine tuberculosis. *Infect Immun* 2002;70:3026-32.
27. Mustafa AS, Amoudy HA, Wiker HG, Abal AT, Ravn P, Oftung F, et al. Comparison of antigen-specific T-cell responses of tuberculosis patients using complex or single antigens of *Mycobacterium tuberculosis*. *Scand J Immunol* 1998;48:535-43.
28. Agger EM, Andersen P. A novel TB vaccine; towards a strategy based on our understanding of BCG failure. *Vaccine* 2002;21:7-14.

Available online at www.sciencedirect.com



Original article

VIPOND, J., VIPOND, R., ALLEN-VERCOE, E., CLARK, S. O., HATCH, G. J., GOOCH, K. E., BACON, J., HAMPSHIRE, T., SHUTTLEWORTH, H., MINTON, N. P., BLAKE, K., WILLIAMS, A. & MARSH, P. D. 2006b. Selection of novel TB vaccine candidates and their evaluation as DNA vaccines against aerosol challenge. *Vaccine*, 24, 6340-50.

Impact factor: 3.269

Contributions by HATCH, G. J.

Home Office – Personal Licence and Deputy Project Licence holder

Animal procedures – In vivo study design, aerosol challenge, necropsy.t

Study management – Liaison and co-ordination with sponsors and in vivo team, scheduling, reporting

Microbiological experimental work and data analysis

Manuscript review

Citation metrics

Google Scholar: 44 citations



Selection of novel TB vaccine candidates and their evaluation as DNA vaccines against aerosol challenge

Julia Vipond*, Richard Vipond, Emma Allen-Vercoe¹,
Simon O. Clark, Graham J. Hatch, Karen E. Gooch,
Joanna Bacon, Toby Hampshire², Helen Shuttleworth,
Nigel P. Minton³, Karen Blake, Ann Williams, Philip D. Marsh

Health Protection Agency, Porton Down, Salisbury SP4 0JG, UK

Received 30 January 2006; received in revised form 9 May 2006; accepted 15 May 2006
Available online 5 June 2006

Abstract

Putative TB vaccine candidates were selected from lists of genes induced in response to *in vivo*-like stimuli, such as low oxygen and carbon starvation or growth in macrophages, and tested as plasmid DNA vaccines for their ability to protect against *Mycobacterium tuberculosis* challenge in a guinea pig aerosol infection model. This vaccination method was chosen as it induces the Th1 cell-mediated immune response required against intracellular pathogens such as *M. tuberculosis*. Protection was assessed in the guinea pig model in terms of mycobacteria present in the lungs at 30 days post-challenge. Protection achieved by the novel candidates was compared to BCG (positive control) and saline (negative control). Four vaccines encoding for proteins such as PE and PPE proteins, a zinc metalloprotease and an acyltransferase, gave a level of protection that was statistically better than saline in the lungs. These findings have enabled us to focus on a sub-set of vaccine candidates for further evaluation using additional vaccination strategies.

© 2006 Elsevier Ltd. All rights reserved.

Keywords: *Mycobacterium tuberculosis*; DNA vaccine; Guinea pig

1. Introduction

Currently, the only available vaccine against tuberculosis (TB) is bacillus Calmette-Guérin (BCG) and has been received by over three billion people worldwide [1]. Although BCG is most effective in protecting children from the disease, its efficacy varies globally, ranging from 0% to 80% [2], so

that the development of an improved vaccine is a research priority [3].

The past two decades have seen a significant increase in the development of potential new vaccines for tuberculosis, due mainly to advances in the discovery and characterisation of *Mycobacterium tuberculosis* virulence factors, aided by the publication of the complete TB genome sequence [4]. Several methods of vaccine delivery have been used in pre-clinical screening of TB vaccines with no particular delivery route or formulation being favoured [5,6]. One method of delivering sub-unit vaccines is the direct delivery of DNA encoding the gene of interest. Here the genes encoding the protein antigens are delivered into host cells thereby enabling antigen production to occur *in vivo*. DNA vaccines stimulate both the MHC Class II restriction and MHC Class I restricted antigen presentation pathways, and the strong

* Corresponding author. Tel.: +44 1980 612584; fax: +44 1980 611310.

E-mail address: julia.vipond@hpa.org.uk (J. Vipond).

¹ Present address: Faculty of Medicine, University of Calgary, Alberta T2N 4N1, UK.

² Present address: Sigma-Aldrich Company Ltd., Fancy Road, Poole, Dorset BH12 4QH, UK.

³ Present address: Institute of Infection, Immunity and Inflammation, University of Nottingham, Nottingham NG7 2RD, UK.

CD8⁺ T cell response resulting from the MHC Class I presentation is a characteristic of DNA vaccines [7]. DNA vaccines have been used as a successful approach for several TB candidates [8–11] and are likely to remain a common formulation method for at least the initial evaluation of vaccine potential, especially with their ease of preparation and stability, plus the adjuvant effect that they elicit upon delivery. To enhance DNA vaccination, plasmids can encode for a secreted form of the protein by fusing the gene to the signal sequence of human tissue plasminogen activator (tPA), often including the 12-residue pro-sequence [12–15]. These are often more immunogenic than plasmids purely encoding the mature form of the protein [16] and inclusion of the pro-sequence is thought to enhance intracellular transport [17].

Two of the main models used for preclinical TB vaccine screening are the low-dose aerosol mouse and guinea pig models. The majority of the work has been carried out in various mouse models due to their low cost and the wealth of immunological reagents. However, there is an increased knowledge and availability of the guinea pig infection model of tuberculosis and new immunological reagents are continuously being developed, thus leading to an increase in vaccine testing in the guinea pig model [6,18–24]. Aerosol infection of guinea pigs with a low-dose of *M. tuberculosis* results in a progression of disease that is similar to that seen in humans [25]. The difference between vaccinated and unvaccinated guinea pigs tends to be greater than similarly treated mice and thus the guinea pig model is more discriminative than mice for vaccine evaluation [23]. Guinea pigs also develop delayed-type hypersensitivity (DTH) reactions that histologically closely resemble those of humans.

An effective sub-unit vaccine would have many advantages over a live, attenuated vaccine such as BCG, and in this study we used two complementary approaches to identify genes required for infection that could subsequently be used as vaccines. Differential fluorescence induction (DFI) was used to reveal genes expressed during mycobacterial growth in macrophages [26], while microarray and transcriptome analyses were undertaken on cells grown under defined and controlled conditions reflecting those likely to be encountered in the host [27,28].

In this study we evaluated DNA vaccines encoding selected genes for their ability to protect guinea pigs against a low-dose of *M. tuberculosis* delivered via the aerosol route. Candidates selected from those identified by DFI or controlled growth conditions were compared against the current vaccine, BCG and a saline control. Vaccine candidate efficacy in guinea pigs was assessed on the basis of reducing the bacterial burden of *M. tuberculosis* in the lungs at 30 days post-aerosol challenge. We report here that four of the selected genes were able to afford protection that was significantly better than the negative control group on two repeat experiments.

2. Materials and methods

2.1. Bacterial strains and plasmids

Escherichia coli strain DH5 α was cultured in Luria-Bertani medium as previously described [29]. Plasmid pVAX1 and Pfx DNA polymerase were obtained from Invitrogen, Paisley, UK. Endotoxin-free plasmid purification kits were used according to the manufacturer's instructions (Qiagen, Crawley, UK).

2.2. Selection of vaccine candidates

Lists of *M. tuberculosis* genes (data not shown) induced during infection of macrophages, were generated using differential fluorescence induction (DFI) as a silent marker of gene expression in a model of infection [26]. Briefly, *M. tuberculosis* H37Rv was transformed with a plasmid promoter library and a macrophage infection assay performed using J774A.1 cells (ECACC, Salisbury, UK). Multiple rounds of differential screening using a CL3-contained FACS sorter (Becton-Dickinson, New Jersey, USA) enabled induced promoters to be identified following sequencing of recovered plasmids from cell-sorted *M. tuberculosis* [30]. Genes that were up- or down-regulated in response to relevant environmental stresses, as determined by DNA microarray analysis, were selected from either an oxygen-depleted continuous culture [27] or a carbon-depleted stationary-phase model [28] of *M. tuberculosis*, respectively. Briefly, a sample of RNA was extracted from four independent chemostat cultures grown under both oxygen-replete and oxygen-depleted conditions, and from one culture grown under carbon-depleted conditions, and then used for DNA microarray as described previously [27,28]. Genes showing statistically significant changes in expression level were selected by at least a 1.5-fold change in expression combined with Welch's approximate *t*-test and a *P*-value cut off of 0.05. Expression levels of at least 5-fold higher or lower at day 50 relative to day 5 were used for those genes identified from the stationary-phase culture. The analysis of expression levels was performed using GeneSpring software and information can be found at the Agilent Technologies website [31]. Selection criteria (e.g., novel, secretory, homology to known virulence factors and predicted expression level) were applied to these lists to identify a sub-set of genes that were likely to provide novel vaccine candidates (Table 1).

2.3. DNA vaccine vector construction

Standard molecular biology techniques were used throughout [29]. The plasmid pVAX1 was designed in accordance with the FDA guidelines for DNA vaccine vectors. The basic vector containing the cytomegalovirus (CMV) immediate/early promoter and bovine growth hormone (bgh) polyadenylation sequence, was modified by the introduction of linkers encoding the signal peptide and pro-sequence

Table 1
Selected vaccine candidates with their predicted functions and conditions from which they were identified

Group number	Vaccine candidate	H37Rv gene	Predicted function	Identifying growth condition
1	1	Rv1477	Putative exported p60 homologue	DFI ^a
		Rv1478	Hypothetical Invasion protein	
	2	Rv1994c	Transcriptional regulatory protein	Up-regulation under low oxygen
	3	Rv1919c	Conserved hypothetical protein	DFI
	4	Rv3174	Probable short-chain dehydrogenase	Up-regulation under low oxygen
	5	Rv3402c	Conserved hypothetical protein	Up-regulation under low oxygen
	6	Rv2462 <i>tig</i>	Probable trigger-factor protein	DFI
2	7	Rv1344	Probable acyl-carrier proteins	Up-regulation under low oxygen
		Rv1345 <i>fadD33</i>	Possible polyketide synthase	
		Rv1346 <i>fadE14</i>	Possible acyl Co-A dehydrogenase	
	8	Rv1130	Conserved hypothetical protein	Up-regulation under low oxygen
		Rv1131 <i>gltA1</i>	Probable citrate synthase	
		Rv1132	Conserved membrane protein	
	9	Rv2386c <i>mbt1</i>	Putative isochorismate synthase	Up-regulation under low oxygen
	10	Rv0251c <i>hsp</i>	Heat shock protein	Up-regulation under low oxygen and carbon starvation
	11	Rv0384c <i>clpB</i>	Probable ATP-binding protein	DFI
	12	Rv1179c	Hypothetical protein	DFI
13	Rv0111	Acyltransferase	Up-regulation under carbon starvation and high oxygen	
3	14	Rv1646 PE17	PE protein	DFI
	15	Rv1799 <i>lppT</i>	Probable lipoprotein	Up-regulation under high oxygen
	16	Rv1917c PPE34	PPE protein	Up-regulation under carbon starvation and high oxygen
		Rv1909c <i>furA</i>	Ferric uptake regulatory protein	DFI
	17	Rv1910c	Probable exported protein	
		Rv1911c <i>lppC</i>	Probable lipoprotein	
		Rv1912c <i>fadB5</i>	Possible oxidoreductase	
		Rv0913c	Possible dioxygenase	Up-regulation under carbon starvation and high oxygen
	18	Rv0914c	Possible lipid carrier protein	
		Rv0915c PPE14	PPE family protein	
Rv0916c PE7		PE family protein		

Table 1 (Continued)

Group number	Vaccine candidate	H37Rv gene	Predicted function	Identifying growth condition
4	19	Rv2671 <i>ribD</i>	Possible riboflavin biosynthesis protein	DFI
		Rv2672	Possible secreted protease	
	20	Rv2673	Possible conserved integral membrane protein	
		Rv2037c	Possible transmembrane protein	DFI and up-regulation under carbon starvation
	21	Rv2038c	Probable sugar-transport ATP-binding protein	
		Rv2039c	Probable sugar-transport integral ABC transporter	
		Rv2040c	Probable sugar-transport integral ABC transporter	
	22	Rv2041c	Probable sugar-binding lipoprotein	
		Rv1167c	Probable regulatory protein	
	23	Rv1168c PPE17	PPE family protein	Up-regulation under low oxygen
Rv1169c PE11		PE family protein		
24	Rv0785	Conserved hypothetical protein	Up-regulation under carbon starvation	
	Rv3639c	Conserved hypothetical protein	Up-regulation under low oxygen	
25	Rv0847 <i>lpqS</i>	Probable lipoprotein	Up-regulation under low oxygen	
	Rv0395	Hypothetical protein	Up-regulation under carbon starvation and low oxygen	
5	26	Rv0396	Hypothetical protein	
		Rv0397	Conserved repeat family protein	
	27	Rv3444c <i>esxT</i>	Putative ESAT-6 like protein	
		Rv3445c <i>esxU</i>	Putative ESAT-6 like protein	
		Rv3446c	Hypothetical alanine and valine rich protein	Up-regulation under low oxygen
28	Rv3447c	Probable conserved membrane protein		
	Rv2316 <i>uspA</i>	Probable ABC sugar transport	Up-regulation under high oxygen	
	Rv2317 <i>uspB</i>	Probable sugar transport membrane protein		
29	Rv2318 <i>uspC</i>	Probable periplasmic sugar-binding lipoprotein		
	Rv0816c <i>thiX</i>	Probable thioredoxin	Up-regulation under high oxygen	
30	Rv0817c	Probable conserved exported protein		
	Rv2667 <i>clpC2</i>	Possible ATP-dependent protease	Up-regulation under high oxygen	
	Rv2668	Possible exported alanine and valine rich protein		
	Rv2669	Conserved hypothetical protein		

Table 1 (Continued)

Group number	Vaccine candidate	H37Rv gene	Predicted function	Identifying growth condition
6	30	Rv1840c	PE-PGRS protein	Up-regulation under low oxygen
		Rv1841c	Conserved hypothetical membrane protein	
		Rv1842c	Conserved hypothetical membrane protein	
	31	Rv0198c	Probable zinc metalloprotease	Down-regulation under carbon starvation
	32	Rv0228	Probable acyltransferase	Up-regulation under carbon starvation
	33	Rv2999 <i>lppY</i>	Probable conserved lipoprotein	
		Rv3000	Conserved hypothetical membrane protein	Up-regulation under low oxygen
	34	Rv1806 PE20	PE protein	Up-regulation under carbon starvation
	35	Rv1807 PPE31 Rv3812 PE-PGRS62	PPE family protein PE-PGRS protein	Up-regulation under low oxygen
	36	Rv1228 <i>lpqX</i>	Probable lipoprotein	Up-regulation under low oxygen
37	Rv2516c	Hypothetical protein	Up-regulation under low oxygen	
7	38	Rv0544c	Possible conserved transmembrane protein	Down-regulation under carbon starvation
		Rv0545c <i>pitA</i>	Probable low affinity inorganic phosphate transporter	
	39	Rv1342c Rv1343c <i>lprD</i>	Conserved membrane protein Probable conserved lipoprotein	Up-regulation under low oxygen
		Rv3756 <i>proZ</i>	Possible osmoprotectant	Up-regulation under low oxygen
	40	Rv3757 <i>proW</i> Rv3758 <i>proV</i> Rv3759 <i>proX</i>	Possible osmoprotectant Possible osmoprotectant Possible osmoprotectant	
41	Rv2896c	Conserved hypothetical protein		
	Rv2897c	Conserved hypothetical protein	Up-regulation under high oxygen	
	Rv2898c	Conserved hypothetical protein		
8	42	Rv1761c	Hypothetical exported proteins	Up-regulation under high oxygen
		Rv1762c	Hypothetical protein	
	43	Rv0848 <i>cysK2</i> Rv0849	Possible cysteine synthase Probable conserved integral membrane transport protein	Up-regulation under carbon starvation
	44	Rv0917 <i>betP</i>	Glycine betaine transporter	Up-regulation under carbon starvation
45	Rv1633 <i>ivrB</i>	Probable exonuclease	Up-regulation under low oxygen	
46	Rv1634	Possible drug efflux membrane protein		
	Rv2144c	Probable transmembrane protein	Down-regulation under carbon starvation	
	Rv2145c <i>wag3I</i>	Conserved hypothetical protein		

Table 1 (Continued)

Group number	Vaccine candidate	H37Rv gene	Predicted function	Identifying growth condition
47		Rv2460c <i>clpP2</i>	Probable ATP-dependent clp protease	DFI
		Rv2461c <i>clpP1</i>	Probable ATP-dependent clp protease	

Where an identified gene formed an operon then each gene within that operon was represented in the vaccine with an equal concentration of DNA. Vaccines were evaluated in eight independent experiments, designated groups 1–8.

^a Differential fluorescence induction, used to identify genes expressed during growth in macrophages.

of tPA to form pVAX1tPA. To allow studies on candidate expression *in vitro*, a linker encoding a 6-His tag was inserted into the vector to form the derivative pVAX1tPAHIS. PCR amplification of the gene encoding eGFP (Clontech, Oxford, UK) and ligation of the amplified fragment into pVAX1tPAHIS created a second *in vitro* expression vector pVAX1tPAeGFPHIS. All vectors contained in-frame cloning sites with compatible cohesive ends corresponding to those introduced into the ends of cloned antigens by PCR; these were AT-rich, and thus rare (*HindIII*) or absent (*PacI*) in the *M. tuberculosis* genome.

2.4. DNA vaccine construction

Selected vaccine candidate genes were screened for the presence of a predicted signal peptide using SignalP [32]. All of the genes were amplified from *M. tuberculosis* H37Rv chromosomal DNA using *Pfx* polymerase (Invitrogen), using primers designed from the *M. tuberculosis* genome sequence database. Primers incorporated restriction sites to allow in-frame fusion to the tPA signal peptide/pro sequence at the start of the mature gene sequence (minus the start codon) and the 6-His tag at the carboxy terminus where required. PCRs were carried out using cycle conditions of 95 °C, 1 min, followed by 30 cycles of 95 °C, 15 s, 60 °C, 15 s, 68 °C, 15 s, followed by a final extension of 68 °C, 7 min. PCR amplified genes were cloned into pVAX1tPA. Selected clones were verified by sequencing, following analysis by restriction digestion. The sequenced gene fragments were sub-cloned into a related vector for *in vitro* studies (pVAX1tPAeGFPHIS). Large-scale endotoxin-free preparations of plasmid (Qiagen) were then made to obtain plasmid DNA at 1 mg/ml (total of 6 mg per candidate). Where the vaccine candidate was comprised of more than one gene (e.g., an operon such as vaccine candidate 7, Table 1) then each gene within that operon was represented in the vaccine with an equal concentration of plasmid DNA.

2.5. *In vitro* expression

Vaccine candidates were sub-cloned into pVAX1tPAeGFPHIS and transfected into COS-7 cells (ECACC, Salisbury, UK) grown on poly-D-lysine coated cover slips

(BD Bioscience) using Lipofectamine 2000™ (Invitrogen). COS-7 cells were maintained in DMEM (supplemented with 100 U/ml penicillin, 100 µg/ml streptomycin, 10% foetal calf serum and 2 mM glutamine) at 37 °C and 5% CO₂ for 24 h. Cells were viewed 24 h post-transfection using a FITC filter on a fluorescence microscope at a wavelength of 460–500 nm.

2.6. Vaccination and aerosol infection of guinea pigs

Female Dunkin–Hartley guinea pigs (David Hall, Burton-on-Trent, UK) were vaccinated with plasmid DNA constitutively expressing selected TB genes. Briefly, 100 µg of DNA was injected intramuscularly into both hind quadriceps muscles of each guinea pig (six animals per group). As it was not possible to evaluate all 47 candidates in 1 experiment, they were divided into 8 groups for evaluation (generally 6 candidates plus controls). Each vaccination group also contained both positive (BCG) and negative (saline) controls against which the vaccine candidates were assessed. One group also included an empty vector control to ensure there were no non-specific mechanisms of protection. The six positive control animals were inoculated sub-cutaneously with 5×10^4 cfu BCG Pasteur, and six negative control animals received saline. DNA-vaccinated animals received booster vaccinations as above after 3 and 6 weeks. Six weeks after the final vaccination animals were aerosol challenged, using a contained Henderson apparatus with *M. tuberculosis* H37Rv (NCTC 7416) to give a retained dose in the lung of approximately 20–50 cfu per animal [33].

Protection was assessed 30 days post-challenge as described previously [33]. Lung tissue was aseptically removed post-mortem and homogenised in 10 ml sterile distilled water. Ten-fold dilutions of these samples were performed (10^{-1} , 10^{-2} , 10^{-3}) and plated onto Middlebrook 7H11 plus OADC selective agar. Plates were incubated at 37 °C and examined after 3 weeks for growth of *M. tuberculosis*. Vaccine efficacy was assessed in terms of reduction in bacterial counts in lungs compared to the saline control group. The mean log₁₀ cfu of test vaccines were compared with the negative controls and differences analysed statistically (see below).

2.7. Statistical analysis

Values for the mean and standard error of the mean were calculated for each data set. Data was analysed both by the Student's *t*-test and ANOVA, using Fisher's pair-wise comparisons to compare the mean values of all the groups in the experiments. Probability values of <0.05 were taken as significant and promising candidates were re-assessed in repeat groups.

3. Results

3.1. Vaccine candidate selection

M. tuberculosis genes initially identified as possible vaccine candidates, included (i) those genes that were induced in response to infection and growth in macrophage (identified by DFI [26,30]), and (ii) those that were up- or down-regulated in response to oxygen and carbon limitation (identified by DNA microarray analysis of mRNA isolated from cultures [27,28]). Lists of genes were then subjected to further selection to reduce the number of candidates. The selection criteria against which the candidates were chosen were:

- (1) Novel: to our knowledge, all candidates that were selected were not patented, published or being investigated by others as a TB vaccine at the time of the study.
- (2) Secretory: secreted antigens were considered to make better candidates for activation of both CD4⁺ and CD8⁺ T cells, thereby explaining why the majority of immunogenic TB antigens are those present in the culture filtrate of *M. tuberculosis*. This was investigated by the use of SignalP (a program that predicts the presence and location of signal peptide cleavage sites based on a combination of several neural networks and hidden Markov models) [32]. Approximately 60% of selected candidates were predicted to be secreted using this approach.
- (3) Supporting data: if the candidate was identified from more than one growth condition then there was more sup-

porting data for its inclusion as a vaccine candidate (six candidates met this criterion). Also, a focus on candidates that had a virulence-associated function, or homology to known virulence factors, increased the chances of the candidate having a potential role in infection.

- (4) Predicted expression levels: where available, published data detailing predicted gene expression levels, indicating genes that are highly expressed, were used to select several candidates (data not shown) [34–36].

Ultimately 47 vaccine candidates (comprising 92 genes) were selected using the above criteria from the lists of DNA microarray analysis of cultures grown under defined conditions and candidates identified by DFI (Table 1).

3.2. Construction of pVAX1tPA and pVAX1tPAeGFPHis vectors

Fig. 1 details pVAX1tPA showing the orientation of the CMV promoter (P_{CMV}), tPA signal peptide/pro-sequence (tPA), restriction cloning site (RCS) and bgh polyadenylation sequence (bgh). Plasmid pVAX1tPAeGFPHis shows the cloned His tag (His) and the eGFP fragment used for immunofluorescence detection. DNA fragments of the selected vaccine candidates obtained by PCR were digested with each restriction endonuclease and ligated into *Pac*I- and *Hind*III-digested plasmid pVAX1tPA. The resultant clones were confirmed by restriction analysis and DNA sequencing (data not shown).

3.3. In vitro expression

Positively identified vaccine clones were sub-cloned into pVAX1tPAeGFPHis to evaluate expression *in vitro* prior to vaccination. COS-7 cells (ECACC, Salisbury, UK) were transfected with the positive clones using Lipofectamine 2000TM (Invitrogen). eGFP fluorescence in COS-7 cells transfected with the positive vaccine clones confirmed the ability of the plasmid to produce the protein. All genes were shown to be expressed prior to vaccination (data not shown).

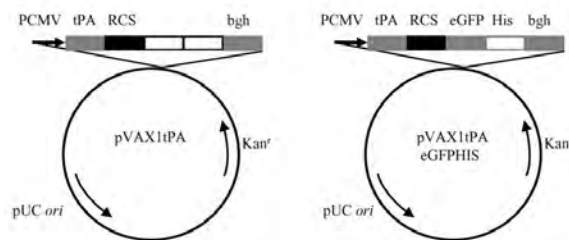


Fig. 1. Schematic diagram of the various forms of pVAX1tPA showing orientation of the CMV promoter (P_{CMV}), tPA signal peptide/pro-sequence (tPA), restriction cloning site (RCS) and bgh polyadenylation sequence (bgh). Plasmid pVAX1tPAeGFPHis shows the cloned eGFP fragment used for immunofluorescence detection.

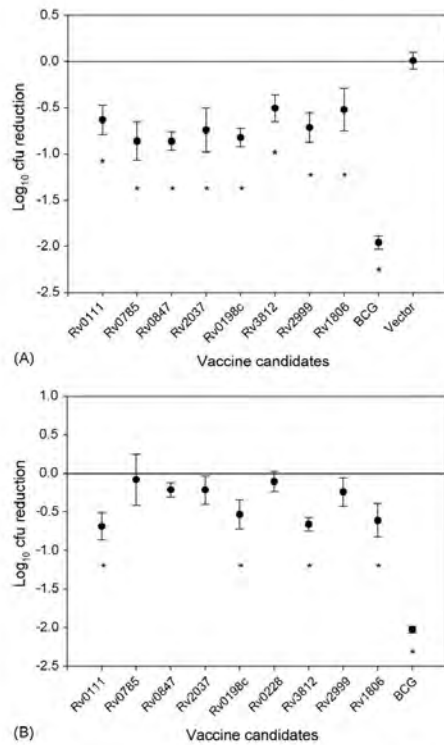


Fig. 2. (A) Bacterial log₁₀ reduction in the lungs, compared to saline control, as a marker of DNA vaccine candidate efficacy following aerosol challenge with *M. tuberculosis* H37Rv. (B) Bacterial log₁₀ reduction following a repeat challenge experiment. The bars indicate the mean ± S.E. (n=6), *P < 0.05 (Student's *t*-test).

3.4. Protection against *M. tuberculosis* aerosol challenge

To evaluate any potential protective effect of the candidate vaccines, groups of six guinea pigs received three DNA vaccinations followed by an aerosol challenge of H37Rv at week 15. Fig. 2(A) shows log₁₀ cfu reduction from saline in lungs of animals challenged with virulent *M. tuberculosis* by the aerosol route. The antigens used for vaccination are indicated and the results are the mean ± S.E. from groups of six guinea pigs. Also included in the evaluation was an empty vector control group to ensure there was no non-specific protection. The experiment was repeated with the DNA vaccine candidates that showed statistically significant cfu reduction in the lungs compared to saline, and these are shown in Fig. 2(B).

In summary, none of the candidates protected better than or as well as BCG, although eight candidates gave a level

of protection that was better than the saline or vector control groups in the lungs on the first evaluation. Four of these candidates (Rv0111, Rv0198c, Rv3812 and Rv1806–1807) displayed protection that was statistically better than saline, by the Student's *t*-test (*p* < 0.05) and ANOVA, after the second repeat experiment (Fig. 2 and Table 2), but there was no statistically significant difference between these candidates.

4. Discussion

Complementary approaches have been used to identify genes that were expressed or up- or down-regulated under conditions that *M. tuberculosis* might encounter in the host and which could, therefore, be considered as potential vaccine candidates. DFI was used as a silent marker of gene expression to reveal TB genes induced during uptake and replication in the macrophage, a key step in the infection process, while the controlled environment culture studies enabled us to grow *M. tuberculosis* in a defined and virulent physiological state under conditions relevant to the host (low oxygen [27], carbon starvation [28]). The strategy for identifying putative protective antigens from the gene lists generated from the DFI studies and from microarray analysis of extracted RNA, was based upon specific selection criteria (e.g., proteins likely to be secreted and thus more accessible to the immune system, genes that were identified by more than one approach, genes that were novel, and any additional supporting data such as putative virulence-associated functions). This enabled a short-list of 47 candidates to be drawn up for evaluation out of a total of several hundred genes. Lists of genes have also been generated by others studying the gene expression profile of *M. tuberculosis* [37,38]. In one of these studies, where changes in the expression profile of H37Rv and a *sigH* mutant were examined in response to the oxidising agent, diamide, two of our vaccine candidates were identified. Rv0251c was shown to be induced due to this general stress response in a *sigH*-independent manner and Rv1130 in a *sigH*-dependent manner [37]. This provided subsequent confirmatory data (to our finding of induction under low oxygen and carbon starvation) that these genes are involved in the response to stresses that may be encountered *in vivo* and therefore could be relevant targets for a directed immune response. The selected 47 candidates were systematically evaluated for their ability to protect guinea pigs against a low-dose of *M. tuberculosis* compared with BCG and a saline control.

There was no obvious relationship between the putative functions of the four candidates that were protective in both the first and second rounds of evaluation. Three of the candidates, PE and PPE proteins (Rv1806–1807, Rv3812) and an acyltransferase (Rv0111), were up-regulated under conditions of stress that may be encountered in the host (oxygen and carbon starvation) and were thought to be important in the stress response or in persistence. Approximately 10% of the *M. tuberculosis* genome is allocated to the PE and PPE gene families, and although their exact function is unknown,

Table 2
Viable *M. tuberculosis* log₁₀ cfu counts in the lungs from guinea pigs vaccinated with DNA vaccines compared to unvaccinated (saline) animals and BCG-vaccinated animals relevant to each experiment group

Vaccine	First evaluation log ₁₀ cfu	Log ₁₀ reduction ^a	Second evaluation log ₁₀ cfu	log ₁₀ reduction ^a
BCG ^b	3.79 ± 0.12	2.11	3.23 ± 0.14	2.01
Saline	5.90 ± 0.21	0.00	5.24 ± 0.08	0.00
Rv0111 ^c	5.21 ± 0.11	0.69	4.55 ± 0.17	0.69
BCG ^b	3.49 ± 0.34	1.77	3.45 ± 0.32	1.96
Saline	5.26 ± 0.33	0.00	5.41 ± 0.20	0.00
Rv0785	4.41 ± 0.20	0.85	5.33 ± 0.33	0.08
Rv0847	4.40 ± 0.10	0.86	5.20 ± 0.09	0.21
Rv2037	4.52 ± 0.23	0.74	5.20 ± 0.18	0.21
BCG ^b	3.23 ± 0.14	2.01	3.45 ± 0.10	2.1
Saline	5.24 ± 0.08	0.00	5.55 ± 0.20	0.00
Rv0198c ^c	4.42 ± 0.10	0.82	5.02 ± 0.19	0.53
Rv3812 ^c	4.73 ± 0.14	0.51	4.89 ± 0.09	0.66
Rv2999	4.53 ± 0.16	0.71	5.31 ± 0.18	0.24
Rv1806 ^c	4.72 ± 0.23	0.52	4.94 ± 0.21	0.61

The values given are means (±S.E.) (n=6) for both the first and second evaluations.

^a log₁₀ reduction in cfu compared to saline.

^b p < 0.01 for first and second evaluations.

^c p < 0.05 for first and second evaluations.

a similar example has been observed where unknown surface antigens of other pathogens that are targets for the host's immune response have been used as vaccine candidates [39]. Interestingly, TB patients have been shown to mount an immune response to PE proteins, in particular Rv1759 and Rv3367 [7,36], and a significant proportion of BCG-vaccinated donors have been found to recognise the PPE protein, Rv3873 [40]. Mice have also been shown to produce antibodies to the PE_PGRS protein encoded by Rv1818c following an aerosol infection with *M. tuberculosis* [41]. These data indicate that at least some of the genes belonging to this family are expressed by *M. tuberculosis in vivo* and could be recognised by the host immune response. Although there is no supporting evidence for the use of an acyltransferase as a vaccine candidate, other than the consistent results we obtained, such a protein may play a critical role in enzyme activity, such as in lipid metabolism and cell wall biosynthesis. We are currently trying to establish a guinea pig model of chronic infection, aimed at simulating latency, and studies to identify whether Rv0111 is expressed in acute or chronically infected guinea pigs are underway. The fourth candidate, a zinc metalloprotease (Rv0198c), was selected based on its possible virulence-associated function. Unlike the other candidates, this gene was down-regulated under carbon starvation. This may reflect a shift in expression towards a general stress response, whereby the bacterium is tightly regulating its virulence factors and expressing them only when required, and in this instance, not during carbon starvation. Zinc metalloproteases are widely distributed in both Gram positive and Gram negative bacteria, and although a role as a virulence factor in *M. tuberculosis* has not been identified, they have been proposed as a major virulence determinant in several pathogens, e.g. *Burkholderia cenocepacia*, *Clostridium botulinum* and *Bacillus anthracis* [42–45].

Many TB vaccine candidates have been identified using the mouse challenge model; however, some of these candidates are not necessarily protective when they are progressed through the hierarchy of animal models, in particular the guinea pig [18,21,46–48]; a notable exception to this is *M. tuberculosis* 72 kDa fusion polypeptide, where survival in the guinea pig has been shown to be comparable with BCG [49,50]. The guinea pig is regarded as a more stringent model of human tuberculosis than the mouse model and for this reason it is widely used to evaluate new vaccines. Consequently, we chose to screen candidates for protective efficacy directly in the guinea pig aerosol infection model. This strategy of using a more discriminatory screening model, together with our selection criteria, enabled us to reduce the number of candidates to be evaluated to a manageable number and to identify four that afforded a significant and reproducible level of protection. The levels of protection seen in our study are comparable to other DNA vaccines tested in the guinea pig model (e.g. Ag85A and Mtb72f), with a cfu log reduction of between 0.5 and 1.0 [18,50,51]. Sub-unit vaccines (delivered as either protein adjuvant or naked DNA) generally afford lower and rarely equal protection to BCG against challenge with *M. tuberculosis* in guinea pigs; however, prime-boost strategies are able to enhance the level of protection. In these strategies DNA can be used to prime the immune response, then a second vaccination is used to induce a greater response, or BCG can be used as the prime followed by a sub-unit boost [52]. The regimen of DNA as a prime for the Th1 and MHC Class I type immune response, followed by a subsequent protein boost has been used successfully with HIV and malaria [53,54]. Thus, the prime-boost regimen may be the most effective approach in the future for DNA vaccination, particularly in larger animal models.

In conclusion, we have demonstrated the success of using our selection process coupled with the more stringent guinea pig model to move from lists of several hundred potential vaccine candidates down to four that afforded a significant level of protection. We have shown that a plasmid-based system is ideal for screening large numbers of candidate vaccines with respect to relative ease of preparation, cost and time; however, DNA vaccination is likely to be more effective in larger animal models and humans when administered as a prime-boost vaccination regimen, or when given as a combination approach with BCG. These delivery approaches will be used to further evaluate a selection of the protective candidates identified in this study.

Acknowledgements

This study was funded by the Department of Health, UK. The views expressed in this publication are those of the authors and not necessarily those of the Department of Health. We acknowledge the support of the staff in the Biological Investigations Group at HPA, Porton Down, the technical expertise of Kim Hatch, and members of the TB group for constructive discussions on vaccine candidate selection.

References

- [1] Andersen P, Doherty TM. TB subunit vaccines—putting the pieces together. *Microbes Infect* 2005;7(5–6):911–21.
- [2] Fine PE. Variation in protection by BCG: implications of and for heterologous immunity. *Lancet* 1995;346(8986):1339–45.
- [3] McMurray DN. Recent progress in the development and testing of vaccines against human tuberculosis. *Int J Parasitol* 2003;33(5–6):547–54.
- [4] Cole ST, Brosch R, Parkhill J, Garnier T, Churcher C, Harris D, et al. Deciphering the biology of *Mycobacterium tuberculosis* from the complete genome sequence. *Nature* 1998;393(6685):537–44.
- [5] Brennan MJ. The tuberculosis vaccine challenge. *Tuberculosis (Edinburgh)* 2005;85(1–2):7–12.
- [6] Izzo A, Brandt L, Lasco T, Kipnis A-P, Orme I. NIH pre-clinical screening program: overview and current status. *Tuberculosis (Edinburgh)* 2005;85(1–2):25–8.
- [7] Doria-Rose NA, Haigwood N. DNA vaccine strategies: candidates for immune modulation and immunization regimens. *Methods* 2003;31(3):207–16.
- [8] Tascon RE, Colston MJ, Ragno S, Stavropoulos E, Gregory D, Lowrie DB. Vaccination against tuberculosis by DNA injection. *Nat Med* 1996;2(8):888–92.
- [9] Huygen K, Content J, Denis O, Montgomery DL, Yawman AM, Deck RR, et al. Immunogenicity and protective efficacy of a tuberculosis DNA vaccine. *Nat Med* 1996;2(8):893–8.
- [10] Lowrie DB, Silva CL, Colston MJ, Ragno S, Tascon RE. Protection against tuberculosis by a plasmid DNA vaccine. *Vaccine* 1997;15(8):834–8.
- [11] Reed SG, Alderson MR, Dalemans W, Lobet Y, Skeiky YAW. Prospects for a better vaccine against tuberculosis. *Tuberculosis (Edinburgh)* 2003;83:213–9.
- [12] Burke RL, Pacht C, Quiroga M, Rosenberg S, Haigwood N, Nordfang O, et al. The functional domains of coagulation factor VIII:C. *J Biol Chem* 1986;261(27):12574–8.
- [13] Chapman BS, Thayer RM, Vincent KA, Haigwood NL. Effect of intron A from human cytomegalovirus (Towne) immediate-early gene on heterologous expression in mammalian cells. *Nucl Acids Res* 1991;19(14):3979–86.
- [14] Leitner WW, Seguin MC, Ballou WR, Seitz JP, Schultz AM, Sheehy MJ, et al. Immune responses induced by intramuscular or gene gun injection of protective deoxyribonucleic acid vaccines that express the circumsporozoite protein from *Plasmodium berghei* malaria parasites. *J Immunol* 1997;159(12):6112–9.
- [15] Berg DT, Grinnell BW. Signal and propeptide processing of human tissue plasminogen activator: activity of a pro-tPA derivative. *Biochem Biophys Res Commun* 1991;179(3):1289–96.
- [16] Baldwin SL, D'Souza CD, Orme IM, Liu MA, Huygen K, Denis O, et al. Immunogenicity and protective efficacy of DNA vaccines encoding secreted and non-secreted forms of *Mycobacterium tuberculosis* Ag85A. *Tuber Lung Dis* 1999;79(4):251–9.
- [17] Kohne C, Johnson A, Tom S, Peers DH, Gehlert RL, Hotaling TA, et al. Secretion of glycosylation site mutants can be rescued by the signal/pro sequence of tissue plasminogen activator. *J Cell Biochem* 1999;75(3):446–61.
- [18] Baldwin SL, D'Souza CD, Roberts AD, Kelly BP, Frank AA, Liu MA, et al. Evaluation of new vaccines in the mouse and guinea pig model of tuberculosis. *Infect Immun* 1998;66(6):2951–9.
- [19] Horwitz MA, Harth G. A new vaccine against tuberculosis affords greater survival after challenge than the current vaccine in the guinea pig model of pulmonary tuberculosis. *Infect Immun* 2003;71(4):1672–9.
- [20] Lasco TM, Cassone L, Kamohara H, Yoshimura T, McMurray DN. Evaluating the role of tumor necrosis factor- α in experimental pulmonary tuberculosis in the guinea pig. *Tuberculosis (Edinburgh)* 2005;85(4):245–58.
- [21] Olsen AW, Williams A, Okkels LM, Hatch G, Andersen P. Protective effect of a tuberculosis subunit vaccine based on a fusion of Antigen85B and ESAT-6 in the aerosol guinea pig model. *Infect Immun* 2004;72(10):6148–50.
- [22] Orme IM. Current progress in tuberculosis vaccine development. *Vaccine* 2005;23(17):2105–8.
- [23] Orme IM, McMurray DN, Belisle JT. Tuberculosis vaccine development: recent progress. *Trends Microbiol* 2001;9(3):115–8.
- [24] Williams A, Hatch GJ, Clark SO, Gooch KE, Hatch KA, Hall GA, et al. Evaluation of vaccines in the EU TB vaccine cluster using a guinea pig aerosol infection model of tuberculosis. *Tuberculosis (Edinburgh)* 2005;85(1–2):29–38.
- [25] McMurray DN. Guinea pig model of tuberculosis. In: Bloom BR, editor. *Tuberculosis: pathogenesis, protection and control*. Washington, DC: ASM Press; 1994. p. 135–47.
- [26] Valdivia RH, Falkow S. Fluorescence-based isolation of bacterial genes expressed within host cells. *Science* 1997;277(5334):2007–11.
- [27] Bacon JB, James BW, Wernisch L, Williams A, Morley KA, Hatch GJ, et al. The influence of reduced oxygen availability on pathogenicity and gene expression in *Mycobacterium tuberculosis*. *Tuberculosis (Edinburgh)* 2004;84(3–4):205–17.
- [28] Hampshire T, Soneji S, Bacon J, James BW, Hinds J, Laing K, et al. Stationary phase gene expression of *Mycobacterium tuberculosis* following a progressive nutrient depletion: a model for persistent organisms? *Tuberculosis (Edinburgh)* 2004;84(3–4):228–38.
- [29] Aulsebrook FM, Brent R, Kingston RE, Moore DD, Seidman JG, Smith JA, et al. *Short protocols in molecular microbiology*. Chichester, USA: Wiley; 1992.
- [30] Shuttleworth H, Ambrose E, Griffiths K, MacDonald-Fyall J, Minton N, Rawkins A, et al. Identification of novel TB vaccine candidates by differential fluorescence induction. *Tuberculosis (Edinburgh)* 2002;82(4–5):209.
- [31] <http://www.chem.agilent.com/scripts/pds.asp?page=27881>.

- [32] Nielsen H, Engelbrecht J, Brunak S, von Heijne G. Identification of prokaryotic and eukaryotic signal peptides and prediction of their cleavage sites. *Protein Eng* 1997;10(1):1–6.
- [33] Williams A, Davies A, Marsh PD, Chambers MA, Hewinson RG. Comparison of the protective efficacy of Bacille Calmette-Guérin vaccination against aerosol challenge with *Mycobacterium tuberculosis* and *Mycobacterium bovis*. *Clin Infect Dis* 2000;30(Suppl 3):S299–301.
- [34] Karlin S, Mrazek J. Predicted highly expressed genes of diverse prokaryotic genomes. *J Bact* 2000;182(18):5238–50.
- [35] Mustafa AS, Oftung F, Amoudy HA, Madi NM, Abal AT, Shaban F, et al. Multiple epitopes from the *Mycobacterium tuberculosis* ESAT-6 antigen are recognized by antigen-specific human T cell lines. *Clin Infect Dis* 2000;30(Suppl 3):S201–5.
- [36] Sasseti CM, Boyd DH, Rubin EJ. Genes required for mycobacterial growth defined by high density mutagenesis. *Mol Micro* 2003;48(1):77–84.
- [37] Manganelli R, Voskuil MI, Schoolnik GK, Dubnau E, Gomez M, Smith I. Role of the extracytoplasmic-function σ factor σ^{H} in *Mycobacterium tuberculosis* global gene expression. *Mol Microbiol* 2002;45(2):365–74.
- [38] Schnappinger D, Ehrt S, Voskuil MI, Liu Y, Mangan JA, Monahan IM, et al. Transcriptome adaptation of *Mycobacterium tuberculosis* within macrophages: insights into the phagosomal environment. *J Exp Med* 2003;198(5):693–704.
- [39] Howard RJ. Vaccination against malaria: recent advances and the problems of antigenic diversity and other parasite evasion mechanisms. *Int J Parasitol* 1987;17(1):17–29.
- [40] Okkels LM, Brock I, Follmann F, Agger EM, Arend SM, Ottenhoff TM, et al. PPE protein (Rv3873) from DNA segment RD1 of *Mycobacterium tuberculosis*: strong recognition of both specific T-cell epitopes and epitopes conserved within the PPE family. *Infect Immun* 2003;71(11):6116–23.
- [41] Delogu G, Brennan MJ. Comparative immune response to PE and PE₂PGRS antigens of *Mycobacterium tuberculosis*. *Infect Immun* 2001;69(9):5606–11.
- [42] Eswaremoorthy S, Kumaran D, Swaminathan S. A novel mechanism for *Clostridium botulinum* neurotoxin inhibition. *Biochemistry* 2002;41(31):9795–802.
- [43] Kochi SK, Schiavo G, Mock M, Montecucco C. Zinc content of the *Bacillus anthracis* lethal factor. *FEMS Microbiol Lett* 1994;124(3):343–8.
- [44] Kooi C, Corbett CR, Sokol PA. Functional analysis of the *Burkholderia cenocepacia* ZmpA metalloprotease. *J Bacteriol* 2005;187(13):4421–9.
- [45] Shoop WL, Xiong Y, Wiltsie J, Woods A, Guo J, Pivnichny JV, et al. Anthrax lethal factor inhibition. *Proc Natl Acad Sci* 2005;102(22):7958–63.
- [46] Derrick SC, Repique C, Snoy P, Yang AL, Morris S. Immunization with a DNA vaccine cocktail protects mice lacking CD4 cells against an aerogenic infection with *Mycobacterium tuberculosis*. *Infect Immun* 2004;72(3):1685–92.
- [47] Lima KM, dos Santos SA, Santos RR, Brandao IT, Rodrigues JM, Silva CL. Efficacy of DNA-isp65 vaccination for tuberculosis varies with method of DNA introduction *in vivo*. *Vaccine* 2003;22(1):49–56.
- [48] Wang R, Doolan DL, Le TP, Hedstrom, Coonan KM, Charoenvit Y, et al. Induction of antigen-specific cytotoxic T lymphocytes in humans by a malaria DNA vaccine. *Science* 1998;282(5388):476–80.
- [49] Brandt L, Skeiky YAW, Alderson MR, Lobet Y, Dalemans W, Turner OC, et al. The protective effect of the *Mycobacterium bovis* BCG vaccine is increased by co administration with the *Mycobacterium tuberculosis* 72-kDa fusion polypeptide Mtb72F in *M. tuberculosis*-infected guinea pigs. *Infect Immun* 2004;72(11):6622–32.
- [50] Skeiky YAW, Alderson MA, Owendale PJ, Gunderian JA, Brandt L, Dillon DC, et al. Differential immune responses and protective efficacy induced by components of a tuberculosis polyprotein vaccine, Mtb72F, delivered as naked DNA or recombinant protein. *J Immunol* 2004;172(12):7618–28.
- [51] Sugawara I, Yamada H, Udagawa T, Huygen K. Vaccination of guinea pigs with DNA encoding Ag85A by gene gun bombardment. *Tuberculosis (Edinburgh)* 2003;83:331–7.
- [52] Mollenkopf HJ, Grode L, Mattow J, Stein M, Mann P, Knapp B, et al. Application of Mycobacterial proteomics to vaccine design: Improved protection by *Mycobacterium bovis* BCG prime-Rv3407 DNA boost vaccination against tuberculosis. *Infect Immun* 2004;72(11):6471–9.
- [53] Giri M, Ugen KE, Weiner DB. DNA vaccines against human immunodeficiency virus type 1 in the past decade. *Clin Microbiol Rev* 2004;17(2):370–89.
- [54] Moore AC, Hill AVS. Progress in DNA-based heterologous prime-boost immunization strategies for malaria. *Immunol Rev* 2004;199:126–43.

Original article

SHARPE, S. A., ESCHELBACH, E., BASARABA, R. J., GLEESON, F., HALL, G. A., MCINTYRE, A., WILLIAMS, A., KRAFT, S. L., CLARK, S., GOOCH, K., HATCH, G., ORME, I. M., MARSH, P. D. & DENNIS, M. J. 2009. Determination of lesion volume by MRI and stereology in a macaque model of tuberculosis. *Tuberculosis (Edinb)*, 89, 405-16.

Impact factor: 1.960

Contributions by HATCH, G. J.

Home Office – Personal Licence holder

Animal procedures – Development and qualification of NHP aerosol challenge and plethysmography systems, performance of aerosol challenge studies.

Study management – Liaison and co-ordination with sponsors and in vivo team, scheduling, reporting

Microbiological experimental work and data analysis

Manuscript review

Citation metrics

Google Scholar: 62 citations



MODEL SYSTEMS

Determination of lesion volume by MRI and stereology in a macaque model of tuberculosis

S.A. Sharpe^{a,*}, E. Eschelbach^b, R.J. Basaraba^b, F. Gleeson^d, G.A. Hall^a, A. McIntyre^c, A. Williams^a, S.L. Kraft^c, S. Clark^a, K. Gooch^a, G. Hatch^a, I.M. Orme^b, P.D. Marsh^a, M.J. Dennis^a^a Health Protection Agency, Centre for Emergency Preparedness and Response, Porton Down, Salisbury, SP4 0JG, UK^b Department of Microbiology Immunology and Pathology, College of Veterinary Medicine and Biomedical Sciences, Colorado State University, Fort Collins, Colorado, USA^c Department of Radiological Health Sciences, College of Veterinary Medicine and Biomedical Sciences, Colorado State University, Fort Collins, Colorado, USA^d Churchill Hospital, Headington, Oxford, UK

ARTICLE INFO

Article history:

Received 28 May 2009

Received in revised form

3 September 2009

Accepted 6 September 2009

Keywords:

Stereology

Tuberculosis

Non-human primate

Pathology

SUMMARY

Sensitive and reproducible methods are needed to measure the impact on the host following experimental challenge with *Mycobacterium tuberculosis*, in order to determine the degree of protection conferred by new vaccines. Here we compare how well different clinical and post-mortem measures of disease burden predict the response by the host to increasing doses of *M. tuberculosis* in rhesus and cynomolgus macaques. The total lung and lesion volume was quantified from magnetic resonance imaging (MRI) digital stacks obtained from lungs of *M. tuberculosis* infected animals that were formalin fixed and scanned *ex-vivo*. The total lung lesion volume relative to the fixed whole lung volume was superior at indicating disease burden when compared to thoracic radiography, pathology scores, changes in body weight and temperature, as well as erythrocyte haemoglobin concentrations and sedimentation rate. The total lesion volume accurately reflected differences in challenge doses of *M. tuberculosis* that ranged from 30 to 500 CFU delivered by aerosol. The determination of total lesion volume from MR images demonstrated a species-dependent difference between rhesus and cynomolgus macaques in susceptibility to *M. tuberculosis* infection. MR stereology provides an accurate, quantifiable and relatively simple assessment, which can be easily standardized between laboratories and should form an essential component of the clinical assessment of disease progression, or vaccine efficacy.

© 2009 Elsevier Ltd. All rights reserved.

1. Introduction

Tuberculosis is one of the leading causes of death of humans from a single infectious agent worldwide. It is estimated that in 2006, there were 9.2 million new cases and 1.7 million deaths due to TB.¹ Of the one third of the world's population estimated to be latently infected with TB, 10% of individuals are at high risk of relapsing with active disease during their lifetime. The emergence of multi-drug resistant and extensively drug resistant strains of *Mycobacterium tuberculosis*, together with the geographical overlap between the HIV and TB epidemics, means that there has never been a more urgent need for better control of TB. Vaccination is the most effective way to control infectious diseases, but the only vaccine currently available against TB, *Mycobacterium bovis* bacillus Calmette-Guérin (BCG), is only partially effective against adult lung

disease, which is where the burden of mortality and morbidity lies.² The global effort to identify and develop novel TB vaccination strategies has resulted in a number of promising candidates being proposed to replace or augment the current vaccination strategies. These candidates include recombinant BCG and BCG boosted by a variety of proteins delivered in adjuvants or delivered by viral vectors.

The development of these approaches has involved the preclinical evaluation of the immunogenicity and protective efficacy of new vaccines in animal models. Mouse models are generally used as a first screen of vaccine candidates and are very useful for studying detailed immunological responses.³ Guinea pigs are considered a more stringent model than mice to discriminate vaccines in terms of protective efficacy since they show a variety of pulmonary and extra-pulmonary lesion types that are similar to those observed in humans.⁴ The different lesion morphologies and the rapid progression of disease in experimentally infected guinea pigs represent a more sensitive model to rapidly demonstrate differences in the response by the host to experimental vaccines.⁵

* Corresponding author. Tel.: +44 1980 612 811; fax: +44 1980 611 310.
E-mail address: sally.sharpe@hpa.org.uk (S.A. Sharpe).

Although small animal models are useful, it is widely accepted that non-human primates are the most relevant model species to predict safety, immunogenicity and protective efficacy of vaccines prior to their introduction in humans.^{6,7} Non-human primates are naturally susceptible to infection with *M. tuberculosis* via the respiratory route and develop a disease which closely mimics the human disease clinically. Radiographic and post-mortem findings at the gross and microscopic levels are similar to those seen in humans. As is seen in other animal models, BCG vaccination of non-human primates provides a limited level of protection against *M. tuberculosis* that can be quantified through a variety of clinical and non-clinical parameters.^{8–12}

One of the greatest challenges in quantifying disease burden associated with *M. tuberculosis* infection in people and in animals is the lack of sensitive and reliable biomarkers that predict the stage or severity of disease. In humans with naturally-occurring *M. tuberculosis* infection, clinical assessments including advanced imaging can be used to determine disease burden and measure treatment outcomes. In experimentally infected animals, the ability to assess lesion burden and quantify bacterial loads in tissue specimens collected at post-mortem examination provides an added advantage and a unique opportunity to correlate clinical parameters with pathology findings. There continues to be a need to identify measures of disease burden in animals that are accurate and sensitive enough to distinguish subtle differences between TB vaccine candidates.

Systems that can be standardized between laboratories and that provide quantitative data based on well defined criteria are necessary to assess the extent of disease and improvement related to vaccination following experimental infection with *M. tuberculosis*. As more vaccine candidates are developed and tested, validated methods that have the power to distinguish subtle differences and benefits afforded by different vaccine candidates will be required. Ideally, new measures developed to fulfil this need should be objective, quantitative and transferable.

MRI has superior contrast resolution and sensitivity when estimating lung lesion burden when compared to gross examination of tissue at necropsy. MRI of *ex-vivo* lung specimens has recently been shown to be an excellent imaging method to visualise lesion distribution and to quantify lesion volume in guinea pigs infected with *M. tuberculosis*.¹³ This study sought to determine the utility of quantifying the total lung/lesion volume obtained from post-mortem MRI to assess lung disease burden in a non-human primate model. These data were compared to existing ante- and post-mortem methods used for the evaluation of TB vaccine candidates. We also investigated the use of total lung lesion volume in rhesus and cynomolgus macaques independently to assess any species differences in susceptibility to infection with *M. tuberculosis* as has been previously suggested.¹⁴ Our results show that the application of new stereology-based techniques to the measurement of lesion volume to lung volume ratio provide a useful new tool to quantify pulmonary disease induced by *M. tuberculosis*.

2. Materials and methods

2.1. Experimental animals

Captive-bred rhesus macaques of Indian origin and cynomolgus macaques of Chinese origin were used for this study. All animals were 4 years old at the time of challenge and naive in terms of prior exposure to mycobacterial antigens (*M. tuberculosis* infection or environmental mycobacteria) as demonstrated by the tuberculin test whilst in their original breeding colony and by the IFN- γ based Primagam™ test kit (Biocor, CSL, USA) just prior to study start. Monkeys were housed according to the Home Office (UK) guidelines

for the care and maintenance of primates and were sedated by intramuscular (i.m.) injection with ketamine hydrochloride (10 mg/kg) (Ketaset, Fort Dodge Animal Health Ltd, Southampton, UK) for all procedures requiring removal from their cages.

2.2. *M. tuberculosis* strain

The *M. tuberculosis* Erdman strain K01 was kindly provided by Dr Amy Yang of CBER/FDA. This repository of the Erdman strain is provided to the TB research community in order to improve standardization of challenge materials between laboratories. The stocks were provided as frozen suspensions at a stated titre of $3.5 \pm 1.5 \times 10^8$ CFU/ml. For challenge, sufficient vials were thawed and diluted appropriately, as stated below, in sterile distilled water.

2.3. Aerosol exposure

The aerosol exposure apparatus used to infect the macaques was an adaptation of the equipment used routinely to aerosol challenge guinea pigs and mice.^{15–17} This system of aerosol generation involved a 3-jet Collision nebuliser (BGI Incorporated, Waltham, MA, USA) to generate mono-dispersed bacteria in particles with a mean diameter of $2 \mu\text{m}$ ¹⁸ in conjunction with a modified Henderson apparatus¹⁹ to provide a controllable supply of air and to maintain the flow of stable aerosols. Delivery of the aerosol to the animals was via a veterinary anaesthesia mask, modified to permit the flow of aerosol over the nose of the subject. Different sizes of mask were used for different sizes of animal to ensure a seal around the nose and mouth thus preventing escape of the aerosol and maintaining the pressures and flow rates within the system. Challenge was performed on sedated animals placed within a 'head-out', plethysmography chamber (Buxco, Wilmington, North Carolina, USA) to enable the aerosol to be delivered simultaneously with the measurement of respiration rate and volume. The principle of the exposure was to deliver the aerosol to the animals whilst measuring the minute volume until such time that a target volume of inhaled aerosol had been reached. As determined by the process outlined below, the target volume of aerosol would contain a known number of viable *M. tuberculosis* bacilli.

2.4. Estimation of dose

The inhaled, retained dose was estimated using the following formulae:

- (1) Presented dose = Cneb \times SF \times AV
- (2) Inhaled, retained dose = Presented dose/retention factor

The spray factor (SF) defines a relationship between the viability of the challenge suspension in the nebulizer (Cneb, colony forming units, CFU/ml) and the concentration of viable bacilli circulating in the aerosol (CFU/litre/min). The SF used in these studies was determined from a large historical data set generated over 15 years of delivering aerosols of *M. tuberculosis* to experimental animals using the Henderson apparatus and Collision nebulizer. Thus for a known Cneb, the aerosol concentration could be estimated and the total accumulated volume (AV) of aerosol to be inspired in order for the macaques to inhale a defined number of bacilli could be determined. The normal respiration rate of each macaque (measured on a separate occasion) was used to estimate the time that it would take to inhale this volume of aerosol and, if necessary, adjustments were made to ensure that the exposure time was between 5 and 15 min. This 'required volume' of inhaled aerosol was typically between 3.5 to 7 litres AV. The AV was fixed for each

animal that was due to receive the same dose and only the time taken to reach the target AV was varied.

Thus, preparations were made in advance to ensure that the concentration of *M. tuberculosis* in the nebulizer was appropriate for the target dose to be delivered. However the final, inhaled dose estimate for each animal was determined by actual measurement of Cneb for each exposure. Doses are quoted as estimated inhaled and retained dose. The retained dose is quoted in order to be consistent with aerosol infection studies in small animals where the actual dose retained in the lungs can be measured by the plating of whole lungs after challenge. This is not possible in macaques, therefore a retention factor was used to convert the presented dose to a retained dose. The retention factor used in this study was derived from data by Harper and Morton²⁰ in macaques exposed to anthrax spores and data from guinea pig and mouse challenge studies with *M. tuberculosis* which measured the proportion of the aerosol that was retained in the lungs relative to the total number of aerosol particles delivered to the animals (using a similar Henderson apparatus and Collison nebulizer to that used here). The retention factor is 21, i.e. approximately 5% of the presented dose was assumed to be retained in the lungs. The factors behind the difference in presented and retained dose are related to the operating conditions of the Porton Henderson apparatus, such as the higher flow rates and negative pressure.

Macaques were challenged with a range of doses from 30 to 500 CFU retained in the lungs (Table 1).

2.5. Clinical assessment

Animal behaviour was observed daily throughout the study for contra-indicators such as depression, withdrawal from the group, aggression, food and water intake, changes in respiration rate, or cough. Animals were sedated every two weeks to measure weight, body temperature, blood haemoglobin levels and erythrocyte sedimentation rate, (ESR) and to collect blood samples for immunology. The time of necropsy if prior to the end of the planned study period was determined by experienced primatology staff based on a combination of the following adverse indicators: depressed or withdrawn behaviour, abnormal respiratory rates (dyspnoea), loss of 20% of peak post-challenge weight, ESR levels elevated above

normal, haemoglobin level below normal limits, increased temperature and severely abnormal chest X-ray.

2.6. Necropsy

Before necropsy, animals were sedated with ketamine (10 mg/ml, i.m.), weighed, photographed, chest x-rays taken and clinical data collected. Anaesthesia was deepened using intravenous pentobarbitone sodium 30 mg/kg (Sagatal, Rhône Mérieux) and exsanguination was effected via the inferior vena cava, before termination by injection of an anaesthetic overdose (Dolethal, Vétquinol UK Ltd, 140 mg/kg). A full necropsy was performed and gross pathology was scored using a relative scoring system (Table 2) based on the number and extent of lesions present in lungs, spleen, liver, kidney and lymph nodes.²¹ The scores attributed to each tissue (lung lobe, organ, lymph node) were summed to give the total pathology score. Samples of spleen, liver, kidneys and hilar, inguinal and axillary lymph nodes were removed and placed in weighed tubes for quantitative bacteriology and into formalin buffered saline for histology, and dissection was performed on sterile trays. The whole lungs were carefully dissected to retain their integrity, removed from the thorax and gently infused with 10% neutral buffered formalin using a 10 ml syringe attached to a 14 CH Nelaton catheter (J.A.K. Marketing, York, UK). The tip of the catheter was inserted via the trachea into the left bronchus at the tracheal bifurcation and the left lung lobes infused; the procedure was repeated on the right side and the trachea was tied off and the lungs immersed in formalin to complete fixation.

2.7. Lung imaging

Thoracic radiographs (SP VET 3.2, Xograph Ltd) using mammography film (Xograph Imaging Systems Ltd, Tetbury, UK) were acquired before and every 2 weeks after exposure to *M. tuberculosis*. Evaluation of disease was performed blind by an experienced consultant thoracic radiologist blinded to the animals inoculation and clinical status using a pre-determined scoring system based on the amount and distribution of infiltrate (Table 3).

2.8. Magnetic resonance imaging

The inflated lungs that had been immersed in formalin were set in agarose for MRI scanning. Images were acquired on a 1.5 T Twinspeed HDX MRI Scanner (General Electric Healthcare, Milwaukee, WI, USA). The sample was placed in a general purpose flexible coil. T1 weighted 3D Fast Spoiled Gradient Echo (FSPGR) images were acquired with the following parameters: TE: 7.7, TR: 4.2, 16 cm field of view, 1 mm slice thickness, –0.5 mm slice gap, 192 × 192 matrix, 15 degree Flip Angle, 3NEX. Each acquisition took approximately 3.5 min.

Table 1
Aerosol challenge doses of *M. tuberculosis* delivered to rhesus and cynomolgus macaques.

Species	Animal Identification number	Presented Dose (cfu)	Estimated Retained Dose (cfu)	
Rhesus macaque	D53	10500	500	
	D12	1575	75	
	D19	1470	70	
	D28	945	45	
	D42	945	45	
	C54	840	40	
	D60	840	40	
	D80	630	30	
	D31	630	30	
	Cynomolgus macaque	1011	1575	75
		1231	1575	75
1191		1575	75	
9181		840	40	
9027		840	40	
9203		840	40	
1163		840	40	
1111		840	40	
2151		840	40	
9187		630	30	
9013		630	30	
4313	630	30		

Table 2
Gross pathology scoring system.

Lung (per lobe) and other organs	Score	Lymph nodes	Score
No visible lesions	0	No visible lesions; no necrosis	0
1 lesion, <10 mm	1	1 small focus	1
2–5 lesions, <10 mm	2	Several foci; necrotic/caseous areas >5 × 5 mm	2
>6 lesions, <10 mm; or 1 lesion, >10 mm	3	Extensive necrosis; extensive caseation	3
>1 lesion >10 mm	4		
Coalescing lesions	5		

Table 3
Thoracic radiograph scoring system.

Level and distribution of infiltrate	Score
No infiltrate (clear radiograph)	0
Modest infiltrate on one side only	1
Extensive infiltrate on one side only	2
Modest infiltrate on both sides of lungs	3
Extensive infiltrate on both sides of lungs	4

2.9. Lesion analysis/quantification (Stereology)

The total lung and lesion volume relative to the fixed tissue was determined using the Cavalieri method applied to MRI image stacks, and then expressed as a ratio to provide a measure of disease burden in each animal.^{22–24}

Analyses of lesion volume on magnetic resonance (MR) images were performed with the investigators reading the images blind to treatment groups. Lung lesions were identified on MR images based on their signal intensity and nodular morphology relative to more normal lung parenchyma. Lesions were typically multifocal to coalescing nodules (Figure 1A) that were substantially more intense compared to the background intensity of the normal lung parenchyma. Care was taken to differentiate lesions from the normal pulmonary vasculature that often had a similar signal intensity but, in contrast to lesions, a smooth linear distribution that was continuous in multiple adjacent slices. Normal lung parenchyma varied somewhat in signal intensity from hypointense to slightly hyperintense relative to the agar media. Selected points for normal lung parenchyma and lesions excluded mediastinal structures.

The total lung and lesion volume for each animal was estimated from MR images using a stereology workstation consisting of a personal computer with frame grabber board, colour digital camera, 24-inch monitor and stereology software (Stere Investigator 8.2, MBF Bioscience, Williston, VT, USA) with the MRI module. MRI digital image stacks in a DICOM format (ranging from 369 to 664 $\mu\text{m}/\text{voxel}$) were uploaded and displayed. Representative sections of the entire lung field were selected by an unbiased, systematic and uniform sampling technique using a random starting point. An average of 8 total sections (average periodicity of 10) were selected from digital stacks that ranged from 72 to 160 slices per sample with a section thickness of 1.0 mm with a -0.5 mm spacing. A grid with spacing of 3.0 mm between points in X and Y axes was randomly placed on the region of interest using

the Stereo Investigator software and Cavalieri Estimator module (Figure 1B). The same grid spacing was used for both lung and lesion with the average total sampling points placed for lung volume being 2394 (range 589–9711) and for lesions 199 (range 23–1324). The total lung and lesion volume was estimated from the sum of points placed in the individual serial sections and the sampling probability according to Cavalieri's principle.^{22,23} The coefficient of error (CE) for total lung and lesion volumes was calculated separately and was maintained at less than 0.1 (Gundersen, $M = 0$).²⁵

2.10. Pathological analysis

On return from scanning, lung lobes were removed from agar and stored in 10% neutral buffered formalin. Lung lobes that had been fixed in buffered formalin were sliced at approximately 5–10 mm intervals and discrete lesions measuring 1–5 mm in diameter were counted. Lesions that had coalesced and measured more than 5 mm in diameter were counted and the dimensions of the sectioned coalesced lesions were measured and recorded. Total lesion count was the sum of the discrete and coalesced lesions. Lesions were classified according to the scheme used by Lin et al.²⁶ Lesions were generally smaller than those seen in the rhesus, which made them easier to count.

2.11. Statistical analysis

Statistical analyses were performed using GraphPad Prism, version 5.01 (GraphPad Software Inc, La Jolla, California, USA). The Spearman correlation test was used to determine the level of correlation between study parameters.

3. Results

3.1. Disease progression in rhesus macaques infected with *M. tuberculosis*

Nine rhesus macaques were exposed to aerosol doses of *M. tuberculosis* ranging from 30 to 500 CFU (estimated retained dose) and monitored for changes in behaviour and clinical parameters for 12 weeks after challenge. All animals showed changes in behaviour and clinical parameters consistent with

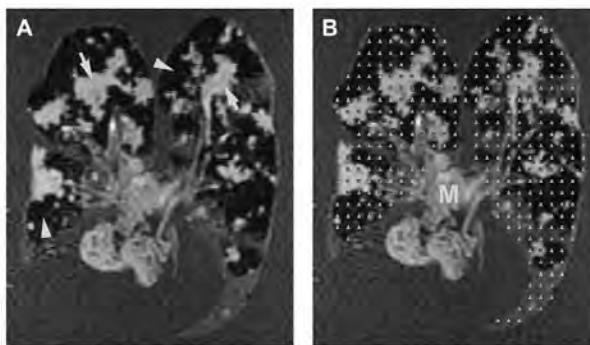


Figure 1. (A) A representative magnetic resonance image from a rhesus macaque illustrating the *M. tuberculosis* lesions (arrows) compared to more normal lung (arrowheads). (B) The same MR image illustrating the use of probes used to quantify the area and volume of lesions (blue stars) and more normal parenchyma (green triangles). Mediastinal structures (M) including anterior heart, mediastinal and hilar lymph nodes and associated connective tissue were excluded from the analysis.

tuberculosis infection. Disease progressed in 4 of the 9 animals to a level that met the humane endpoint criteria and these were euthanized before the end of the planned 12 week study period. The 4 animals in which disease progressed rapidly (D53, D12, D19,

D28) received the four highest aerosol doses of *M. tuberculosis*. All four animals showed changes in their behaviour, becoming withdrawn or depressed, cough was observed, and respiration rates were seen to be more rapid (Table 3). Three of the animals (D53,

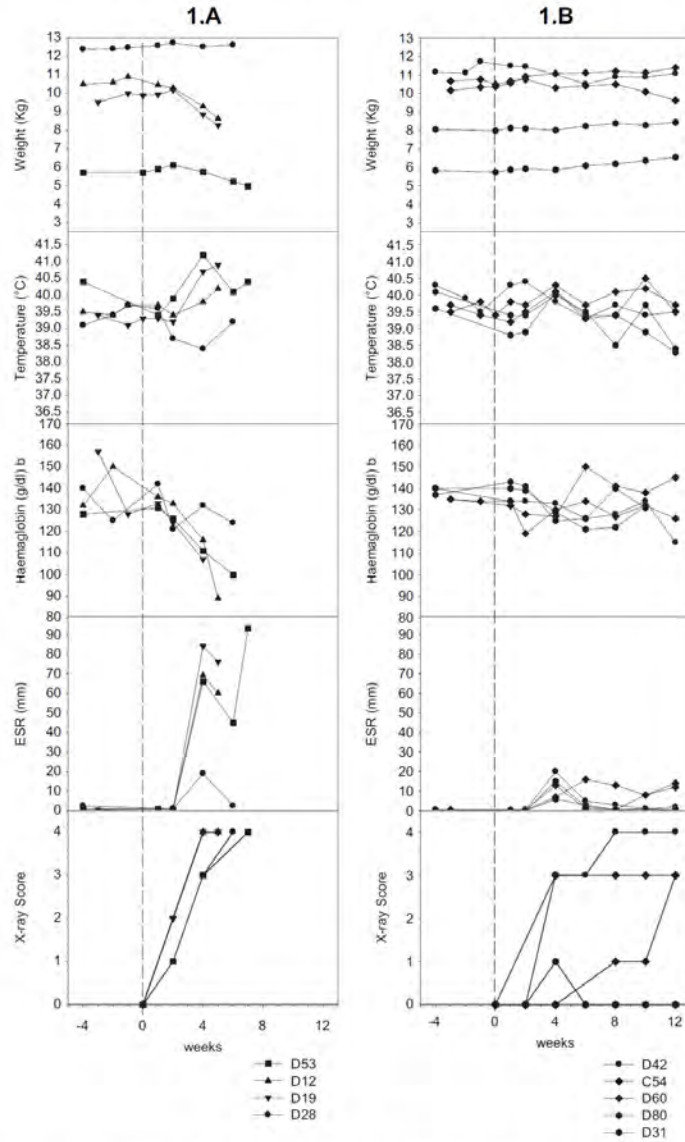


Figure 2. Changes in clinical parameters in rhesus macaques following aerosol infection with *M. tuberculosis*; A: Animals in which disease progressed to meet humane endpoints before the end of the planned study period. B: Animals in which disease levels remained below set endpoints for study period.

D19 and D12) showed clear changes in clinical parameters that included weight loss, haemoglobin loss, increased ESR and abnormal thoracic radiographs (Figure 2). Changes in these clinical parameters were not as marked in D28; however, the behavioural indicators were sufficiently adverse to require that the animal was euthanized. The behaviour of the other 5 animals remained normal; only two animals (C54, D60) showed rapid and shallow breathing when sedated but coughing was not observed (Table 4). Changes in weight, haemoglobin level, temperature and ESR did not exceed the normal limits, while abnormalities in chest X-ray appeared to be dose dependent (Figure 2). These five animals were euthanized as planned, 12 weeks after challenge.

3.2. Visualisation of tuberculosis-induced pulmonary disease in rhesus macaques by magnetic resonance (MR) imaging

Following necropsy, and prior to histological examination, MR images of the lungs of each animal were collected. Images from each sequential tissue slice were reconstructed into three dimensional images of the entire lung using computer software for all study subjects. Representative images from animals that were exposed to different doses of *M. tuberculosis* are shown in Figure 3A. In all animals, lesions were evenly distributed throughout all of the lobes of the lung and the level of pulmonary disease increased with aerosol dose delivered. No abnormalities were observed in the lungs of rhesus macaques that had not been exposed to *M. tuberculosis*.

3.3. Quantification of the level of pulmonary disease in rhesus macaques at the end of the study period

Total lesion volume determined from MR images was compared to post-mortem lesion counting and other approaches conventionally used for the evaluation of TB vaccine efficacy including gross pathology score, pulmonary pathology score and chest X-ray. The level of pulmonary disease measured by each of the approaches generally increased in line with the increasing dose of *M. tuberculosis* to which the animal was exposed (Figure 4A).

Total lesion volume expressed as lesion to lung volume ratio reflected the initial exposure dose and this measurement was able to demonstrate subtle differences in the level of pulmonary disease at both the upper and lower ranges. Lesion to lung volume ratio significantly correlated with all other measures of pulmonary disease (Figure 5A, B, C, D) and the clinical markers of disease severity provided by weight loss and erythrocyte sedimentation rate (Figure 5E, F). Estimation of total lesion numbers in the lung, by serial sectioning and manual counting of both discrete and coalesced lesions, was laborious and in animals with more severe disease the individual lesions became difficult to distinguish, and eventually too numerous to count. This was particularly the case

with the animal (D53) which was exposed to the highest aerosol dose of *M. tuberculosis*. Subjective histopathology revealed lung lesions consistent with descriptions given by Lin et al.²⁶ although no differences between exposure doses were detected.

Gross pathology scores and chest X-ray scores, which are dependent on the use of previously defined arbitrary scoring systems, were less sensitive than measures based on quantitative data, such as lesion to lung volume ratio and lesion counting. The gross pulmonary pathology score system did not differentiate between the level of disease in the three animals exposed to the three highest doses, while the X-ray system did not show any differences between animals which received the 4 highest doses. The chest X-ray score system also lacked sensitivity at the lower end of the disease spectrum, as animals either appeared normal, or progressed directly to the relatively high score of 3.

The level of pulmonary disease by all scoring systems also agreed with the level of changes determined in the clinical measures of disease severity, namely, weight loss, decreased erythrocyte haemoglobin concentration and increase in ESR (Figure 4B), with most changes occurring in the animals with the greatest level of pulmonary disease.

3.4. Quantification of the level of pulmonary disease in cynomolgus macaques

Following the successful demonstration of the utility of lesion-lung volume ratio for the quantification of pulmonary disease in tuberculosis-infected rhesus macaques this method was used in a second study to determine the level of pulmonary disease in tuberculosis-infected cynomolgus macaques.

Twelve cynomolgus macaques were exposed to pre-defined estimated aerosol doses of *M. tuberculosis* ranging from 30 to 75 CFU and monitored for changes in behaviour and clinical parameters. Most changes were observed in two of the three animals that were exposed to the highest dose of *M. tuberculosis*. Symptoms were most severe in animal 201011 which showed a weight loss of 15% over the course of the study, a significantly elevated ESR (89 mm) at termination, and was observed to have an increased respiration rate and a cough. Symptoms were observed in 111231 that included a cough and an increased respiration rate when sedated for assessment. Slightly laboured respiration on sedation was observed in one animal (9027) exposed to 40 CFU; however, other clinical parameters in these two animals remained within normal ranges. Normal behaviour was exhibited by all the other animals during the study period (Table 5). None of the changes observed in any of the animals over the study period were sufficient to meet humane endpoint criteria and at study termination clinical parameters in all animals remained within normal ranges (Figure 6).

Table 4
Behavioural indicators at termination in rhesus macaques following aerosol infection with *M. tuberculosis*.

Animal I. D.	Dose <i>M. tuberculosis</i>	Behaviour	Respiration rate		Eating/drinking	Cough	Other indicators
			Normal	Under sedation			
D53	500	Withdrawn	Rapid, heavy	Very laboured	Normal	Yes	Ruffled coat, Subdued
D12	75	Depressed	Rapid, shallow breathing	Rapid/shallow	Much reduced intake	Yes	Very inactive
D19	70	Withdrawn	Rapid	Rapid/shallow	No	Yes	Ruffled coat, watery eyes
D28	45	Depressed	Rapid/shallow	Normal	Much reduced intake	Yes	Very inactive
D42	45	Normal	Normal	Normal	Normal	Yes	NAD
C54	40	Normal	Normal	Rapid/shallow	Normal	No	Ruffled coat
D60	40	Normal	Normal	Rapid/shallow	Normal	No	Ruffled coat,
D80	30	Normal	Normal	Normal	Normal	No	NAD
D31	30	Normal	Normal	Normal	Normal	No	NAD

NAD = No abnormalities detected.

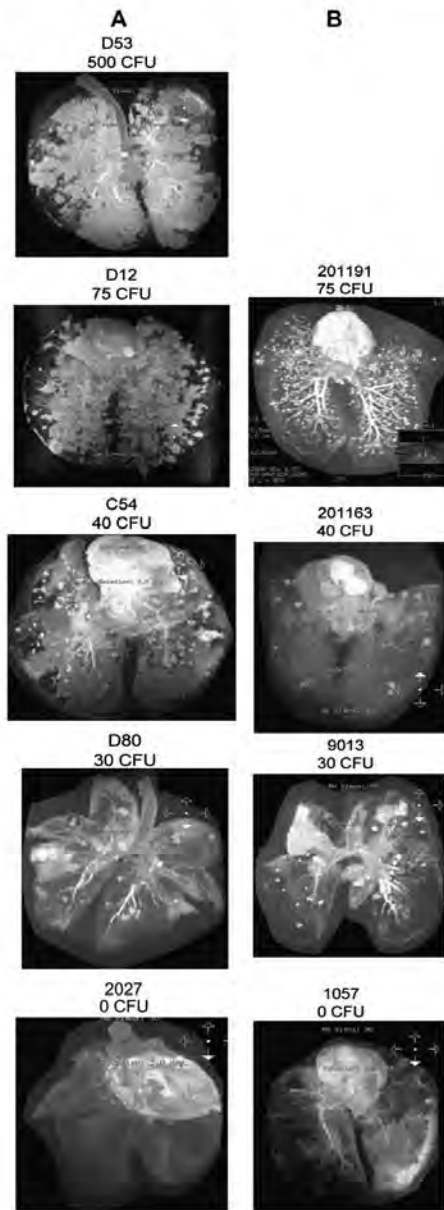


Figure 3. Typical examples of magnetic resonance (MR) images of lungs from rhesus (3A) and cynomolgus (3B) macaques following aerosol infection with a range of doses of *M. tuberculosis*.

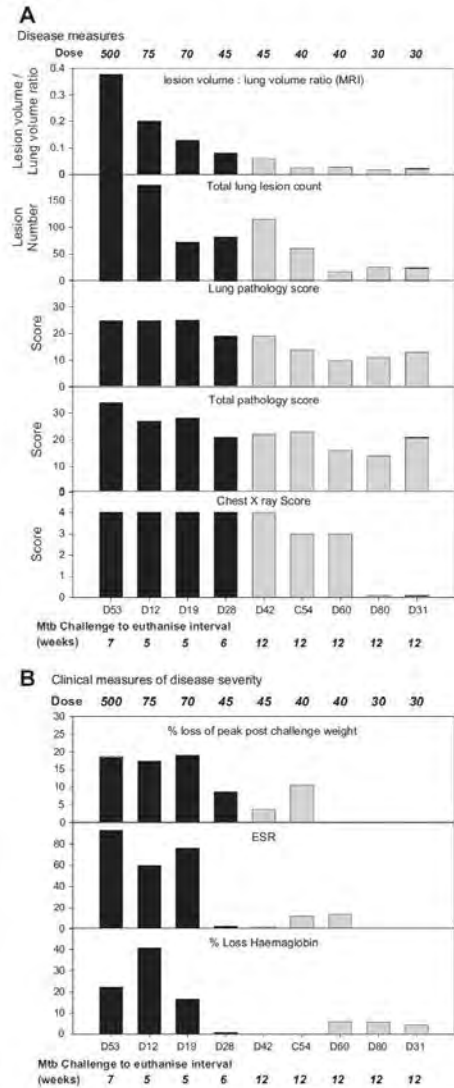


Figure 4. Measures of pulmonary disease (A) and clinical disease (B) severity in rhesus macaques following aerosol exposure to a range of doses of *M. tuberculosis*. Black fill colour represents animals in which disease progressed rapidly.

Animals were euthanized 12 or 13 weeks after exposure and examined using the same techniques described for the rhesus macaque study above. MR imaging of the lungs revealed a trend for an increase in the number of lesions with the increase in exposure dose (representative examples are shown in Figure 3B). Animals exposed to 75 CFU showed a uniformly large number of lesions; in

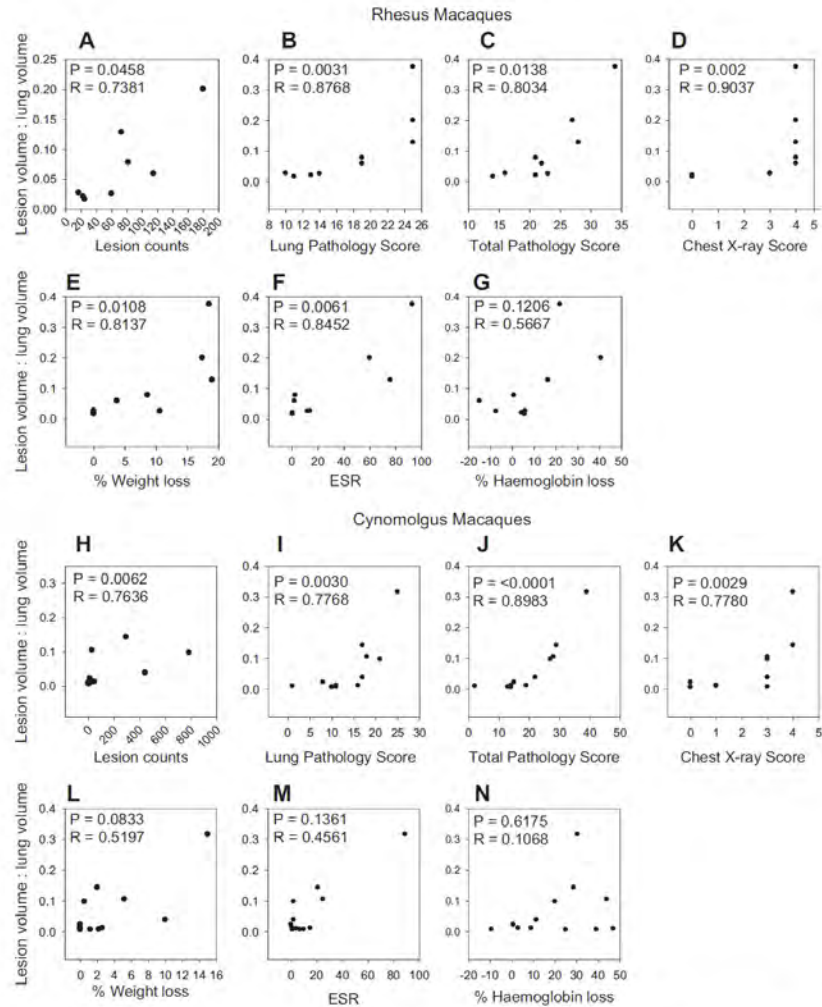


Figure 5. Correlation of lesion volume: lung volume ratio with other measures of pulmonary disease level or clinical disease severity.

contrast, considerable variation was seen in the numbers of lesions induced in animals exposed to a dose of 40 CFU or 30 CFU. Lesions were evenly distributed throughout the lung in all animals exposed to *M. tuberculosis* and were not detected in the animal that was not exposed (1057). Lesions were of a type consistent with descriptions from Lin et al.²⁵ but were not related to exposure dose.

The level of pulmonary disease determined by both of the measures based on quantitative data, or the arbitrary scoring systems, generally agreed for individual animals (Figure 6). The variation in outcome following exposure to lower doses of *M.*

tuberculosis observed in the MR images was confirmed by all of the measurements, although the ability of each approach to reveal the extent of the differences in the level of disease between animals depended on the inherent sensitivity of the approach used. For example, chest X-ray suggested most variation in outcome amongst animals exposed to 40 CFU compared to groups receiving either 75 or 30 CFU.

The extent of pulmonary disease revealed through the determination of lesion to lung volume ratio correlated significantly with all the pulmonary disease measures used (Figure 5H, I, J, K) but

Table 5
Behavioural indicators at termination in cynomolgus macaques following aerosol infection with *M. tuberculosis*.

Animal I. D.	Dose <i>M. tuberculosis</i>	Behaviour	Respiration rate		Eating/drinking	Cough	Other indicators
			Normal	Under sedation			
201011	75	Normal	Rapid	Slightly laboured	Normal	Yes	NAD
111231	75	Normal	Normal	Slightly rapid	Normal	Yes	NAD
201191	75	Normal	Normal	Normal	Normal	No	NAD
9181	40	Normal	Normal	Normal	Normal	No	NAD
9027	40	Normal	Normal	Slightly laboured	Normal	No	NAD
9203	40	Normal	Normal	Normal	Normal	No	NAD
201163	40	Normal	Normal	Normal	Normal	No	NAD
201111	40	Normal	Normal	Normal	Normal	No	NAD
112151	40	Normal	Normal	Normal	Normal	No	NAD
9187	30	Normal	Normal	Normal	Normal	No	NAD
9013	30	Normal	Normal	Normal	Normal	No	NAD
4313	30	Normal	Normal	Normal	Normal	No	NAD

NAD = no abnormalities detected.

correlation with clinical measures of disease severity was not significant (Figure 5L, M, N).

4. Discussion

The susceptibility of rhesus macaques to aerosols of *M. tuberculosis* is well established and the use of the aerosol model for the assessment of vaccine efficacy was first described over 30 years ago.^{9,27} The infection of rhesus macaques by aerosol exposure to *M. tuberculosis* reported here caused changes in clinical parameters and behaviour consistent with that in similar animals described in the early reports of the aerosol model, and also in more recent studies in rhesus macaques infected by intra-tracheal administration.^{14,28} Aerosol infection induced rapid disease progression following exposure to higher doses supporting previous studies following intratracheal²⁷ and aerosol infection.²⁹

This is the first report of infection of cynomolgus macaques with *M. tuberculosis* using low dose aerosol exposure, as previous studies have used the intra-tracheal route of challenge.^{14,21,7,30–33}

Clinical symptoms in cynomolgus macaques, such as weight loss and cough, were only induced in animals that were exposed to the highest dose of *M. tuberculosis* (75 CFU) and disease did not progress as rapidly as in rhesus macaques exposed to the same dose, which supports previous observations.¹⁴ The disease induced in the cynomolgus macaques following exposure to the same doses of *M. tuberculosis* showed greater variation than in the rhesus macaques. The induction of a spectrum of disease in cynomolgus macaques following inoculation with a low dose of *M. tuberculosis* by the intra-tracheal route has also been reported previously.^{7,34}

The most common method used to quantify gross and microscopic lesions is based on subjective scoring schemes that often include parameters of lesion size in combination with morphological criteria indicating stage of disease.^{35,36} Lesion scoring schemes at the time of examination *post-mortem* represent a rapid yet simplified estimate of disease severity. Similar scoring schemes when applied to microscopic lesions are also subjective and often lack sensitivity. Scoring of lesions at the microscopic level provide limited information about stage of disease or chronicity unless specialized staining techniques are used. In non-human primate studies, the disease burden is traditionally measured by gross and microscopic pathology, bacterial burden, chest X-ray and changes in clinical parameters such as inflammatory markers (C reactive protein or ESR) and weight loss. Since the clinical manifestations of TB in humans and animals are directly correlated to the pulmonary and extra-pulmonary lesion burden, assessment *post-mortem* of pathology is critical in the evaluation of experimental vaccines. However, there are limitations to the current methods used. Scoring methods have limited usefulness in discerning subtle

differences in disease burden because they are subjective and lack standardization between laboratories. Lesion scores at the gross and microscopic level often indicate the extent of disease (lesion size) with distribution and limited morphologic features that may reflect different stages of disease. Because these systems are not based on linear scores they are not readily quantifiable, and this accounts for the lack of sensitivity and consistency.

In this regard, there is a need for more sensitive and reproducible methods to quantify disease burden at both the gross and microscopic level. Our study therefore assessed the use of a stereological approach applied to MR image stacks to determine the total lung and lesion volume to quantify *M. tuberculosis*-induced pulmonary disease. One of the most powerful and efficient methods to evaluate disease burden at the gross and microscopic level is through the use of stereology.^{37–40} This is a statistical method applied to morphological features that recovers most of the three dimensional structural information lost by sectioning. Design-based stereology uses a set of probes selected and applied by the investigator using criteria that include strict sampling strategies.^{23,25,37} These methods are assumption free and mathematically rigorous and can be applied to any sample type. Stereology uses two dimensional sections (gross or microscopic specimens) to accurately estimate measurements of three dimensional structures.³⁸ In previous studies using the guinea pig model, estimates of lesion volume and numbers were determined by computer assisted image segmentation which correlated with the pathology assessment.¹³ The combination of MR images and stereology in the current study represents a more mathematically strenuous and therefore less biased method of lesion quantification. The advantage of using stereology combined with MR images to quantify disease severity is that important data such as total lesion volume can be obtained. These methods are both quantitative and more sensitive than other scoring methods. A further advantage is that if performed correctly, lesion data are reproducible and comparable between laboratories. In principle, stereology could also be applied to other methods of imaging, including CT.

In both non-human primate species, the data revealed a trend for an increasing level of disease that aligned with exposure dose, particularly in the rhesus macaques. The strength of this approach is that it is based on quantitative data, which provides the sensitivity and the power to discriminate both at the upper and lower levels of disease, and lends itself to a more rigorous analysis compared to more subjective interpretations of disease severity.

We also used conventional scoring techniques such as total gross pathology score and chest X-ray previously reported as quantification of disease severity, as used in assessment of vaccine efficacy as endpoints in non-human primate model studies.^{14,21,41} The variation in disease severity induced following exposure to the range of doses of tuberculosis was reflected by each of the different systems. All

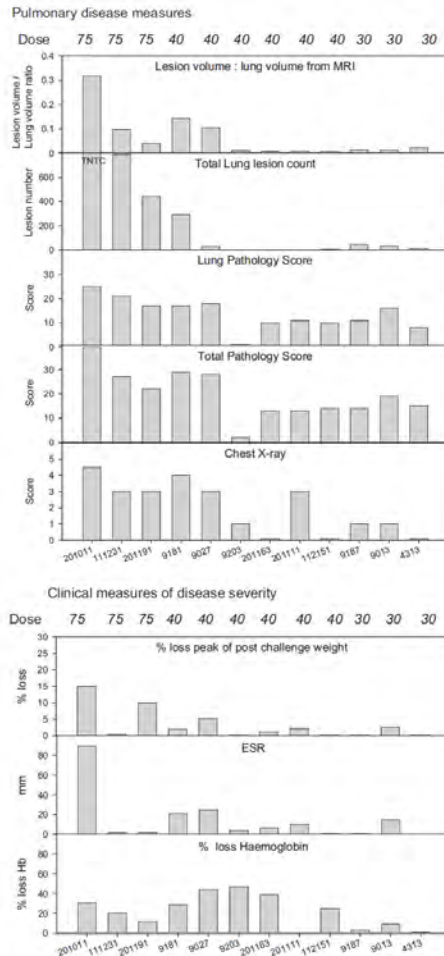


Figure 6. Measures of pulmonary disease and clinical disease severity in cynomolgus macaques following aerosol exposure to a range of doses of *M. tuberculosis*.

measures demonstrated the disease to be more consistent in the rhesus macaques than the cynomolgus macaques and more severe in those exposed to aerosol doses of tuberculosis of 45 CFU or more. A similar trend of increased disease severity with aerosol dose was seen in the cynomolgus macaques, although there was less consistency in the course of disease induced by different doses. In the two species, the variation in the discriminatory capacity and sensitivity at the upper and lower ends of the disease spectrum varied according to the approach used to measure disease.

In our study, we used the gross pathology arbitrary scoring system previously reported by Langermans et al.^{14,21} and Verreck et al.,^{2009³³} based on the number and size of lesions visible on the surface of organs and each lung lobe; the pulmonary component of the

scoring system has a maximum score of 25. This system when applied to animals in our study was able to show differences at necropsy in both the total level of pathology and pulmonary disease induced by higher and lower doses for both species, but the upper limit could not be used to distinguish the severity at higher levels of disease. This system was principally developed to score disease in non-human primates exposed to *M. tuberculosis* via the trachea which targets a single lobe resulting in the induction of often extensive disease in this lobe whilst involvement of the other lobes is reduced and is potentially caused by secondary spread from the original site of infection.^{8,31} Therefore, such a system may not be optimal for the measurement of disease induced following aerosol delivery which, in contrast, delivers bacilli evenly throughout the entire lung.

Previous studies in the aerosol challenge model^{9,26} employed an alternative disease severity scoring system based on experience with rhesus monkeys, and provided a comparative measure of resistance of various treatments.⁹ The scoring system assigned a numerical score dependent on the relationship between the number of tubercles counted in the lung (following fixation and cutting into thin slices) with the number of bacilli inhaled, with the highest scores given for cavitation, caseation or lung destruction. These studies used low doses of *M. tuberculosis* and resulted in numbers of lesions which were easily countable. In contrast, in the studies reported here, as the number of lesions increased, the accuracy of the manual count reduced as lesions became more difficult to distinguish and, in fact, the number of lesions induced in the animal of each species exposed to the highest doses of bacilli (D53, 201011) were too numerous to count by this method. Despite the limitations at the higher levels of disease, lesion counting does provide an overall view of disease severity, although this is not a complete insight into the level of pulmonary disease because, unlike the lesion volume to lung volume ratio, it does not take into account lesion size. Lesion counting provides a useful readout in the short term, low dose, fixed endpoint studies of vaccine efficacy, but the value of this approach may be less in long-term survival studies where high numbers of lesions would be predicted in animals in which disease progresses to specified humane endpoints.

The progress of pulmonary disease induced by *M. tuberculosis* infection in non-human primate studies is commonly followed on serial chest radiographs which are examined by an experienced radiologist and scored using an arbitrary system. For this study, a qualitative scoring system based on the occurrence, position and extent of pulmonary infiltrate similar to that proposed to the WHO by Langermans, Reed and Flynn in 2004 (J Langermans personal communication), was used. The trend in scores allocated to the thoracic radiograph of each animal taken on the day of necropsy agreed with the other measures described, but the system suffers from similar limitations in sensitivity and discriminatory power particularly at the upper and lower limits as with the gross pathology system described above. The system was developed from work using the intra-tracheal route of delivery, and the score for the presence of infiltrate in both sides of the lung (score 3) is higher than for the presence of extensive infiltrate on a single side (score 2). The scoring system is less applicable for aerosol delivery because the inoculum is evenly distributed to all lung lobes and, as a consequence, disease develops evenly. Hence, a scoring system weighted to reflect more uniformly progressive disease, such as that described by Good⁸ in which the criterion for measuring involvement is the proportion of each lung lobe affected by disease, is more appropriate. This suggests that qualitative systems need to be tailored for the model in which they are used.

MR imaging could have many applications in vaccine efficacy studies. For example, if MR images of the lungs of animals could be collected from live animals throughout the study period, a comprehensive picture of disease progression over time could be

built up for each study subject as has been achieved CT.³¹ Terminal ex-vivo MR imaging precludes the conventional read out of organ-specific CFU, but has other advantages, and future developments such as in-study MRI would increase the power of this approach still further. Historically MR imaging has not been ideal for the lung due to artefacts induced from respiratory motion and low signal intensity in air filled lung tissue. However, the recent advent of faster MR imaging sequences now enables improved lung imaging with increased resolution in living patients. The exceptional contrast between more normal lung parenchyma and granulomatous lesions in the current study is made possible by high signal intensity. Such information could be used to inform on appropriate times to terminate animals. This would minimise the risk of terminating an animal prematurely and would avoid situations, such as occurred in this study with D28, where termination was predominantly based on behavioural criteria, in contrast to the lower level of disease suggested by the clinical measures. Such discrepancies can reduce the discriminatory power of a vaccine study. In-study stereology could also provide an opportunity to refine studies; if clear differences seen between control and vaccine groups could be identified, studies could be terminated early which would be beneficial both in terms of animal welfare and the cost of the study. The introduction of modern multichannel MRI systems capable of fast acquisition times may make the use of *in vivo* MR image scanning possible, with the alternative of Multislice CT scanning also worthy of consideration. Whilst MR has the advantage over CT in providing better soft tissue contrast that enables easy detection of necrosis in pulmonary nodules and lymph nodes it has the disadvantage of slower scanning speed and decreased spatial resolution.

In conclusion, therefore, this study has shown that the application of new stereology-based techniques applied to the measurement of lesion volume to lung volume ratio from lung images provides a useful new tool to quantify pulmonary disease induced by *M. tuberculosis* that can be used to evaluate disease severity and, as a quantitative system, provides advantages over existing qualitative systems. Studies are in progress to determine the utility of this new tool as a measure of vaccine efficacy.

Acknowledgements

The views expressed in this publication are those of the authors and not necessarily those of the Department of Health. We thank the staff of the Biological Investigations Group at HPA for assistance in conducting studies and Ms Susan Gray for histology support.

Funding: This work was supported by Department of Health, UK and NIH grant (U01 AI070456).

Competing interests: None declared.

Ethical approval: Not required.

References

- Global tuberculosis control: surveillance, planning, financing: WHO report: 2008. WHO/htm/TB/2008.393.
- Colditz GA, Brewer TF, Berkley ME, Wilson E, Burdick HV, Fineberg, et al. Efficacy of BCG vaccine in the prevention of tuberculosis. Meta analysis of the published literature. *JAMA* 1994; **271**: 698–702.
- Orme IM, McMurray DN, Belisle JT. Tuberculosis vaccine development: recent progress. *Trends Microbiol* 2001; **9**: 115–8.
- Basaraba RJ. Experimental tuberculosis: the role of comparative pathology in the discovery of improved tuberculosis treatment strategies. *Tuberculosis (Edinb)* 2008 Aug; **88**(Suppl. 1):S35–47. Review.
- McMurray DN, Collins FM, Dannenberg Jr AM, Smith DW. Pathogenesis of experimental tuberculosis in animal models. *Curr Top Microbiol Immunol* 1996; **215**: 157–79.
- McMurray DN. A non-human primate model for the preclinical testing of new tuberculosis vaccines. *Clin Infect Dis* 2000; **30**(Suppl. 3):S210–2.
- Capuano SV, Croix DA, Pawar S, Zinovit A, Myers A, Lin PL, et al. Experimental *Mycobacterium tuberculosis* infection of cynomolgus macaques closely resembles the various manifestations of human *M. tuberculosis* infection. *Infect Immun*; 2003;5831–44.
- Good RC. Simian tuberculosis: immunologic aspects. *Annals NY Acad Sci* 1968; **154**:200–13.
- Barclay WR, Anacker RL, Brehmer W, Leif W, Ribi E. Aerosol-induced tuberculosis in sub-human primates and the course of the disease after intravenous BCG vaccination. *Infect Immun*; 1970;574–82.
- Barclay WR, Busey WM, Dalgard DW, Good RC, Janicki BW, Kasik JE, et al. Protection of monkeys against airborne tuberculosis by aerosol vaccination with bacillus Calmette-Guerin. *Am Rev Respir Dis* 1973 Mar; **107**(3):351–8.
- Janicki BW, Good RC, Mioden P, Affronti LF, Hymes WF. Immune responses in rhesus monkeys after bacille Calmette-Guerin vaccination and aerosol challenge with *Mycobacterium tuberculosis*. *Am Rev Respir Dis* 1973; **107**:359–66.
- Chaparas SD, Good RC, Janicki BW. Tuberculin-induced lymphocyte transformation and skin reactivity monkeys vaccinated or not vaccinated with bacille Calmette-Guerin, then challenged with virulent *Mycobacterium tuberculosis*. *Am Rev Respir Dis* 1975; **112**:43–7.
- Kraft SL, Dailey D, Kovach M, Stasiak KL, Bennett J, McFarland CT, et al. Magnetic resonance imaging of pulmonary lesions in guinea pigs infected with *Mycobacterium tuberculosis*. *Infect Immun* 2004 Oct; **72**(10):5963–71.
- Langermans JAM, Anderson P, van Soelingen D, Verenne RAW, Frost PA, van der Laan T, et al. Divergent effect of bacillus Calmette-Guerin (BCG) vaccination on *Mycobacterium tuberculosis* infection in highly related macaque species: implications for primate models in tuberculosis vaccine research. *Proc Natl Acad Sci USA* 2000; **98**(20):11497–502.
- Williams A, Davies AC, Marsh PD, Chambers MA, Hewinson RG. Evaluation of the protective efficacy of Bacille Calmette-Guerin vaccination against aerosol challenge by *M. tuberculosis* and *M. bovis*. *Clinical Infectious Diseases* 2000; **30**(Suppl. 3):S299–301.
- Williams A, Reljic R, Naylor I, Clark SO, Falero-diaz G, Singh M, et al. Passive protection with IgA antibodies against tuberculous early infection of the lungs. *Immunology* 2004; **111**:328–33.
- Williams A, James BW, Bacon J, Hatch KA, Hatch GJ, Hall GA, et al. An assay to compare the infectivity of *Mycobacterium tuberculosis* isolates based on aerosol infection of guinea pigs and assessment of bacteriology. *Tuberculosis* 2005; **85**:177–84.
- Lever MS, Williams A, Bennett AM. Survival of mycobacterial species in aerosols generated from artificial saliva. *Letts Appl Microbiol* 2000; **31**:238–41.
- Druett HA. A mobile form of the Henderson apparatus. *J Hyg(Lond)* 1969; **67**:437–48.
- Harper GJ, Morton JD. The respiratory retention of bacterial aerosols: experiments with radioactive spores. *J Hyg (Lond)* 1953; **51**:372–85.
- Langermans JAM, Doherty TM, Verenne RAW, van der Laan T, Lyashchenko K, Greenwald R, et al. Protection of macaques against *Mycobacterium tuberculosis* infection by a subunit vaccine based on a fusion protein of antigen 85B and ESAT6. *Vaccine* 2005; **23**:270–5.
- Michel RP, Cruz-Orive LM. Application of the Cavalieri principle and vertical sections method to lung: estimation of volume and pleural surface area. *J Microsc* 1988; **150**(Pt. 2):117–36.
- Cruz-Orive LM, Weibel ER. Sampling designs for stereology. *J Microsc* 1981; **122**(Pt. 3):235–57.
- Knust J, Ochs M, Gundersen HJ, Nyengaard JR. Stereological estimates of alveolar number and size and capillary length and surface area in mice lungs. *Anat Rec (Hoboken)* 2009; **292**(1):113–22.
- Nyengaard JR, Gundersen HJG. Sampling for stereology in lungs. *Eur Respir Rev* 2006; **15**(101):107–14.
- Lin PL, Pawar S, Myers A, Pergu A, Fuhrman C, Reinhart TA, et al. Early events in *Mycobacterium tuberculosis* infection in cynomolgus macaques. *Infect Immun* 2006; **74**:3790–803.
- Ribi E, Anacker RL, Barclay WR, Brehmer W, Harris SC, Leif WR, et al. Efficacy of mycobacterial cell walls as a vaccine against airborne tuberculosis in the rhesus monkey. *J Infect Dis* 1971; **123**:527–38.
- Gormus BJ, Blanchard JL, Alvarez XH, Didier PJ. Evidence for a rhesus monkey model of asymptomatic tuberculosis. *J Med Primatol* 2004; **33**:134–45.
- Shen Y, Zhou D, Qiu L, Lai X, Simon M, Shen L, et al. Adaptive immune responses of V γ 2V δ 2+T cells during mycobacterial infections. *Science* 2002; **295**:2255–8.
- Walsh GP, Tan EV, dela Cruz EC, Abalos RM, Villahermosa LG, Young LJ, et al. The Philippine cynomolgus monkey (*Macaca fascicularis*) provides a new non-human primate model of tuberculosis that resembles human disease. *Nat Med* 1996; **2**:237–40.
- Lewinson DM, Tydemans IS, Frieder M, Grotzke JE, Lines RA, Ahmed S, et al. High resolution radiographic and fine immunologic definition of TB disease progression in the rhesus macaque. *Microbes Infect* 2006; **8**:2587–98.
- Sugawara I, Li Z, Sun L, Udagawa T, Taniyama T. Recombinant BCG Tokyo (Ag85A) protects cynomolgus monkeys (macaca fascicularis) infected with H37Rv *Mycobacterium tuberculosis*. *Tuberculosis* 2007; **87**:518–25.
- Reed SG, Coler RN, Dalemans W, Tan EV, Dela Cruz EC, Basaraba RJ, et al. Defined tuberculosis vaccine, Mt672F/AS02A, evidence of protection in cynomolgus monkeys. *Proc Natl Acad Sci USA* 2009; **106**:2301–6.

34. Lin PL, Rodgers M, Smith L, Bigbee M, Myers A, Bigbee C, et al. Quantitative comparison of active and latent tuberculosis in the cynomolgus macaque model. *Infect Immun*. ia.asm.org/; 2009. published on line ahead of print from.
35. Basaraba RJ, Smith EE, Shanley CA, Orme IM. Pulmonary lymphatics are primary sites of *Mycobacterium tuberculosis* infection in guinea pigs infected by aerosol. *Infect Immun* 2006;**74**:5397–401.
36. Palanisamy GS, Smith EE, Shanley CA, Ordway DJ, Orme IM, Basaraba RJ. Disseminated disease severity as a measure of virulence of *Mycobacterium tuberculosis* in the guinea pig model. *Tuberculosis (Edinb)* 2008;**88**:295–306.
37. Hyde DM, Tyler NK, Plopper CG. Morphometry of the respiratory tract: avoiding the sampling, size, orientation, and reference traps. *Toxicol Pathol* 2007;**35**:41–8.
38. Oberholzer M, Bianchi L, Dalquen P, Landmann L, Heitz PU. Stereology in the extraction of information from images. *Anal Quant Cytol Histol* 1985;**7**:197.
39. Weibel ER. Quantitation in morphology: possibilities and limits. *Beitr Pathol* 1975;**155**:1–17.
40. Weibel ER, Hsia CC, Ochs M. How much is there really? Why stereology is essential in lung morphometry. *J Appl Physiol* 2007;**102**(1):459–67.
41. Verreck FAW, Vervenne RAW, Kondova I, van Kralingen KW, Remarque EJ, Braskamp G, et al. MVA.85A boosting of BCG and an attenuated *phoP* deficient *M. tuberculosis* vaccine both show protective efficacy against tuberculosis in rhesus macaques. *PLoS ONE* 2009;**4**:e5264, 1–11.

Original article

CLARK, S. O., HALL, Y., KELLY, D. L., HATCH, G. J. & WILLIAMS, A. 2011. Survival of *Mycobacterium tuberculosis* during experimental aerosolization and implications for aerosol challenge models. *J Appl Microbiol*, 111, 350-9.

Impact factor: 2.683

Contributions by HATCH, G. J.

Development of aerosol challenge systems, study design,

Microbiological experimental work and data analysis

Manuscript review

Citation metrics

Google Scholar: 38 citations

ORIGINAL ARTICLE

Survival of *Mycobacterium tuberculosis* during experimental aerosolization and implications for aerosol challenge models

S.O. Clark, Y. Hall, D.L.F. Kelly, G.J. Hatch and A. Williams

Health Protection Agency – Porton Down, Porton Down, Salisbury, UK

Keywords

disease(s), infection, modelling, mycobacteria.

Correspondence

Simon O. Clark, Health Protection Agency (HPA), Porton Down, Salisbury SP4 0JG, UK.
E-mail: simon.clark@hpa.org.uk

2011/0032: received 6 January 2011, revised 5 May 2011 and accepted 23 May 2011

doi:10.1111/j.1365-2672.2011.05069.x

Abstract

Aims: We undertook a series of experiments to investigate factors that contribute to variation in *Mycobacterium tuberculosis* viability and infectivity, during experimental aerosolization, with an aim to optimize a strategy to enable a more reproducible delivered dose within animal models of tuberculosis.

Methods and results: The viability and infectivity of the challenge suspension was determined in relation to aerosolization time, concentration, method of preparation and *M. tuberculosis* strain. Challenge stocks generated from frozen aliquots of *M. tuberculosis* were shown to undergo a $1 \log_{10}$ CFU ml^{-1} decrease in viability during the first 10 min of aerosolization. This correlated with a decrease in surface lung lesions developing in guinea pigs challenged during this time. The phenomenon of decreased viability *in vitro* was not observed when using freshly grown, nonfrozen cells of *M. tuberculosis*. The viability of aerosolized bacilli at the point of inhalation relative to the point of aerosolization always remained constant.

Conclusion: Based on these findings, we have developed an improved strategy by which to reproducibly deliver aerosol infection doses to individually challenged animals and separately challenged groups of animals.

Significance and Impact of the Study: Study of the aerobiological characteristics of micro-organisms is a critical step in the validation of methodology for aerosol infection animal models, particularly where large numbers of animals and nonhuman primates are used.

Introduction

The natural route of human infection with *Mycobacterium tuberculosis* is via inhalation of droplet nuclei. Therefore, aerosol challenge is deemed the most relevant route of infection for animal models used to study the natural history of tuberculosis disease (Riley 1957; Riley and O'Grady 1961; Riley *et al.* 1995; Escombe *et al.* 2007). It is important to develop these models thoroughly to measure disease burden accurately and sensitively, and that each animal is challenged in a reproducible manner. Several research groups use aerosol challenge models, and amongst them, different challenge apparatus are employed (Dannenberg 1994; McMurray

1994; Orme and Collins 1994; Lever *et al.* 2000; Williams *et al.* 2000; Chambers *et al.* 2001; Corner *et al.* 2001); however, there are very few reports of the aerobiological characteristics of the challenge organism under the conditions employed during challenge. In many cases, estimates of the delivered dose rely on empirical information or are extrapolated from data obtained from a small number of animals whose lungs are sampled post-challenge and assumptions are made that all animals challenged by the same process will receive the same inhaled dose (Guyton 1947; Bide *et al.* 2000). Previous published work can provide data on the aerobiological characteristics of organisms, but differences in the micro-organisms themselves and equipment used for

aerosolization mean that it is preferable to conduct studies specific to each aerosol challenge model.

Critical to the aerosolization of any pathogenic micro-organism is its ability to survive the stresses incurred whilst being generated and suspended as an aerosol. Factors known to influence the airborne survival of vegetative bacteria include temperature and relative humidity (Cox 1995). Aerosol droplet size, number of inhaled organisms and infectious dose all have an influence on the pathogen's ability to infect (Cox 1987, 1995). Aerosol exposure systems should be designed to provide a homogeneous aerosol to each group of animals challenged at any one time, irrespective of their position in the exposure system. The fully contained Henderson apparatus equipment used for aerosol challenges at the Health Protection Agency, Porton Down (HPA-PD), is a device for studying the infectivity and virulence of micro-organisms whilst in the form of aerosol particles is used, in conjunction with a Collison nebulizer, to deliver reproducible aerosol particles of micro-organisms to experimental animals whilst controlling parameters such as presented dose, air flow, temperature and relative humidity (Druett 1969). Groups of animals (up to 20 mice or 10 guinea pigs) are simultaneously exposed by inhalation of a continuous stream of homogeneous bioaerosol, in a manner that will deliver a reproducible dose to each animal, controlled through the parameters described above. In studies with larger numbers of small animals, these must be challenged in separate exposure groups, and animals that are physically larger must be challenged individually. Both scenarios require separate challenge suspensions, which introduces an additional variable to the system. To evaluate the factors that may contribute to animal-to-animal variation and to validate the aerosol challenge methodology for animal models of TB, we examined the viability of *M. tuberculosis* during experimental aerosolization by determining the viability of organisms in the Collison nebulizer over time and the subsequent concentration of viable bacilli at the point of inhalation. The studies were performed as 'mock challenges' using the same conditions as those employed during aerosol exposure of animals. We undertook a series of experiments to investigate factors that contribute to variation in organism viability and infectivity; these were duration of aerosolization, effect of the concentration of organisms in the nebulizer and the effect of freeze/thawing of the challenge suspension. We have developed a system of exposing nonhuman primates (NHPs) to *M. tuberculosis* by modifying the usual exposure system to deliver the aerosol via a veterinary anaesthesia mask, modified to permit the flow of aerosol over the nose of the subject (Jemski and Philips 1965). Evaluating the kinetics of *M. tuberculosis* during the aerosolization process and correlating this with disease in

the guinea pig model have allowed us to develop a robust strategy for the aerosol challenge of groups of small animals and individually challenged NHPs.

Materials and Methods

Bacterial strains and growth conditions

The *M. tuberculosis* H37Rv (National Collection of Type Cultures (NCTC) 7416) challenge stock was generated from a chemostat grown to steady state under controlled conditions at 37°C ± 0.1, pH 7.0 ± 0.1 and a dissolved oxygen tension of 10% ± 0.1, in a defined medium, the details of which have been previously described (James et al. 2000). Briefly, the chemically defined medium is an optimized nutrient-rich source that contains amino acids such as L-serine, L-alanine, L-asparagine and L-leucine that are known to be utilized during steady-state aerobic chemostat culture and also contains biotin (100 µg l⁻¹) and Tween 80 (0.2% v/v). High-concentration culture (approximately 1 × 10⁸ colony-forming units (CFU) ml⁻¹) was aliquoted and frozen at -80°C. *M. tuberculosis* Erdman strain lot K01, originally from the Trudeau Institute, USA, was supplied as frozen suspensions at a stated concentration of 3.5 ± 1.5 × 10⁸ CFU ml⁻¹ by Dr Amy Yang, Center for Biologics Evaluation and Research (CBER)/United States Food and Drug Administration. The *M. tuberculosis* strains described earlier are the stock cultures typically used in challenge studies at HPA-PD. Additionally, *M. tuberculosis* H37Rv was grown to late exponential phase in a chemically defined medium (Bacon and Hatch 2008) in a shaking incubator at 37°C and 220 rev min⁻¹. High-concentration culture (approximately 1 × 10⁸ CFU ml⁻¹) was then aliquoted to be used either fresh or frozen at -80°C and subsequently thawed for use.

The Henderson apparatus

The principal assembly of the Henderson apparatus consists of three components: (i) A three-jet Collison nebulizer generates aerosol particles from a biological suspension and within a few seconds can be delivered through the (ii) 'piccolo' apparatus that is a chamber designed to allow the particles of bacilli in the aerosol to equilibrate with the main air flow before inhalation. An air flow of 55 l min⁻¹ through the apparatus is controlled by a critical orifice set within the apparatus (iii) The aerosol continues through the apparatus to the exposure unit named a 'sow' where animals are nose-only exposed to the aerosol for a set duration of time. The sow can be replaced (or supplemented) with biological samplers (e.g. all-glass impinger AGI-30) where the aerosol particles are

impinged into a collection medium for assay of viable micro-organisms in the circulating aerosol (Druett 1969). Characterization of the aerosol particle size distribution of *M. tuberculosis* using the Henderson apparatus has been performed previously (Lever et al. 2000).

Impact of aerosol generation time on infectious dose of *M. tuberculosis*

Aerosol challenge of guinea pigs

The infectivity of aerosolized *M. tuberculosis* culture suspension was determined using surface lesion counts as a read-out. Guinea pig experimental work was conducted according to UK Home Office legislation for animal experimentation and was approved by the local ethical committee. The impact on infectivity of different aerosolization parameters of *M. tuberculosis* was evaluated by exposing groups of guinea pigs to aerosols generated from a single suspension over a time course. Groups of six female Dunkin Hartley guinea pigs were exposed for

5 min each at time points of 0, 10 or 20 min postinital aerosolization. A total of 36 guinea pigs were used in this study. The experiment was performed with both *M. tuberculosis* H37Rv and *M. tuberculosis* Erdman.

Aerosol particles of *M. tuberculosis* with a mean diameter of $2 \mu\text{m}$ (diameter range of $0.5\text{--}7.0 \mu\text{m}$) were generated using a three-jet Collison nebulizer (BGI Inc., Waltham, MA, USA), used in conjunction with a controlled pressurized air supply, and a controllable air flow system was used to deliver the aerosols to animals placed in a nose-only exposure system (sow) (Fig. 1a) (Williams et al. 2000). Relative humidity, r.h. ($65 \pm 1\%$), temperature ($21 \pm 1^\circ\text{C}$) and air flow rates (55 and 7.5 l min^{-1} for circulating aerosol and Collison nebulizer, respectively) were maintained at the same level throughout an aerosol delivery. The aerosols of *M. tuberculosis* were generated from a saline suspension containing between 1×10^6 and $1 \times 10^7 \text{ CFU ml}^{-1}$, which has previously been shown to result in the delivery of approximately 10–100 surface lesions in the lungs over a 5-min exposure time

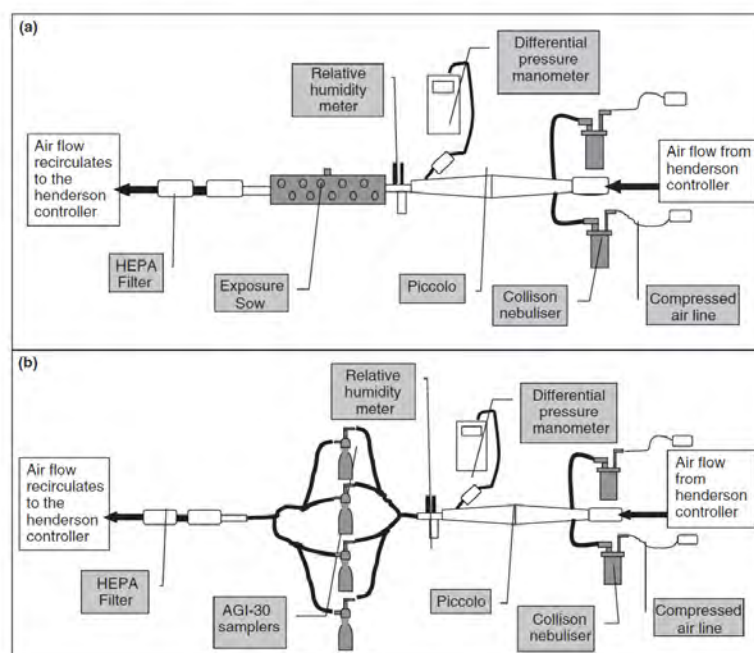


Figure 1 Schematic of CEPR, HPA Henderson apparatus (a), showing the position of the Collison nebulizer and aerosol flow in relation to the point of inhalation (exposure sow) and (b) the AGI-30 samplers positioned at the point of inhalation (replacing the exposure sow).

(Chambers *et al.* 2001). A second Collison nebulizer, as shown in Fig. 1a,b, contained only sterile saline and was used to purge the apparatus in between separate aerosolizations of mycobacterial cultures. Following aerosol challenge, the animals were housed for 28 days at Advisory Committee on Dangerous Pathogens (ACDP) containment level 3 within the Biological Investigations Group (BIG) containment facility at HPA, PD.

Surface lung lesion score on fixed lung tissue in the guinea pig after inhalation

At 28 days postchallenge, guinea pigs were euthanized by intraperitoneal injection of sodium pentobarbital. Lungs were removed from each guinea pig and placed into 10% neutral buffered formalin to fix the tissue. Once fixed, the lungs were analysed lobe by lobe and lesions counted to obtain total surface lesion count per animal.

Impact of aerosol generation time on viability of *M. tuberculosis*

*Sampling and determination of *M. tuberculosis* viability during aerosolization*

For the studies described later, approximately 20 ml of culture suspension was diluted in distilled water and was placed into a Collison nebulizer; 500 μ l sample aliquots of *M. tuberculosis* suspension was taken from the liquid phase of the Collison nebulizer at 0, 5, 10, 15, 20, 25 and 30 min after initial aerosolization. AGI-30 all-glass impingers (AGI-30) (Ace Glass, Brighton, UK) containing 5 ml of sterile water were used to sample the circulating air at a position equivalent to the exposure sow for periods of 5 min starting at 0, 5, 10, 15, 20 and 25 min after initial aerosolization. Four AGI-30 samplers were used allowing quadruplicate measurements at each time point (Fig. 1b). The aerosol was captured in the fluid of the AGI-30 impinger, and the concentration of viable organisms in the fluid was measured by serial dilution in sterile water and 100 μ l plated onto 7H11 OADC selective agar (Bio-Merieux, Basingstoke, UK) and incubated at 37°C for at least 3 weeks. Following incubation, agar plates were examined for growth of *M. tuberculosis* and colony counts determined and expressed as colony-forming units (CFU) ml⁻¹ of the sample fluid. The concentration of organisms in the liquid phase of the nebulizer was determined in the same way. These data were used to calculate the concentrations of viable organisms in the aerosol phase, as described later.

*Determination of spray factor of *M. tuberculosis* during aerosolization in the Henderson apparatus*

The spray factor (SF) defines a relationship between the viability of a challenge suspension in the nebulizer (C_{neb} ,

CFU ml⁻¹) and the concentration of viable bacilli in the circulating aerosol (C_{aero} , CFU l⁻¹) as per the following formula (Hartings and Roy 2004):

$$SF = C_{aero}/C_{neb} \quad (1)$$

The concentration of bacilli in the circulating aerosol (C_{aero}) was calculated using the formula below:

$$C_{aero} = (C_{imp} \times V_{imp}/Q_{imp} \times t_{exp})/1000 \quad (2)$$

where C_{imp} is the concentration of bacilli (CFU ml⁻¹), V_{imp} is the volume of collection fluid in the impinger (Litre), Q_{imp} is the sample flow rate of the impinger (l min⁻¹), and t_{exp} is the exposure time (min).

*Impact of viability in the Collison nebulizer of *M. tuberculosis* strains during nebulization*

Aerosol stability was evaluated in two common laboratory strains of *M. tuberculosis*, H37Rv and Erdman, to determine whether these strains differed in viability during aerosolization. The evaluation was conducted by sampling from the culture suspension of the Collison nebulizer at 5-min intervals in between aerosol challenge runs of groups of guinea pigs, described earlier. A concentration of 1×10^6 CFU ml⁻¹ of both *M. tuberculosis* strains was used in the Collison nebulizer, similar to the concentration normally used to infect animals with low-dose aerosols.

Impact of starting concentration of challenge suspension on viability over time

In a separate study, three different concentrations of *M. tuberculosis* H37Rv, 1×10^6 , 5×10^6 and 1×10^7 CFU ml⁻¹ in the Collison nebulizer, were tested to determine whether *M. tuberculosis* viability in the nebulizer and in the circulating aerosol was influenced by the starting concentration of organisms. Sampling and determination of *M. tuberculosis* viability during aerosolization was performed as described earlier.

Impact of freshly grown vs freeze/thawed stock suspension preparation on viability during nebulization

Fresh and frozen/thawed stocks of *M. tuberculosis* H37Rv were tested at two different concentrations, 1×10^6 and 1×10^7 CFU ml⁻¹ in the Collison nebulizer, to determine whether the viability of *M. tuberculosis* in the suspension liquid phase was influenced by the freeze/thawing of suspensions prior to aerosolization. Sampling and determination of *M. tuberculosis* viability during aerosolization was performed as described earlier.

Impact of freshly grown vs freeze/thawed stock suspensions on the spray factor

To determine whether freeze/thawing of the challenge suspension had an effect on the spray factor during aerosolization, the concentration of bacilli in the circulating aerosol was determined using the method described earlier, at 0–5, 5–10, 10–15, 15–20, 20–25 and 25–30 min post-aerosolization, using a concentration of 1×10^7 CFU ml⁻¹ *M. tuberculosis* H37Rv generated from freeze/thawed or fresh stock suspensions, in the Collison nebulizer.

Optimization of parameters required for aerosol challenge of nonhuman primates

Large animals are required to be exposed by aerosol challenge individually. In an infection study involving >12 NHPs, the aerosol challenge may need to occur more than 1 day. Therefore, we investigated important parameters of the aerosol challenge that specifically relate to the exposure of large animals, such as NHPs.

Comparison of the viability during nebulization of different frozen vials of challenge stocks

In a separate study, the effect of vial to vial variation on the viability of freeze/thawed *M. tuberculosis* Erdman suspensions was tested to determine whether challenge studies performed using separate aliquots of suspension would be reproducible.

Also, the effect of challenge suspension storage prior to aerosolization on the viability of *M. tuberculosis* Erdman (in the liquid phase of the nebulizer) was tested to determine whether aerosol challenges performed on separate days using the same aliquot of suspension would be reproducible. Individual frozen vials of *M. tuberculosis*

Erdman were thawed and diluted in sterile water to a working concentration of 1×10^6 CFU ml⁻¹ in the Collison nebulizer. The effect of overnight storage of the thawed *M. tuberculosis* suspensions at either room temperature or 2–8°C was compared to suspensions that were thawed immediately prior to aerosolization. Evaluations were conducted in quadruplicate. Sampling and determination of *M. tuberculosis* viability during aerosolization was performed as described earlier.

Statistical analysis

Statistical analyses were performed using MINITAB (ver. 13.32). Differences in lesion counts and differences in vial to vial *M. tuberculosis* viability were analysed via unpaired *t*-test. *P* values of <0.05 observed between compared groups were deemed as statistically significantly different.

Results

Impact of aerosol generation time on infectious dose of *M. tuberculosis*. Viability in Collison nebulizer vs surface lung lesion score at 28 days postchallenge

Figure 2 shows that a decrease of approximately 1 log₁₀ CFU ml⁻¹ in viable bacilli (derived from a frozen/thawed suspension preparation) occurred in the liquid phase of the Collison nebulizer during the initial 10 min of aerosolization. Between 10 and 30 min, the concentration of viable bacilli in the nebulizer was more stable and showed less of a decline in concentration over time (Fig. 2). The decline in infectivity followed a similar pattern to the decline in viability in the nebulizer. The average number of surface lesions per group counted in

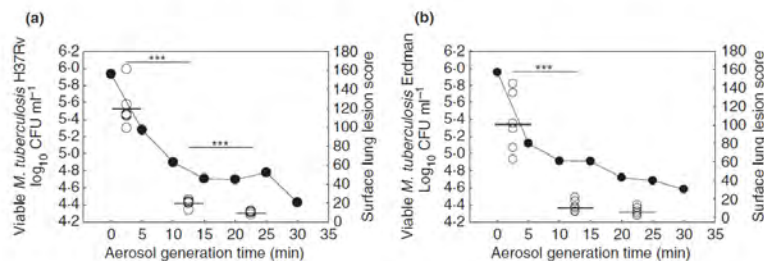


Figure 2 Impact of aerosol generation time on challenge dose of *M. tuberculosis* H37Rv (a) and *M. tuberculosis* Erdman (b): viability in Collison nebulizer vs surface lung lesion score 28 days postchallenge. The data are representative of two independent experiments of 18 guinea pigs in each study. Filled circles represent viability of *M. tuberculosis* in the Collison during aerosolization expressed as log₁₀ CFU ml⁻¹. Open circles represent dot plot of individual animal lung surface lesion counts expressed as total surface lesion count. Solid line represents mean lung surface lesion counts of animal groups (***) *P* < 0.001).

the guinea pigs exposed during the first 5 min of aerosolization was approximately 10-fold higher than the average number of lesions in animals exposed at 10 or 20 min post-aerosolization (Fig. 2). Differences in the number of lesions between all three time points (0–5, 10–15 and 20–25 min) were very highly statistically significant ($P < 0.001$), although the number of lesions in the latter two groups of animals was more similar. Similar data were obtained using two different commonly used laboratory strains of *M. tuberculosis*, H37Rv and Erdman, although in the latter case, no statistical difference in group lesion count was observed between 10 and 20 min (Fig. 2). The greatest variability of surface lesion counts within animal groups was in the first 5 min (group mean lesion count of 121 ± 9 and 89 ± 10 standard error of the mean, SEM) from infection with *M. tuberculosis* H37Rv and Erdman, respectively. After 10 min, the surface lesion counts were reproducible within animal groups (group mean lesion count of 20 ± 2 and 12 ± 2 SEM at 10 min and 10 ± 1 and 8 ± 2 SEM at 20 min post-aerosolization from infection with *M. tuberculosis* H37Rv and Erdman, respectively).

Impact of aerosol generation time on viability of *M. tuberculosis*

Impact of starting concentration of challenge suspension on viability over time

Three different concentrations of *M. tuberculosis* H37Rv challenge suspension (frozen/thawed preparation) (1×10^6 , 5×10^6 and 1×10^7 CFU ml⁻¹) in the Collison nebulizer each showed a decrease of approximately 1 log₁₀ CFU ml⁻¹ in viable bacilli during the initial 10 min of aerosolization (Fig. 3). However, between 10 and 30 min, the concentration of viable bacilli in the liquid phase of the nebulizer of all three challenge suspension concentrations was more stable and showed less of a decline in concentration over time (Fig. 3). The rate of decline in viable bacilli during the initial 10 min of aerosolization was comparable between all three suspension concentrations in the Collison nebulizer (Fig. 3).

Impact of freshly grown vs freeze/thawed suspensions on viability in the Collison nebulizer

No decrease in viable bacilli during the initial 10 min of aerosolization was observed when a freshly prepared *M. tuberculosis* H37Rv suspension (Fig. 4a) was compared with a frozen/thawed suspension (Fig. 4b). Between 10 and 30 min, the concentration of viable bacilli in the nebulizer containing a freshly grown suspension remained stable but did show a decline in concentration over time compared to viability in the first 10 min (Fig. 4a). Similar data were obtained for two different suspension concen-

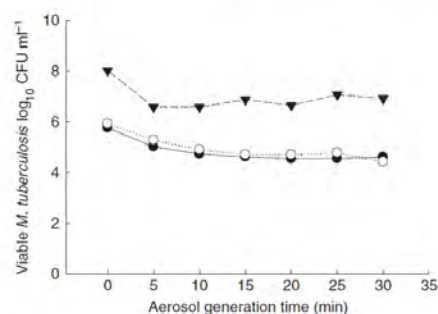


Figure 3 Impact of *M. tuberculosis* H37Rv concentration on its viability during aerosol generation. Viable *M. tuberculosis* log₁₀ CFU ml⁻¹ during aerosol generation. The data are representative of three independent experiments. Filled circles: 1×10^6 CFU ml⁻¹ in Collison nebulizer (a concentration designed to deliver a very low dose), open circles: 5×10^6 CFU ml⁻¹ in Collison nebulizer (a concentration designed to deliver a low dose) and filled triangles: 5×10^7 CFU ml⁻¹ in the Collison nebulizer (a concentration designed to deliver a high dose).

trations, 1×10^6 and 1×10^7 CFU ml⁻¹, in the Collison nebulizer (Fig. 4a,b).

Impact of freshly grown vs freeze/thawed suspensions on the spray factor

No changes in the spray factor were seen (derived from the concentration of bacilli in the Collison nebulizer and the circulating aerosol), sampled at either 0–5, 5–10, 10–15, 15–20, 20–25 or 25–30 min post-initial aerosolization, and no differences in spray factor were observed between freshly prepared and frozen/thawed challenge suspensions of *M. tuberculosis* H37Rv. The calculated average spray factor (ratio) was 9.54×10^{-7} (data not shown).

Optimization of parameters required for aerosol challenge of nonhuman primates

We investigated additional parameters pertinent to the aerosol challenge of large animals, such as NHPs. There is a requirement for large animals to be exposed individually. In an infection study involving >12 NHPs, the aerosol challenge may need to occur more than 1 day. We investigated the effects of storage of freeze/thawed challenge suspension on the viability of bacilli to determine whether NHPs could be challenged reproducibly on separate days with the same challenge suspension.

The pattern of decreasing viability over time was reproducibly observed in four separate frozen vials of *M. tuberculosis* (Erdman K01) challenge stocks. However,

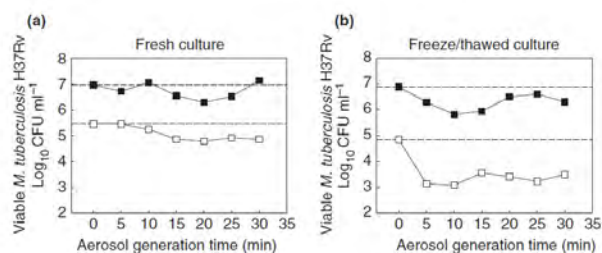


Figure 4 Impact of aerosol generation time on concentration of fresh and frozen/thawed *M. tuberculosis* H37Rv. Viability of (a) fresh and (b) freeze/thawed bacterial suspension in the Collision nebulizer expressed as fold change in viability relative to starting concentration. The data are representative of four independent experiments. Open squares: 1×10^6 CFU ml⁻¹ in Collision, and closed squares: 1×10^7 CFU ml⁻¹ in Collision represent viability of *M. tuberculosis* in the Collision during aerosolization expressed as fold change relative to the initial concentration log₁₀ CFU ml⁻¹.

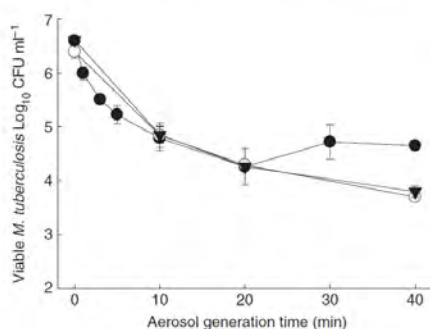


Figure 5 Impact of *M. tuberculosis* Erdman storage conditions on viability during aerosol generation. The data are representative of 12 independent experiments. Filled circles: frozen stocks of *M. tuberculosis* Erdman suspension thawed immediately prior to time of challenge, open circles: stocks of *M. tuberculosis* Erdman suspension thawed and then stored for 28 h at room temperature before challenge, closed triangles: stocks of *M. tuberculosis* Erdman suspension thawed and then stored for 28 h at 2–8°C before challenge. Four replicate vials used under each test condition. Viability expressed as log₁₀ CFU ml⁻¹ ± SEM.

there were differences in the level of reduction in viability of *M. tuberculosis* between vials with some vials showing a greater reduction in viability than others with SEM ranging from 0.045 to 0.343 (Fig. 5).

Storage of diluted suspensions at either 4°C or room temperature for 28 h did not alter the profile of reduced viability between 0 and 20 min ($P = 0.286$) (Fig. 5). However, after 40-min aerosol generation time, there was a statistically significant decrease in viability between storage of diluted suspensions at 4°C or at room temperature

for 28 h compared to suspensions that were used immediately after preparation ($P = 0.007$ and <0.001 , respectively) (Fig. 5).

Discussion

These studies describe a series of investigations into the viability and infectivity of suspensions of *M. tuberculosis* over various time periods. It is conventional to generate frozen stock suspensions of organisms for challenge experiments to increase reproducibility between studies. Pooling a number of freeze/thawed vials together as part of the protocol for generating a bacterial suspension for challenge would greatly reduce the variability seen between separate vials and would therefore reduce the variability of infectious dose between studies. Aerosolization of suspensions of freshly grown *M. tuberculosis* did not lose viability over time. However, freeze/thawed suspensions of *M. tuberculosis* showed reductions in viability (in the liquid phase) of approximately 1 log₁₀ CFU ml⁻¹ within the first 10 min post-aerosolization. However, it is widely accepted that there are inaccuracies associated with viable counts as measured by colony-forming units because of possible populations of viable nonculturable bacilli present. This effect, observed by the measure of bacterial viability in the Collision nebulizer, was verified to have an impact on infectivity *in vivo* by the measure of surface lesion development in guinea pig lungs 4 weeks postchallenge in groups of animals challenged for 5 min at each of the time periods post-aerosolization as the measure of suspension viability in the Collision nebulizer. A reduction of approximately 1 log₁₀ surface lesion count was observed in animals challenged during the first 10 min post-aerosolization of the bacteria. This indicates that the reduction in viability in the challenge suspension was unlikely to be as a result of the presence of a

sub-population of viable nonculturable bacilli within the challenge suspension because the reduction in viability was mirrored by a similar reduction in infectivity as measured by lung surface lesion counts. This reduction in viability in the nebulizer fluid needs to be considered for all systems that use a Collison nebulizer to generate the aerosols, especially when the suspension concentration is the critical factor for determining the estimated challenge dose, and no additional measures (e.g. air sampling or bacterial load in lungs on day of challenge) are applied to confirm the dose. It is necessary for us to know the relationship between Collison suspension concentration, circulating aerosol and inhaled/retained dose as we use the strategy of altering inhaled/retained dose in our models by altering the concentration of suspension in the Collison nebulizer. Because of the relatively low numbers of bacilli in the circulating aerosol during aerosolization within this apparatus, although not ideal, a 5 ml volume of sampling fluid was used, smaller than the recommended 20 ml volume, but was necessary to obtain an accurate colony count on solid agar.

Despite the variation in the viability of freeze/thawed *M. tuberculosis* suspensions in the Collison nebulizer, the spray factor (a function of the nebulizer, the bacilli and dilution effects within the Henderson apparatus) remained unchanged throughout the 30 min of aerosolization when using either freshly prepared or freeze/thawed challenge suspensions. This indicates that once aerosolized, the viability of bacilli in the circulating aerosol generated by the Henderson apparatus is reproducible during a time period appropriate for animal exposure. A possible reason for the 1 log₁₀ reduction in suspension viability in the Collison nebulizer in the first 10 min could be attributed to the presence of a sub-population of bacilli that are more susceptible, as a result of freeze/thawing, to the high physical fluid shearing forces generated by the aerosolization process. The Collison nebulizer works by applying sterile high pressure air to a reservoir of liquid culture suspension that aspirates the liquid into a sonic velocity gas jet wherein it is sheared into droplets. This liquid/gas jet is further impacted against the inside of the Collison nebulizer jar to remove the larger fraction of the droplets from the aerosol (May 1973). The susceptibility of bacilli to nebulization has been shown to affect viability in the suspended aerosol (Cox 1976; Griffiths *et al.* 1996; Heidelberg *et al.* 1997; Stone and Johnson 2002) and the liquid phase (Stone and Johnson 2002). Whilst our findings may suggest that fresh cultures are preferable in terms of improved viability during the aerosolization process, the variation associated with different culture techniques/conditions between small stock batches may outweigh the benefit of the reproducibility associated with preparing a large stock of

frozen material for use in many experiments. An equivalent initial decrease in viability in the nebulizer over time was observed when using diluted suspensions of challenge stock that had been stored overnight. However, after 40 min post-aerosolization, a significant decrease in viability was observed from suspensions of challenge stocks stored overnight. Therefore, using the same bacterial suspension to challenge larger animals on separate days, but not aerosolizing the suspension for more than 10 min, should deliver equivalent infectious doses between animals challenged on those separate days. The factors that did not affect the kinetics in viability of aerosolized *M. tuberculosis* over time were the concentration of suspension in the Collison nebulizer, the concentration of bacilli in the circulating aerosol (C_{aero}) and the spray factor. These observations are important because they provide flexibility in challenge studies as sometimes it is necessary to challenge animals with very low or relatively high doses but within a range relevant for modelling TB disease (Williams *et al.* 2005).

Our observations with *M. tuberculosis* under the experimental conditions used in these studies may not be expected for other micro-organisms. Hambleton *et al.* describe variable survival of aerosols in a Goldberg drum with different bacterial species and different strains. Interestingly, a 1 log₁₀ decrease in viability in the first 10 min of aerosol survival was observed with *E. coli* substrains B and JEPP but not with other strains and species (Heidelberg *et al.* 1997).

The loss of viability of aerosolized bacteria has been described in two stages by Ferry *et al.* (Ferry *et al.* 1958b; Gannon *et al.* 2007). The first stage is described as a relatively rapid loss in the viability of bacilli within the first minute of aerosolization. The mechanisms responsible for stage 1 of loss in viability are still unclear, but it is proposed that characteristic properties of individual bacterial suspensions used for aerosol generation are responsible (Ferry *et al.* 1958a). The second stage is described as a relatively slower loss in viability over a prolonged period of time. Experiments described by Ferry *et al.* have shown that factors such as rapid changes in atmospheric oxygen are attributable to stage 2 loss in viability. In terms of survival in the aerosol phase, the two published studies on *M. tuberculosis* report apparently contradictory results. The first documented approximately 65% survival after 3h (Loudon *et al.* 1969a,b), whilst the second study of Lever and colleagues at HPA-PD reported a 50% decrease in viability within the first 5 min and survival at below 1% at 1 h (Lever *et al.* 2000). It is important to note that the study described in this paper is aimed at validation of methodology for aerosol infection models and are focused upon aerosolization processes generated over a relatively short time frame rather than in understanding

the long-term impact of environmental factors on the ability of *M. tuberculosis* to survive in an aerosolized form.

When using a system where some animals may receive aerosolized bacilli at a later time point to others, the initial decrease in viability will have an influence on homogeneity of the dose delivered over an entire experiment. This may be the case in systems where separate groups of animals are exposed to the same suspension over several 'challenge runs' or in systems where there may be a time delay in the aerosol reaching some of the animals, e.g. in an exposure chamber. In the latter case, the aerosol inlet location versus the animal position in an exposure chamber should be considered carefully. Evaluating the kinetics of *M. tuberculosis* during the aerosolization process and correlating this with disease in the guinea pig model has allowed a validation of methodology for the aerosol challenge of groups of small animals and individually challenged NHPs.

Based on these findings, we have optimized a strategy to enable a more reproducible delivered dose to individually challenged animals and separately challenged groups of animals (Sharpe et al. 2009, 2010). Our strategy is to pool individual vials of *M. tuberculosis* challenge suspension to reduce vial to vial variation, perform a prechallenge aerosolization (when no animals are exposed) for a fixed period of time to allow initial period of decay in viability to occur prior to animal exposure, calculate the desired circulating aerosol concentration based on the decline in the nebulizer and to further subdivide the 'pre-treated' suspension for separate groups or individual animals to avoid the continued decline in viability.

Therefore, we conclude that the study of the aerobiological characteristics of micro-organisms is a critical step in the development of robust aerosol infection animal models, particularly where large numbers of animals and nonhuman primates are used.

Acknowledgements

This study was funded by the Department of Health, UK. The views expressed in this publication are those of the authors and not necessarily those of the Department of Health. We acknowledge the support of the staff in the Biological Investigations Group at HPA, Porton Down, and thank Prof. P.D. Marsh for providing comments on the manuscript.

References

- Bacon, J. and Hatch, K.A. (2008) Continuous culture of mycobacteria. In *Mycobacteria Protocols* ed. Parish, T. and Brown, A.C. pp. 153–171. New York: Humana Press.
- Bide, R.W., Armour, S.J. and Yee, E. (2000) Allometric respiration/body mass data for animals to be used for estimates of inhalation toxicity to young adult humans. *J Appl Toxicol* **20**, 273–290.
- Chambers, M.A., Williams, A., Gavier-Widen, D., Whelan, A., Hughes, C., Hall, G., Lever, M.S., Marsh, P.D. et al. (2001) A guinea pig model of low-dose *Mycobacterium bovis* aerogenic infection. *Vet Microbiol* **80**, 213–226.
- Corner, L.A., Buddle, B.M., Pfeiffer, D.U. and Morris, R.S. (2001) Aerosol vaccination of the brushtail possum (*Trichosurus vulpecula*) with bacille Calmette-Guérin: the duration of protection. *Vet Microbiol* **81**, 181–191.
- Cox, C.S. (1976) Inactivation kinetics of some microorganisms subjected to a variety of stresses. *Appl Environ Microbiol* **31**, 836–846.
- Cox, C.S. (1987) *The Aerobiological Pathway of Microorganisms*. pp. 244–254. Chichester, England: Wiley-Interscience.
- Cox, C.S. (1995) Stability of airborne microbes and allergens. In *Bioaerosol Handbook* ed. Cox, C.S. and Wathes, C.M. pp. 77–99. Boca Raton: CRC Press Inc.
- Dannenber, A.M. (1994) Rabbit Model of tuberculosis. In *Tuberculosis, Pathogenesis, Protection and Control* ed. Bloom, B.R. pp. 149–156. Washington, DC: ASM Press.
- Druett, H.A. (1969) A mobile form of the Henderson apparatus. *J Hyg* **67**, 437–448.
- Escombe, A.R., Oeser, C., Gilman, R.H., Navincopa, M., Ticona, E., Martinez, C., Caviedes, L., Sheen, P. et al. (2007) The detection of airborne transmission of tuberculosis from HIV-infected patients, using an in vivo air sampling model. *Clin Infect Dis* **44**, 1349–1357.
- Ferry, R.M., Brown, W.F. and Damon, E.B. (1958a) [Studies of the loss of viability of bacterial aerosols. III. Factors affecting death rates of certain non-pathogens.] *J Hyg* **56**, 389–403.
- Ferry, R.M., Brown, W.F. and Damon, E.B. (1958b) Studies of the loss of viability of stored bacterial aerosols. II. Death rates of several non-pathogenic organisms in relation to biological and structural characteristics. *J Hyg* **56**, 125–150.
- Gannon, B.W., Hayes, C.M. and Roe, J.M. (2007) Survival rate of airborne *Mycobacterium bovis*. *Res Vet Sci* **82**, 169–172.
- Griffiths, W.D., Stewart, I.W., Reading, A.R. and Fitter, S.J. (1996) Effect of aerosolisation, growth phase and residence time in spray and collection fluids on the culturability of cells and spores. *J Aerosol Sci* **27**, 803–820.
- Guyton, A.C. (1947) Measurement of the respiratory volumes of laboratory animals. *Am J Physiol* **150**, 70–77.
- Hartings, J.M. and Roy, C.J. (2004) The automated bioaerosol exposure system: preclinical platform development and a respiratory dosimetry application with nonhuman primates. *J Pharmacol Toxicol Methods* **49**, 39–55.
- Heidelberg, J.F., Shahamat, M., Levin, M., Rahman, I., Stelma, G., Grim, C. and Colwell, R.R. (1997) Effect of aerosolization on culturability and viability of gram-negative bacteria. *Appl Environ Microbiol* **63**, 3585–3588.
- James, B.W., Williams, A. and Marsh, P.D. (2000) The physiology and pathogenicity of *Mycobacterium tuberculosis* grown under controlled conditions in a defined medium. *J Appl Microbiol* **88**, 669–677.

- Jemski, J.V. and Philips, G.B. (1965) Aerosol challenge of animals. In *Methods of Animal Experimentation* ed. Gay, W. pp. 274–341. New York: Academic Press.
- Lever, M.S., Williams, A. and Bennett, A.M. (2000) Survival of mycobacterial species in aerosols generated from artificial saliva. *Lett Appl Microbiol* **31**, 238–241.
- Loudon, R.G., Bumgarner, L.R. and Coffman, G.K. (1969a) Isoniazid and the survival of tubercle bacilli in airborne droplet nuclei. *Am Rev Respir Dis* **100**, 172–176.
- Loudon, R.G., Bumgarner, L.R., Lacy, J. and Coffman, G.K. (1969b) Aerial transmission of mycobacteria. *Am Rev Respir Dis* **100**, 165–171.
- May, K.R. (1973) The Collision Nebulizer. Description, Performance & Application. *J Aerosol Sci* **4**, 235.
- McMurray, D.N. (1994) Guinea pig model of tuberculosis. In *Tuberculosis, Pathogenesis, Protection and Control* ed. Bloom, B.R. pp. 135–147. Washington, DC: ASM Press.
- Orme, I.M. and Collins, F.M. (1994) Mouse model of tuberculosis. In *Tuberculosis, Pathogenesis, Protection and Control* ed. Bloom, B.R. pp. 113–114. Washington, DC: ASM Press.
- Riley, R.L. (1957) Aerial dissemination of pulmonary tuberculosis. *Am Rev Tuberc* **76**, 931–941.
- Riley, R.L. and O'Grady, F. (1961) *Airborne Infection*. New York: Macmillan.
- Riley, R.L., Mills, C.C., Nyka, W., Weinstock, N., Storey, P.B., Sultan, L.U., Riley, M.C. and Wells, W.F. (1995) Aerial dissemination of pulmonary tuberculosis. A two-year study of contagion in a tuberculosis ward. 1959. *Am J Epidemiol* **142**, 3–14.
- Sharpe, S.A., Eschelbach, E., Basaraba, R.J., Gleeson, F., Hall, G.A., McIntyre, A., Williams, A., Kraft, S.L. *et al.* (2009) Determination of lesion volume by MRI and stereology in a macaque model of tuberculosis. *Tuberculosis (Edinburgh, Scotland)* **89**, 405–416.
- Sharpe, S.A., McShane, H., Dennis, M.J., Basaraba, R.J., Gleeson, F., Hall, G., McIntyre, A., Gooch, K. *et al.* (2010) Establishment of an aerosol challenge model of tuberculosis in rhesus macaques and an evaluation of endpoints for vaccine testing. *Clin Vaccine Immunol* **17**, 1170–1182.
- Stone, R.C. and Johnson, D.L. (2002) A Note on the Effect of Nebulization Time and Pressure on the Culturability of *Bacillus subtilis* and *Pseudomonas Fluorescens*. *Aerosol Sci Technol* **36**, 536–539.
- Williams, A., Davies, A., Marsh, P.D., Chambers, M.A. and Hewinson, R.G. (2000) Comparison of the protective efficacy of *bacille calmette-Guerin* vaccination against aerosol challenge with *Mycobacterium tuberculosis* and *Mycobacterium bovis*. *Clin Infect Dis* **30**(Suppl 3), S299–S301.
- Williams, A., Hatch, G.J., Clark, S.O., Gooch, K.E., Hatch, K.A., Hall, G.A., Huygen, K., Ottenhoff, T.H. *et al.* (2005) Evaluation of vaccines in the EU TB Vaccine Cluster using a guinea pig aerosol infection model of tuberculosis. *Tuberculosis (Edinburgh, Scotland)* **85**, 29–38.

Original article

HATCH, G. J., GRAHAM, V. A., BEWLEY, K. R., TREE, J. A., DENNIS, M., TAYLOR, I., FUNNELL, S. G., BATE, S. R., STEEDS, K., TIPTON, T., BEAN, T., HUDSON, L., ATKINSON, D. J., MCLUCKIE, G., CHARLWOOD, M., ROBERTS, A. D. & VIPOND, J. 2013a. Assessment of the protective effect of Imvamune and Acam2000 vaccines against aerosolized monkeypox virus in cynomolgus macaques. *J Virol*, 87, 7805-15.

Impact factor: 4.324

Contributions by HATCH, G. J.

Home Office – Personal Licence holder

Development and qualification of aerosol, biocontainment and clinical parameter systems. Performance of aerosol challenge.

Study management – Study design, liaison and co-ordination with sponsors, virology, immunology, histology and in vivo teams. scheduling, reporting

Data analysis and manuscript preparation

Citation metrics

Google Scholar: 36 citations

Assessment of the Protective Effect of Imvamune and Acam2000 Vaccines against Aerosolized Monkeypox Virus in *Cynomolgus* Macaques

Graham J. Hatch, Victoria A. Graham, Kevin R. Bewley, Julia A. Tree, Mike Dennis, Irene Taylor, Simon G. P. Funnell, Simon R. Bate, Kimberley Steeds, Thomas Tipton, Thomas Bean, Laura Hudson, Deborah J. Atkinson, Gemma McLuckie, Melanie Charwood, Allen D. G. Roberts, Julia Vipond

Microbiological Services, Public Health England, Salisbury, Wiltshire, United Kingdom

To support the licensure of a new and safer vaccine to protect people against smallpox, a monkeypox model of infection in cynomolgus macaques, which simulates smallpox in humans, was used to evaluate two vaccines, Acam2000 and Imvamune, for protection against disease. Animals vaccinated with a single immunization of Imvamune were not protected completely from severe and/or lethal infection, whereas those receiving either a prime and boost of Imvamune or a single immunization with Acam2000 were protected completely. Additional parameters, including clinical observations, radiographs, viral load in blood, throat swabs, and selected tissues, vaccinia virus-specific antibody responses, immunophenotyping, extracellular cytokine levels, and histopathology were assessed. There was no significant difference ($P > 0.05$) between the levels of neutralizing antibody in animals vaccinated with a single immunization of Acam2000 (132 U/ml) and the prime-boost Imvamune regime (69 U/ml) prior to challenge with monkeypox virus. After challenge, there was evidence of viral excretion from the throats of 2 of 6 animals in the prime-boost Imvamune group, whereas there was no confirmation of excreted live virus in the Acam2000 group. This evaluation of different human smallpox vaccines in cynomolgus macaques helps to provide information about optimal vaccine strategies in the absence of human challenge studies.

Variola virus, the etiological agent of smallpox, is highly contagious and causes disease with a high mortality rate (1). Endemic smallpox was eradicated through a successful global immunization campaign by the World Health Organization more than 30 years ago (2), with the final natural case of smallpox recorded in Somalia in 1977 (3). Since the eradication, widespread vaccination against this pathogen has been discontinued, and so the majority of the world's population currently lacks protective immunity (4). As a consequence, the use of variola virus as a biological weapon poses a current major public health threat. Other orthopoxviruses, for example, human monkeypox, cowpox virus, and a variety of vaccinia virus-like viruses (5–8), also threaten public well-being. These orthopoxviruses are naturally occurring and usually spread to human beings by zoonotic infection. Since all of these orthopoxviruses pose a risk to public health, there is a renewed effort to develop and stockpile medical countermeasures such as safe, effective orthopoxvirus vaccines and therapeutic agents.

The traditional calf-lymph derived, smallpox vaccines (e.g., Dryvax) used in the eradication of smallpox are based on replicating vaccinia virus. They are highly efficacious; however, their use is associated with rare but severe side effects, particularly in immunocompromised individuals (9, 10). Adverse events include progressive vaccinia, eczema vaccinatum, myo/pericarditis, Stevens-Johnson syndrome, fetal vaccinia, encephalitis, and occasionally death (11). Second-generation smallpox vaccines, for example, Acam2000, have subsequently been developed and licensed. These vaccines are produced using the Lister-Elstree or New York City Board of Health vaccinia virus strains in qualified cell cultures according to Good Manufacturing Practice standards (12, 13). Although these qualified vaccine preparations are cleaner and appear to be as effective as earlier vaccines, there are still adverse events following vaccination (11). Thus, if these vaccines

were used today, in a public health emergency, it is estimated that 25% of the general population would be at risk of developing complications (14).

Third-generation smallpox vaccines, such as Imvamune, manufactured by Bavarian Nordic (Martinsried, Germany), are currently being developed as safe and effective vaccines without the complications associated with traditional smallpox vaccines (15). Imvamune is based on a strain of the modified vaccinia Ankara (MVA) virus, which is a highly attenuated, replication-deficient strain of vaccinia virus. It was generated by more than 500 passages of vaccinia virus in chicken embryo fibroblasts, during which time it acquired multiple deletions and mutations and lost the capacity to replicate efficiently in people and most mammalian cells (16). In Germany, in the 1970s, MVA was tested in ~120,000 people. It was given as a preimmunization vaccine in combination with the Lister vaccine (a second-generation vaccine). Several high-risk groups were vaccinated, including young children with skin conditions (15–18), and there were no reports of serious adverse events using this two-step inoculation process (15).

It is not feasible to assess the protective efficacy of single or multiple doses of Imvamune vaccine in phase III human clinical trials because smallpox is no longer endemic in any part of the

Received 18 March 2013 Accepted 30 April 2013

Published ahead of print 8 May 2013

Address correspondence to Graham J. Hatch, graham.hatch@phe.gov.uk, or Julia A. Tree, julia.tree@phe.gov.uk

Copyright © 2013, American Society for Microbiology. All Rights Reserved.

doi:10.1128/JVI.03481-12

The authors have paid a fee to allow immediate free access to this article.

world. In order to progress licensing of effective medical countermeasures for biodefense, such as Imvamune, the U.S. Food and Drug Administration (FDA) has published the "Animal Rule" (19). This rule permits the approval or licensing of drugs and biological compounds based upon results obtained from an animal model that appropriately replicates the human condition. In the past, macaques have been used in studies employing both variola virus and monkeypox virus in order to model the ordinary disease presentation of smallpox infection in people (1). Since there are difficulties with working with variola virus, monkeypox virus infection in macaques has now become an acceptable surrogate model for human smallpox disease (20, 21), provided an appropriate dose and route of challenge such as aerosolization is used (1). Thus, this animal model is supported by the FDA and may provide valuable information on vaccine efficacy that could be used to aid licensing.

The purpose of the present study was to evaluate the protective effect of either a single dose of Imvamune, a prime and a boost of Imvamune, or a single dose of the licensed vaccine Acam2000 against disease following an aerosolized severe or lethal dose of the central African strain (Zaire 79) of monkeypox virus in cynomolgus macaques. Humoral and cell-mediated responses to vaccination were also examined.

MATERIALS AND METHODS

Experimental animals. Twenty-four captive bred, healthy, cynomolgus macaques (*Macaca fascicularis*) of Mauritian origin (12 male and 12 female) were obtained from a United Kingdom breeding colony for use in the present study. All of the animals weighed between 2.5 and 4.5 kg and were between 2 and 4 years of age at challenge. The monkeys were negative for neutralizing antibodies to orthopoxvirus prior to the start of the study. Animals were housed according to the United Kingdom Home Office Code of Practice for the Housing and Care of Animals Used in Scientific Procedures (1989) and the National Committee for Refinement, Reduction, and Replacement (NC3Rs) Guidelines on Primate Accommodation, Care and Use, August 2006. If a procedure required the removal of a primate from a cage it was sedated by intramuscular (i.m.) injection with ketamine hydrochloride (10 mg/kg; Ketaset, Fort Dodge Animal Health, Ltd., Southampton, United Kingdom). All procedures were conducted under a Project License approved by the Ethical Review Process of the Health Protection Agency, Salisbury, United Kingdom, and the United Kingdom Home Office. None of the animals had been used previously for experimental procedures.

Vaccines. Acam2000 Smallpox (vaccinia) vaccine was obtained from Acambis, Inc., Cambridge, MA. The freeze-dried vaccine was reconstituted in 0.3 ml of diluent, according to the manufacturer's instructions. Imvamune, modified vaccine virus Ankara-BN (MVA-BN), was manufactured by IDT Biologika GmbH (Germany) and was supplied by Bavarian Nordic A/S, Denmark, as a homogenous suspension. It was diluted in the diluent provided (Tris-buffered saline [TBS]) to give a final concentration of 2×10^8 50% tissue culture infective doses (TCID₅₀)/ml. The negative control for the experiment was TBS, the diluent used for the Imvamune vaccine.

Four treatment groups of six cynomolgus macaques were established. The first group of animals (TBS negative control) were inoculated with 0.5 ml of TBS 28 days prior to challenge. The second group of animals (Acam2000 × 1) were vaccinated with one dose of Acam2000 vaccine (2.5×10^5 to 12.5×10^5 PFU) at the same time. Both the TBS and the Acam2000 vaccines were delivered by scarification to the midscapular area with the use of a bifurcated-end needle. In the third group (Imvamune × 1), animals were vaccinated once with Imvamune (10^8 TCID₅₀ in a total volume of 0.5 ml) 28 days prior to challenge via the subcutaneous route. In the fourth group (Imvamune × 2), animals were vaccinated via

the subcutaneous route with an Imvamune primer dose of 10^8 TCID₅₀ in a 0.5-ml total volume, 56 days prior to challenge, and an Imvamune booster dose (10^8 TCID₅₀ in a 0.5-ml total volume) 28 days prior to challenge. The distribution of male and female macaques in the study was as follows: the TBS negative control animals were male ($n = 6$), the Acam2000-vaccinated animals were female ($n = 6$), the Imvamune × 1-vaccinated animals were male ($n = 6$), and the Imvamune × 2-treated animals were female ($n = 6$). Each group of animals was kept separate to avoid cross contamination and/or spreading of the vaccine.

Monkeypox virus challenge strain. Monkeypox virus strain Zaire 79, NR-2324, was obtained from the Biodefense and Emerging Infections Research Resources Repository (BEI Resources, Manassas, VA). On the day of challenge, stocks of virus were thawed and diluted appropriately in minimum essential medium containing Earl's salts (Sigma, Poole, United Kingdom), 2 mM L-glutamine (Sigma), and 2% (vol/vol) fetal calf serum (Sigma).

Aerosol exposure and sampling. Monkeys were challenged with a target dose of 10^5 PFU of monkeypox virus using the AeroMP-Henderson apparatus: a flexible, highly configurable system in which the challenge aerosol was generated using a six-jet Collision nebulizer (BGI, Waltham, MA). The aerosol was mixed with conditioned air in the spray tube (22) and delivered to the nose of each animal via a modified veterinary anesthesia mask. Samples of the aerosol were taken using an SKC BioSampler (SKC, Ltd., Dorset, United Kingdom) and an aerodynamic particle sizer (TSI Instruments, Ltd., Bucks, United Kingdom); these processes were controlled and monitored using the AeroMP management platform (Bi-aera Technologies, LLC, Frederick, MD). To enable delivery of consistent doses to individuals each animal was sedated and placed within a "head-out" plethysmograph (Buxco, Wilmington, NC). The aerosol was delivered simultaneously with a measurement of the respiration rate. A back titration of the aerosol samples taken at the time of challenge was performed to calculate the presented/inhaled dose. The challenge was performed on 2 days and the mean presented dose on each day was 2.1×10^5 and 3.1×10^5 PFU/animal (the overall mean presented dose was 2.6×10^5 PFU).

Antibody concentrations, cellular-immune populations, and cytokines were monitored in the blood pre- and postchallenge. After challenge, the viral loads were monitored in the blood and throat. For the latter, a flocced swab (Copan Diagnostics, Murrieta, CA) was gently stroked six times across the back of the throat in the tonsillar area.

Lung imaging. Thoracic, dorsoventral, and ventrodorsal radiographs (SP VET 3.2; Xograph Imaging Systems, Ltd., Tetbury, United Kingdom) were acquired at day 9 postchallenge using Xograph mammography film. Lung pathology was evaluated by two consultant thoracic radiologists blinded to the animals' vaccination and clinical status, using a predetermined scoring system.

ELISA. Samples of blood were taken at various time points throughout the study. Serum was isolated and assayed for immunoglobulin G (IgG) serum antibodies to vaccinia virus using an enzyme-linked immunosorbent assay (ELISA). Maxisorp 96-well plates (Nunc, Roskilde, Denmark) were coated overnight at 4°C with a preparation of commercially prepared psoralen/UV-inactivated, sucrose density gradient-purified vaccinia virus (Lister strain; Autogen Bioclear UK, Ltd., Wiltshire, United Kingdom) in calcium carbonate buffer at 2.5 µg/ml. Unbound antigen was removed by washing the plates three times. The plates were blocked with blocking buffer (phosphate-buffered saline [PBS], 5% milk powder [Sigma], 0.1% Tween 20 [Sigma]) for 1 h at room temperature with shaking. Unbound blocking solution was removed by washing three times. Fourfold serially diluted serum samples (starting at 1:50) were added to the plate for 2 h at room temperature with shaking. Unbound antibodies were removed from the plate by three washes. The plates were then incubated for 2 h with shaking with horseradish peroxidase-labeled anti-monkey-IgG (Kirkegaard & Perry Laboratories, Gaithersburg, MD). Unbound detection antibody was removed by five washes and then developed using an ABTS [2,2'-azino-bis(3-ethylbenzothiazolinesulfonic acid)] peroxidase

substrate system (Kirkegaard & Perry). The development of the ELISA was stopped using the ABTS stop solution (Kirkegaard & Perry). ELISA titers were calculated and compared to a vaccinia virus immune globulin standard (BEI Research Repository Resource, Manassas, VA), which was used to convert the titer into arbitrary international units (AIU)/ml.

Flow cytometry. Whole blood was collected at time points throughout the study by using heparin as the anticoagulant. Antibodies to CD3e, CD4, CD20, and CD16 (BD Biosciences, Oxford, United Kingdom) and to CD8a (Invitrogen, United Kingdom) conjugated to R-phycoerythrin (PE)-cyanine dye (Cy7), allophycocyanin, PE, fluorescein isothiocyanate, and PE-Texas Red, respectively, were incubated with the blood for 30 min at room temperature. The red blood cells were removed from the whole blood by lysing them with Uti-Lyse reagent (Dako, Cambridgeshire, United Kingdom). Flow count beads (Beckman Coulter, High Wycombe, United Kingdom) were added to provide a standard to enable cell counts per μl of blood, before being acquired on the flow cytometer. The data were collected on an FC500 flow cytometer (Beckman Coulter) and analyzed with CXP analysis version 2.1 software (Applied Cytometry Systems).

Luminex analysis of cytokines. The concentrations of interleukin-6 (IL-6) and gamma interferon (IFN- γ) were determined in serum samples using a NHP 23 Plex kit (Merck Millipore, Billerica, MA) according to the manufacturer's instructions. Samples were acquired using a Luminex 200 system (Luminex, Austin, TX), and the data were analyzed using the Xponent software (version 3.0). The concentration of each cytokine in the serum was calculated based on a comparison with the corresponding standard curve generated using purified cytokines from the kit.

Monkeypox virus plaque assay. During the course of the study, EDTA-treated blood and throat swabs were collected and frozen at -80°C and, at necropsy, tissues were collected and snap-frozen in liquid nitrogen. Prior to testing, the tissue was thawed and homogenized in PBS by using a Precellys24 tissue homogenizer (Bertin Technologies, Villeurbanne, France). The titers of live infectious virus in the tissues, blood, and throat swabs were determined by plaque assay. Samples were incubated in 24-well plates (Nunc/Thermo Fisher Scientific, Loughborough, United Kingdom) with Vero E6 (ATCC CRL-1586; American Type Culture Collection, Manassas, VA) cell monolayers under MEM (Life Technologies, Foster City, CA) containing 1.5% carboxymethyl cellulose (Sigma), 5% (vol/vol) fetal calf serum (Life Technologies), and 25 mM HEPES buffer (Sigma). After incubation at 37°C for 72 h, the samples were fixed overnight with 20% (wt/vol) formalin-PBS, washed with tap water, and stained with methyl crystal violet solution (0.2% [vol/vol]; Sigma).

PRNT assay. Samples of blood were collected at designated time points prior to challenge and neutralizing, anti-vaccinia virus antibody titers were measured by plaque reduction neutralization (PRNT) assay. Heat-inactivated sera (56°C for 30 min) were serially diluted and incubated with ~ 50 PFU of wild-type Lister-Elstree vaccinia virus for 1 h at 37°C in 5% CO_2 . The samples were then incubated with Vero E6 monolayers using the method described above. The neutralizing antibody titers were defined as the serum dilutions resulting in a 50% reduction relative to the total number of plaques counted without antibody, according to the Behrens-Karber formula (23). Titers were standardized to a standard preparation of human Vaccinia Immune Globulin CNJ-016 (BEI Research Repository Resource).

Virus detection by quantitative PCR. Tissue samples collected post-challenge and snap-frozen in liquid nitrogen were defrosted and homogenized in PBS using a Precellys24 tissue homogenizer. Viral DNA was isolated from homogenates by using a tissue kit (Qiagen, Crawley, West Sussex, United Kingdom) according to the manufacturer's instructions. Blood and throat swabs were processed using a Qiagen blood DNA mini-kit according to the manufacturer's instructions. Real-time PCR was performed using an Applied Biosystems 7500 Fast instrument (Life Technologies) with an in-house TaqMan assay targeted at the viral hemagglutinin (HA) gene and residues in the Z79 genome (GenBank accession no.

HQ857562.1 [V79-I-005]; monkeypox virus, residues 158734 to 158798, inclusive).

Clinical and euthanasia observations. The clinical observations were scored, and routine in-house welfare assessments were made at regular intervals pre- and postchallenge. These included measurements of the rectal temperature and body weight. These parameters also fed into a euthanasia scoring scheme. Both clinical and euthanasia scoring schemes used a scale to indicate severity (0 = none, 1 = mild, 2 = substantial, and 3 = intense). Clinical observation score sheets were used to record anorexia, behavioral changes (depression/unresponsiveness/repetitive activity), nasal discharge, cough, dyspnea, and rash/skin swelling, whereas euthanasia score sheets were used to record appearance and provoked and natural behavior. The criteria for immediate euthanasia included signs of severe systemic infection, $>20\%$ loss in body weight, convulsions, hemorrhagic rash, and persistent prostration. Postchallenge detailed clinical and euthanasia assessments were made on all animals every four to 6 h until recovery, at which time the frequency was reduced to twice daily.

Euthanasia and necropsy procedures. Animals were sedated with ketamine hydrochloride (10 mg/ml, i.m.; Fort Dodge Animal Health, Ltd.). Anesthesia was deepened using intravenous pentobarbitone sodium at 30 mg/kg (Sagatal; Rhone Merieux), and exsanguination was effected via the heart, before termination by injection of an anesthetic overdose (Dolethal, 140 mg/kg; Vetquinol UK, Ltd.). A full necropsy was performed immediately to provide tissues.

Pathological studies. At necropsy, gross observations, including skin lesions, were recorded, and samples were collected of all lung lobes, trachea, heart, liver, kidneys, spleen, tongue, tonsil, esophagus, stomach, ileum, descending colon, lymph nodes (tracheobronchial, axillary, mesenteric, mandibular, and inguinal), adrenal gland, ovary or testis, skin (with or without lesion), and brain. The samples were placed in 10% neutral buffered formalin; fixed tissues were then processed routinely to paraffin wax, and sections cut at $5\ \mu\text{m}$ and stained with hematoxylin and eosin (H&E).

Statistical analysis. Flow cytometry data and antibody titers as measured by ELISA and PRNT assays were compared across treatments using one-way Mann-Whitney tests. A Pearson product-moment correlation was performed on the transformed (\log_{10}) real-time PCR data set and the transformed (\log_{10}) PFU/ml data set for the blood and throat samples. All statistical analyses were performed using Minitab version 15.1. Differences were considered significant at P values of <0.05 .

RESULTS

Local effects at site of vaccination. Red patches were observed on all animals at the vaccination site 4 days postvaccination by scarification with Acam2000. These developed into raised scabbed sites ~ 10 mm in diameter by day 6 postvaccination. Dry scabs persisted for ~ 3 weeks postscarification. No reactive signs were detected at the vaccination sites of any Imvamune-vaccinated animals. Similarly no vaccination-specific marks were seen on the TBS negative control animals.

Vaccine-induced humoral immune responses. Sera from MVA vaccinated (Imvamune), vaccinia-virus vaccinated (Acam2000), and TBS negative control animals were tested with a PRNT assay against one antigen, wild-type Lister-Elstree vaccinia virus to determine the levels of vaccinia virus-specific neutralizing antibodies (Fig. 1a) prior to challenge. Antibodies were induced and continued to rise after vaccination with Acam2000 (Fig. 1a), with a maximum median titer of 132 U/ml 6 days prior to challenge. Significantly lower levels ($P < 0.01$) of neutralizing antibodies were detected by PRNT assay in animals vaccinated with a single dose of Imvamune (13 U/ml, 6 days prior to challenge). Animals that received a second boost of Imvamune showed a rise in neutralizing antibodies after the booster vaccination (Imvamune

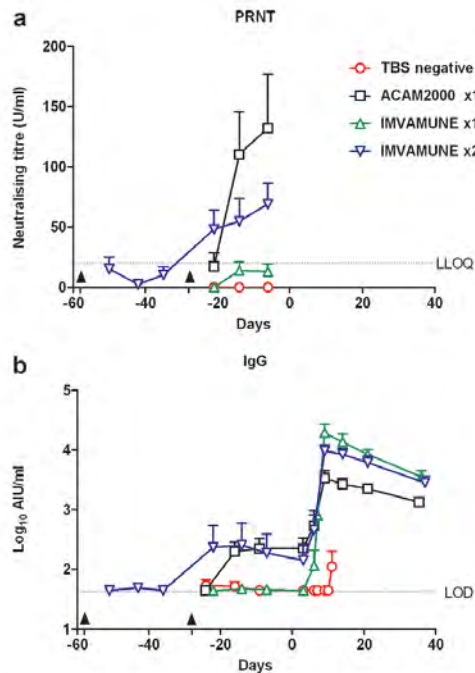


FIG 1 Vaccine-induced humoral immune responses. (a) Vaccinia virus-specific neutralizing serum antibody titres (median + 1 standard error [SE], $n = 6$) in samples collected on different days during the study, measured by PRNT assay. (b) Development of specific serum IgG responses in samples collected pre- and postchallenge, measured by ELISA (mean + 1 SE, $n = 6$), day 0, time of challenge with monkeypox. TBS negative, TBS negative control groups; closed triangles, times of immunization; LOD, limit of detection; LLOQ, lower limit of quantification.

$\times 2$). This reached 69 U/ml 6 days prior to challenge and was significantly higher ($P < 0.05$) than the titer in single-dose Imvamune group. Although higher concentrations of neutralizing antibody were detected in the Acam2000 group, this was not significantly different from the amount of antibody detected in the two-dose Imvamune group ($P > 0.05$) (Imvamune $\times 2$) (Fig. 1a).

The levels of circulating IgG antibodies were detected by ELISA pre- and postchallenge using only one antigen, vaccinia virus. Prior to challenge, no rise in IgG antibody was seen in the TBS negative control or the single Imvamune dose group. In the Acam2000 group after vaccination, IgG rose to 2.4 log₁₀ AUI/ml, 9 days prior to challenge (Fig. 1b). A similar rise in antibody was seen after the second dose of Imvamune in animals (Imvamune $\times 2$) (2.3 log₁₀ AUI/ml, 7 days prior to challenge) (Fig. 1b). After infection, the kinetics of the antibody responses for the Acam2000, Imvamune $\times 1$, and Imvamune $\times 2$ groups were similar; large increases in antibody titer from baseline levels were found which peaked at day 9 postchallenge and then decreased slowly to the end of the study. Vaccinia virus-specific IgG was not

detected in the TBS negative control group until day 11 (2.0 log₁₀ AUI/ml). Significantly ($P < 0.05$) higher levels of antibody were detected in the two-dose Imvamune group (4.0 log₁₀ AUI/ml) on day 9 postchallenge than in the Acam2000 group, where a peak of 3.5 log₁₀ AUI/ml was seen. Antibody concentrations in the single and two-dose Imvamune groups remained significantly ($P < 0.05$) higher than the Acam2000 group on days 14 and 21 (Fig. 1b) postchallenge.

Vaccine-induced cell-mediated immune responses. The cell-mediated immune responses after vaccination and challenge were monitored by flow cytometry. Lymphocyte numbers rose in the TBS negative control, and Acam2000 groups after vaccination by scarification (Fig. 2a to c). These small peaks were probably caused by local irritation at the site of vaccination caused by scarification. Small rises in CD3⁺, CD4⁺, and CD8⁺ cells were seen initially, following vaccination with one dose of Imvamune, but there was no marked increase following the second vaccination (Fig. 2). After challenge, however, there were noticeable rises in the different cell populations in animals that succumbed to disease in the TBS negative control group. For example, on day 9, there were significant differences ($P < 0.05$) between the TBS control and the Imvamune $\times 2$ group. On closer inspection, these differences were caused by the significant rise in circulating NK cells in the TBS control ($P < 0.05$). By day 14, there were significantly higher ($P < 0.05$) numbers of B cells and CD8⁺ T cells in the surviving animals (4/6) of the one-dose Imvamune group compared to the Acam2000 group. Also, by day 14 significantly higher ($P < 0.05$) numbers of CD4⁺ and CD8⁺ cells were recorded in single Imvamune group than in the two-dose Imvamune group (Imvamune $\times 2$).

Elevated concentrations of IFN- γ , as detected by Luminex assay, were seen in the TBS negative control group on day 6 after challenge (4630%) (Fig. 3a). In contrast, no rise in serum gamma-IFN was observed in animals in Acam2000 and two-dose Imvamune groups (Fig. 3a) as they were protected by vaccination. The single Imvamune dose group also had raised concentrations of serum gamma-IFN 6 days after challenge (Fig. 3a).

A significant rise in IL-6 cytokine was seen in the TBS negative control group following aerosol challenge, which continued to increase until the animals succumbed to infection on day 11 (4592% change from baseline) (Fig. 3b). Smaller increases in IL-6 were seen (day 6) in the single-dose Imvamune group (Fig. 3b).

Clinical signs of disease and mortality. Aerosol challenge with monkeypox virus at a mean presented dose of 2.6×10^5 PFU resulted in a severe or lethal infection in susceptible individuals. Most animals showed a decline in weight from their prechallenge weights (Fig. 4). This was most severe in the TBS negative control group, with a 10 to 18% loss in weight prior to euthanasia (Fig. 4a). All surviving animals in the vaccination groups—Acam2000, Imvamune $\times 1$, and Imvamune $\times 2$ —had a consistent increase in body weight from day 14 postexposure, indicating recovery from the infection (Fig. 4b to d).

Signs of infection generally appeared from day 5 postchallenge. Animals in the TBS negative control displayed progressing depression, dyspnea, and nasal discharge. All six animals succumbed to infection between days 7 to 11 postchallenge. In the single-dose Imvamune group, two animals succumbed to infection on different days. Both animals displayed mild depression and dyspnea and were recumbent from day 6 postchallenge; animal M064F was found dead in cage on day 7 postchallenge, and animal I320I had

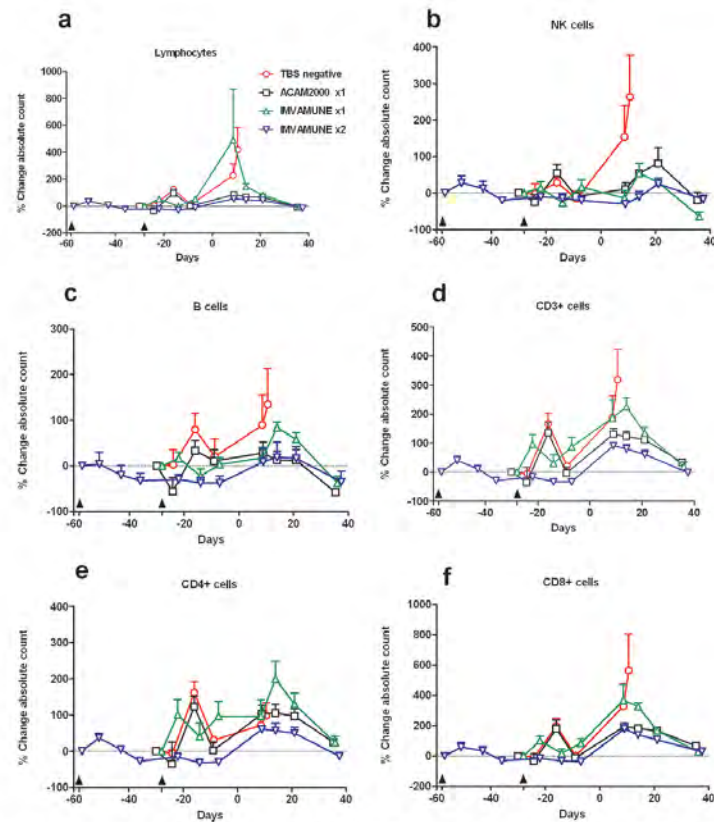


FIG 2 Cell-mediated immune responses, indicated as the mean percent (%) change compared to baseline levels (± 1 SE, $n = 6$), in different cellular populations in whole blood on various days in the study. Different cellular populations were evaluated. (a) Lymphocytes; (b) natural killer (NK) cells; (c) B lymphocytes; (d) CD3+ T lymphocytes; (e) CD4+ T lymphocytes; (f) CD8+ T lymphocytes. Day 0, time of challenge with monkeypox; TBS negative, TBS negative control group; closed triangles, times of immunization.

clinical signs that progressed to severe and met the criteria for immediate euthanasia on day 9 postchallenge. The remaining four animals in the one-dose Imvamune group were generally free of clinical signs and survived to the end of the study (67% survival). All of the animals vaccinated with Acam2000 or two doses of Imvamune survived the monkeypox virus challenge. The animals appeared to be clinically normal, although there were differences in the level of protection afforded by these vaccines, as demonstrated in some of the test parameters, such as radiographs, lesion counts, and viral load (Table 1).

Skin lesions, as a result of monkeypox virus infection, first appeared at day 6 after challenge (Table 1). There was a peak in the mean number of lesions, across all vaccination and control groups at day 9. The greatest mean number of lesions was 51 per animal (range, 5 to 169) in the TBS negative control group (Table 1). Fewer lesions were detected in the vaccination groups. Vaccina-

tion with one or two doses of Imvamune led to fewer lesions on day 9, with means of 10 (range, 0 to 42) and 7 (range, 0 to 18) lesions per animal, respectively. The lowest mean number of lesions was 3 (range, 0 to 7) per animal in the Acam2000 treatment group.

Radiographs were taken postchallenge at the time when clinical signs were most severe (9 days). They were scored independently against a corresponding baseline image. Animals in the TBS negative control group generally displayed the most severe clinical signs (Table 1). Radiographs taken from animals in the Acam2000 vaccination group were normal. A wide spectrum of conditions was observed in the Imvamune single- and two-dose groups ranging from normal to severe edema (Table 1). One animal (Z385A) in the two-dose Imvamune group had moderate to severe pulmonary edema but recovered fully.

Whole blood, throat, and tissue viral loads of NHP exposed to

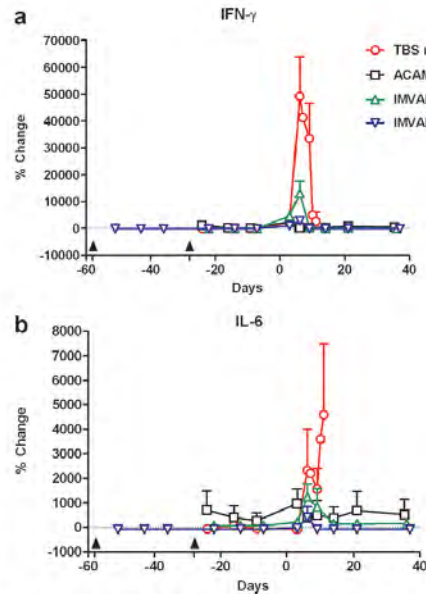


FIG 3 Cytokine profiles in the serum of cynomolgus macaques. The mean percent (%) change from baseline levels (± 1 SE, $n = 6$) in cytokine levels, on various days during the study, was determined. The IFN- α (a) and IL-6 (b) responses are shown. TBS negative, TBS negative control group; day 0, time of challenge with monkeypox; closed triangles, times of immunization.

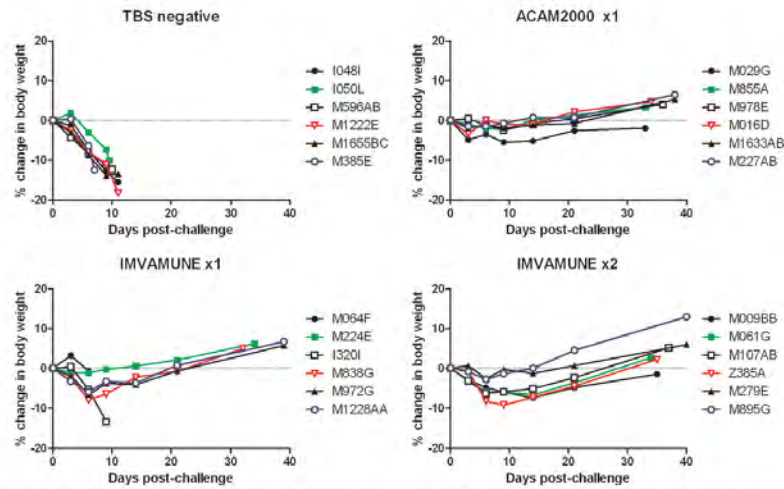


FIG 4 Change in the body weight of cynomolgus macaques. The percent (%) change in body weight compared to baseline levels in animals challenged with aerosolized monkeypox, over time, following vaccination, was determined. The results for individual animals are plotted. TBS negative, TBS negative control group.

aerosolized monkeypox virus: the monkeypox viral load of blood and throat swabs were assessed by plaque assay (PFU/ml) (Fig. 5a and b) and real-time quantitative PCR (genomes/ml) (Fig. 5c and d) (there was a strong correlation [$r = 0.746$; $df = 26$, $P < 0.001$, Pearson product-moment correlation] between plaque assay and real-time PCR data). The peak in the mean load of viral DNA (4×10^8 genomes/ml) in the blood of animals from the TBS negative control group (Fig. 5c) occurred on day 7 postchallenge. In contrast, no viral DNA was also detected in the group that received the Acam2000 vaccine on any day examined postchallenge. A peak in the mean level of viral DNA in the blood was detected in animals that had received one (6×10^7 genomes/ml; day 7 postchallenge) and two (1×10^4 genomes/ml; day 6 postchallenge) doses of Imvamune (Fig. 5c). Low levels of live virus were detected in the blood by day 3 postchallenge in all three vaccination groups and the TBS negative control group, ranging from 25 to 200 PFU/ml (Fig. 5a).

In the TBS negative control group, live virus (10^5 PFU/ml) and viral DNA (10^7 genome copies/ml) were detected in the throats of all animals challenged with monkeypox virus (Fig. 5b and d). Live virus (10^4 to 10^5 PFU/ml) was also detected in the throats of animals that had received a single dose of Imvamune (Fig. 5b and d). In the two-dose Imvamune group, four of six animals did not excrete virus in the throat (within the sensitivity of the plaque assay [<25 PFU/ml]). Live virus was detected at low levels (50 PFU/ml) in one of six animals, and one animal (Z385A) excreted high levels of virus that peaked (4.6×10^4 PFU/ml) on day 9 postchallenge. In contrast, live virus was not detected in the throats of animals (5/6 animals) vaccinated with Acam2000. Note that no plaque assay data were obtained for one remaining animal (M016D) in the Acam2000 group due to contamination of the cell monolayer.

TABLE 1 Clinical signs of monkeypox disease^d

Measurement	Treatment group			
	TBS negative control	Acam2000 ×1	Imvamune ×1	Imvamune ×2
Temp	Normal	Normal	Normal	Normal
Clinical signs ^b	+++	+	++ ^c	+
Mean no. of lesions (day 9)	51	3	10	7
Onset of lesions	Day 6	Day 9	Day 9	Day 6
Resolution of lesions	Not resolved	Within 5 days	Within 5 days	Within 5 days
Thoracic radiography ^d	+++	—	++	+
Survival (%)	0 ^e	100	67 ^f	100

^a Clinical signs were monitored every 4 to 6 h until disease recovery and thereafter twice daily. Treatment groups are as described in Materials and Methods.

^b Clinical signs: —, none; +, mild; ++, substantial; +++, intense signs.

^c Two of the that animals succumbed to infection had intense clinical signs (+++).

^d A thoracic radiograph was obtained 9 days postchallenge. Findings were scored as follows: —, normal; +, minor pulmonary edema; ++, mild pulmonary edema; +++, moderate pulmonary edema.

^e All animals died between 7 and 11 days postchallenge and displayed high euthanasia scores.

^f Two animals succumbed to infection on day 7 and day 9 postchallenge; the animal that died on day 7 had low euthanasia scores prior to death.

In addition to blood and throat swabs, tissues were collected postmortem and assayed by real-time quantitative PCR for viral load. The majority of tissues were positive for monkeypox virus in the TBS negative control group (Fig. 6a). The greatest viral loads were found in the tonsil and lung tissues, with between 10^6 and 10^7 genomes/mg. Two animals (M064F and I320I) vaccinated with a

single dose of Imvamune also succumbed to monkeypox infection. These two animals also showed similar patterns of viral load, as seen in the TBS negative control group. Both tonsil and lung tissue reflected the greatest values of between 10^5 and 10^6 copies/mg (Fig. 6c). The remaining animals in the Imvamune ×1 group that survived to the end of the study (>30 days postchal-

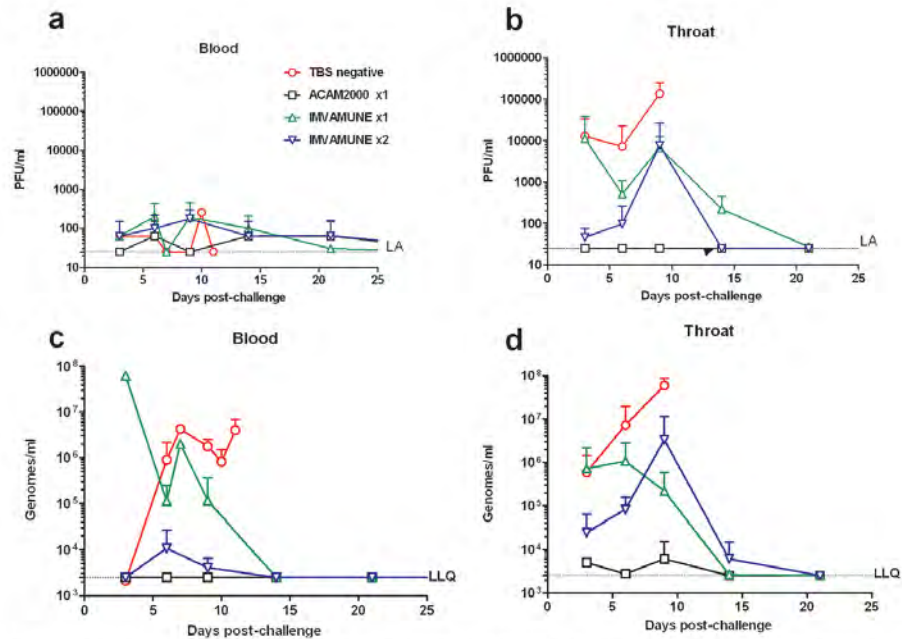


FIG 5 Mean detectable levels (± 1 SD) of live monkeypox virus in the blood (a) and throats (b) of macaques after a challenge with aerosolized virus (the limit of plaque assay sensitivity was 25 PFU/ml). The numbers of viral genomes (HA gene), as determined from quantitative PCR analyses in the blood (c) and throats (d) in samples postchallenge, are shown. TBS negative, TBS negative control group; LLQ, the lower limit of quantification for quantitative PCR was 2,500 genomes/ml; LA, limit of plaque assay sensitivity. The plaque assay result for 1/4 animals in the Imvamune ×2 was lost due to monolayer contamination on day 14.

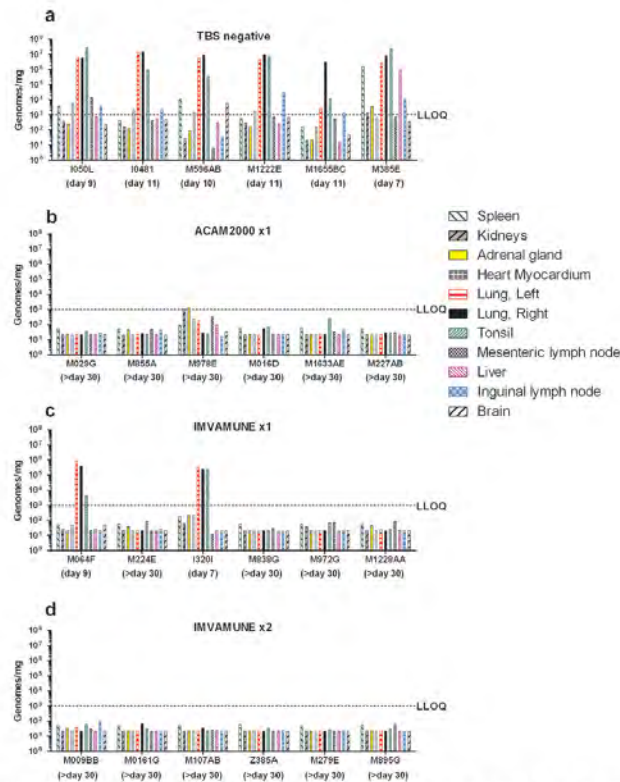


FIG 6 Viral load in tissues after challenge with monkeypox virus. The viral load, as determined by real-time PCR, in the tissues of different animals in the treatment groups. Individual animals in the TBS negative control (a), Acam2000 \times 1 (b), Imvamune \times 1 (c), and Imvamune \times 2 (d) groups were evaluated. LLOQ, lower limit of quantification was 1,000 genomes/mg (the time postmortem is given as the number of days postchallenge). TBS, TBS negative control group.

lunge) did not have any detectable viral loads by PCR in their tissue postmortem. No detectable viral loads were seen in the tissue of animals from the Acam2000 vaccination or the two doses of Imvamune (Fig. 6b and d). All of these animals also survived to the end of the study (between 30 and 40 days).

Pathological and histopathological findings. Gross findings on postmortem examination revealed that the main gross lesions associated with monkeypox infection consisted of lung consolidation in all animals in the TBS negative control and in two of the six animals in Imvamune \times 1 group. An enlarged spleen was seen in five of six animals in the TBS negative control and in one of six animals in the Imvamune \times 1 group.

On histological examination, changes consistent with acute monkeypox infection were observed in the TBS negative control group in the lungs, comprising (i) focal, acute necrotizing bronchitis and bronchopneumonia (Fig. 7a); (ii) focal, fibrinous, necrotizing alveolitis (Fig. 7b), often accompanied by edema; and (iii) focal acute vasculitis, sometimes together with thrombosis and perivascular edema. In addition, focal necrosis with or with-

out neutrophil infiltration was observed in the trachea, larynx, and tracheobronchial lymph node. In the skin (with lesion), spleen, tonsils, the axillary, inguinal, and mandibular lymph nodes, and the descending colon, focal necrosis—with or without neutrophil infiltration—was observed.

In animals vaccinated with Acam2000, which were killed 33 to 38 days postchallenge, only mild, chronic lesions were observed. These comprised focal alveolar epithelialization and/or infiltration of alveolar walls by lymphocytes and macrophages, which were seen in two (M016D and M978E) of the six animals (Fig. 7c). Hyperplasia of bronchus-associated lymphoid tissue (BALT) was recorded in five of six animals.

Animals vaccinated with a single dose of Imvamune that died (M064F) or were killed for welfare reasons (I3021) (days 7 and 9 postchallenge, respectively) had lesions of acute disease in all lung lobes, similar to those described above in the TBS negative control group (Fig. 7d). In the trachea of one animal and in the larynx of another, focal necrosis, with or without neutrophil infiltration, was also observed. Hyperplasia of BALT was observed in one of

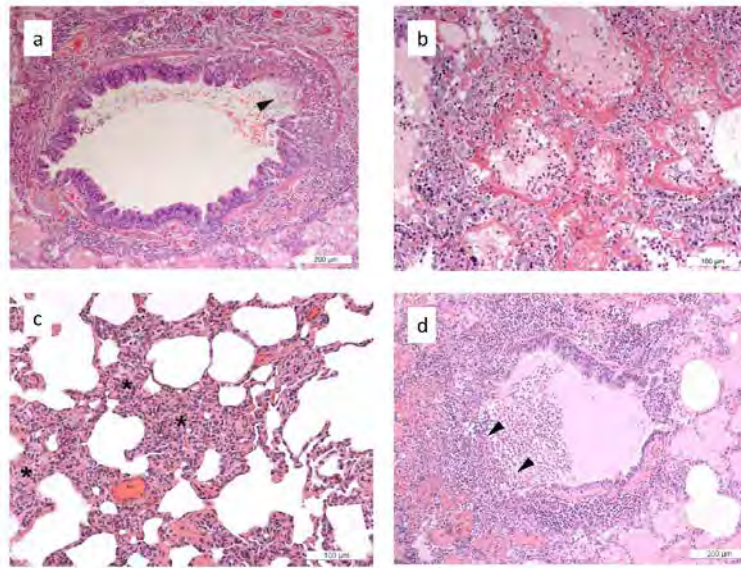


FIG 7 Histological lesions associated with monkeypox infection in the lung. (a) TBS negative control, animal M596AB (lung; focal, acute, and necrotising bronchiolitis [arrowhead]; H&E staining). (b) TBS negative control, animal M595AB (lung; focal, fibrinous, and necrotising alveolitis; H&E staining). (c) Acam2000 vaccination group, animal M016D (lung; patchy infiltration of alveolar walls by lymphocytes and macrophages [asterisks]; H&E staining). (d) Single Imvamune dose, animal I3201 (lung; focal, acute, and necrotising bronchiolitis [arrowheads]; H&E staining).

four animals that were euthanized as scheduled 32 to 39 days after challenge. In all animals in the single-dose Imvamune group, mild changes of focal alveolar epithelialization and/or infiltration of alveolar walls by lymphocytes and macrophages, a finding consistent with chronic or resolving lesions, were recorded.

In animals that received two doses of Imvamune and were euthanized as scheduled 35 to 40 days after challenge, only mild lesions of chronic disease, comprising focal alveolar epithelialization and/or infiltration of alveolar walls by lymphocytes and macrophages were seen in two of the six animals. Hyperplasia of BALT was recorded in four of six animals.

Lesions attributable to monkeypox infection were not detected in the liver, kidney, heart, tongue, esophagus, stomach, ileum, mesenteric lymph node, adrenal gland, ovary, testis, or brain of any animal.

DISCUSSION

Since smallpox has been eradicated, the future licensing of a new generation of smallpox vaccines relies, in part, on the demonstration of efficacy in animal models of monkeypox (19). When monkeypox virus infects people as an epizootic pathogen, it presents a clinical disease similar to smallpox in that the time course and manifestation of disease is similar to that seen with human smallpox, particularly the rash which progresses through the macular, papular, vesicular, and pustular phases (24). Thus, a well-defined animal model using monkeypox virus should mimic the natural course of smallpox disease. Macaques have been used at various stages of smallpox vaccine and antiviral research (16, 25–36), and

in each case the route of infection, dose, and choice of challenge strain have been key factors in determining whether the macaque model of monkeypox resembles human clinical variola virus infection.

Imvamune is a more recent smallpox vaccine and is being fast-tracked by the FDA for use in humans (37). This vaccine is currently stockpiled in the United States for use during an emergency, such as an imminent bioterrorist attack, to protect individuals who are at risk of developing side effects from older vaccines (37). Studies have been published demonstrating the safety, immunogenicity (4), and protective efficacy against vaccinia virus scarification in humans (38) of Imvamune delivered in a single- or two-dose regime. Several studies have also shown its protective potency in animals (33, 39, 40). In the present study, for the first time, the efficacy of both one and two doses of Imvamune vaccine was assessed in cynomolgus macaques following challenge with an aerosolized dose of 2.6×10^5 PFU of monkeypox Zaire Z9. Inhalation of aerosolized virus more closely resembles the natural route of infection of smallpox in humans (41) and therefore initiates the onset of clinical signs that are similar to human clinical disease (20, 42).

When aerosolized monkeypox virus was used at a dose (2.6×10^5 PFU) to produce severe or lethal disease in naive cynomolgus macaques, animals in the TBS negative control group succumbed to infection within 7 to 11 days. Pock lesions began to appear on day 6 postchallenge, and there was a peak in the number of lesions by day 9 (a mean of 51 lesions per animal). These data are in sharp

alignment with other natural history and pathology studies conducted at our laboratories, as well as with work performed by Nalca et al. (36). In contrast, in other vaccine trials where control animals have been challenged by a different route, such as the intravenous route with a dose 5×10^7 PFU (16) or 2×10^7 PFU (32), pock lesions ranging from 250 to >500 per animal appeared from days 3 to 6. These differences highlight the importance of the challenge route and the dose.

All of the animals that received the second-generation vaccine (Acam2000) survived the monkeypox virus challenge, although some signs of viral infection were observed, such as lesions (mean number of three per animal) on day 9 and low levels of viremia. The animals were generally well and lost very little weight. Both humoral and cell-mediated immune responses were primed, and high concentrations of neutralizing antibody and IgG antibody were detected after vaccination.

The optimal and intended vaccination regime for Imvamune is a prime-boost approach, and results from the present study highlight the importance of this vaccination strategy. The use of a prime-boost regime with Imvamune protected all of the animals challenged (100% survival). Both antibody and cell-mediated immune responses were stimulated, and high titers of neutralizing and IgG antibody were detected following the second dose of Imvamune. There was still some evidence of monkeypox virus infection in the group, as indicated by the presence of pock lesions on day 9 and minor pulmonary edema; nevertheless, this is comparable to the results from the Acam2000-vaccinated animals. In addition, however, there was evidence of virus excretion in the throats of two of six animals. Viral excretion in the throat after MVA vaccination has previously been shown when using the intratracheal (33) and intravenous (32) challenge routes (a different source of MVA and a different route of vaccination was used in the intravenous challenge study).

In the present study, a single dose of Imvamune did not protect all of the animals in the group, and two animals succumbed to infection. Postmortem, the virus was isolated from the lungs and tonsils of both animals. The titer of vaccinia virus-specific IgG antibody and neutralizing antibody prior to challenge was very low, and this may have contributed to the poorer outcome in this group. It should be noted that a single dose is not the optimal regime for Imvamune vaccination; however, one dose does give partial protection and thus may potentially be useful as a primer vaccine, in certain groups of people, which are then subsequently boosted during an emergency. Further work is clearly needed in this area.

Our data not only provide supportive information for the use of Imvamune as a vaccine against variola virus but also show that it could be useful as a vaccine to protect against human infections with monkeypox virus. Recent epidemiologic studies suggest that human monkeypox is currently exhibiting a robust emergence in the Democratic Republic of the Congo (7, 43, 44). Cessation of smallpox vaccination worldwide has resulted in diminished vaccine-induced orthopoxvirus immunity, creating a new "immunologic niche" for the emergence of human monkeypox (45). The use of next-generation smallpox vaccines for the prevention of human monkeypox is currently being discussed (45, 46).

Overall, we have demonstrated here that a prime-boost vaccination regime with Imvamune provides complete protection, as does the comparator vaccine Acam2000. Two doses of Imvamune should be used rather a single dose which only offers partial pro-

tection. This evaluation of different human smallpox vaccines in cynomolgus macaques helps to address questions about optimal vaccine strategies, in the absence of human challenge studies, during a time when the efficacy of Imvamune is being established under the "Animal Rule."

ACKNOWLEDGMENTS

This study was funded by the National Institute of Allergy and Infectious Diseases.

The views expressed in this manuscript are those of the authors and not necessarily those of the funding body.

We thank Geoff Pearson for critically reviewing the manuscript. We are also grateful to Graham Hall, Emma Rayner, and Kim Hatch for performing the histopathology. We thank the Biological Investigations Group at the HPA for conducting the animal procedures.

REFERENCES

- Chapman JL, Nichols DK, Martinez MJ, Raymond JW. 2010. Animal models of orthopoxvirus infection. *Vet. Pathol.* 47:852–870.
- Jacobs BL, Langland JO, Kibler KV, Denzler KL, White SD, Holeček SA, Wong SAS, Huynh T, Baskin CR. 2009. Vaccinia virus vaccines: past, present, and future. *Antivir. Res.* 84:1–13.
- World Health Organization. 2001. Smallpox. *Wkly. Epidemiol. Rec.* 76:337–344.
- von Krempelhuber A, Vollmar J, Pokorny R, Rapp P, Wulff N, Petzold B, Handley A, Mateo L, Siersbol H, Kollaritsch H, Chaplin P. 2010. A randomized, double-blind, dose-finding phase II study to evaluate immunogenicity and safety of the third-generation smallpox vaccine candidate Imvamune. *Vaccine* 28:1209–1216.
- Bhanuprakash V, Venkatesan G, Balamurugan V, Hosamani M, Yogisharadhya R, Gandhale P, Reddy KV, Damle AS, Kher HN, Chandel BS, Chauhan HC, Singh RK. 2010. Zoonotic infections of buffalopox in India. *Zoonoses Public Health* 57:e149–155.
- Glatz M, Richter S, Ginter-Hanselmayer G, Aberer W, Mullegger RR. 2010. Human cowpox in a veterinary student. *Lancet Infect. Dis.* 10:288.
- Rimoin AW, Mulembakani PM, Johnston SC, Lloyd Smith JO, Kisalu NK, Kinkela TL, Blumberg S, Thomassen HA, Pike BL, Fair JN, Wolfe ND, Shongo RL, Graham BS, Formenty P, Okitolonda E, Hensley LE, Meyer H, Wright L, Muyembe JJ. 2010. Major increase in human monkeypox incidence 30 years after smallpox vaccination campaigns cease in the Democratic Republic of Congo. *Proc. Natl. Acad. Sci. U. S. A.* 107:16262–16267.
- Trindade GS, Emerson GL, Carroll DS, Kroon EG, Damon IK. 2007. Brazilian vaccinia viruses and their origins. *Emerg. Infect. Dis.* 13:965–972.
- Bray M, Wright ME. 2003. Progressive vaccinia. *Clin. Infect. Dis.* 36:766–774.
- Mayr A. 2003. Smallpox vaccination and bioterrorism with pox viruses. *Comp. Immunol. Microbiol. Infect. Dis.* 26:423–430.
- Metzger W, Mordmueller BG. 2007. Vaccines for preventing smallpox. *Cochrane Database Syst. Rev.* 2007:CD004913.
- Monath TP, Caldwell JR, Mundt W, Fusco J, Johnson CS, Buller M, Liu J, Gardner B, Downing G, Blum PS, Kemp T, Nichols R, Weltzin R. 2004. Acam2000 clonal Vero cell culture vaccinia virus (New York City Board of Health strain): a second-generation smallpox vaccine for biological defense. *Int. J. Infect. Dis.* 8:S31–S44.
- Greenberg RN, Kennedy JS. 2008. Acam2000: a newly licensed cell culture-based live vaccinia smallpox vaccine. *Expert Opin. Invest. Drugs* 17:555–564.
- Kemper AR, Davis MM, Freed GL. 2002. Expected adverse events in a mass smallpox vaccination campaign. *Eff. Clin. Pract.* 5:84–90.
- Kennedy JS, Greenberg RN. 2009. Imvamune: modified vaccinia Ankara strain as an attenuated smallpox vaccine. *Expert Rev. Vaccines* 8:13–24.
- Earl PL, Americo JL, Wyatt LS, Eller LA, Whitbeck JC, Cohen GH, Eisenberg RJ, Hartmann CJ, Jackson DL, Kulesh DA, Martinez MJ, Miller DM, Mucker EM, Shamblyn JD, Zwiers SH, Huggins JW, Jahrling PB, Moss B. 2004. Immunogenicity of a highly attenuated MVA smallpox vaccine and protection against monkeypox. *Nature* 428:182–185.
- Stückl H, Hochstein-Mintzel V, Mayr A, Huber HC, Schafer H, Holzner

- A. 1974. MVA vaccination against smallpox: clinical tests with an attenuated live vaccinia virus strain (MVA). *Deutsch. Med. Wochenschr.* 99: 2386–2392. (In German.)
18. Mayr A, Stickl H, Muller HK, Danner K, Singer H. 1978. The smallpox vaccination strain MVA: marker, genetic structure, experience gained with the parenteral vaccination and behavior in organisms with a debilitated defense mechanism. *Zentralbl. Bakteriol. B* 167:375–390. (In German.)
 19. FDA. 2002. New drug and biologics and drug products; evidence needed to demonstrate effectiveness of new drugs when human efficacy studies are not ethical or feasible. *Fed. Regist.* 67:37988–37998.
 20. Zaucha GM, Jahrling PB, Geisbert TW, Swearengen JR, Hensley L. 2001. The pathology of experimental aerosolized monkeypox virus infection in cynomolgus monkeys (*Macaca fascicularis*). *Lab. Invest.* 81:1581–1600.
 21. Cann JA, Jahrling PB, Hensley LE, Wahl-Jensen V. 2012. Comparative pathology of smallpox and monkeypox in man and macaques. *J. Comp. Pathol.* [Epub ahead of print.]
 22. Drutt HA. 1969. A mobile form of the Henderson apparatus. *J. Hyg. (Lond.)* 67:437–448.
 23. Gilles HJ. 1974. Calculation of the index of acute toxicity by the method of linear regression. Comparison with the method of "Karber and Behrens." *Eur. J. Toxicol. Environ. Hyg.* 7:77–84.
 24. Jezek Z, Nakano JH, Arita I, Mutombo M, Szczeniowski M, Dunn C. 1987. Serological survey for human monkeypox infections in a selected population in Zaire. *J. Trop. Med. Hyg.* 90:31–38.
 25. Huggins J, Goff A, Hensley L, Mucker E, Shamblyn J, Wlazlowski C, Johnson W, Chapman J, Larsen T, Twenhafel N, Karem K, Damon IK, Byrd CM, Bolken TC, Jordan Hruby RD. 2009. Nonhuman primates are protected from smallpox virus or monkeypox virus challenges by the antiviral drug ST-246. *Antimicrob. Agents Chemother.* 53:2620–2625.
 26. Jordan R, Goff A, Frimm A, Corrado ML, Hensley LE, Byrd CM, Mucker E, Shamblyn J, Bolken TC, Wlazlowski C, Johnson W, Chapman J, Twenhafel N, Tyavanagimatt S, Amantana A, Chinsangaram J, Hruby DE, Huggins J. 2009. ST-246 antiviral efficacy in a nonhuman primate monkeypox model: determination of the minimal effective dose and human dose justification. *Antimicrob. Agents Chemother.* 53:1817–1822.
 27. Shao L, Huang D, Wei H, Wang RC, Chen CY, Shen L, Zhang W, Jin J, Chen ZW. 2009. Expansion, reexpansion, and recall-like expansion of Vγ2Vδ2 T cells in smallpox vaccination and monkeypox virus infection. *J. Virol.* 83:11959–11965.
 28. Keasey S, Pugh C, Tikhonov A, Chen G, Schweitzer B, Nalca A, Ulrich RG. 2010. Proteomic basis of the antibody response to monkeypox virus infection examined in cynomolgus macaques and a comparison to human smallpox vaccination. *PLoS One* 5:e15547. doi:10.1371/journal.pone.0015547.
 29. Zielinski RJ, Smedley JV, Perera PY, Silvera PM, Waldmann TA, Capala J, Perera LP. 2010. Smallpox vaccine with integrated IL-15 demonstrates enhanced *in vivo* viral clearance in immunodeficient mice and confers long-term protection against a lethal monkeypox challenge in cynomolgus monkeys. *Vaccine* 28:7081–7091.
 30. Estep RD, Messaoudi I, O'Connor MA, Li H, Sprague J, Barron A, Engelmann AF, Yen B, Powers MF, Jones JM, Robinson BA, Orzechowska BU, Manoharan M, Legasse A, Planer S, Wilk J, Axthelm Wong MKSW. 2011. Deletion of the monkeypox virus inhibitor of complement enzymes locus impacts the adaptive immune response to monkeypox virus in a nonhuman primate model of infection. *J. Virol.* 85: 9527–9542.
 31. Hiraio LA, Draghia-Akli R, Prigge JT, Yang M, Satishchandran A, Wu L, Hammarlund E, Khan AS, Babas T, Rhodes L, Silvera P, Slika M, Sardesai NY, Weiner DB. 2011. Multivalent smallpox DNA vaccine delivered by intradermal electroporation drives protective immunity in non-human primates against lethal monkeypox challenge. *J. Infect. Dis.* 203: 95–102.
 32. Golden JW, Joselyn M, Mucker EM, Hung CF, Loudon PT, Wu TC, Hooper JW. 2012. Side-by-side comparison of gene-based smallpox vaccine with MVA in nonhuman primates. *PLoS One* 7:e42353. doi:10.1371/journal.pone.0042353.
 33. Stittelaar KJ, van Amerongen G, Kondova I, Kuiken T, van Lavieren RF, Pistorio FH, Niesters HG, van Doornum G, van der Zeijst BA, Mateo L, Chaplin PJ, Osterhaus AD. 2005. Modified vaccinia virus Ankara protects macaques against respiratory challenge with monkeypox virus. *J. Virol.* 79:7845–7851.
 34. Buchman GW, Cohen ME, Xiao Y, Richardson-Harman N, Silvera P, DeTolla LJ, Davis HL, Eisenberg RJ, Cohen GH, Isaacs SN. 2010. A protein-based smallpox vaccine protects non-human primates from a lethal monkeypox virus challenge. *Vaccine* 28:6627–6636.
 35. Denzler KL, Babas T, Rippeon A, Huynh T, Fukushima N, Rhodes L, Silvera PM, Jacobs BL. 2011. Attenuated NYCBH vaccinia virus deleted for the E3L gene confers partial protection against lethal monkeypox virus disease in cynomolgus macaques. *Vaccine* 29:9684–9690.
 36. Nalca A, Livingston VA, Garza NL, Zumbrun EE, Frick OM, Chapman JL, Hartings JM. 2010. Experimental infection of cynomolgus macaques (*Macaca fascicularis*) with aerosolized monkeypox virus. *PLoS One* 5:12880. doi:10.1371/journal.pone.0012880.
 37. Anonymous. 2010. FDA fast track status for Imvamune. *Hum. Vaccin.* 6:368–372.
 38. Frey SE, Newman FK, Kennedy JS, Sobek V, Ennis FA, Hill H, Yan LK, Chaplin P, Vollmar J, Chaitman BR. 2007. Clinical and immunologic responses to multiple doses of Imvamune (modified vaccinia Ankara) followed by Dryvax challenge. *Vaccine* 25:8562–8573.
 39. Garza NL, Hatkin JM, Livingston V, Nichols DK, Chaplin PJ, Volkman A, Fisher D, Nalca A. 2009. Evaluation of the efficacy of modified vaccinia Ankara (MVA)/Imvamune against aerosolized rabbitpox virus in a rabbit model. *Vaccine* 27:5496–5504.
 40. Keckler MS, Carroll DS, Gallardo-Romero NF, Lash RR, Salzer JS, Weiss SL, Patel N, Clemmons CJ, Smith SK, Hutson CL, Karem Damon KLIK. 2011. Establishment of the black-tailed prairie dog (*Cynomys ludovicianus*) as a novel animal model for comparing smallpox vaccines administered preexposure in both high- and low-dose monkeypox virus challenges. *J. Virol.* 85:7683–7698.
 41. Barnewall RE, Fisher DA, Robertson AB, Vales PA, Knostman KA, Bigger JE. 2012. Inhalational monkeypox virus infection in cynomolgus macaques. *Front. Cell Infect. Microbiol.* 2:117.
 42. Goff AJ, Chapman J, Foster C, Wlazlowski C, Shamblyn J, Lin K, Kreiselmeier N, Mucker E, Paragas J, Lawler J, Hensley L. 2011. A novel respiratory model of infection with monkeypox virus in cynomolgus macaques. *J. Virol.* 85:4898–4909.
 43. Hutin YJ, Williams RJ, Malfait P, Pebody R, Loparev VN, Ropp SL, Rodriguez M, Knight JC, Tshioke FK, Khan AS, Szczeniowski MV, Esposito JJ. 2001. 1996. Outbreak of human monkeypox, Democratic Republic of Congo, to 1997. *Emerg. Infect. Dis.* 7:434–438.
 44. Meyer H, Perrichot M, Stemmler M, Emmerich P, Schnitz H, Varaine F, Shungu R, Tshioke F, Formenty P. 2002. 2001. Outbreaks of disease suspected of being due to human monkeypox virus infection in the Democratic Republic of Congo. *J. Clin. Microbiol.* 40:2919–2921.
 45. Reynolds MG, Damon IK. 2012. Outbreaks of human monkeypox after cessation of smallpox vaccination. *Trends Microbiol.* 20:80–87.
 46. Rimoin AW, Graham BS. 2011. Whither monkeypox vaccination. *Vaccine* 29:D60–D64.

Original article

GRAHAM, V. A., HATCH, G. J., BEWLEY, K. R., STEEDS, K., LANSLEY, A., BATE, S. R. & FUNNELL, S. G. 2014. Efficacy of primate humoral passive transfer in a murine model of pneumonic plague is mouse strain-dependent. *J Immunol Res*, 2014, 807564.

Impact factor: 3.404

Contributions by HATCH, G. J.

Home Office – Personal Licence holder

Development and qualification of aerosol, biocontainment and clinical parameter systems. Performance of aerosol challenge.

Study management – Study design, liaison and co-ordination with sponsors, bacteriology, immunology and in vivo teams, scheduling, reporting.

Data analysis and manuscript review

Citation metrics

Google Scholar: 2 citations

Research Article

Efficacy of Primate Humoral Passive Transfer in a Murine Model of Pneumonic Plague Is Mouse Strain-Dependent

V. A. Graham, G. J. Hatch, K. R. Bewley, K. Steeds, A. Lansley,
S. R. Bate, and S. G. P. Funnell

Microbiological Services, Public Health England, Porton Down, Salisbury, Wiltshire SP4 0JG, UK

Correspondence should be addressed to S. G. P. Funnell; simon.funnell@phe.gov.uk

Received 28 February 2014; Revised 21 May 2014; Accepted 18 June 2014; Published 6 July 2014

Academic Editor: E. Diane Williamson

Copyright © 2014 V. A. Graham et al. This is an open access article distributed under the Creative Commons Attribution License, which permits unrestricted use, distribution, and reproduction in any medium, provided the original work is properly cited.

New vaccines against biodefense-related and emerging pathogens are being prepared for licensure using the US Federal Drug Administration's "Animal Rule." This allows licensure of drugs and vaccines using protection data generated in animal models. A new acellular plague vaccine composed of two separate recombinant proteins (rF1 and rV) has been developed and assessed for immunogenicity in humans. Using serum obtained from human volunteers immunised with various doses of this vaccine and from immunised cynomolgus macaques, we assessed the pharmacokinetic properties of human and cynomolgus macaque IgG in BALB/c and the NIH Swiss derived Hsd:NIHS mice, respectively. Using human and cynomolgus macaque serum with known ELISA antibody titres against both vaccine components, we have shown that passive immunisation of human and nonhuman primate serum provides a reproducible delay in median time to death in mice exposed to a lethal aerosol of plague. In addition, we have shown that Hsd:NIHS mice are a better model for humoral passive transfer studies than BALB/c mice.

1. Introduction

Plague is caused by the gram-negative bacterium *Yersinia pestis*; it is primarily a disease of rodents, which can cause zoonotic disease directly via the aerosol route or indirectly via arthropod vectors. Throughout history, human pandemics have been caused, the greatest being during the Middle Ages where at least 25% of the population was killed [1]. There is a general perception that plague is nonexistent; however, there are several regions in the world where plague is still endemic and there is a consistent annual morbidity and mortality rate with the potential to cause large outbreaks [2]. Worldwide, from 2000 to 2009, at least 21,725 people were infected with plague and 1,612 people died, including 7 deaths in the United States [3].

Humans are extremely susceptible to plague and the aetiology of the disease is dependent upon the route and source of the infection, resulting in one of the three principal clinical forms: bubonic, septicaemic, and pneumonic plague [2]. Pneumonic plague follows inhalation of aerosolised droplets containing *Y. pestis*. It has the highest fatality rate of the three forms of plague, with a 1–3 day incubation period.

It has a 100% fatality rate unless antibiotics are given the same day as symptoms develop [3]. Once inhaled the plague bacteria multiply in the alveolar spaces, and the patient is usually infectious 1–2 days after infection; during this time the patient produces highly contagious aerosolised *Y. pestis* in fine droplets, which can be inhaled deep into the respiratory tract of close contacts [2].

Antibiotics have been used for the treatment of plague and, to date, there have been two reports of antibiotic resistant plague strains [4, 5]. Laboratory experiments have shown that it is possible for *Y. pestis* to acquire plasmids which contain antibiotic resistant genes [3, 5]. Due to the rapid onset and the high case fatality rate of pneumonic plague, the potential bioterrorist threat, and the potential emergence of antibiotic resistant strains, the production of a vaccine to enable protection from this form of plague is required.

Vaccines against plague have previously been limited to live-attenuated or formalin-killed whole cell *Y. pestis*. They have not shown protection against primary pneumonic plague and have shown adverse reactions to the vaccine

itself [6, 7]. Therefore, there is a requirement for vaccines which will provide long-lasting protection against all forms of plague infection with minimal side-effects.

It has been shown that both humoral and cellular immunity are required for complete plague immunity [8–12]; however, antibodies against two natural virulence proteins F1 and V are associated with protection during a natural infection and have been shown to be protective in mouse models of pneumonic plague when given as recombinant proteins [11, 13–15]. The F1 capsular protein is unique to *Y. pestis* and is an antiphagocytic protein capsule, the gene for which is located on the pFra plasmid. The V protein is an outer membrane protein encoded by the pYV plasmid and is part of the Type III secretion system [3, 8, 11]. These (rF1 and rV) are the major constituents of new subunit plague vaccines [12, 16–24].

Due to the lack of an endemic population within which new plague vaccines could be assessed the FDA will allow licensure based on the animal rule (21CFR 601.91 Subpart H). There are several critical components in evaluating vaccine efficacy under this rule. Licensure will require the use of an assay(s) that measures a functional component of the immune response and is reasonably likely to predict clinical benefit. Scientists and regulatory authorities have for many years been looking for a functional assay which will enable measurement of a correlate of protection against pneumonic plague. Passive immune protection studies in animals, using antibodies isolated from vaccinated individuals, may provide this assay [14, 15, 25, 26].

The experiments described here detail the development of a pneumonic plague mouse model and the subsequent use of this model to test the *Y. pestis* subunit vaccine containing recombinant F1 and recombinant V (rF1 and rV) by the passive transfer of unfractionated serum and plasma from immunised cynomolgus macaques and humans.

This is the first paper to assess the ability of the rF1 and rV vaccine to generate protection from an aerosol challenge of the CO92 strain of *Y. pestis* by passive transfer of unfractionated serum. Previous papers have assessed the combined rF1V fusion protein [13]. Known titres of anti-rF1 and anti-rV antibodies were then transferred into groups of immunologically naïve mice to assess the ability of humoral immunity to protect against pneumonic plague.

2. Materials and Methods

2.1. Bacterial Strain. *Y. pestis* strain CO92 (biovar Orientalis, NR641, BEI Repositories) was supplied by the Biodefence and Emerging Infections (BEI) Research Repository (USA) in accordance with International Export and Import Regulatory Requirements. The organism was stored and handled in accordance with US Biological Select Agent or Toxin requirements.

2.2. Bacterial Growth and Subculture. The generation of the master stock was performed by streaking *Y. pestis* onto tryptic soy agar (TSA) (VWR, UK) and incubated at 26°C for 48 hours. This was used to inoculate tryptone soya broth

(TSB) (Media Services, PHE) which was incubated overnight at 26°C. This broth was then used to inoculate a further suspension of TSB, which was incubated at 26°C overnight. A 50% glycerol (Sigma, UK) solution was added to the broth to a final concentration of 40% (v/v) glycerol. The master stocks were frozen at –80°C. Working stocks were generated from a vial of master stock. This was performed by streaking the master stock of *Y. pestis* onto TSA and incubating at 26°C for 72 hours. A strike through of the lawn was used to inoculate a large volume of TSB and was incubated overnight at 26°C. A 50% glycerol solution was added to the broth to a final concentration of 40% (v/v) glycerol. The working stocks were frozen at –80°C. Master stock certificate of analysis was produced; characterisation of these stocks included microscopic staining (Wayson's), colony morphology and purity checks on TSA, Congo red uptake on Congo red agar, multiple loci (5 target) PCR, 16S rRNA sequencing, and VNTR for genetic integrity checks. Subcutaneous lethality checks were performed on BALB/c mice and stocks were 100% lethal (data not shown). All experimental and confirmatory studies were performed using the working stock vials; therefore they had a maximum passage number of 3.

2.3. Preparation of Inoculum. All inocula were prepared in the same way. A vial from the working stock was thawed at ambient temperature and then streaked onto TSA and incubated at 26°C for 54 hours for subculture and purity check. The contents of individual streak plates were washed into 25 mL total of TSB. To obtain maximal yields, the broth was incubated with orbital agitation at 26°C for 18 hours. Following incubation, 25 mL fresh TSB was added and the optical density was measured at 600 nm wavelength. The broths were then reincubated with orbital agitation for 3 hours at 26°C. The broths were harvested when the OD_{600nm} values were over 3, with an aliquot taken for real time PCR analysis.

2.4. Determination of Bacterial Challenge Dose. Retrospective quantification of colony forming unit concentration of inocula was conducted using a spread plate method. Briefly, serial ten-fold dilutions were created to bring the bacterial suspensions into a countable range. In duplicate, 100 µL of each diluted bacterial suspension was spread across the surface of a TSA plate. After 48 hours incubation, the plates were manually counted for colony forming unit content and the average counts used to determine colony forming unit concentration (CFU/mL). Immediately prior to aerosol exposure of mice all inocula were checked for the presence of plasmids and essential genetic characteristics by PCR, as described below. *In vivo* studies were not initiated without confirmation of genetic integrity by PCR for each batch of inocula culture.

2.5. Confirmation of Strain Virulence. A four target real time PCR was utilised to ensure genetic integrity and stability for each batch of inocula used for *in vivo* studies. This confirmed the presence of all three plasmids and the *pgm* virulence locus

TABLE 1: Genetic primer targets of the PCR test used to ensure integrity of the inoculum. All primer probe design was based on GenBank accession number NC_003143 (*Yersinia pestis* CO92, complete genome). MGB is *minor groove binder/nonfluorescent quencher* covalently bound to the 3' end of the probe. All probes have a 5' fluorescein (FAM) label.

Gene	Sequence (5' → 3')
HmsF (chromosomal <i>pgm</i> locus)	
Forward	CGGAGAAGCCAACGTTTCGT
Reverse	TCTTCACTTTGCGGCAATG
Probe (MGB)	CCGCCTGCACAACG
F1 (pMT1)	
Forward	TTGGCGGCTATAAACAGGAA
Reverse	CACCCGCGGCATCTGTA
Probe (MGB)	CACTAGCACATCTGTTAAC
Pst (pPCPI)	
Forward	CGGCAATCGTTCCTCAA
Reverse	GGTCAGGAAAAAGACGGTGTGA
Probe (MGB)	AACCATGACACGGTAGACT
VAg (pCD1)	
Forward	CGGCGGTAAAGAGAAATGC
Reverse	CATCGCGAATACACAATGG
Probe (MGB)	TACTGCCATGAACGCC

[27] of the bacterial chromosome. The PCR was based on the targets detailed in Table 1. PCR reaction constituents consist of 2× fast universal master mix (Applied Biosystems) 10 µL; forward primer (900 nM); reverse primer (900 nM); probe (250 nM); DNA template 2 µL; and nuclease-free water to a final volume of 20 µL. PCR thermal cycling consisted of 40 cycles (ABI 7500 fast protocol) comprising 95°C, 3 seconds, and 60°C, 30 seconds.

2.6. Mice. In accordance with UK Home Office regulations, BALB/c and Hsd:NIHS mice were obtained from UK accredited suppliers (Harlan, UK, or Charles River, UK). In all studies described, mice were required to comply with both age and weight selective criteria: age minimum 8–10 weeks and a minimum body weight of 17 grams. Mice were randomly assigned and housed in groups of between five and ten. Food and water available to all mic *ad libitum*, and were exposed to 12 hour. Pilot studies were performed with groups of 5 or 6 mice. Details for all the challenge experiments can be found in Table 2. All animal procedures were conducted under the authority of and in accordance with a UK Home Office license.

2.7. Health Monitoring. For three days before infection and throughout the remainder of the studies, mice were weighed in the morning and afternoon to monitor diurnal body-weight fluctuation. In addition, the health status of each

mouse was checked on at least two occasions every day. When mice began to show signs of infection, the monitoring frequency was increased to at least four occasions every day. When mice were seen to have restricted movement and reflexes they were humanely euthanised using a UK Home Office schedule 1 procedure.

2.8. Human Serum. All human serum samples were from individuals vaccinated with either 40, 80, or 120 µg of recombinant plague vaccine using the same dosing regimen and serum isolated 35, 196, or 365 days postvaccination. All human serum samples were provided by NIAID (through Avecia and PharmAthene) under contract number N01-AI30062.

2.9. Pharmacokinetic Analysis of Human Antibodies. Pooled human serum with known ELISA titres against rF1 and rV proteins was injected into four groups of five BALB/c mice via the intraperitoneal route (250 µL/mouse). Groups of mice were serially sacrificed at 1.5, 3, 6, and 12 hours after injection. One group of 5 mice was injected with 250 µL/mouse negative control serum for a control. The levels of circulating human IgG antibody levels specific for rF1 and rV were determined by ELISA (performed by Huntingdon Life Sciences, UK).

2.10. Passive Humoral Therapy of Human Serum. Three to six hours before aerosol infection, groups of five mice were administered with 250 µL of human serum via the intraperitoneal route. Mice were administered with either test, positive control or negative control human serum. The mice were then transferred into high-containment isolators before being loaded into restraint tubes for aerosol administration.

2.11. Aerosol Challenge of Mice. Groups of mice were challenged for 10 minutes with a dynamic aerosol of *Y. pestis* (<2 µm, mass median aerodynamic diameter) using a contained modified Henderson apparatus [28]. The challenge aerosol was generated using a three-jet Collison nebulizer (BGI, Waltham, USA) containing 20 mL *Y. pestis* in TSB. The resulting aerosol was mixed with conditioned air (65% relative humidity, 22°C) in the spray tube and delivered to the nose of each animal via an exposure tube in which the unanaesthetised mice are held in restraint tubes. Samples of the aerosol were collected into 20 mL TSB using an SKC Biosampler (SKC, Dorset, UK) operating at 12.5 L/min. In the later studies using the Hsd:NIHS mice, aerosol samples were collected using an All Glass Impinger (AGI30, Ace Glass, USA) [29] operating at 6 L/min and an Aerodynamic Particle Sizer (TSI Instruments Ltd., Bucks, UK), controlled using the AeroMP management platform (Biaera Technologies LLC., MD, USA). Counts were used to calculate the inhaled dose using a derived respiratory minute volume estimated from the average weight of the animals [30].

2.12. ELISA. Recombinant F protein (rF1) and V protein (rV) (provided by PharmAthene via NIAID) were coated

TABLE 2: A tabular summary of the murine data for each of the challenge experiments described.

Study	Number of mice per group	Minimum body weight (g)	Sex of mice	Source of mice	Strain of mice
Study 1	6	17.7	Female	Harlan	BALB/c
Study 2	10	17.5	Female	Charles Rivers	BALB/c
Study 3	10	17.1	Female	Charles Rivers	BALB/c
Study 4	5	18.0	Female Male	Harlan	BALB/c Hsd:NIHS
Study 5	10	18.0	Female	Harlan	BALB/c Hsd:NIHS
Study 6	10	18.0	Female	Harlan	Hsd:NIHS

in carbonate coating buffer separately into wells of 96-well microplate (Nunc Maxisorp C96, Fisher Scientific, UK) and incubated overnight at 4°C. The plates were washed in PBS containing 0.05% w/v Tween-20 (Sigma, UK) before and after each absorptive reagent addition. Plates were blocked for 2 hours with PBS containing 3% w/v bovine serum albumin (BSA) (Sigma, UK). Where necessary, samples were pre-diluted using PBS containing 1% w/v BSA and 0.05% Tween-20. Murine samples containing human antibody were incubated for 1 hour, and vaccinated-goat serum was used as a positive control (rF1 14182 Pro-Sci, USA; rV 14181 Pro-Sci, USA). Bound antibody was detected with horseradish peroxidase conjugated to protein-G (Pierce, USA). Bound conjugate was detected by addition of ABTS peroxidase substrate system (Kirkegaard and Perry Laboratories, USA), and the reaction stopped with ABTS peroxidase stop solution (Kirkegaard and Perry Laboratories, USA). Plates were read at a wavelength of 405 nm using an automated ELISA reader (VersaMax, Molecular Devices, CA, USA) and data was analysed using Softmax Pro version 4.7.1. (Molecular Devices, CA, USA). The goat positive control sera (anti-rF1 or anti-rV) were assigned arbitrary values of 10000 units per mL. The human and cynomolgus macaque sera titres were extrapolated from the goat positive control sera.

2.13. Cynomolgus Macaques (*Macaca fascicularis*). Two female cynomolgus macaques of Mauritian origin were obtained from a UK breeding colony for use in this study. Both animals weighed more than 2.5 kg and were over 2 years of age at immunization. Animals were housed according to the Home Office (UK) Code of Practice for the Housing and Care of Animals Used in Scientific Procedures (1989) and the National Committee for Refinement, Reduction and Replacement (NC3Rs) Guidelines on Primate Accommodation, Care and Use, August 2006. When a procedure required the removal of a primate from a cage it was sedated by intramuscular (*i.m.*) injection with ketamine hydrochloride (10 mg/kg) (Ketaset, Fort Dodge Animal Health Ltd., Southampton, UK). All procedures were conducted under a project license approved by the Ethical Review Process of Public Health England, Salisbury, UK, and the UK Home Office. None of the animals had previously been used for experimental procedures.

2.14. Generation of Cynomolgus Macaque Immune Serum. Two cynomolgus macaques were immunized then twice boosted with a recombinant plague vaccine consisting of rF1 and rV antigens with an alhydrogel adjuvant (plague (recombinant) vaccine suspension, 873082-H01, Batch 7051, Avidia Biologics Ltd., UK). A 20 µg/mL solution was prepared by adding 0.25 mL of the vaccine (which contained 240 µg/mL of each antigen adjuvanted with 0.26% (w/w) alhydrogel) to 2.75 mL 0.26% (w/w) alhydrogel in a sterile vessel and mixed thoroughly. The vaccination schedule comprised of three intramuscular injections of 10 µg of total antigen with a 21 day interval between injections.

2.15. Pharmacokinetic Analysis of Cynomolgus Macaque Antibodies. Pooled cynomolgus macaque serum with known ELISA titres against rF1 and rV proteins was injected into groups of five Hsd:NIHS mice via the intraperitoneal route (250 µL/animal). Groups of five mice were serially sacrificed, preinjection or at 1.5, 3, 6, and 12 hours postinjection. The levels of circulating cynomolgus macaque IgG antibody were determined by ELISA as previously described.

2.16. Passive Humoral Therapy of Cynomolgus Macaque Serum. Three to six hours before aerosol infection, groups of five mice were administered with 250 µL/mouse of test cynomolgus macaque serum, positive control vaccinated human serum, or as a negative control nonvaccinated human serum via the intraperitoneal route. The mice were then transferred into high containment isolators before being loaded into restraint tubes for aerosol administration.

2.17. Statistical Analysis. Survival analysis was performed using Kaplan-Meier survival curves and comparisons were performed using Wilcoxon rank sum for *P* values [31].

3. Results

3.1. Aerosol BALB/c Murine Infection Model. An aerosol model of plague was developed using BALB/c mice to enable assessment of the efficacy of passive transfer of antibodies against pneumonic plague. An exposure to 2.4 LD₅₀

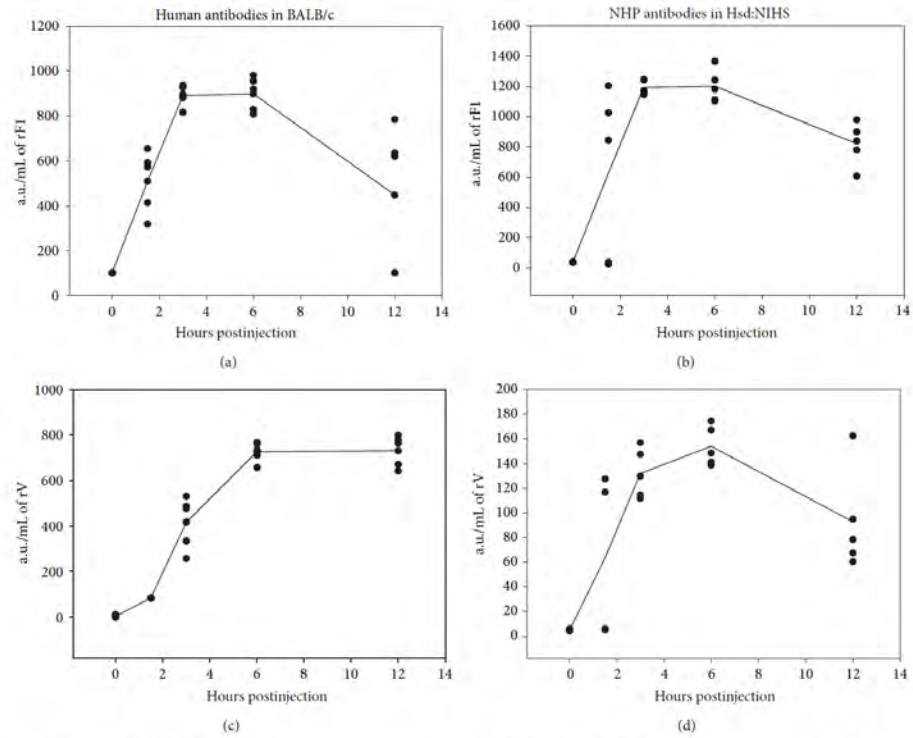


FIGURE 1: Pharmacokinetics of human or cynomolgus macaque antibody in BALB/c and Hsd:NIHS mice, respectively. 0.25 mL human ((a) and (c)) or cynomolgus macaque ((b) and (d)) plague vaccine serum was injected via the intraperitoneal route into BALB/c ($n = 20$) or Hsd:NIHS ($n = 20$) mice, respectively. The mice were serially sacrificed and the presence of anti-rF1 ((a) and (b)) or anti-rV ((c) and (d)) antibody was assessed by ELISA. Additional groups of mice ($n = 5$) were sacrificed preinjection to provide baseline data. The data suggests that the time delay between passive antibody administration and optimal serum concentration in the murine serum was between 3 and 6 hours. a.u., arbitrary units.

aerosolised *Y. pestis* CO92 or above was found to produce a mean time to death of 4.2 days (± 0.5 SE).

The presented dose used in a range of humoral passive transfer experiments was extremely consistent and only varied between 10.6 and 13.9 LD₅₀s.

3.2. Passive Protection of Human Antibody within BALB/c Mice. To maximise the efficacy of passively transferred antibodies, we examined the pharmacokinetics of human antibody in the circulating blood stream of BALB/c mice (Figure 1). The results indicated that optimal human antibody concentrations were reached between three and six hours after intraperitoneal administration into mice.

A pool of high titre serum obtained from human volunteers that had been vaccinated with experimental

recombinant plague vaccine was initially used to assess the concept that passive human antibody therapy would provide some form of protection against pneumonic plague in BALB/c mice. The combined Kaplan-Meier survival curves of three studies are presented in Figure 2. All BALB/c mice were infected three hours after intraperitoneal administration of 250 μ L of either nonimmune human serum or a pool of serum from vaccinated volunteers. The serum had a significant protective effect ($P < 0.001$, Wilcoxon test), as defined by a delay of the median time to death (MTD) of 1 to 2 days (Table 3).

3.3. Assessment of Vaccine Dose and Longevity of Protection. The dose of the vaccine required to provide protection was investigated by examining the protective effect of human sera taken from vaccines 35 days after they received one

TABLE 3: A tabular summary of presented dose of aerosolised *Y. pestis*, passive immune therapy treatment, and MTD in BALB/c and Hsd:NIHS mice. The median time to death (MTD) was calculated using a Kaplan-Meier survival plot. N/D: not determined; over 50% of the mice survived to the end of these experiments; therefore an MTD could not be calculated.

Presented dose		Mouse strain	Study	Passive immune treatment	MTD
(CFU)	LD ₅₀				
240	0.05	BALB/c	4	No treatment	N/D
3,000	0.6	BALB/c	4	No treatment	N/D
12,000	2.4	BALB/c	4	No treatment	3.7
62,026	12.4	BALB/c	1	Human reference serum	4.92
57,746	11.5	BALB/c	2	Human reference serum	4.18
69,390	13.9	BALB/c	3	Human reference serum	4.71
62,026	12.4	BALB/c	1	Human control negative serum	3.42
57,746	11.5	BALB/c	2	Human control negative serum	2.94
69,390	13.9	BALB/c	3	Human control negative serum	3.17
57,746	11.5	BALB/c	2	D35 40 µg	3.94
57,746	11.5	BALB/c	2	D35 80 µg	4.18
57,746	11.5	BALB/c	2	D35 120 µg	4.18
69,390	13.9	BALB/c	3	D196 40 µg	5.17
69,390	13.9	BALB/c	3	D196 80 µg	5.17
69,390	13.9	BALB/c	3	D196 120 µg	4.71
69,390	13.9	BALB/c	3	D365 40 µg	4.33
69,390	13.9	BALB/c	3	D365 80 µg	4.71
69,390	13.9	BALB/c	3	D365 120 µg	4.71
240	0.05	Hsd:NIHS	4	No treatment	N/D
3,000	0.6	Hsd:NIHS	4	No treatment	3.46
12,000	2.4	Hsd:NIHS	4	No treatment	3.96
53,000	10.6	BALB/c	5	Human vaccine serum	5.48
53,000	10.6	BALB/c	5	Human control negative serum	3.48
53,000	10.6	Hsd:NIHS	5	Human vaccine serum	7.73
53,000	10.6	Hsd:NIHS	5	Human control negative serum	3.48
62,000	12	Hsd:NIHS	6	Human vaccine serum	7.75
62,000	12	Hsd:NIHS	6	Human control negative serum	3.25
62,000	12	Hsd:NIHS	6	Cynomolgus macaque vaccinated serum	N/D

of three different doses (40 µg, 80 µg, and 120 µg). The sera showed a significant protective effect ($P < 0.001$, Wilcoxon test) in survival analysis (Figure 3) as defined by a delay of the MTD from 2.94 days to between 3.92 and 4.18 days (Table 3). However, there was no significant difference ($P > 0.02$, Wilcoxon test) between the three doses of vaccine.

The length of the protective effect of immunisation was also tested by comparing the passive protective effect of human vaccine sera taken at 35, 196, and 365 days postimmunisation in the BALB/c pneumonic plague model (Figures 3 and 4). There was no significant difference ($P > 0.02$, Wilcoxon test) in the passive protection of the mice from the human sera from three different doses and 35, 196, and 365 days postvaccination.

In order to assess the relationship between ELISA titre and MTD, all the data from the different dose experiments

were combined. As illustrated in Figure 5, a good correlation was obtained between MTD and the ELISA titre of the sera against both rF1 ($R^2 = 0.91$) and rV ($R^2 = 0.92$).

The pneumonic plague model was initially developed in BALB/c mice. However, even when using the highest titre human sera available, passive transfer only resulted in a delay in the MTD in BALB/c mice in our hands. We were aware that other published literature had previously described 100% survival in other murine strains [13]. As a result, Hsd:NIHS mice were investigated to determine whether the protection conferred by the human antibodies would be more effective in the different mouse strain.

3.4. Aerosol Hsd:NIHS Murine Infection Model. An aerosol model of murine plague using Hsd:NIHS mice was developed to enable assessment of the efficacy of passive transfer of

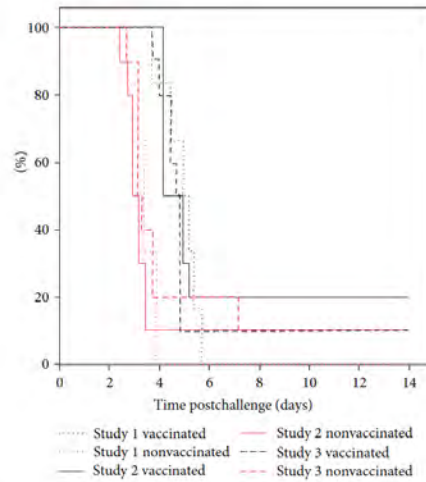


FIGURE 2: Combined survival plots of 3 studies following passive therapy of mice with either nonimmune or plague vaccinated volunteer serum. Study (1), $n = 6$ per group, study (2), $n = 10$ per group, and study (3), $n = 10$ per group. Mice were administered $250 \mu\text{L}$ human serum into the peritoneal cavity, 3 hours before being exposed to more than 10 LD_{50} aerosolised *Y. pestis* using a modified contained Henderson apparatus. The median time to death (MTD) was calculated using a Kaplan-Meier survival plot.

human antibodies. Results showed that there was no difference in the time to death of Hsd:NIHS mice ($P > 0.02$, Mann-Whitney) compared to BALB/c mice after aerosol challenge of *Y. pestis* (Figure 6), and Table 3 demonstrates that a presented dose of 2.4 LD_{50} or above results in an average MTD of 5.3 days ($\pm 0.8 \text{ SE}$).

3.5. Comparison of Passive Protection of Human Antibody within Hsd:NIHS and BALB/c Mice. The highest titre human serum available was used to compare the suitability of BALB/c and Hsd:NIHS mouse strains for the assessment of passive protection against pneumonic plague. After exposure to 10.6 LD_{50} of *Y. pestis*, the MTD of BALB/c and Hsd:NIHS with negative control sera was the same at 3.5 days (Figure 7). However, after intraperitoneal administration of high titre human vaccine serum, there were statistically significant ($P < 0.02$, Wilcoxon test) delays in the MTD in both BALB/c and Hsd:NIHS mice of 5.5 to 7.7 days, respectively (Table 3).

3.6. Use of Cynomolgus Macaque Serum to Provide Passive Protection

3.6.1. Cynomolgus Macaque Immunisation. To confirm that cynomolgus macaque serum can provide a significant level

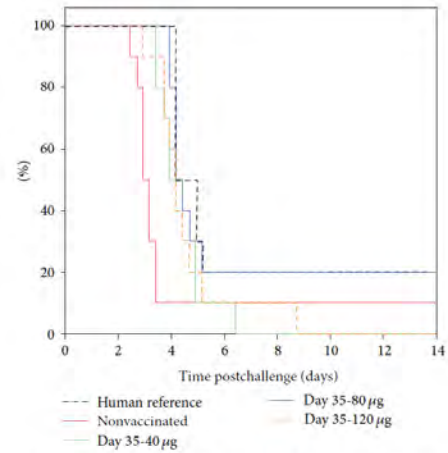


FIGURE 3: Combined survival plots of BALB/c mice following passive transfer of human serum from vaccinates 35 days after receiving different doses of vaccine. Study (2), $n = 10$ per group. Mice were administered $250 \mu\text{L}$ human serum into the peritoneal cavity, 3 hours before being exposed to more than 10 LD_{50} aerosolised *Y. pestis* using a modified contained Henderson apparatus. The median time to death (MTD) was calculated using a Kaplan-Meier survival plot.

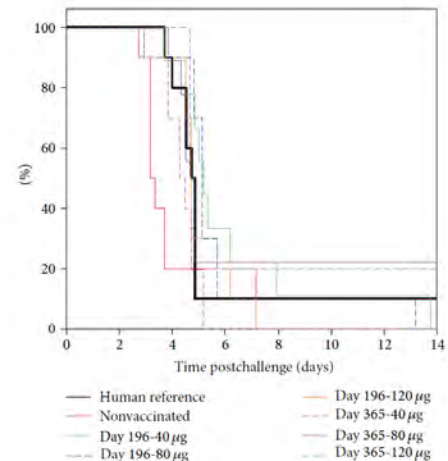


FIGURE 4: Combined survival plots of mice following passive therapy of either nonimmune or plague vaccinated volunteer serum from 196 to 365 days postinoculation. Study (3), $n = 10$ per group. BALB/c mice were administered $250 \mu\text{L}$ human serum into the peritoneal cavity, 3 hours before being exposed to *Y. pestis* using a modified contained Henderson apparatus. The median time to death (MTD) was calculated using a Kaplan-Meier survival plot.

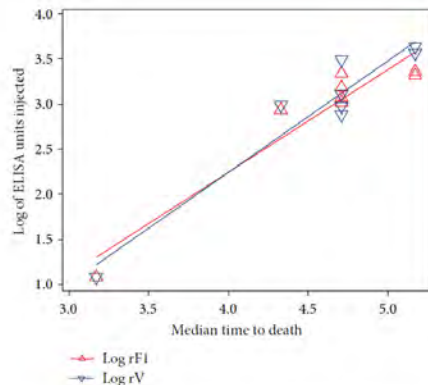


FIGURE 5: When all of the passive protection data from BALB/c mice were pooled, the log ELISA titre against both rF1 and rV correlated with survival time.

of protection against pneumonic plague, two cynomolgus macaques were immunised intramuscularly with three $10 \mu\text{g}$ doses of rF1 and rV vaccine 21 days apart. The antibody titres were monitored and the study terminated after the peak of the anti-rF1 and anti-rV antibody responses. The serum isolated at termination was pooled and the anti-rF1 and anti-rV antibody titres were assessed by ELISA (Figure 8).

3.6.2. Pharmacokinetics of Primate Antibody in Mice. To maximise the efficacy of passively transferred antibodies, we examined the pharmacokinetics of cynomolgus macaque serum in the circulating blood stream of Hsd:NIHS mice (Figure 1). The results showed that optimal primate antibody concentrations were reached between three and six hours after intraperitoneal administration of $250 \mu\text{L}$. This had a similar profile to human antibodies in BALB/c mice.

3.6.3. Passive Protection with Primate Sera. The cynomolgus macaque serum was used in an assessment of passive protection in Hsd:NIHS mice against an aerosolised challenge of *Y. pestis*. The MTD of the untreated mice was observed to be 3.5 days, whereas the MTD of mice treated with the highest titre of human serum was 7.7 days (Figure 9). The MTD for the mice treated with the cynomolgus macaque serum could not be determined because 60% of the mice survived until day 14. However, there was no statistical difference ($P > 0.02$, Wilcoxon) between the passive protective effect of human and cynomolgus macaque vaccine sera in Hsd:NIHS mice.

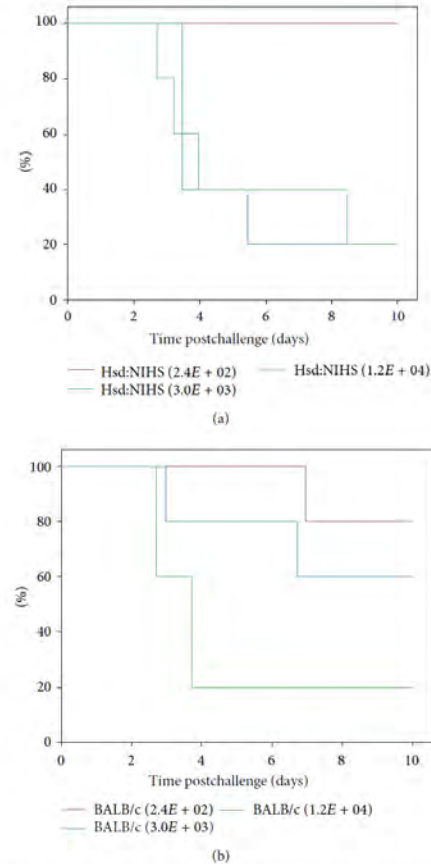


FIGURE 6: Mouse strain BALB/c and Hsd:NIHS had similar susceptibility to aerosolised *Y. pestis*. (a) shows the survival plots for Hsd:NIHS and (b) shows the survival plots for BALB/c mice. Study (4), $n = 5$ per group. The MTD was calculated using a Kaplan-Meier survival plot.

4. Discussion

The rF1 and rV vaccine was developed to protect against pneumonic plague in humans. In order to enable the licensure of the plague vaccine, information regarding efficacy will need to be provided using animals and the FDAs "animal rule" [32]. In addition, linkage between the human disease and animal studies is essential. An assessment of the protective effect following the passive transfer of antibodies from human vaccines to mice may provide this link.

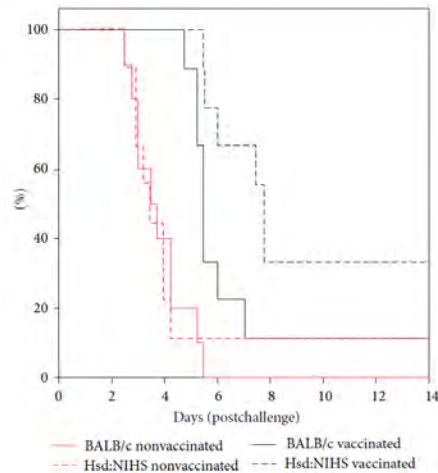


FIGURE 7: Hsd:NIHS mice had better survival outcomes than BALB/c mice after administration of human serum. Study (5), $n = 10$ mice per group. Mice were injected with $250 \mu\text{L}$ human serum into the peritoneal cavity, 3–6 hours before being exposed to aerosolised *Y. pestis* using a modified contained Henderson apparatus. The MTD was calculated using a Kaplan-Meier survival plot.

A model of pneumonic plague was successfully set up by challenging BALB/c mice with aerosolised *Y. pestis* (CO92). This system was both robust and reproducible. To determine whether the antibody response raised against the rF1 and rV plague vaccine was sufficient to protect against pneumonic plague, a passive transfer model in BALB/c mice using human serum was developed. Serum from rF1 and rV vaccines provided significant protection in the pneumonic plague mouse model, as defined by a delay in MTD of between 1 and 2 days. The protective effect of human vaccine sera in mice was found to extend up to 365 days postimmunisation. In addition, this protective effect was not found to be dose dependent as no difference was observed between sera from vaccines that received 40, 80, or $120 \mu\text{g}$.

By examining the relationship between human IgG ELISA titre to either rF1 or rV and the MTD, we have demonstrated that the ELISA titres are proportional to the extent of the protective effect. This supports the findings by Fellows et al. [13, 32] which used the recombinant rF1V vaccine and Green et al. [33] who used the rF1 and rV vaccine used within this paper. However, in contrast with the findings of Fellows et al., [13] the passive transfer of human antibody was not providing complete protection as expected. Therefore, we used a mouse strain more closely related to that used by Fellows et al., the outbred Hsd:NIHS strain, and compared them to the inbred BALB/c mouse strain which was used in our earlier studies.

When we compared the susceptibility of Hsd:NIHS and BALB/c mice to aerosolised *Y. pestis* CO92, we found no statistical differences in the mean time to death. To determine whether the antibody response raised against the rF1 and rV plague vaccine was sufficient to protect against pneumonic plague, a passive transfer model in Hsd:NIHS mice using human serum was developed. This was compared to the BALB/c model. Serum from human rF1 and rV vaccines provided significant protection in both the BALB/c and Hsd:NIHS mice strains, as defined by a delay in MTD of between 2 and 4 days, respectively. Restrictions in the quantity of human vaccine trial serum available prevented a repeat pharmacokinetic study of human antibody in Hsd:NIHS mice. The outcome of the pharmacological analysis of cynomolgus macaque antibodies in Hsd:NIHS mice did, however, provide sufficient similarity in the clearance rate of primate antibody for us to be confident that the delay between passive antibody administration and infection was optimal in both murine species.

Cynomolgus macaque sera were also used to assess protection in Hsd:NIHS mice against an aerosolised challenge of *Y. pestis*. The MTD of untreated mice was 3.5 days, whereas those treated with the highest titre of human serum was 7.7. We were unable to provide a median time to death for the NHP serum, as 60% of the mice survived until the end of the experiment.

The passive transfer data presented in this paper supports the findings of previous passive transfer studies from plague vaccine studies [13, 25, 34]. However an interesting result from this study was the difference between the ability of the outbred Hsd:NIHS and the inbred BALB/c to utilise human serum to protect against pneumonic plague. The duration of protection with the human serum was significantly longer in Hsd:NIHS mice than in BALB/c mice. The reason for this difference in protection is unknown and could have important implications when evaluating the efficacy of human antibodies in other passive transfer experiments and should be investigated further. New murine IgG Fc receptors are continually being discovered [35] and are currently being evaluated for their specificity to human IgG. The possibility that Hsd:NIHS mice are able to bind human IgG more effectively than BALB/c mice should be further investigated.

In summary, the results presented in this study demonstrate that passive transfer of human and cynomolgus macaque antibodies raised in response to vaccination with rF1 and rV provides protection in the form of delay in the median time to death in murine pneumonic plague. The data indicate that increasing levels of antibodies result in an increase in the MTD. Our data also demonstrates a good correlation between IgG ELISA titres to rF1 and rV with biological protection. In addition, human serum was better utilized for protection in Hsd:NIHS mice than in BALB/c mice.

Conflict of Interests

The authors declare that there is no conflict of interests regarding the publication of this paper.

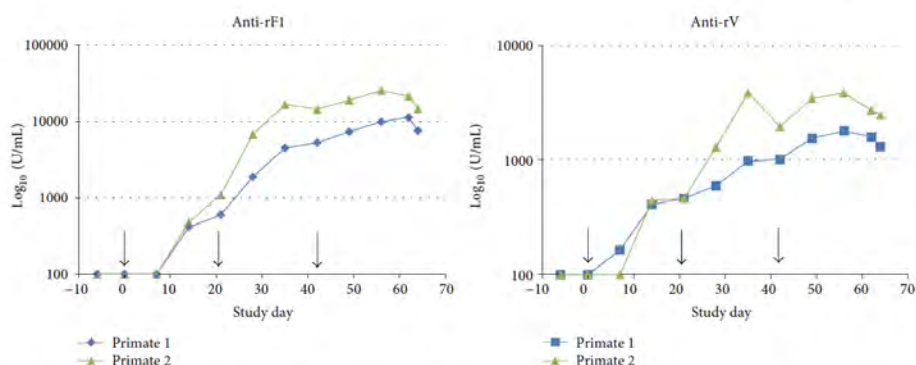


FIGURE 8: Assessment of anti-rF1 and anti-rV antibody titres in NHP serum after 3 intramuscular immunizations of 10 μ g of rF1 and rV antigen. Detectable amounts of anti-rF1 and anti-rV antibodies were found in the serum 2 weeks after the primary immunization, with anti-rF1 consistently having a higher titre.

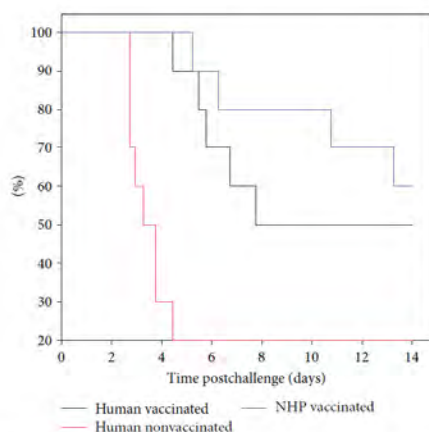


FIGURE 9: Passive immune therapy with NHP serum provided better protection in Hsd:NIHS mice than human serum after a lethal challenge of *Y. pestis*. Study (6), $n = 10$ mice per group. Mice were administered 250 μ L serum into the peritoneal cavity, 3–6 hours before being exposed to aerosolised *Y. pestis* using a modified contained Henderson apparatus. The MTD was calculated using a Kaplan-Meier survival plot.

Acknowledgments

This study was funded by the National Institute for Allergy and Infectious Diseases, Contract no. N01-AI-30062. The authors would like to thank the Biological Investigation Group for their help and support with the animal work, all members of the bacteriology and immunology teams,

past and present, who contributed to this work, HLS for performing and analysing the first pharmacokinetic study, NIAID for the provision of the vaccinated human serum, Allen Roberts for supervision and acquisition of funding, Julia Vipond, Julia Tree, and Stuart Dowall for their assistance and support with the preparation and reviewing of the paper. In addition, the authors thank Dstl for their permission to use the human ELISA assay conducted at HLS in the human PK study.

References

- [1] M. B. Prentice and L. Rahalison, "Plague," *The Lancet*, vol. 369, no. 9568, pp. 1196–1207, 2007.
- [2] E. D. Williamson, "Plague," *Vaccine*, vol. 27, supplement 4, pp. D56–D60, 2009.
- [3] T. Butler, "Plague gives surprises in the first decade of the 21st century in the United States and worldwide," *The American Journal of Tropical Medicine and Hygiene*, vol. 89, no. 4, pp. 788–793, 2013.
- [4] M. Galimand, A. Guiyoule, G. Gerbaud et al., "Multidrug resistance in *Yersinia pestis* mediated by a transferable plasmid," *The New England Journal of Medicine*, vol. 337, no. 10, pp. 677–680, 1997.
- [5] A. Guiyoule, G. Gerbaud, C. Buchrieser et al., "Transferable plasmid-mediated resistance to streptomycin in a clinical isolate of *Yersinia pestis*," *Emerging Infectious Diseases*, vol. 7, no. 1, pp. 43–48, 2001.
- [6] K. F. Meyer, "Effectiveness of live or killed plague vaccines in man," *Bulletin of the World Health Organization*, vol. 42, no. 5, pp. 653–666, 1970.
- [7] J. D. Marshall Jr., P. J. Bartelloni, D. C. Cavanaugh, P. J. Kadull, and K. F. Meyer, "Plague immunization. II. Relation of adverse clinical reactions to multiple immunizations with killed vaccine," *Journal of Infectious Diseases*, vol. 129, pp. S19–S25, 1974.

- [8] G. W. Anderson Jr., P. L. Worsham, C. R. Bolt et al., "Protection of mice from fatal bubonic and pneumonic plague by passive immunization with monoclonal antibodies against the F1 protein of *Yersinia pestis*," *The American Journal of Tropical Medicine and Hygiene*, vol. 56, no. 4, pp. 471–473, 1997.
- [9] R. Kingston, F. Burke, J. H. Robinson et al., "The fraction 1 and V protein antigens of *Yersinia pestis* activate dendritic cells to induce primary T cell responses," *Clinical and Experimental Immunology*, vol. 149, no. 3, pp. 561–569, 2007.
- [10] Y. Levy, Y. Flashner, A. Tidhar et al., "T cells play an essential role in anti-F1 mediated rapid protection against bubonic plague," *Vaccine*, vol. 29, no. 40, pp. 6866–6873, 2011.
- [11] V. L. Motin, R. Nakajima, G. B. Smirnov, and R. R. Brubaker, "Passive immunity to yersiniae mediated by anti-recombinant V antigen and protein A-V antigen fusion peptide," *Infection and Immunity*, vol. 62, no. 10, pp. 4192–4201, 1994.
- [12] E. D. Williamson, S. M. Eley, A. J. Stagg, M. Green, P. Russell, and R. W. Titball, "A sub-unit vaccine elicits IgG in serum, spleen cell cultures and bronchial washings and protects immunized animals against pneumonic plague," *Vaccine*, vol. 15, no. 10, pp. 1079–1084, 1997.
- [13] P. Fellows, J. Adamovicz, J. Hartings et al., "Protection in mice passively immunized with serum from cynomolgus macaques and humans vaccinated with recombinant plague vaccine (rFIV)," *Vaccine*, vol. 28, no. 49, pp. 7748–7756, 2010.
- [14] J. Hill, C. Cope, S. Leary, A. J. Stagg, E. D. Williamson, and R. W. Titball, "Synergistic protection of mice against plague with monoclonal antibodies specific for the F1 and V antigens of *Yersinia pestis*," *Infection and Immunity*, vol. 71, no. 4, pp. 2234–2238, 2003.
- [15] J. Hill, J. E. Eyles, S. J. Elvin, G. D. Healey, R. A. Lukaszewski, and R. W. Titball, "Administration of antibody to the lung protects mice against pneumonic plague," *Infection and Immunity*, vol. 74, no. 5, pp. 3068–3070, 2006.
- [16] S. M. Jones, F. Day, A. J. Stagg, and E. D. Williamson, "Protection conferred by a fully recombinant sub-unit vaccine against *Yersinia pestis* in male and female mice of four inbred strains," *Vaccine*, vol. 19, no. 2-3, pp. 358–366, 2000.
- [17] D. G. Heath, G. W. Anderson Jr., J. M. Mauro et al., "Protection against experimental bubonic and pneumonic plague by a recombinant capsular F1-V antigen fusion protein vaccine," *Vaccine*, vol. 16, no. 11-12, pp. 1131–1137, 1998.
- [18] S. M. Jones, K. F. Griffin, I. Hodgson, and E. D. Williamson, "Protective efficacy of a fully recombinant plague vaccine in the guinea pig," *Vaccine*, vol. 21, no. 25-26, pp. 3912–3918, 2003.
- [19] L. E. Quenee, N. A. Ciletti, D. Elli, T. M. Hermanas, and O. Schneewind, "Prevention of pneumonic plague in mice, rats, guinea pigs and non-human primates with clinical grade rV10, rV10-2 or F1-V vaccines," *Vaccine*, vol. 29, no. 38, pp. 6572–6583, 2011.
- [20] P. Russell, S. M. Eley, S. E. Hibbs, R. J. Manchec, A. J. Stagg, and R. W. Titball, "A comparison of Plague vaccine, USP and EV76 vaccine induced protection against *Yersinia pestis* in a murine model," *Vaccine*, vol. 13, no. 16, pp. 1551–1556, 1995.
- [21] E. D. Williamson and P. C. F. Oyston, "Protecting against plague: towards a next-generation vaccine," *Clinical and Experimental Immunology*, vol. 172, no. 1, pp. 1–8, 2013.
- [22] E. D. Williamson, S. M. Eley, K. F. Griffin et al., "A new improved sub-unit vaccine for plague: the basis of protection," *FEMS Immunology and Medical Microbiology*, vol. 12, no. 3-4, pp. 223–230, 1995.
- [23] E. D. Williamson, S. M. Eley, A. J. Stagg, M. Green, P. Russell, and R. W. Titball, "A single dose sub-unit vaccine protects against pneumonic plague," *Vaccine*, vol. 19, no. 4-5, pp. 566–571, 2000.
- [24] M. K. Hart, G. A. Saviolakis, S. L. Welkos, and R. V. House, "Advanced development of the rFIV and rBV A/B vaccines: progress and challenges," *Advances in Preventive Medicine*, vol. 2012, Article ID 731604, 14 pages, 2012.
- [25] E. D. Williamson, H. C. Flick-Smith, E. Waters et al., "Immunogenicity of the rF1+rV vaccine for plague with identification of potential immune correlates," *Microbial Pathogenesis*, vol. 42, no. 1, pp. 11–21, 2007.
- [26] E. D. Williamson, P. M. Vesey, K. J. Gillhespy, S. M. Eley, M. Green, and R. W. Titball, "An IgG1 titre to the F1 and V antigens correlates with protection against plague in the mouse model," *Clinical and Experimental Immunology*, vol. 116, no. 1, pp. 107–114, 1999.
- [27] C. Buchrieser, M. Prentice, and E. Carniel, "The 102-kilobase unstable region of *Yersinia pestis* comprises a high-pathogenicity island linked to a pigmentation segment which undergoes internal rearrangement," *Journal of Bacteriology*, vol. 180, no. 9, pp. 2321–2329, 1998.
- [28] H. A. Druett, "A mobile form of the Henderson apparatus," *Journal of Hygiene*, vol. 67, no. 3, pp. 437–448, 1969.
- [29] K. R. MAY and G. J. HARPER, "The efficiency of various liquid impinger samplers in bacterial aerosols," *British Journal of Industrial Medicine*, vol. 14, no. 4, pp. 287–297, 1957.
- [30] A. C. Guyton, "Measurement of the respiratory volumes of laboratory animals," *American Journal of Physiology*, vol. 150, no. 1, pp. 70–71, 1947.
- [31] E. Pietersen, "Long-term outcomes of patients with extensively drug-resistant tuberculosis in South Africa: A Cohort Study," *The Lancet*, vol. 383, no. 9924, pp. 1230–1239, 2014.
- [32] P. Fellows, W. Lin, C. Detrisac et al., "Establishment of a Swiss webster mouse model of pneumonic plague to meet essential data elements under the animal rule," *Clinical and Vaccine Immunology*, vol. 19, no. 4, pp. 468–476, 2012.
- [33] M. Green, D. Rogers, P. Russell et al., "The SCID/Beige mouse as a model to investigate protection against *Yersinia pestis*," *FEMS Immunology and Medical Microbiology*, vol. 23, no. 2, pp. 107–113, 1999.
- [34] E. D. Williamson, H. C. Flick-Smith, C. LeButt et al., "Human immune response to a plague vaccine comprising recombinant F1 and V antigens," *Infection and Immunity*, vol. 73, no. 6, pp. 3598–3608, 2005.
- [35] P. Bruhns, "Properties of mouse and human IgG receptors and their contribution to disease models," *Blood*, vol. 119, no. 24, pp. 5640–5649, 2012.

Original article

HATCH, G. J., BATE, S. R., CROOK, A., JONES, N., FUNNELL, S. G. & VIPOND, J. 2014. Efficacy testing of orally administered antibiotics against an inhalational *Bacillus anthracis* infection in BALB/c mice. *Journal of Infectious Diseases and Therapy*, 02, 1000175.

Impact factor: 1.650

Contributions by HATCH, G. J.

Home Office – Personal Licence holder

Development and qualification of aerosol, biocontainment and clinical parameter systems. Performance of aerosol challenge.

Study management – Study design, liaison and co-ordination with sponsors, bacteriology and in vivo teams., scheduling, reporting

Data analysis and manuscript preparation

Citation metrics

Google Scholar: 2 citations



Efficacy Testing of Orally Administered Antibiotics against an Inhalational *Bacillus anthracis* Infection in BALB/C Mice

Graham J Hatch, Simon R Bate, Anthony Crook, Nicola Jones, Simon G Funnell and Julia Vipond*

Public Health England, Porton Down, Salisbury, SP4 0JG, UK

*Corresponding author: Julia Vipond, Public Health England, Porton Down, Salisbury, UK, Tel: +4401980 612584; Fax: +44 (0)1980 619894; E-mail: julia.vipond@phe.gov.uk

Rec date: August 15, 2014; Acc date: October 16, 2014; Pub date: October 28, 2014

Copyright: © 2014 Hatch GJ, et al. This is an open-access article distributed under the terms of the Creative Commons Attribution License, which permits unrestricted use, distribution, and reproduction in any medium, provided the original author and source are credited.

Abstract

Anthrax is a potentially fatal disease in man, and events of the last decade have highlighted the possibility for *Bacillus anthracis* to be used as a biological weapon through deliberate release. Whilst outbreaks of anthrax occur in several countries, there are only a few areas in which outbreaks of inhalational anthrax occur, so it is not possible to test therapies using conventional clinical trials. To overcome these problems, the FDA published the 'Animal Rule' in 2002; a rule designed to permit licensure of drugs and biologics intended to reduce or prevent serious conditions caused by exposure to biological and other agents.

Due to limited proven post-exposure prophylaxis after inhalational exposure for use in humans, it is essential to have a robust animal model of disease. In a series of three studies conducted in BALB/c mice, the efficacy of post-exposure, orally administered antibiotics in preventing disease following inhalational exposure to *B. anthracis* was evaluated. Mice treated with either azithromycin or clarithromycin displayed a near identical disease progression to the control, untreated mice; in contrast, those treated with levofloxacin, amoxicillin and co-amoxiclav were generally protected with survival of 97%, 95% and 79%, respectively. The details of the assessments and future direction of these studies are presented.

Keywords: *Bacillus anthracis*; Anthrax; Co-amoxiclav; Orally administered antibiotics

Introduction

Bacillus anthracis, a Gram-positive, spore-forming bacillus, is the causative agent of anthrax, a disease that manifests via the gastrointestinal, cutaneous or inhalational route of exposure. Whilst human infection is rare, it generally occurs with low lethality via the cutaneous or gastrointestinal route following people handling infected animals or by ingesting infected meat. The disease, however, is potentially lethal via the inhalational route due to internalization of the spores [1], and the threat posed to public health and safety have caused it to be included on the US Centers for Disease Control and Prevention (CDC) list of select agents as a Category A biological threat agent [2]; indeed the human inhalational mortality rate ranges from 45%-80% [3,4].

The current recommended antibiotic (ciprofloxacin) of choice against *B. anthracis* is based upon empirical treatments for sepsis, as there are no clinical studies of the treatment of anthrax in humans [4]; although recently the CDC has updated their guidelines on treatment of post-exposure inhalational anthrax, to include doxycycline and levofloxacin as well as ciprofloxacin [5]. Ciprofloxacin has been investigated in many animal models of inhalational infection, ranging from mice, guinea pigs and rabbits [6-10] through to marmoset and rhesus macaques [11-16] and it has proved effective. Whilst antibiotics are still considered to be the most effective therapeutic approach in the treatment of many pathogens, it is important to look at different antibiotics or indeed different combinations of antibiotics to combat potential antibiotic resistance. In addition, treatment with

ciprofloxacin alone during the Amerithrax incident was seen to fail to protect 5 out of 11 individuals against inhalational anthrax. Some have speculated that this apparent antibiotic failure was due to continued action of toxin in the absence of viable organisms [17] and suggest a combination of antibiotics (e.g. bactericidal agents with protein synthesis inhibitors) would be more effective. This suggestion is supported by the fact that 53% of the human cases of inhalational anthrax that survived were treated with a combination of antibiotics [5].

Inhalational anthrax has an incredibly rapid disease course, with death occurring within a few days of exposure if no treatment is administered, thereby making this a lethal form of the disease [18]. To evaluate the efficacy of different antibiotics following aerosol exposure to virulent *B. anthracis* (Ames strain), a model utilising BALB/c mice was established. This manuscript focuses on the survival and clinical signs of infection in BALB/c mice following orally administered antibiotics post-aerosol challenge with *B. anthracis* spores.

Material and Methods

Bacillus anthracis challenge strain

Bacillus anthracis, AMES (NR-2324) was obtained from the Biodefense and Emerging Infections Research Resources Repository (BEI Resources, Manassas, VA). *B. anthracis* spores were produced by fed batch culture in a 2 L bioreactor for approximately 26 h at 37°C ± 2°C, 400 rpm ± 10 rpm. The spores were concentrated and washed in sterile distilled water by centrifugation, with final suspension in sterile distilled water to an approximate titre of 8E+09 CFU/ml.

Confirmation of spores was by phase-bright microscopy; the final suspension was 100% phase-bright.

Experimental animals

All animal studies were carried out in accordance with the UK Animals (Scientific Procedures) Act, 1986 and the Codes of Practice for the Housing and Care of Animals used in Scientific Procedures, 1989. Female BALB/c mice aged over 8 weeks (sexually mature), free of inter-current infection, were obtained from a commercial supplier (Charles River, UK) with an approximate body weight of 20 grams. Mice were housed in groups of five on a 12 hour day-night light cycle, with food and water available *ad libitum*.

Aerosol challenge

Over three sequential experiments, groups of up to 20 mice (Table 1) were challenged for 10 minutes with a dynamic aerosol of *B. anthracis* spores using the AeroMP-Henderson apparatus; the

challenge aerosol was generated using a three-jet Collison nebuliser (BGI, Waltham, USA) containing 20 ml *B. anthracis* spores in sterile water. The resulting aerosol was mixed with conditioned air ($65 \pm 5\%$ relative humidity, $21 \pm 1^\circ\text{C}$) in the spray tube [19] and delivered to the nose of each animal via an exposure tube (sow) in which the unanaesthetised mice were held in restraint tubes. Samples of the aerosol were taken using an All Glass Impinger (AGI30, Ace Glass, USA), [20] operating at 6 L/min containing 20 ml sterile water and an Aerodynamic Particle Sizer (TSI Instruments Ltd, Bucks, UK); these processes were controlled and monitored using the AeroMP management platform (Biaera Technologies LLC, MD, USA).

Back titrations of the aerosol samples, taken at the time of challenge, were performed by serial dilution and plating out onto trypticase soy agar (TSA) incubated at 37°C for 16-24 h. These titrations were used to calculate the inhaled dose using a derived respiratory minute volume of 19.9 ml estimated from the average weight of the animals [21].

	Levofloxacin	Control (water)	Amoxicillin	Co-amoxiclav	Azithromycin	Clarithromycin
Study 1	20	19 ^a	N/A	N/A	N/A	N/A
Study 2	5	20	20	19 ^b	N/A	N/A
Study 3	5	20	N/A	N/A	20	20

^aOne death during aerosolisation
^bOne death during antibiotic administration
 N/A Not applicable; no animals in these study groups

Table 1: Experimental design detailing number of animals per group

Antibiotic Dosing

Antibiotics were obtained from a registered pharmacy. Levofloxacin tablets were dissolved with the aid of sonication in sterile water to a concentration of 8 mg/ml. Liquid preparations of amoxicillin, co-amoxiclav, clarithromycin and azithromycin were prepared in sterile

water according to manufacturer's instructions. Immediately prior to administration, amoxicillin, co-amoxiclav and clarithromycin were further diluted in sterile water to achieve concentrations of 3 mg/ml; azithromycin was diluted to 1.2 mg/ml for the first dose and 0.6 mg/ml thereafter (Table 2).

Antibiotic treatment	Name/supplier	Treatment dose	% survival	Median time to death (days)	Log-rank statistic compared to control
			(survivors/total)		
Levofloxacin	Tavanic/Sanofi-Aventis	80 mg/Kg BID	97 (29/30)	>45	p<0.001
Amoxicillin	Amoxil/GSK	30 mg/Kg QD	95 (19/20)	>45	p<0.001
Co-amoxiclav	Augmentin/GSK	30 mg/Kg QD	79 (15/19)	>45	p<0.001
Azithromycin	Zithromax/Pfizer	12.6 mg/Kg QD	5 (1/20)	1.92	p=0.198
Clarithromycin	Klaricid/Abbott Healthcare	30 mg/Kg QD	0 (0/20)	1.67	p=0.815
Control (water)		0.2 ml BID	3 (2/59)	1.92	-

BID – Twice daily; QD – Once daily

Table 2: Summary of antibiotic treatment and the observed protective effect of each antibiotic tested

From one day post-exposure, once or twice daily oral gavage of 0.2 ml of either the test antibiotic or carrier control commenced. Treatment continued for thirty days after which the animals were observed for a further fourteen days. Each treatment dose was verified

from peak and trough serum samples taken from a separate group of three animals, 1 h after treatment and 1 h prior to the following treatment dose. Sera were filter sterilised prior to analyses. These animals were exposed to *B. anthracis* prior to antibiotic administration as in the main studies. Analyses were performed at Huntington Life Sciences, UK. Briefly, protein precipitation was used to extract test antibiotic from the mouse serum. Mouse serum (20 µl) was spiked with 10 µl of ciprofloxacin (internal standard), then precipitated with 300 µl of acetonitrile. Samples were centrifuged for 5 minutes at +4°C (ca 12000 g). The supernatant was transferred and evaporated to dryness, after which the sample was reconstituted in 300 µl of mobile phase, and ca. 10 µl was then injected onto the LC MS/MS system.

Monitoring/Sampling

Challenged mice were returned to their home cages within an ACDP (U.K. Advisory Committee on Dangerous Pathogens) animal containment level 3 facility. Animals were closely observed at least twice daily over the 45-day period for the development of clinical signs. A clinical score was attributed based upon ruffled fur, eyes closed, arched back and immobility. The humane endpoint of immobility was strictly observed so that no animal became distressed. 'Time to death' figures include those animals killed according to the humane endpoint. Cause of death was confirmed by the presence of bacteraemia by streaking 10 µl blood onto TSA and incubating at 37°C for 24 h. Any animals that reached the end of the study (45 days post-challenge) were designated as survivors. Survivors were humanely euthanized and lung tissue subsequently removed and frozen at less than minus 60°C.

Bacterial Enumeration

Lung tissue was thawed, weighed and homogenised in sterile water using a Precellys24 tissue homogenizer (Bertin Technologies, Villeurbanne). Tissue samples were serially diluted in sterile water and then plated out onto TSA. Plates were incubated at 37°C for 16-24 h before enumeration using a well-developed and characterised standard procedure.

Minimum Inhibitory Concentration (MIC)

The MICs of the test antibiotics were assessed using 12 *B. anthracis* isolates recovered from murine survivors' lung tissue. Antibiotics were serially diluted two-fold in Mueller-Hinton broth so that four wells of a 96-well test plate contained 100 µl in the following concentration range: amoxicillin (4-0.004 µg/ml), co-amoxiclav (4-0.004 µg/ml), levofloxacin (2-0.002 µg/ml), clarithromycin (4-0.004 µg/ml), azithromycin (16-0.015 µg/ml) and ciprofloxacin (2-0.002 µg/ml). Lung tissue isolates and *B. anthracis* controls (*B. anthracis*, Ames working cell bank) were grown for 20-24 h at 37°C on Columbia blood agar. A sample from each was suspended in 10 ml Mueller-Hinton broth to an optical density measured at 600 nm of 0.08 to 0.12. The bacterial suspensions were further diluted 150-fold; 100 µl was added to each well of the test plates and then incubated for 18-24 h at 35 ± 2°C. Following incubation, the optical density of each well was measured at 600 nm and the MIC curve and values calculated.

Statistical Analysis

Analysis of survival rates between mice in treatment groups was performed using the log-rank test.

Results and Discussion

Aerosol exposure to *B. anthracis*

Groups of 20 mice were challenged with a mean inhaled dose of *B. anthracis* of 1.2E+06 CFU equating to 20 LD₅₀ (range 11-31 LD₅₀); the mass median aerodynamic diameter of the challenge aerosols was <2 µm.

Clinical observations and mortality

Administration of antibiotics by oral gavage once or twice daily for 30 days was well tolerated. In addition to mortality data, in order to generate a numerical assessment of the observable well-being of groups of animals, a cumulative overall scoring system was devised which was based on clinical observations indicative of the disease. Clinical observations were scored in the following manner; healthy, score=0; ruffled fur, score=2; eyes closed, score=3; arched back, score=3; immobility, score=9 and death in cage or humane euthanasia, score=10.

A graphical summary of the survival of animals from all of these studies is displayed in Figure 1. Analysis of the combined Kaplan Meier curves with the Log-Rank statistic shows that, compared to the negative control, levofloxacin, amoxicillin and co-amoxiclav all conferred significant protection (p<0.001) from inhalational anthrax when administered for 30 days post-aerosol challenge. Azithromycin and clarithromycin failed to protect (p=0.198 and 0.815, respectively) from morbidity or mortality in this murine model.

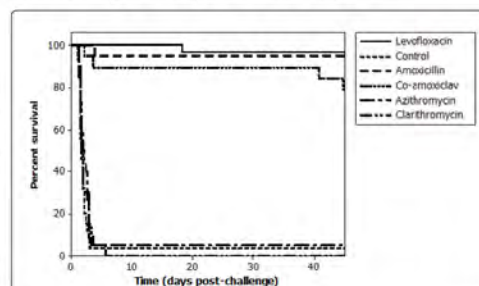


Figure 1: Combined Kaplan-Meier survival plots for all treatment groups

In all experiments, any mouse showing signs of severe disease (immobility) was immediately humanely euthanized. In animals that did not succumb to disease, clinical signs were largely absent with the exception of two levofloxacin-treated animals (Figures 2 and 3). Control, sham-treated mice generally displayed a rapid onset of clinical signs from 1 day post-challenge with the appearance of ruffled fur followed by immobility/death/euthanasia with a median time of 1.92 days post-challenge (Figures 2-4). Mice treated with either azithromycin or clarithromycin displayed a near identical disease progression to that of the control mice with rapid onset and escalation of clinical signs leading to immobility/death/euthanasia in a median time of 1.92 and 1.67 days, respectively (Figure 3 and Table 3). Levofloxacin, amoxicillin and co-amoxiclav generally protected mice from disease conferring survival 97%, 95% and 79%, respectively

(Table 2). A summary of the protective efficacy of the test antibiotics is presented in Table 2.

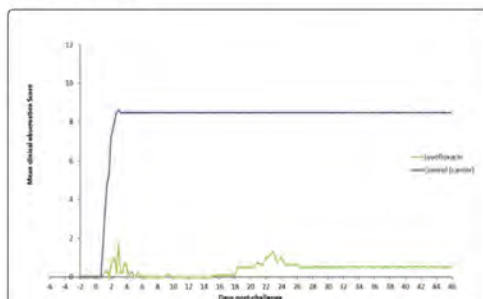


Figure 2: Cumulative mean clinical observation scores for the levofloxacin efficacy study

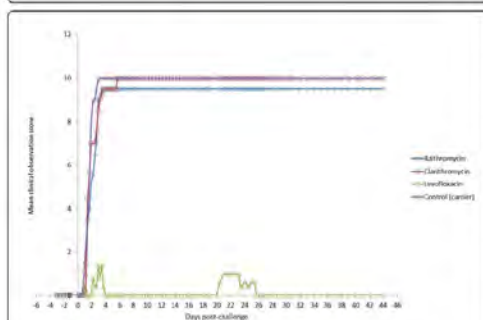


Figure 3: Cumulative mean clinical observation scores for the first antibiotic trial

The presence of a low but detectable level of anthrax persistence was noted in all groups of survivors, irrespective of antibiotic treatment. The probability that the presence of these few colonies was due to cross-contamination from inside the containment isolator during manual enumeration can be discounted due to the fact that the colonies tended only to grow from plates inoculated with most concentrated lung homogenate samples. This is because cross-contamination from within the isolator would have presented randomly across all plates.

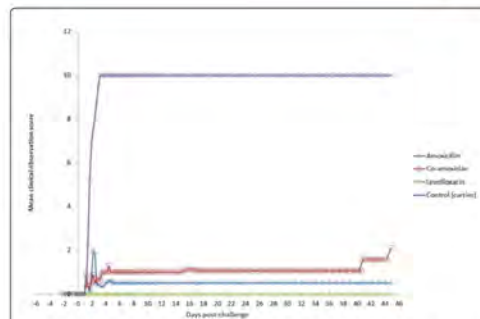


Figure 4: Cumulative mean clinical observation scores for the second antibiotic trial, Tissue bacterial load

An increase in antibiotic resistance in these persistent colonies was not detected. The reason for the presence of these persistent anthrax cells in apparently healthy survivors cannot, therefore, be attributed to an increase in antibiotic resistance. It is possible that these colonies represent spores which did not germinate in the lung or they could represent viable partially-germinated anthrax spores which resided in an intracellular or otherwise sheltered location which was protected from the bactericidal concentration of test antibiotics. This interpretation of our data is consistent with the opinion of others [5] and is further supported by the recent observations of Jenkins and Xu [22] that anthrax spores may reside intracellularly, specifically within epithelial cells of the respiratory tract, in BALB/c mice after intranasal inoculation with *B. anthracis* spores.

Serum concentrations of antibiotics

The antibiotic concentrations present in the mouse sera at peak and trough times are displayed in Table 3. Levels of azithromycin and clarithromycin were below that expected, even taking into consideration the potential for the development of resistance in Gram positive bacteria to macrolides (including clarithromycin); however, this may have been a result of an additional freeze/thaw cycle of the mouse serum that was required to prove sterility prior to analyses. Confirmation that no antibiotic resistance was incurred during the animal study is confirmed by the results presented in Table 4. The MIC of the *B. anthracis* isolates recovered from the lungs of surviving mice were the same or very similar to the MIC of the control cell bank; thus indicating that the persistence of these viable anthrax cells was not attributable to the development of increased antibiotic resistance.

Antibiotic treatment	Peak serum level (ng/ml)	Trough serum level (ng/ml)
Levofloxacin	4013	56
Amoxicillin	6220	BLQ
Co-amoxiclav	2702	BLQ
Azithromycin	50	BLQ

Clarithromycin	49	BLQ
Control (water)	BLQ	BLQ
BLQ – below limit of quantification		

Table 3: Antibiotic serum concentrations detected after dosing

Sample	Minimum inhibitory concentration (µg/ml)					
	Amoxicillin	Co-amoxiclav	Azithromycin	Clarithromycin	Levofloxacin	Ciprofloxacin
1	-	-	2	0.03	0.06	0.12
2	0.03	0.03	-	-	0.12	0.03
3	0.015	0.03	-	-	0.12	0.03
4	0.03	0.03	-	-	0.25	0.03
5	0.015	0.06	-	-	0.06	0.03
6	0.03	0.03	-	-	0.06	0.03
7	0.03	0.12	-	-	0.06	0.12
8	0.06	0.03	-	-	0.25	0.03
9	0.015	0.03	-	-	0.12	0.03
10	0.03	0.06	-	-	0.12	0.03
11	0.06	0.03	-	-	0.12	0.03
12	0.03	0.03	-	-	0.12	0.12
Control-WCB	0.06	0.12	2	0.03	0.12	0.12

WCB – Working cell bank

Table 4: MIC values on *B. anthracis* isolates recovered from the lungs of survivors

Conclusions

In this set of studies, BALB/c mice were demonstrated to be reproducibly susceptible to aerosol challenge with virulent *B. anthracis* (Ames) spores. In addition, this BALB/c model was found to be appropriate for the assessment of different antibiotic treatment regimes. Orally delivered levofloxacin, amoxicillin and to a slightly lesser extent, co-amoxiclav, were found to significantly reduce mortality when compared against azithromycin and clarithromycin at the doses evaluated. The presence of a low, but detectable, level of anthrax in some survivors from treatment groups was unexpected and could not be attributed to an increase in antibiotic resistance.

Based on the presented data (and corresponding bacterial burden; not presented), levofloxacin, amoxicillin and co-amoxiclav will be evaluated further in a cynomolgus macaque model. The FDA 2002 draft guidance recommends the use of an appropriate macaque model [2] and subsequent guidance and publications support the use of the African green, rhesus or cynomolgus macaque [23,12-16]. For this reason we have characterised the cynomolgus macaque model and will be evaluating the post-exposure efficacy of these three orally administered antibiotics in terms of animal survival, bacterial burden and time course of progression of diseases (including disease manifestations e.g. pathologic features and immune status) ultimately

aiming to increase the therapeutic options to support further post-exposure prophylaxis indications for inhalational anthrax. In addition we will investigate if these antibiotics have the ability to prevent systemic replication and dormancy, as this aspect has not been clearly defined to date.

Acknowledgement

These studies have been funded in whole with Federal funds from the National Institute of Allergy and Infectious Diseases contract number N01-AI-30062. The authors would like to thank all PHE employees from the Biological Investigations Group and bacteriology group who helped support this work. They would also like to acknowledge the work conducted by the Bio-analytical group at HLS.

Ethical approval: All animal studies were carried out in accordance with the Scientific Procedures Act of 1986 and the Codes of Practice for the Housing and Care of Animals used in Scientific Procedures 1989. Work was authorised by a Home Office Project Licence.

References

1. Mock M, Fouet A (2001) Anthrax. *Annu Rev Microbiol* 55: 647-671.

2. Food and Drug Administration, HHS (2002) New drug and biological drug products; evidence needed to demonstrate effectiveness of new drugs when human efficacy studies are not ethical or feasible. Final rule. *Fed Regist* 67: 37988-37998.
3. Holty JE, Bravata DM, Liu H, Olshen RA, McDonald KM, et al. (2006) Systematic review: a century of inhalational anthrax cases from 1900 to 2005. *Ann Intern Med* 144: 270-280.
4. Inglesby TV, Henderson DA, Bartlett JG, Ascher MS, Eitzen E, et al. (1999) Anthrax as a biological weapon: medical and public health management. Working Group on Civilian Biodefense. *JAMA* 281: 1735-1745.
5. Hendricks KA, Wright ME, Shadomy SV, Bradley JS, Morrow MG, et al. (2014) Centers for disease control and prevention expert panel meetings on prevention and treatment of anthrax in adults. *Emerg Infect Dis* 20.
6. Steward J, Lever MS, Simpson AJ, Sefton AM, Brooks TJ (2004) Post-exposure prophylaxis of systemic anthrax in mice and treatment with fluoroquinolones. *J Antimicrob Chemother* 54: 95-99.
7. Altboum Z, Gozes Y, Barnea A, Pass A, White M, et al. (2002) Postexposure prophylaxis against anthrax: evaluation of various treatment regimens in intranasally infected guinea pigs. *Infect Immun* 70: 6231-6241.
8. Heine HS, Bassett J, Miller L, Hartings JM, Ivins BE, et al. (2007) Determination of antibiotic efficacy against *Bacillus anthracis* in a mouse aerosol challenge model. *Antimicrob Agents Ch* 51: 1373-1379.
9. Peterson JW, Moen ST, Healy D, Pawlik JE, Taormina J, et al. (2010) Protection Afforded by Fluoroquinolones in Animal Models of Respiratory Infections with *Bacillus anthracis*, *Yersinia pestis*, and *Francisella tularensis*. *Open Microbiol J* 4: 34-46.
10. Vietri NJ, Purcell BK, Tobery SA, Rasmussen SL, Leffel EK, et al. (2009) A short course of antibiotic treatment is effective in preventing death from experimental inhalational anthrax after discontinuing antibiotics. *J Infect Dis* 99: 336-341.
11. Nelson M, Stagg AJ, Stevens DJ, Brown MA, Pearce PC, et al. (2011) Post-exposure therapy of inhalational anthrax in the common marmoset. *Int J Antimicrob Agents* 38: 60-64.
12. Friedlander AM, Welkos SL, Pitt ML, Ezzell JW, Worsham PL, et al. (1993) Postexposure prophylaxis against experimental inhalation anthrax. *J Infect Dis* 167: 1239-1243.
13. Fritz DL, Jaax NK, Lawrence WB, Davis KJ, Pitt ML, et al. (1995) Pathology of experimental inhalation anthrax in the rhesus monkey. *Lab Invest* 73: 691-702.
14. Kao LM, Bush K, Barnewall R, Estep J, Thalacker FW, et al. (2006) Pharmacokinetic considerations and efficacy of levofloxacin in an inhalational anthrax (postexposure) rhesus monkey model. *Antimicrob Agents Chemother* 50: 3535-3542.
15. Vasconcelos D, Barnewall R, Babin M, Hunt R, Estep J, et al. (2003) Pathology of inhalation anthrax in cynomolgus monkeys (*Macaca fascicularis*). *Lab Invest* 83: 1201-1209.
16. Twenhafel NA, Leffel E, Pitt ML (2007) Pathology of inhalational anthrax infection in the african green monkey. *Vet Pathol* 44: 716-721.
17. Karginov VA, Robinson TM, Riemenschneider J, Golding B, Kennedy M, et al. (2004) Treatment of anthrax infection with combination of ciprofloxacin and antibodies to protective antigen of *Bacillus anthracis*. *FEMS Immunol Med Microbiol* 40: 71-74.
18. Twenhafel NA (2010) Pathology of inhalational anthrax animal models. *Vet Pathol* 47: 819-830.
19. Druett HA (1969) A mobile form of the Henderson apparatus. *J Hyg (Lond)* 67: 437-448.
20. May KR, Harper GJ (1957) The efficiency of various liquid impinger samplers in bacterial aerosols. *Br J Ind Med* 14: 287-297.
21. Guyton AC (1947) Measurement of the respiratory volumes of laboratory animals. *Am J Physiol* 150: 70-77.
22. Jenkins SA, Xu Y (2013) Characterization of *Bacillus anthracis* persistence in vivo. *PLoS One* 8: e66177.
23. Food and Drug Administration; HHS (2009) Guidance for Industry: Animal Models - Essential Elements to Address Efficacy Under the Animal Rule.

Original article

NORVILLE, I. H., HATCH, G. J., BEWLEY, K. R., ATKINSON, D. J., HAMBLIN, K. A., BLANCHARD, J. D., ARMSTRONG, S. J., PITMAN, J. K., RAYNER, E., HALL, G., VIPOND, J. & ATKINS, T. P. 2014. Efficacy of liposome-encapsulated ciprofloxacin in a murine model of Q fever. *Antimicrob Agents Chemother*, 58, 5510-8.

Impact factor: 4.715

Contributions by HATCH, G. J.

Home Office – Personal Licence holder

Development and qualification of aerosol, biocontainment and clinical parameter systems. Performance aerosol of challenge.

Study management – Study design, liaison and co-ordination with sponsors, virology, histology and in vivo teams, scheduling, reporting

Data analysis and manuscript review

Citation metrics

Google Scholar: 26 citations

Efficacy of Liposome-Encapsulated Ciprofloxacin in a Murine Model of Q Fever

I. H. Norville,^a G. J. Hatch,^b K. R. Bewley,^b D. J. Atkinson,^a K. A. Hamblin,^a J. D. Blanchard,^d S. J. Armstrong,^a J. K. Pitman,^b E. Rayner,^b G. Hall,^b J. Vipond,^b T. P. Atkins^{a,c}

Defence Science and Technology Laboratory, Porton Down, Salisbury, United Kingdom^a; Public Health England, Porton Down, Salisbury, United Kingdom^b; College of Life and Environmental Sciences, University of Exeter, Exeter, United Kingdom^c; Aradigm Corporation, Hayward, California, USA^d

Encapsulation of antibiotics may improve treatment of intracellular infections by prolonging antibiotic release and improving antibiotic uptake into cells. In this study, liposome-encapsulated ciprofloxacin for inhalation (CFI) was evaluated as a postexposure therapeutic for the treatment of *Coxiella burnetii*, the causative agent of Q fever. Intranasal treatment of male A/Jola (A/J) mice with CFI (50 mg/kg of body weight) once daily for 7 days protected mice against weight loss and clinical signs following an aerosol challenge with *C. burnetii*. In comparison, mice treated twice daily with oral ciprofloxacin or doxycycline (50 mg/kg) or phosphate-buffered saline (PBS) lost 15 to 20% body weight and exhibited ruffled fur, arched backs, and dehydration. Mice were culled at day 14 postchallenge. The weights and bacterial burdens of organs were determined. Mice treated with CFI exhibited reduced splenomegaly and reduced bacterial numbers in the lungs and spleen compared to mice treated with oral ciprofloxacin or doxycycline. When a single dose of CFI was administered, it provided better protection against body weight loss than 7 days of treatment with oral doxycycline, the current antibiotic of choice to treat Q fever. These data suggest that CFI has potential as a superior antibiotic to treat Q fever.

Coxiella burnetii is a Gram-negative intracellular bacterium and the etiological agent of the disease Q fever. Q fever is prevalent throughout the world, with the exception of New Zealand, and is a zoonosis that typically presents as an acute, self-limiting febrile disease or atypical pneumonia in humans (1). In addition, there are several recent reports of outbreaks among military personnel serving in Iraq and Afghanistan, and *C. burnetii* is listed as a category B agent by the Centers for Disease Control and Prevention (CDC) (2–4). Recovery from acute disease usually occurs within 2 weeks and can be accelerated by treatment twice daily with oral doxycycline. However, delays in diagnosis of acute Q fever or an incorrect diagnosis often result in ineffective or inappropriate antibiotic treatment (5). *C. burnetii* can also cause a chronic form of disease which is a severe, and sometimes life-threatening, manifestation, often characterized by endocarditis or hepatitis (6). Chronic infections are treated with a combination of doxycycline and chloroquine for at least 18 months and up to 4 years (7). A recent fatal case of Q fever was caused by a doxycycline-resistant strain, and cases presenting with endocarditis are associated with frequent relapses, despite antibiotic treatment (8, 9).

Encapsulation of antibiotics in delivery vesicles, such as liposomes, has been shown to enhance drug availability and activity and reduce toxicity in general (10), and antibiotics delivered by inhalation particularly display these characteristics (11). Ciprofloxacin is a broad-spectrum fluoroquinolone that demonstrates *in vitro* bactericidal effects against several respiratory pathogens, including *C. burnetii*, *Mycobacterium tuberculosis*, and *Neisseria meningitidis* (12–14). However, oral or intravenous delivery of ciprofloxacin results in a suboptimal pharmacokinetic profile in the lower respiratory tract, and emergence of antibiotic resistance makes treatment problematic (15–17). Formulations of liposome-encapsulated ciprofloxacin have been developed and shown to improve antibiotic efficacy in *Francisella tularensis*,

Mycobacterium avium, and *Streptococcus pneumoniae* *in vivo* models (18–21).

The liposome-encapsulated ciprofloxacin tested in this study, ciprofloxacin for inhalation (CFI), is an advanced formulation specifically designed for inhalation that has already been shown to be highly efficacious *in vivo* against several intracellular pathogens, specifically *F. tularensis* LVS and Schu S4 strains (22) and *Yersinia pestis* CO92 strain (K. A. Hamblin, J. D. Blanchard, C. Davies, and S. V. Harding, presented at the 19th Congress of the International Society of Aerosols in Medicine, April 2013, Chapel Hill, NC) in mouse models of lung infection.

In this study, we report for the first time the evaluation of antibiotic efficacy in an aerosol murine model of Q fever. The efficacy of CFI, ciprofloxacin, and doxycycline as postexposure therapeutics were compared, and single-dose pharmacokinetic profiles were determined.

MATERIALS AND METHODS

Bacteria. *C. burnetii* strain Nine Mile was grown axenically in ACCM-2 in 250-ml Erlenmeyer flasks containing 100 ml medium (23). Cultures were incubated at 37°C, shaking at 75 rpm for 6 days, with a GENbox microaer atmosphere generator (bioMérieux, France) to displace oxygen. Bacteria were harvested by centrifugation at 10,000 × g at 21°C for 20 min and resuspended in sterile phosphate-buffered saline (PBS) at a concentration of approximately 1 × 10⁹ genome equivalents (GE)/ml. All manipulations of *C. burnetii* were carried out in a class III microbiological safety cabinet complying with the 2000 European standard EN 12469 (24). Using the

Received 23 May 2014 Returned for modification 19 June 2014

Accepted 1 July 2014

Published ahead of print 7 July 2014

Address correspondence to T. P. Atkins, tpatkins@dstl.gov.uk.

Copyright © 2014, American Society for Microbiology. All Rights Reserved.

doi:10.1128/AAC.03443-14

criteria within the "Proposed Framework for the Oversight of Dual Use Life Sciences Research: Strategies for Minimizing the Potential Misuse of Research Information" (25) by the National Science Advisory Board for Biosecurity (NSABB), this research does not fall into any of the categories for dual-use research of concern.

Bacterial enumeration. *C. burnetii* was enumerated using real-time PCR (RT-PCR) targeting the *sod* gene using the forward primer TCTTC AACAAATGCAGCACAACAT and reverse primer TGAAGCCAATTCCG CAGAA. The probe sequence was CATTATTGGCACTGCATGAGCC CTG, and the probe was covalently labeled at the 5' end with the reporter dye 6-carboxyfluorescein (FAM) and at the 3' end with the quencher dye black hole quencher 1 (BHQ-1). Chromosomal DNA was extracted by addition using Qiagen QIAmp DNA minikit/blood mini/tissue depending on the sample type. Real-time PCR mixtures comprised 2 μ l template DNA, forward primer (900 nM), reverse primer (900 nM), probe (250 nM) and ABI Fast TaqMan mastermix. PCR cycling conditions comprised 3 min at 95°C, 30 s at 60°C, followed by 50 two-step cycles, with 1 cycle consisting of 15 s at 95°C and 30 s at 60°C. For each PCR, a control of linearized synthetic plasmid that contains a single copy of the target was included. The synthetic plasmid was quantitated after linearization and purification using a ND-2500 NanoDrop spectrophotometer. For each reaction, a standard curve of the synthetic plasmid was run in duplicate in the range 1×10^7 GE/ml to 1×10^3 GE/ml. Plasmid concentration of 1×10^3 GE/ml in triplicate is used as a lower-limit check in every assay. The lower limit of detection for this assay is 2.5×10^3 GE/ml culture or 4.4×10^1 GE/mg spleen or 2.2×10^1 GE/mg lung/liver/testes.

Mice. Groups of age-matched male A/Jola (A/J) mice (Charles River) were housed on a 12-h day-night light cycle, with food and water available *ad libitum* in an Advisory Committee on Dangerous Pathogens (ACDP) (United Kingdom) level 3 flexible-film isolator, complying with the 2000 European Standard EN 12469 (24), and allowed to acclimatize before challenge. All procedures were conducted under a project license approved by internal ethical review, and in accordance with both the Animal (Scientific Procedures) Act (1986) (26) and the 1989 Codes of Practice for the Housing and Care of Animals used in Scientific Procedures (27).

Antimicrobial agents. Ciprofloxacin (Bayer, Newbury, United Kingdom) or doxycycline hyclate (Sigma-Aldrich, United Kingdom) were dissolved in distilled water to a working concentration of 25 mg/ml or 40 mg/ml, respectively. Ciprofloxacin for inhalation (CFI) was provided by Aradigm Corporation (Hayward, CA, USA) and diluted in PBS to a working concentration of 25 mg/ml. All antibiotics were prepared freshly each day prior to dosing.

Infection of mice and antibiotic efficacy studies. Mice were challenged with an aerosol produced from 10-ml suspension of *C. burnetii* at a concentration of 2.3×10^9 GE/ml (study 1), 6×10^9 GE/ml (study 2), or 1×10^{10} GE/ml (study 3) using the AeroMP-Henderson apparatus. The challenge aerosol was generated using a six-jet Collison nebulizer (BGI, Waltham, MA) operating at 15 liters/min. The aerosol was mixed with conditioned air in the spray tube and delivered via a head-only exposure chamber. Samples of the aerosol were taken using an AGI-30 (Ace Glass Inc., USA) at 6 liters/min containing PBS and an aerodynamic particle sizer (TSI Instruments, Ltd., Bucks, United Kingdom); these processes were controlled and monitored using the AeroMP management platform (Biaera Technologies, LLC, Frederick, MD). A back titration of the aerosol samples taken at the time of challenge was performed using RT-PCR as described above. Direct bacterial enumeration was used to calculate the presented dose using a derived respiratory minute volume of 19.9 ml estimated using the average weight of the animals (28).

For study 1, groups of six infected mice were observed, and clinical signs (piloerection, arched back, dehydration, eyes shut, wasp-waisted appearance, immobile, and death) and weight were evaluated twice daily. Mice were culled on days 3, 4, 5, 6, 7, 8, 9, 11, and 13 postchallenge (p.c.), and the lungs, spleen, liver, testes, and blood were aseptically removed. Organs were weighed and homogenized using a Precellys24 homogenizer, and bacteria were enumerated using RT-PCR as described above. Anti-

body titers were determined using Q fever phase I IgG and phase II IgM Novalisa kits (Novatec, Germany).

For study 2, groups of 10 infected mice were treated from 24 h p.c. for 7 consecutive days with 40 μ l of a 25-mg/ml ciprofloxacin (50 mg/kg of body weight) solution administered orally via pipette twice daily (12-h intervals) or as 40 μ l of a 25-mg/ml solution of CFI (50 mg/kg) delivered once daily (24-h intervals) by intranasal (i.n.) instillation using a pipette. Control mice received PBS orally twice daily for 7 days postchallenge. At day 14 p.c., mice were culled, and the lungs and spleens were aseptically removed. The lungs and spleens were weighed, and half the organ was placed in 10% neutral buffered formalin for histological analysis. The remaining organ was homogenized using a Precellys24 instrument, and bacteria were enumerated using RT-PCR as described above. Mice were monitored as discussed above for study 1.

For study 3, groups of 20 infected mice were treated from 24 h p.c. for 1, 3, or 7 consecutive days with 25 μ l of a 40-mg/ml (50-mg/kg) doxycycline solution administered orally via pipette twice daily (12-h intervals) to mimic treatment of human Q fever or as CFI delivered once daily (24-h intervals) by i.n. instillation (as described above for study 2). Control mice received PBS orally twice daily for the same number of days postchallenge as the respective treatment groups. At day 7 or 14 postchallenge, 10 mice from each treatment group were culled, and the lungs and spleens were aseptically removed and weighed. Mice were monitored as described above for study 1, and the organs were processed as described above for study 2.

Pharmacokinetic studies. Ciprofloxacin was administered to mice ($n = 30$) by the oral route at a dose of 50 mg/kg. Groups of three mice were culled at 10 min, 20 min, 30 min, 45 min, 1 h, 1.5 h, 2 h, 4 h, 8 h, and 24 h after dosing.

Doxycycline was administered to mice ($n = 30$) by the oral route at a dose of 50 mg/kg. Groups of three mice were culled at 10 min, 20 min, 30 min, 45 min, 1 h, 2 h, 4 h, 8 h, 16 h, and 24 h after dosing.

CFI was administered to mice ($n = 30$) by the i.n. route at a dose of 50 mg/kg. Groups of three mice were culled at 1 min, 15 min, 30 min, 2 h, 4 h, 8 h, 12 h, 16 h, 20 h, and 24 h after dosing.

Lungs and blood samples were collected from all animals immediately postmortem. All blood samples were heparinized and centrifuged to separate the plasma fraction from the whole blood. Samples were immediately frozen and stored at -80°C until further analysis. Three untreated control mice were included with each antibiotic group.

Histopathology. Samples of lung and spleen were processed and embedded in paraffin wax. Sections were cut at 5 to 6 μ m and stained with hematoxylin and eosin. Microscopic lesions in lung and spleen were assessed and recorded as within normal limits (where *C. burnetii*-associated lesions were not detected) or minimal, mild, moderate, and marked where *C. burnetii*-associated lesions were detected. The slides were assessed independently by two pathologists in a blind manner (unaware of the treatment).

Determination of antibiotic concentrations in plasma and lung tissues by liquid chromatography-mass spectrometry (LC-MS). Lung samples were weighed and mixed with $3 \times$ the volume of 0.1% (vol/vol) aqueous formic acid. Tissue was homogenized in a Precellys24-Dual bead homogenizer using 2.8-mm beads for two 20-s cycles at 5,000 rpm. The lung homogenate was mixed with an equal volume of 1- μ g/ml internal standard solution (ciprofloxacin-d8 hydrochloride hydrate or demeclocycline hydrochloride hydrate; Fluka, United Kingdom), and 2 volumes of dichloromethane were added. The plasma samples were mixed with an equal volume of internal standard solution and 3 volumes of acetonitrile. Following centrifugation, the supernatant was removed and reduced in volume to remove the acetonitrile using a centrifugal evaporator (Genevac Ltd., Ipswich, United Kingdom) and injected onto the LC-MS system consisting of an Agilent 1100 binary pump (Agilent Technologies UK Ltd., Wokingham, United Kingdom), CTC PAL injector (Presearch Ltd., Basingstoke, United Kingdom), Sciex API3000 LC-MS (AB Sciex, Warrington, United Kingdom) using an ACE-3-C18HL 20- by 2.1-mm column (Hichrom, Theale, United Kingdom) and a gradient mobile phase. Mobile-phase solvent A consisted of 0.1% (vol/vol) aqueous formic acid

TABLE 1 Natural history of *C. burnetii* infection in A/J mice^a

Day postchallenge	Organ wt (mg) (mean ± SD)			Bacterial burden (GE/mg or GE/ml) ^b (mean ± SD) in:					
	Lung	Spleen		Lung	Spleen	Liver	Testes ^c	Blood	
3	146.10 ± 14.50	59.87 ± 4.10		2.98 × 10 ⁵ ± 5 × 10 ⁴	5.67 × 10 ² ± 1.39 × 10 ²	0	0	3.60 × 10 ⁴ ± 7.05 × 10 ⁴	
4	175.95 ± 26.96	64.42 ± 16.02		1.43 × 10 ⁶ ± 9.31 × 10 ⁵	9.64 × 10 ² ± 1.75 × 10 ²	2.9 × 10 ³ ± 2.71 × 10 ⁴	0	1.10 × 10 ⁴ ± 4.30 × 10 ³	
5	250.58 ± 55.58	75.60 ± 8.30		1.07 × 10 ⁶ ± 3.54 × 10 ⁵	3.53 × 10 ³ ± 8.89 × 10 ²	1.98 × 10 ² ± 9.06 × 10 ¹	0	1.70 × 10 ⁴ ± 0.00	
6	230.38 ± 23.65	94.13 ± 10.99		9.50 × 10 ⁵ ± 4.80 × 10 ⁵	2.67 × 10 ³ ± 4.55 × 10 ²	3.36 × 10 ³ ± 2.12 × 10 ³	2.93 × 10 ³ ± 4.29 × 10 ⁴	6.00 × 10 ⁵ ± 1.01 × 10 ⁶	
7	266.85 ± 29.88	86.80 ± 19.54		6.95 × 10 ⁵ ± 2.02 × 10 ⁵	1.15 × 10 ³ ± 5.82 × 10 ²	6.95 × 10 ³ ± 5.37 × 10 ³	<LOD	3.50 × 10 ⁵ ± 4.02 × 10 ⁵	
8	273.40 ± 35.02	164.13 ± 14.53		6.38 × 10 ⁵ ± 3.22 × 10 ⁵	1.01 × 10 ³ ± 7.40 × 10 ²	2.58 × 10 ³ ± 1.31 × 10 ⁴	7.62 × 10 ³ ± 9.92 × 10 ⁴	1.70 × 10 ⁴ ± 0.00	
9	252.92 ± 24.36	176.53 ± 20.92		4.83 × 10 ⁵ ± 1.44 × 10 ⁵	4.6 × 10 ² ± 4.85 × 10 ²	1.99 × 10 ³ ± 1.81 × 10 ⁴	8.57 × 10 ³ ± 1.04 × 10 ⁴	4.40 × 10 ³ ± 1.06 × 10 ⁶	
11	260.15 ± 36.69	141.93 ± 25.98		8.95 × 10 ⁵ ± 2.18 × 10 ⁵	1.13 × 10 ³ ± 9.48 × 10 ²	2.60 × 10 ³ ± 1.90 × 10 ⁴	2.49 × 10 ³ ± 2.27 × 10 ²	2.80 × 10 ³ ± 2.72 × 10 ³	
13	303.02 ± 70.36	156.20 ± 12.48		6.03 × 10 ⁵ ± 4.91 × 10 ⁵	4.07 × 10 ³ ± 2.78 × 10 ²	2.61 × 10 ³ ± 1.55 × 10 ⁴	1.05 × 10 ³ ± 1.16 × 10 ²	2.10 × 10 ⁵ ± 4.56 × 10 ³	

^aIn uninfected animals, no changes in organ weight were observed, and no bacteria were detected.

^bBacterial burden shown in genome equivalents (GE) per milligram for the solid organs (lung, spleen, liver, and testes) or GE per milliliter for blood.

^c<LOD, less than the limit of detection.

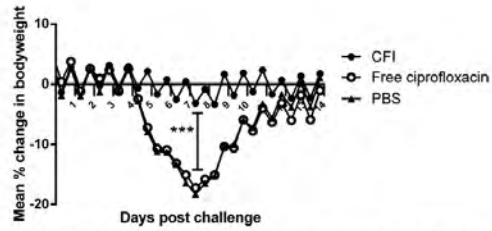


FIG 1 Efficacy of ciprofloxacin or CFI against *C. burnetii* in vivo ($n = 10$). Mean percentage change in body weight of mice infected with 2.8×10^6 GE of *C. burnetii* per ml and treated with free ciprofloxacin (by oral administration) or CFI (by i.n. administration) for 7 days postchallenge.

in water, and mobile-phase solvent B consisted of 0.1% (vol/vol) aqueous formic acid in acetonitrile. The initial mobile-phase composition was 95% solvent A and 5% solvent B. For ciprofloxacin analysis, the gradient was increased from 1 to 4 min to 95% solvent B, maintained for 1 min, then decreased back to 5% solvent B, and maintained for 3 min. For doxycycline analysis, the gradient was increased from 1 to 8 min to 55% solvent B, maintained for 1 min, then decreased back to 5% solvent B, and maintained for 3 min. The solvents were pumped at a flow rate of 250 μ l/min. The LC-MS system was controlled by Analyst software (AB Sciex, United Kingdom). Calibration curves were prepared in naive mouse plasma or lung tissue samples, using reference standards ciprofloxacin (>98%; Fluka, United Kingdom) and doxycycline hyclate (>98%; Sigma-Aldrich) and consisted of 11 points from 1 ng/ml to 20,000 ng/ml. All calibration curves had r of ≥ 0.99 and were fitted using linear regression with $1/x^2$ weighting.

Pharmacokinetic calculations. The pharmacokinetic parameters terminal half-life ($t_{1/2}$), rate of clearance (CL), maximum concentration (C_{max}), time of maximum concentration (T_{max}), and area under the concentration-time curve (AUC) were determined by noncompartmental pharmacokinetic analysis using WinNonlin Phoenix (v6.1; Pharsight Corp., USA) on mean concentration data. The relative bioavailability of oral ciprofloxacin and i.n. ciprofloxacin quantified in lung homogenate was calculated using an equation adapted from Rowland and Tozer (29), with the error associated with the relative bioavailability equation adapted from Taylor (30).

Statistical analysis. All statistical analysis was performed using SPSS v18.0 (IBM). All graphs were produced using Graphpad Prism v5. Analysis of mouse body weight loss compared to controls was carried out using a parametric univariate model of variance and Bonferroni's post test. Bacterial burden data were first transformed by \log_{10} and then analyzed using a univariate linear model and Bonferroni's post test. Organ weight (as a percentage of body weight) was first transformed by square root function and then analyzed using a univariate linear model and Bonferroni's post test. The validity of the univariate model approach (general linear model [GLM]) was tested by Levene's test for unequal variance. Statistical significance was indicated as follows: *, $P < 0.05$; **, $P < 0.01$; ***, $P < 0.001$.

RESULTS

Study 1 (development of a murine model of Q fever). In order to establish a model suitable for antibiotic efficacy studies, mice were challenged by the aerosol route with a mean presented dose of 5×10^6 GE of *C. burnetii*. Infected mice showed clinical signs between 5 and 9 days after challenge, exhibiting ruffled coats, arched backs, and a wasp-waisted appearance. In addition, weight loss was apparent in all animals from day 5 postchallenge, with peak weight loss observed between days 7 and 8. In order to characterize the pathogenesis of disease over time, groups of six mice were culled at

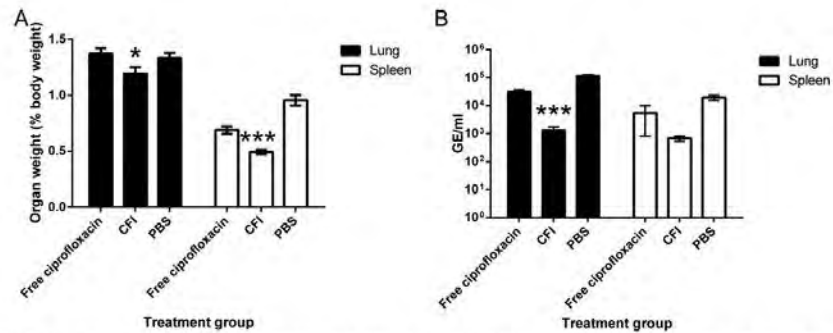


FIG 2 Weight and bacterial colonization of lungs and spleen at day 14 p.c. ($n = 10$). (A) Weight of lungs and spleens from mice challenged with 2.8×10^6 GE of *C. burnetii* per ml and treated with PBS, free ciprofloxacin, or CFI for 7 days. (B) Bacterial colonization of lungs and spleens from mice challenged with 2.8×10^6 GE of *C. burnetii*/ml and treated with PBS, free ciprofloxacin, or CFI for 7 days. Values are means \pm standard errors (error bars). Values that are significantly different from the value for the ciprofloxacin control are indicated by asterisks as follows: *, $P < 0.05$; ***, $P < 0.001$.

multiple time points after challenge, and the organs were harvested. During the 13-day course of this experiment, no significant changes in organ weight in uninfected mice were observed (sampled at 0, 7, and 13 days; $P = 0.981$ for the spleen and $P =$

0.795 for the lung). In contrast, the weights of both the spleen and the lung (but not liver and testes) from infected mice increased over time ($P < 0.001$) (Table 1), with the difference in the spleen weight becoming statistically significant at day 8 postinfection

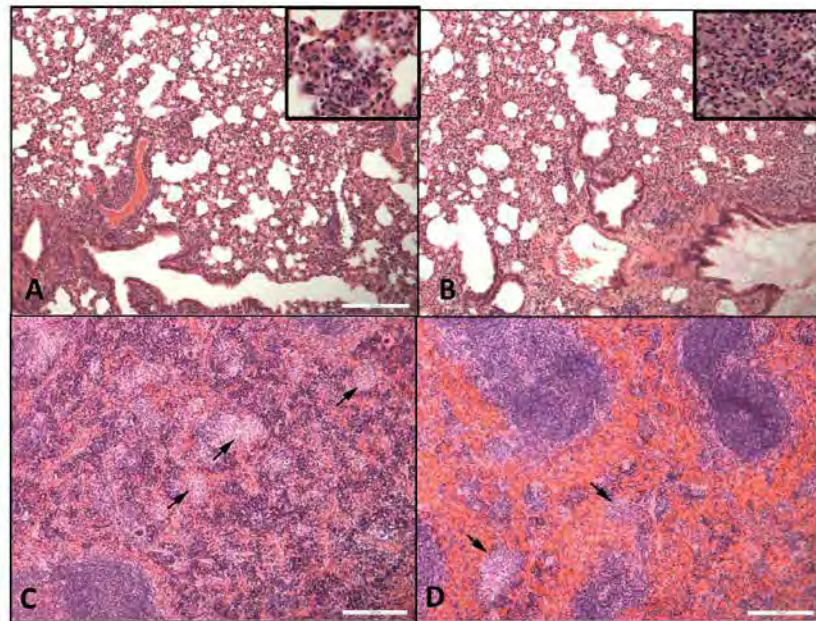


FIG 3 Hematoxylin-and-eosin-stained spleen and lung tissues from mice at day 14 p.c. (A) Lung from a mouse treated with PBS for 7 days. Moderate granulomatous alveolitis is present. (B) Lung from a mouse treated with CFI for 7 days. Moderate granulomatous alveolitis is present. (C) Spleen from a mouse treated with PBS for 7 days. The sites of moderate, multifocal, granulomatous lesions are indicated by black arrows. (D) Spleen from a mouse treated with CFI for 7 days. The sites of minimal granulomatous lesions are indicated by black arrows. Bar, 200 μ m.

($P < 0.001$) and the difference in the lung weight becoming statistically significant at 5 days ($P = 0.033$). *C. burnetii* was isolated from all tissues postchallenge, with consistently high levels of bacteria (10^5 to 10^6 GE/ml) in the lungs. The bacterial burden in the spleen, liver, testes, and blood increased throughout the course of infection (Table 1). In addition, all infected mice culled at day 13 had developed antibodies to *C. burnetii* phase I and II antigens (phase I IgG titers of $<1:200$; phase II IgM titers from 1:200 to 1:1,600).

Study 2 (in vivo efficacy of free ciprofloxacin and CFI). The efficacy of ciprofloxacin or CFI for the treatment of mice infected with *C. burnetii* was determined (Fig. 1). Mice were challenged with a mean presented dose of 2.8×10^6 GE and treated with free ciprofloxacin or PBS lost almost 20% body weight by day 7 post-challenge (p.c.) and exhibited clinical signs such as piloerection and arched backs from days 4 to 9 p.c. In contrast, mice treated with CFI were significantly protected against weight loss from day 4 p.c. ($P < 0.001$) and showed no clinical signs of disease.

Infection of mice with *C. burnetii* significantly increased the weight of the spleen and lungs ($P < 0.001$; data not shown). Treatment with CFI significantly moderated lung and spleen weight increases compared to treatment with ciprofloxacin or PBS (controls) at day 14 p.c. ($P < 0.05$ for the lung; $P < 0.001$ for the spleen; Fig. 2A). In addition, while mice treated with PBS were colonized with approximately 10^5 to 10^6 GE/ml or 10^4 to 10^5 GE/ml in the lungs or spleen, respectively, treatment with CFI reduced bacterial numbers by 10- to 100-fold, which was significant in the lungs ($P < 0.001$; Fig. 2B).

On histological examination, in the lungs of all challenged animals, focal or diffuse granulomatous alveolitis was observed, and the severity of alveolitis was similar in treated and PBS control groups (Fig. 3A and B). In the spleen, multifocal granulomatous foci were observed in mice treated with free ciprofloxacin or in PBS control groups (Fig. 3C), but reduced severity or absence of lesions was observed following treatment with CFI (Fig. 3D).

Study 3 (in vivo efficacy of doxycycline and CFI). Doxycycline is the standard antibiotic of choice to treat Q fever. Thus, the efficacy of 1 day, 3 days, and 7 days of doxycycline or CFI treatment postchallenge of mice challenged with a mean presented dose of 7×10^6 GE of *C. burnetii* was determined (Fig. 4). Mice treated with PBS lost 15% body weight by day 7 p.c., and 80% of the mice exhibited clinical signs such as piloerection at least once during the postchallenge period. Mice treated with doxycycline for 1 day, 3 days, or 7 days also lost 13 to 15% body weight; however, there was a delay in initiation of weight loss of 1, 3, or 7 days, respectively, compared to PBS-treated control mice. In all doxycycline treatment groups, 70% of mice exhibited clinical signs that correlated with peak weight loss. In contrast, mice treated with CFI had significantly reduced weight loss from day 8 p.c. compared to the corresponding doxycycline treatment regime (Fig. 4A and B) ($P < 0.001$). In addition, from day 12 to day 14 p.c., mice treated with a single dose of CFI had significantly reduced weight loss compared to mice treated with doxycycline for 1, 3, or 7 days ($P < 0.01$). The proportion of mice treated with CFI presenting with clinical signs ranged from 50% (1 day of CFI treatment) to 0% (7 days of CFI treatment).

Treatment with CFI for 7 days significantly moderated lung weight increases compared to treatment with doxycycline for 7 days at day 14 p.c. ($P < 0.01$; Fig. 5A). Spleen weight gain of CFI-treated mice was significantly moderated compared to PBS-

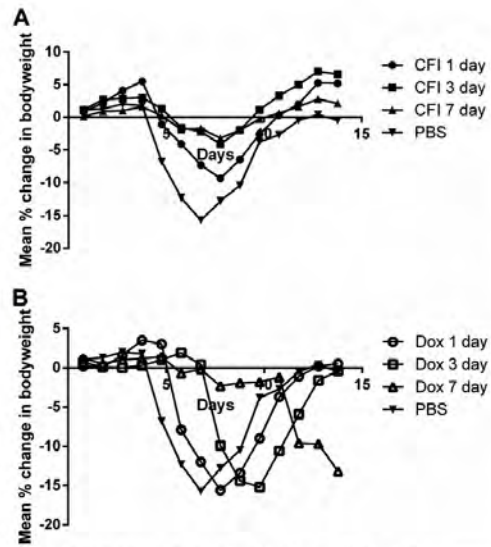


FIG 4 Efficacy of doxycycline or CFI against *C. burnetii* in vivo ($n = 10$) versus PBS-treated control mice. Mean percentage change in body weight of mice infected with 7×10^7 GE of *C. burnetii*/ml and treated with CFI (A) (by i.n. administration) or free doxycycline (Dox) (B) (by oral administration) for 1 day, 3 days, or 7 days postchallenge.

treated control mice ($P < 0.05$), but not doxycycline-treated mice. In addition, mice treated with CFI for 7 days had significantly reduced bacterial numbers in the lungs and spleen compared to mice treated with doxycycline for 7 days ($P < 0.001$; Fig. 5B).

On histopathological examination, in the lungs of all challenged animals, focal or diffuse granulomatous alveolitis was observed, with no differences observed between control and treated animals (Fig. 6A and B). In the spleen, multifocal granulomatous foci were observed in mice in the PBS control group, and lesion severity was reduced in mice receiving CFI, but not in mice receiving doxycycline (Fig. 6C and D).

Pharmacokinetic profile. In order to determine drug concentrations in treated mice, ciprofloxacin, doxycycline, and CFI were administered to naive animals. Animals were culled at set time points over a 24-h period, and lungs and plasma samples were collected postmortem. The concentration of ciprofloxacin after oral administration decreased rapidly over time in both the lungs and plasma, with terminal half-lives of 1.3 and 0.8 h, respectively (Fig. 7). Pharmacokinetic parameters are shown in Table 2. In contrast, mice receiving i.n. CFI had 100-fold-greater concentration of drug in the lung, with an extended terminal half-life of 4.1 h. In addition, the C_{max} of CFI in the lung was higher than that of oral doxycycline. Importantly, the AUC in the lung following CFI administration was almost 3 orders of magnitude greater than the AUC following the same dose of oral ciprofloxacin, resulting both from the superior C_{max} and the duration in the lung. The relative bioavailability of oral ciprofloxacin in the lung compared to i.n. CFI is 0.0014; in contrast, the relative bioavailability of oral ciprofloxacin in the plasma compared to i.n. CFI is 0.363.

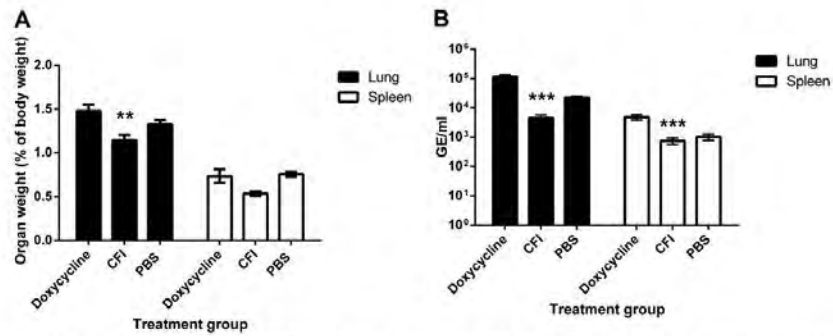


FIG 5 Weight and bacterial colonization of lungs and spleen at day 14 p.c. ($n = 10$). (A) Weight of lungs and spleens from mice challenged with 7×10^6 GE of *C. burnetii*/ml and treated with doxycycline or CFI for 7 days. (B) Bacterial colonization of lungs and spleen from mice challenged with 9.68×10^7 GE of *C. burnetii*/ml and treated with doxycycline or CFI for 7 days. Values are means \pm standard errors. Values that are significantly different from the value for the doxycycline control are indicated by asterisks as follows: **, $P < 0.01$; ***, $P < 0.001$.

DISCUSSION

The recommended antibiotic used in the treatment of Q fever is doxycycline, a bacteriostatic tetracycline used to treat several respiratory diseases, including pneumonic plague and anthrax (31).

Antibiotic activity against *C. burnetii* can be determined in embryonated eggs, tissue culture, animal models, and more recently in axenic media (23, 32). The susceptibility of *C. burnetii*, *in vitro*, to doxycycline has been determined with a MIC ranging from 0.05 to

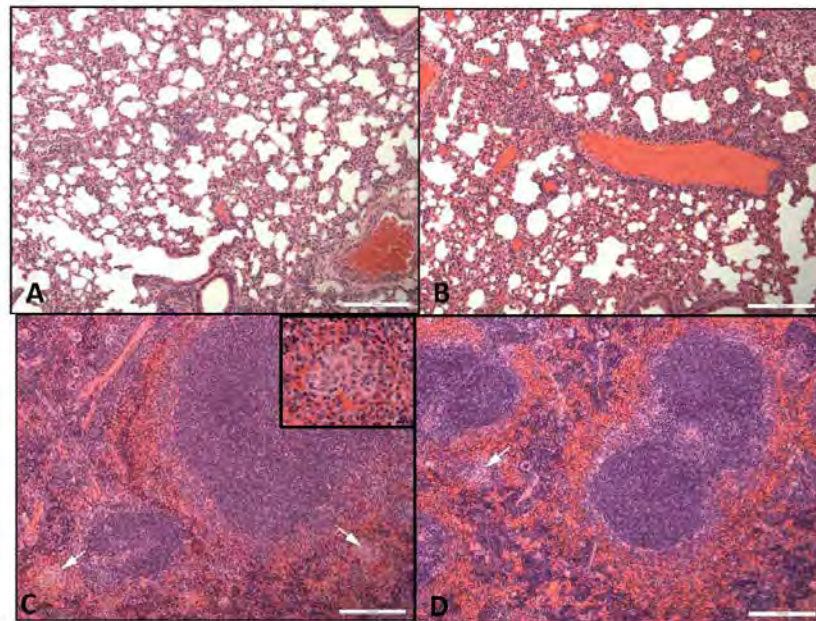


FIG 6 Hematoxylin-and-eosin-stained spleen and lung tissues from mice at day 14 p.c. (A) Lung from a mouse treated with PBS for 7 days. Mild granulomatous alveolitis is present. (B) Lung from a mouse treated with CFI for 7 days. Mild granulomatous alveolitis is present. (C) Spleen from a mouse treated with PBS for 7 days. Mild granulomatous lesions are present (indicated by white arrows). (D) Spleen from a mouse treated with CFI for 7 days. Mild granulomatous lesions are present (indicated by white arrows). Bars, 200 μ m.

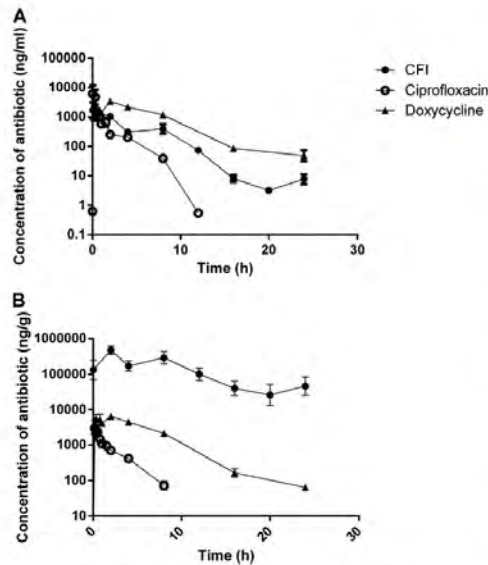


FIG 7 Profiles of the drug concentration in the plasma (A) or lungs (B) of mice ($n = 3$ per time point) after i.n. administration of CFI or oral administration of ciprofloxacin or doxycycline. All compounds were given at a dose of 50 mg/kg. Values are means \pm standard errors.

2 $\mu\text{g}/\text{ml}$ (14, 33). Treatment of chronic Q fever endocarditis with doxycycline alone resulted in $>50\%$ mortality and frequent relapse and requires the addition of alkalinization agents, such as hydroxychloroquine (7, 34). In addition, at least one doxycycline-resistant *C. burnetii* strain has been isolated from a patient who died following unsuccessful antibiotic treatment (6). Although ciprofloxacin is not commonly used to treat acute Q fever, it has been used to successfully treat Q fever endocarditis (35, 36). *In vitro*, the MIC of ciprofloxacin is slightly higher than the MIC of doxycycline (1 to 4 $\mu\text{g}/\text{ml}$), and resistance to fluoroquinolones has been observed in some clinical isolates of *C. burnetii* (14, 33, 36). To date, there is only one report evaluating antibiotic treatment in an animal model of Q fever (37). Therefore, the development of

novel methods to overcome resistance and improve treatment of Q fever is desirable.

In order to assess the efficacy of novel antibiotics against *C. burnetii in vivo*, an aerosol model of Q fever was established. There are several reported animal models of *C. burnetii* infection, using invertebrates, mice, guinea pigs, and nonhuman primates (38, 39). A/J mice have been previously shown to be the most susceptible immunocompetent mouse strain, and the aerosol route of infection is of relevance to the majority of human Q fever cases (40). The model is nonlethal, and therefore, five alternative parameters were used in order to monitor progression of disease, namely, weight loss, clinical signs, organ weight, bacterial burden, and histopathology. Weight loss and clinical signs were used as key indicators of disease severity, as all infected mice showed significant weight loss and reproducible clinical signs, such as piloerection and arched backs. These signs resolve, in the absence of treatment, within 14 days of infection, which is a similar length of time to resolution of acute disease in human Q fever cases (32). The lungs and spleen were selected for monitoring, as both exhibited a significant increase in weight and high levels of bacteria throughout the course of *C. burnetii* infection. In addition, these organs are of particular relevance, as the lungs are the foci of infection following an aerosol challenge, and the spleen may provide an indication of the extent of dissemination of the bacteria during a systemic infection.

Using this murine model, we report for the first time that doxycycline acts to delay the onset of body weight loss, reduce clinical signs, and reduce pathology associated with Q fever. However, following the cessation of doxycycline treatment, infected mice still succumb to infection. This is unlikely to be due to toxicity of oral doxycycline and instead may be due to relapse of infection due to suboptimal antibiotic treatment. A possible reason for this is that A/J mice are deficient in C5 complement and subsequently may not be able to clear the infection. Alternatively, this could be attributed to the antibiotic mechanism of action, with doxycycline having a bacteriostatic mode of action that may also explain why relapse is often observed in Q fever patients, in particular associated with cessation of the antibiotic regime (7). We have also confirmed that, when given by the oral route, ciprofloxacin is not an appropriate treatment for acute Q fever. However, we have identified a novel, encapsulated formulation of ciprofloxacin, specifically designed for inhalation that enables pulmonary delivery into the lung, which significantly improves efficacy in a mouse model of *C. burnetii* infection. Mice treated with CFI exhibit significantly reduced, rather than delayed, body weight loss through-

TABLE 2 Pharmacokinetic parameters in mice for intranasal CFI or oral ciprofloxacin or doxycycline^a

Antibiotic	Formulation	Route	Sampling site	Terminal half-life (h)	Clearance (g/h/kg or liter/h/kg) ^b	C_{max} ($\mu\text{g}/\text{ml}$)	T_{max} (h)	AUC_{0-24} ($\mu\text{g} \cdot \text{h}/\text{ml}$) ^c
Doxycycline	PBS vehicle	Oral	Lung	3.6	1,015	6.4	2	43.6
			Plasma	3.5	2.1	3.4	2	21.3
Ciprofloxacin	PBS vehicle	Oral	Lung	0.8	14,500	3.0	0.17	4.9
			Plasma	1.3	25.4	1.4	0.5	2.4
	CFI	i.n.	Lung	4.1	131	483	2	3,461
			Plasma	2.2	8.5	1.7	0.017	6.5

^a All antibiotic doses were 50 mg/kg. Values are means for three individual animals per time point.

^b Clearance is shown in grams/hour/kilogram for the lung and in liters/hour/kilogram for plasma.

^c AUC_{0-24} , area under the concentration-time curve from 0 h to the last measurable concentration.

out the course of the study compared to mice treated with doxycycline or with PBS (control).

Other *in vivo* studies have demonstrated the broad-spectrum antibiotic activity of CFI. It is highly efficacious against several intracellular pathogens, specifically *F. tularensis* LVS and Schu S4 strains (22) and *Y. pestis* CO92 strain (K. A. Hamblin, J. D. Blanchard, C. Davies, and S. V. Harding, presented at the 19th Congress of the International Society of Aerosols in Medicine, April 2013, Chapel Hill, NC), with only a single dose being needed to provide full protection against all three pathogens in mouse models of lung infection. This formulation is also very efficacious against the extracellular pathogen *Pseudomonas aeruginosa* and has completed multiple phase 2 clinical trials for infection in cystic fibrosis and non-cystic fibrosis bronchiectasis patients (41, 42).

Encapsulation of drugs in liposomes has been shown to be effective for the pulmonary delivery of various therapeutic agents, including antibiotics (11, 19, 43, 44). Liposomes are taken up by phagocytic cells, improving delivery of antibiotics into the primary site of infection for facultative intracellular pathogens, such as *C. burnetii* (45). *In vivo*, *C. burnetii* multiplies in monocytes within an acidic vacuole, and most antibiotics, including doxycycline and ciprofloxacin, exhibit reduced activity in such a low-pH environment (46, 47). Encapsulation of antibiotics enhances intracellular uptake and subsequent accumulation to higher therapeutic levels within the intracellular site of infection. Inhaled liposomally encapsulated antibiotics can be a particularly attractive means to provide high sustained concentrations at the sites of action within the respiratory tract, reducing local side effects and systemic exposure and providing more convenient therapy such as once-daily dosing (11) and smaller number of total doses administered for prophylaxis or treatment as shown in this paper and previous studies with CFI (22).

As shown in this study, in addition to improving uptake into cells, encapsulation of ciprofloxacin allows effective delivery by the *i.n.* route, resulting in high initial concentrations of antibiotic in the lungs. This is demonstrated by the C_{max} for CFI in the lungs, which is 100-fold higher than for free ciprofloxacin or doxycycline. Previous studies have also shown that free ciprofloxacin is ineffective when delivered by the *i.n.* or aerosol route, whereas liposome-encapsulated ciprofloxacin, which is specifically developed for inhalational delivery, has been shown to be efficacious at 50 mg/kg (19, 21). This is because unencapsulated ciprofloxacin is rapidly absorbed and cleared from the lungs (19, 21). The enhanced therapeutic efficacy of CFI can therefore be partly attributed to the increased initial retained dose of antibiotic in the lungs (21). This property is particularly important for the treatment of diseases such as Q fever, where the initial site of infection is the lung. We have shown that treatment with CFI also improves the overall exposure within the lungs over a 24-h period, as demonstrated by the increased area under the curve (AUC) (~1,000-fold) compared to free ciprofloxacin. Delivery of ciprofloxacin in a liposome results in a sustained release of antibiotics, indicated by a prolonged half-life both in the lungs and in plasma. In addition, the bioavailability of ciprofloxacin in the lungs was improved by 99.9% when delivered in the encapsulated formulation compared to oral ciprofloxacin.

We also evaluated the effect of length of antibiotic treatment on outcome of disease. The length of treatment with doxycycline correlates with a delay in body weight loss and clinical signs. However, the length of treatment with CFI correlates with overall prog-

nosis of disease, with mice receiving 7 days treatment exhibiting minimal weight loss and no clinical signs. This result, taken together with the use of a single daily dose of CFI compared to a twice-daily dose of doxycycline, indicates that fewer doses of CFI may be required to treat Q fever. The CDC currently recommends 100 mg of doxycycline, given orally, twice daily for 14 days for treating acute Q fever. The efficacy of doxycycline has been correlated with the AUC pharmacokinetic parameter (48). Published average human AUCs for plasma following 100-mg oral dose of doxycycline range from 13 to 40 mg · h/liter (49). The selected doxycycline dose in the AJ mouse model, 50 mg/kg, results in an average plasma AUC within this range (21.3 mg · h/liter). The differences observed in organ weight and bacterial burden between doxycycline- and CFI-treated mice were less marked. Both antibiotics did not significantly reduce lung or spleen organ weight compared to the PBS-treated control mice; in fact, treatment with doxycycline appeared to increase bacterial numbers within organs compared to the PBS-treated control mice. This finding may be due to using RT-PCR to detect residual bacterial DNA in the organs. An alternative method to enumerate viable bacteria would be to plate organ homogenates onto ACCM-2 agarose (23).

In conclusion, our study demonstrates that liposome encapsulation of ciprofloxacin allows effective pulmonary delivery and improves efficacy of an alternative antibiotic against *C. burnetii* infection. Furthermore, we report that treatment of infected mice with encapsulated ciprofloxacin shows significant improvements over doxycycline, the current treatment for Q fever. We have developed an animal model suitable for testing novel antibiotic therapies, which will allow evaluation and progression of next-generation antimicrobial treatments against Q fever.

ACKNOWLEDGMENTS

We acknowledge Tom Laws for assistance with statistical analysis and Geoff Pearson and Igor Gonda for critical reviewing the manuscript. We thank the Biological Investigations Group at Public Health England (PHE) for conducting the animal procedures and also Melanie Davison, Simon Bate, and Gemma McLuckie for technical assistance.

This work was funded by the United Kingdom Ministry of Defense. J.D.B. is an employee of and owns stock in Aradigm Corporation, which produces the liposome-encapsulated ciprofloxacin for inhalation (CFI) formulation that was tested. He is also a coinventor on Aradigm patents on inhaled formulations involving CFI, though not CFI alone.

REFERENCES

- Hilbink F, Penrose M, Kovacova E, Kazar J. 1993. Q fever is absent from Zealand. *Int. J. Epidemiol.* 22:945–949. <http://dx.doi.org/10.1093/ije/22.5.945>.
- Moodie CE, Thompson HA, Meltzer MI, Swerdlow DL. 2008. Prophylaxis after exposure to *Coxiella burnetii*. *Emerg. Infect. Dis.* 14:1558–1566. <http://dx.doi.org/10.3201/eid1410.080576>.
- Faix DJ, Harrison DJ, Riddle MS, Vaughn AF, Yingst SL, Earhart K, Thibault G. 2008. Outbreak of Q fever among US military in western Iraq, June–July 2005. *Clin. Infect. Dis.* 46:e65–e68. <http://dx.doi.org/10.1086/528866>.
- Bailey MS, Trinick TR, Dunbar JA, Hatch R, Osborne JC, Brooks TJ, Green AD. 2011. Undifferentiated febrile illnesses amongst British troops in Helmand, Afghanistan. *J. R. Army Med. Corps* 157:150–155. <http://dx.doi.org/10.1136/jramc-157-02-05>.
- Fournier PE, Marrie TJ, Raoult D. 1998. Diagnosis of Q fever. *J. Clin. Microbiol.* 36:1823–1834.
- Brouqui P, Dupont HT, Drancourt M, Berland Y, Etienne J, Lepout C, Goldstein F, Massip P, Micoud M, Bertrand A, Raoult D. 1993. Chronic Q fever. Ninety-two cases from France, including 27 cases without endocarditis. *Arch. Intern. Med.* 153:642–648.
- Raoult D, Houpiqian P, Dupont H, Riss J, Arditi-Djiane JJ, Brouqui P.

1999. Treatment of Q fever endocarditis: comparison of 2 regimens containing doxycycline and ofloxacin or hydroxychloroquine. *Arch. Intern. Med.* 159:167–173. <http://dx.doi.org/10.1001/archinte.159.2.167>.
8. Million M, Thuny F, Richet H, Raoult D. 2010. Long-term outcome of Q fever endocarditis: a 26-year personal survey. *Lancet Infect. Dis.* 10: 527–535. [http://dx.doi.org/10.1016/S1473-3099\(10\)70135-3](http://dx.doi.org/10.1016/S1473-3099(10)70135-3).
9. Rouli L, Rolain JM, El Filali A, Robert C, Raoult D. 2012. Genome sequence of *Coxiella burnetii* 109, a doxycycline-resistant clinical isolate. *J. Bacteriol.* 194:6939. <http://dx.doi.org/10.1128/JB.01856-12>.
10. Allison SD. 2007. Liposomal drug delivery. *J. Infus. Nurs.* 30:89–120. <http://dx.doi.org/10.1097/01.NAN.0000264712.26219.67>.
11. Cipolla D, Gonda I, Chan HK. 2013. Liposomal formulations for inhalation. *Ther. Deliv.* 4:1047–1072. <http://dx.doi.org/10.4155/tde.13.71>.
12. Gay JD, Deyoung DR, Roberts GD. 1984. In vitro activities of norfloxacin and ciprofloxacin against *Mycobacterium tuberculosis*, *M. avium* complex, *M. chelonae*, *M. fortuitum*, and *M. kansasii*. *Antimicrob. Agents Chemother.* 26:94–96. <http://dx.doi.org/10.1128/AAC.26.1.94>.
13. Gaunt PN. 1988. Ciprofloxacin vs ceftriaxone for eradication of meningococcal carriage. *Lancet* 2:218–219.
14. Gikas A, Spyridaki I, Psaroulaki A, Kofferithis D, Tselentis Y. 1998. In vitro susceptibility of *Coxiella burnetii* to trovafloxacin in comparison with susceptibilities to pefloxacin, ciprofloxacin, ofloxacin, doxycycline, and clarithromycin. *Antimicrob. Agents Chemother.* 42:2747–2748.
15. Bergogne-Berezin E. 1993. Interpretation of pharmacologic data in respiratory tract infections. *Int. J. Antimicrob. Agents* 3(Suppl 1):S3–S14. [http://dx.doi.org/10.1016/0924-8579\(93\)90030-9](http://dx.doi.org/10.1016/0924-8579(93)90030-9).
16. Campos J, Roman F, Georgiou M, Garcia C, Gomez-Lus R, Canton R, Escobar H, Baquero F. 1996. Long-term persistence of ciprofloxacin-resistant *Haemophilus influenzae* in patients with cystic fibrosis. *J. Infect. Dis.* 174:1345–1347. <http://dx.doi.org/10.1093/infdis/174.6.1345>.
17. Grimaldo ER, Tupasi TE, Rivera AB, Quelapio MID, Cardano RC, Derilo JO, Belen VA. 2001. Increased resistance to ciprofloxacin and ofloxacin in multidrug-resistant *Mycobacterium tuberculosis* isolates from patients seen at a tertiary hospital in the Philippines. *Int. J. Tuberc. Lung Dis.* 5:546–550.
18. Oh YK, Nix DE, Straubinger RM. 1995. Formulation and efficacy of liposome-encapsulated antibiotics for therapy of intracellular *Mycobacterium avium* infection. *Antimicrob. Agents Chemother.* 39:2104–2111. <http://dx.doi.org/10.1128/AAC.39.9.2104>.
19. Conley J, Yang HM, Wilson T, Blasetti K, DiNunno V, Schnell G, Wong JP. 1997. Aerosol delivery of liposome-encapsulated ciprofloxacin: aerosol characterization and efficacy against *Francisella tularensis* infection in mice. *Antimicrob. Agents Chemother.* 41:1288–1292.
20. Ellbogen MH, Olsen KM, Gentry-Nielsen MJ, Preheim LC. 2003. Efficacy of liposome-encapsulated ciprofloxacin compared with ciprofloxacin and ceftriaxone in a rat model of pneumococcal pneumonia. *J. Antimicrob. Chemother.* 51:83–91. <http://dx.doi.org/10.1093/jac/dkg024>.
21. Wong JP, Yang HM, Blasetti KL, Schnell G, Conley J, Schofield LN. 2003. Liposome delivery of ciprofloxacin against intracellular *Francisella tularensis* infection. *J. Control. Release* 92:265–273. [http://dx.doi.org/10.1016/S0168-3659\(03\)00358-4](http://dx.doi.org/10.1016/S0168-3659(03)00358-4).
22. Hamblin KA, Armstrong SJ, Barnes KB, Davies C, Wong JP, Blanchard JD, Harding SV, Simpson AJH, Atkins HS. 17 March 2014. Liposome encapsulation of ciprofloxacin improves protection against highly virulent *Francisella tularensis* Schu S4 strain. *Antimicrob. Agents Chemother.* <http://dx.doi.org/10.1128/AAC.02555-13>.
23. Omsland A, Beare PA, Hill J, Cockrell DC, Howe D, Hansen B, Samuel JE, Heinzen RA. 2011. Isolation from animal tissue and genetic transformation of *Coxiella burnetii* are facilitated by an improved axenic growth medium. *Appl. Environ. Microbiol.* 77:3720–3725. <http://dx.doi.org/10.1128/AEM.02826-10>.
24. European Committee for Standardization. 2000. Biotechnology – performance criteria for microbiological safety cabinets. European standard EN 12469. European Committee for Standardization, Brussels, Belgium.
25. National Science Advisory Board for Biosecurity. 2007. Proposed framework for the oversight of dual use life sciences research: strategies for minimizing the potential misuse of research information. A report of the National Science Advisory Board for Biosecurity (NSABB). National Science Advisory Board for Biosecurity, Office of Biotechnology Activities, Office of Science Policy, Office of the Director, National Institutes of Health, Bethesda, MD.
26. United Kingdom Act of Parliament. 1986. Animals (Scientific Procedures) Act 1986. Her Majesty's Stationery Office, London, United Kingdom.
27. United Kingdom Home Office. 1989. Code of practice for the housing and care of animals used in scientific procedures. Home Office Animals (Scientific Procedures) Act 1986. Her Majesty's Stationery Office, London, United Kingdom.
28. Guyton AC. 1947. Measurement of the respiratory minute volume of laboratory animals. *Am. J. Physiol.* 150:70–77.
29. Rowland M, Tozer TM. 2010. Clinical pharmacokinetics and pharmacodynamics: concepts and applications. Lippincott Williams and Wilkins, Philadelphia, PA.
30. Taylor JR. 1997. An introduction to error analysis: the study of uncertainties in physical measurements. University Science Books, Sausalito, CA.
31. Whithy M, Ruff TA, Street AC, Fenner FJ. 2002. Biological agents as weapons 2: anthrax and plague. *Med. J. Aust.* 176:605–608.
32. Maurin M, Raoult D. 1999. Q fever. *Clin. Microbiol. Rev.* 12:518–553.
33. Lever MS, Bewley KR, Dowsett B, Lloyd G. 2004. In vitro susceptibility of *Coxiella burnetii* to azithromycin, doxycycline, ciprofloxacin and a range of newer fluoroquinolones. *Int. J. Antimicrob. Agents* 24:194–196. <http://dx.doi.org/10.1016/j.ijantimicag.2004.05.001>.
34. Rolain JM, Gouriet F, Brouqui P, Larrey D, Janbon F, Vene S, Jarnestrom V, Raoult D. 2005. Concomitant or consecutive infection with *Coxiella burnetii* and tickborne diseases. *Clin. Infect. Dis.* 40:82–88. <http://dx.doi.org/10.1086/426440>.
35. Yebra M, Ortigosa J, Albarran F, Crespo MG. 1990. Ciprofloxacin in a case of Q fever endocarditis. *N. Engl. J. Med.* 323:614. <http://dx.doi.org/10.1056/NEJM199008303230916>.
36. Zekanovic D, Morovic M, Borcilo MN, Rode OD. 2010. First case of Q fever endocarditis in Croatia and a short review. *Coll. Antropol.* 34:1135–1137.
37. Huebner RJ, Hottle GA, Robinson EB. 1948. Action of streptomycin in experimental infection with Q fever. *Public Health Rep.* 63:357–362. <http://dx.doi.org/10.2307/4586483>.
38. Bewley KR. 2013. Animal models of Q fever (*Coxiella burnetii*). *Comp. Med.* 63:469–476.
39. Norville IH, Hartley MG, Martinez E, Cantet F, Bonazzi M, Atkins TP. 27 March 2014. *Galleria mellonella* as an alternative model of *Coxiella burnetii* infection. *Microbiology* <http://dx.doi.org/10.1099/mic.0.077230-0>.
40. Scott GH, Williams JC, Stephenson EH. 1987. Animal models in Q fever: pathological responses of inbred mice to phase I *Coxiella burnetii*. *J. Gen. Microbiol.* 133:691–700.
41. Bruinenberg P, Blanchard DJ, Cipolla D, Dayton F, Mudumba S, Gonda I. 2010. Inhaled liposomal ciprofloxacin: once a day management of respiratory infections. *Proc. Respir. Drug Deliv.* 2010 1:73–82.
42. Serisier D. 2012. Inhaled antibiotics for lower respiratory tract infections: focus on ciprofloxacin. *Drugs Today* 48:339–351. <http://dx.doi.org/10.1358/dot.2012.48.5.1789474>.
43. Fountain MW, Weiss SJ, Fountain AG, Shen A, Lenk RP. 1985. Treatment of *Brucella canis* and *Brucella abortus* in vitro and in vivo by stable plurilamellar vesicle-encapsulated aminoglycosides. *J. Infect. Dis.* 152: 529–535. <http://dx.doi.org/10.1093/infdis/152.3.529>.
44. Nightingale SD, Saletan SL, Swenson CE, Lawrence AJ, Watson DA, Palkiewicz FG, Silverman EG, Cal SX. 1993. Liposome-encapsulated gentamicin treatment of *Mycobacterium avium-Mycobacterium intracellulare* complex bacteremia in AIDS patients. *Antimicrob. Agents Chemother.* 37:1869–1872. <http://dx.doi.org/10.1128/AAC.37.9.1869>.
45. Pinto-Alphandary H, Andreumont A, Couvreur P. 2000. Targeted delivery of antibiotics using liposomes and nanoparticles: research and applications. *Int. J. Antimicrob. Agents* 13:155–168. [http://dx.doi.org/10.1016/S0924-8579\(99\)00121-1](http://dx.doi.org/10.1016/S0924-8579(99)00121-1).
46. Maurin M, Benoliel AM, Bongrand P, Raoult D. 1992. Phagolysosomes of *Coxiella burnetii*-infected cell lines maintain an acidic pH during persistent infection. *Infect. Immun.* 60:5013–5016.
47. Carryn S, Chanteux H, Seral C, Mingeot-Leclercq MP, Van Bambeke F, Tulkens PM. 2003. Intracellular pharmacodynamics of antibiotics. *Infect. Dis. Clin. North Am.* 17:615–634. [http://dx.doi.org/10.1016/S0891-5520\(03\)00066-7](http://dx.doi.org/10.1016/S0891-5520(03)00066-7).
48. Agwuh KN, Macgowan A. 2006. Pharmacokinetics and pharmacodynamics of the tetracyclines including glycylicyclines. *J. Antimicrob. Chemother.* 58:256–265. <http://dx.doi.org/10.1093/jac/dkl224>.
49. Craig WA. 2002. Pharmacodynamics of antimicrobials: general concepts and applications, p 1–22. In Nightingale CH, Murakawa T, Ambrose PG (ed), *Antimicrobial pharmacodynamics in theory and clinical practice*. Marcel Dekker, Oxford, United Kingdom.

Original article

NEGUS, D., VIPOND, J., HATCH, G. J., RAYNER, E. L. & TAYLOR, P. W. 2015. Parenteral administration of capsule depolymerase EnvD prevents lethal inhalation anthrax infection. *Antimicrob Agents Chemother*, 59, 7687-92.

Impact factor: 4.715

Contributions by HATCH, G. J.

Home Office – Personal Licence holder

Development and qualification of aerosol, biocontainment and clinical parameter systems. Performance of aerosol challenge.

Study management – Study design, liaison and co-ordination with sponsor, bacteriology histology and in vivo teams, scheduling, reporting

Data analysis and manuscript review

Citation metrics

Google Scholar: 5 citations

Parenteral Administration of Capsule Depolymerase EnvD Prevents Lethal Inhalation Anthrax Infection

David Negus,^a Julia Vipond,^b Graham J. Hatch,^b Emma L. Rayner,^b Peter W. Taylor^a

School of Pharmacy, University College London, London, United Kingdom^a; Public Health England, Porton Down, Salisbury, United Kingdom^b

Left untreated, inhalation anthrax is usually fatal. Vegetative forms of *Bacillus anthracis* survive in blood and tissues during infection due to elaboration of a protective poly- γ -D-glutamic acid (PDGA) capsule that permits uncontrolled bacterial growth *in vivo*, eventually leading to overwhelming bacillosis and death. As a measure to counter threats from multidrug-resistant strains, we are evaluating the prophylactic and therapeutic potential of the PDGA depolymerase EnvD, a stable and potent enzyme which rapidly and selectively removes the capsule from the surface of vegetative cells. Repeated intravenous administration of 10 mg/kg recombinant EnvD (rEnvD) to mice infected with lethal doses of *B. anthracis* Ames spores by inhalation prevented the emergence of symptoms of anthrax and death; all animals survived the 5-day treatment period, and 70% survived to the end of the 14-day observation period. In contrast to results in sham-treated animals, the lungs and spleen of rEnvD-dosed animals were free of gross pathological changes. We conclude that rEnvD has potential as an agent to prevent the emergence of inhalation anthrax in infected animals and is likely to be effective against drug-resistant forms of the pathogen.

Bacillus anthracis featured in offensive weapons programs in the United States and former Soviet Union during the last century (1) and has been identified by the World Health Organization, the United Nations, and the Working Group on Civilian Defense (WGCB) as a pathogen of great concern. The WGCB has highlighted a limited number of microorganisms that could cause infections in sufficient numbers to cripple a city or region, and *B. anthracis* is one of the most serious of such threat agents (2). The bacteria's spores are able to survive in hostile environments for many decades and, in aerosolized form, can travel significant distances on prevailing winds, disseminating over a wide area. Accidental release of anthrax spores as an aerosol from a military facility in Sverdlovsk in 1979 resulted in at least 79 cases of anthrax and 68 deaths, demonstrating the bacteria's lethal potential (3). These traits define *B. anthracis* as a potential threat agent, attractive to both rogue states and terrorist groups, and a cause of human and animal disease globally. The vegetative bacilli release toxin complexes that cause hemorrhage, edema, and necrosis and are protected from host innate defenses by a capsule comprised of poly- γ -D-glutamic acid (PDGA) (4). In inhalation anthrax, endospores gain access to the alveolar spaces and are ingested by macrophages; they are then transported to regional lymph nodes where spore germination occurs after a variable period of dormancy (4, 5). Toxin-mediated clinical symptoms typically arise soon after the onset of rapid bacillary growth (2).

Effective treatment requires prompt and aggressive antibiotic therapy; a fluoroquinolone and an agent that inhibits protein synthesis such as linezolid are currently recommended by the Centers for Disease Control and Prevention (6). The consensus approach to prophylaxis and treatment of inhalation anthrax could be compromised by the release of *B. anthracis* carrying engineered antibiotic resistance genes, and occasional reports have emerged of naturally occurring strains resistant to currently useful antibiotics (7, 8). Clearly, new agents or novel therapeutic and prophylactic modalities should be developed as a part of a comprehensive preparedness strategy. We previously demonstrated that parenteral administration of a capsule depolymerase with the capacity to rapidly and selectively remove the protective capsule from the

bacterial surface can resolve potentially lethal *Escherichia coli* infection in the neonatal rat (9, 10). Systemic anthrax is an attractive candidate for this approach as infections are attributable to a single, phylogenetically homogeneous bacterial species, all strains elaborate the unique PDGA capsule essential for pathogenesis (11), and hydrolysis of the outermost layer of the bacilli would confound attempts to circumvent antibiotic chemotherapy by the introduction of antibiotic resistance genes into *B. anthracis*. Here, we report that early intravenous administration of recombinant EnvD (rEnvD), a recombinant PDGA hydrolase elaborated by a consortium culture of soil bacteria, is able to prevent anthrax in mice infected by the inhalation route.

MATERIALS AND METHODS

Bacteria. *B. anthracis* Ames (NR-2324/pXO1⁺/pXO2⁺) was obtained from the Biodefense and Emerging Infections Research Resources Repository (Manassas, VA). Spores were prepared by fed batch culture in a 2-liter bioreactor for 26 h at 37°C with stirring at 400 rpm, collected by centrifugation, and washed in sterile distilled water. For spore challenge tests, suspensions (8×10^9 CFU/ml) were prepared in sterile water. *Bacillus licheniformis* ATCC 9945a was purchased from the American Type Culture Collection and grown in medium E containing 615 μ M MnSO₄ in an orbital incubator (200 orbits/min) at 37°C (12).

Recombinant EnvD. The enzyme was expressed, refolded, and purified as described previously (12). Endotoxin was removed using Proteus Endotoxin Removal columns (Abd Serotec, Oxford, United Kingdom), and removal was confirmed with a Pierce LAL (*Limulus* amoebocyte lysate) Chromogenic Endotoxin Quantitation kit (Thermo Fisher, Rockford,

Received 7 July 2015. Returned for modification 4 August 2015.

Accepted 20 September 2015.

Accepted manuscript posted online 5 October 2015.

Citation: Negus D, Vipond J, Hatch GJ, Rayner EL, Taylor PW. 2015. Parenteral administration of capsule depolymerase EnvD prevents lethal inhalation anthrax infection. *Antimicrob Agents Chemother* 59:7687–7692. doi:10.1128/AAC.01547-15.

Address correspondence to Peter W. Taylor, peter.taylor@ucl.ac.uk.

Copyright © 2015, American Society for Microbiology. All Rights Reserved.

USA). Purified rEnvD was stored in 20 mM Tris (pH 8.5) at -20°C until required.

Impact of rEnvD on bacterial viability. A culture (50 ml) from a single, heavily mucoid colony of *B. licheniformis* 9945a was grown to an optical density at 600 nm (OD_{600}) of 0.6 and examined by light microscopy to ensure that only vegetative bacilli were present. Two aliquots of 1 ml were removed, and rEnvD was added to one aliquot to give a final protein concentration of 1 $\mu\text{g}/\text{ml}$. An equal volume of phosphate-buffered saline (PBS) was added to the second aliquot. Both samples were incubated at 37°C for 15 min, serially diluted in PBS, and plated onto Luria-Bertani agar. Plates were incubated at 37°C for 16 h, and bacteria were enumerated.

Stability of rEnvD in serum. Aliquots of rEnvD (final concentration of 100 nM in 1.6-ml Eppendorf tubes) were incubated at 37°C in serum from BALB/c mice (total volume, 200 μl ; Sigma) for up to 24 h, and EnvD activity was determined at regular intervals by Förster resonance energy transfer (FRET) utilizing the fluorescently labeled synthetic peptide substrate 5-FAM-(D-Glu- γ -K(QXL520)-NH₂) (where FAM is 6-carboxyfluorescein) as previously described (12). Two tubes were used for each time point to provide duplicate readings. In some experiments heat-inactivated (56°C for 30 min) serum was used, and some assays were conducted in the presence of Roche complete protease inhibitor cocktail (Roche, Basel, Switzerland) at concentrations specified by manufacturer's guidelines.

Serum half-life ($t_{1/2}$). Pairs of female adult BALB/c mice were dosed with 10 mg/kg rEnvD in 180 μl of 20 mM Tris, pH 8.5, by tail vein injection. Paired animals were sacrificed over a 24-h period, blood was withdrawn by cardiac puncture, and serum was obtained. Serum was diluted 2-fold with 0.1 M Tricine and 0.1% CHAPS (3-[(3-cholamidopropyl)-dimethylammonio]-1-propanesulfonate), pH 8.5, to a final volume of 200 μl , and 100 μl was transferred to each well of a black 96-well microtiter plate. All assays were run in duplicate. rEnvD activity was measured using the FRET assay described above with the exception that fluorescence was measured over a 4-min period. The concentration of enzyme in each sample was determined using a standard curve prepared in mouse serum. The area under the curve (AUC) was calculated by GraphPad Prism (GraphPad Software Inc., La Jolla, CA) using the trapezoid rule.

Infection of mice with *B. anthracis*. All animal studies were carried out in accordance with the United Kingdom's Animals (Scientific Procedures) Act 1986 and the Codes of Practice for the Housing and Care of Animals used in Scientific Procedures 1989, following approval by the local ethical committee and the United Kingdom's Home Office. Female BALB/c mice (minimum age, 10 weeks; approximate body weight, 20 g; food and water available *ad libitum*) were obtained from Charles River (Canterbury, United Kingdom) and infected by aerosol (13). Groups of 10 mice were challenged with 10 to 50 minimum lethal doses (50% lethal dose [LD_{50}], 6×10^4 CFU; presented dose, $\sim 1.45 \times 10^6$ CFU) of *B. anthracis* spores with an AeroMP-Henderson apparatus. The challenge aerosol was generated using a six-jet Collision Nebulizer (BGI, Inc., Waltham, MA); the aerosol was mixed with conditioned air in the spray tube and delivered to the nose of each animal through an exposure tube in which nonanesthetized mice were held in restraint tubes. Samples of the aerosol were obtained with an AGI30 glass impinger (Ace Glass, Inc., Vineland, NJ), and the mean particle size was determined with an aerodynamic particle sizer (TSI Instruments, Ltd., High Wycombe, United Kingdom). These processes were controlled and monitored from an AeroMP management platform (Biaera Technologies, Hagerstown, MD). All-glass impinger samples were titrated by serial dilution and plated on Trypticase soy agar prior to incubation at 37°C for 16 to 24 h.

Intravenous (i.v.) administration of rEnvD was initiated 12 h after spore challenge. The dosing regimen was guided by the stability of the enzyme in commercial mouse serum and by the rate of clearance of rEnvD from the circulation of adult female BALB/c mice. Each mouse received rEnvD (0.5 to 10 mg/kg) by injection at regular intervals up to 120 h after spore challenge; groups were comprised of 10 individual animals. Control

mice received i.v. injections of PBS (180 μl) at these time points. Additional groups of 10 mice received oral doses of ciprofloxacin (118 mg/kg every 12 h for 14 days). Animals were monitored and assigned a clinical score at least twice daily up to 14 days after spore challenge and at least four times daily during critical periods (13). Clinical scores were based on severity of symptoms (ruffled fur, closed eyes, arched back, immobility, and weight loss). Animals surpassing a threshold score were euthanized humanely by pentobarbital overdose. Surviving mice from each group were euthanized at day 14 after challenge. *Postmortem*, blood, lung, and spleen samples were taken for enumeration of bacterial load, as follows: tissues were weighed and homogenized in sterile water using a Precellys 24 tissue homogenizer (Bertin Technologies, Villeurbanne, France), the homogenates were serially diluted in sterile water and plated onto Trypticase soy agar, and the plates were incubated at 37°C for 16 to 24 h before enumeration. Further lung and spleen samples were placed in 10% neutral buffered formalin for pathological evaluation. An additional group of 10 mice was employed to evaluate pathological changes 6 days after spore challenge; animals were culled 24 h after receiving their final dose of rEnvD on day 5, and blood and tissue samples were removed. A Kaplan-Meier log rank test was used to determine the significance of differences in survival between groups of animals, and GraphPad Prism software (GraphPad, La Jolla, CA, USA) was employed. For histological evaluation, formalin-fixed tissue samples were processed to paraffin wax, and 3- to 5- μm sections were cut and stained with hematoxylin and eosin. Sections were examined by light microscopy and evaluated subjectively. Slides were randomized by a third party before microscopic examination to avoid prior knowledge of group or treatment.

RESULTS

rEnvD is a promising candidate for *in vivo* attenuation of *B. anthracis* capsule expression. Unusually, *envD* resides on the genome of a strain of *Pseudomonas noertemannii*, but the enzyme is produced only when the bacteria are cocultured with a strain of *Pseudomonas fluorescens* (12, 14). rEnvD shows strong sequence homology to bacterial diene lactone hydrolases, and its enzymatic activity is restricted to the hydrolysis of γ -linkages in D- and L-glutamic acid-containing polymers (k_{cat} , 72.6 h^{-1} ; K_m , $0.65 \mu\text{M}$; k_{cat}/K_m , $3.08 \times 10^4 \text{ M}^{-1} \text{ s}^{-1}$ at 37°C). The enzyme retained enzymatic activity after accelerated storage at 37°C for 30 days and completely removed the capsule from *B. anthracis* Pasteur strain within 5 min at 37°C (12). Exposure of *Bacillus licheniformis* ATCC 9945a (induced to elaborate a PDGA polymer) to rEnvD resulted in rapid stripping of the capsule (12), but the viability of this surrogate strain was not significantly altered (2.5×10^8 to 2.9×10^9 CFU/ml over 15 min; $n = 6$; Student's t , $P > 0.05$).

There is limited capacity for repeated parenteral injections in small animals. To guide the design of dosing regimens for the administration of rEnvD to infected BALB/c mice, we determined the retention of depolymerase activity in mouse serum and the serum half-life ($t_{1/2}$) following intravenous (i.v.) administration. The reduction in rEnvD activity following incubation at 37°C in murine serum as determined by FRET assay (12) followed first-order kinetics, with a $t_{1/2}$ of 177 min (Fig. 1A); approximately 20% of activity remained after 8 h of incubation. Neither heat inactivation of serum nor the presence of protease inhibitors had any impact on the rate of reduction of activity. Elimination of rEnvD from the blood circulation of BALB/c mice was biphasic, with an initial rapid decrease in serum concentration (0.5 h to 1 h) followed by a slower elimination phase (2 h to 24 h) characteristic of first-order kinetics (Fig. 1B). This elimination profile is typical of agents administered by the intravenous route (15), with a rapid decrease in serum concentration due to distribution from the cen-

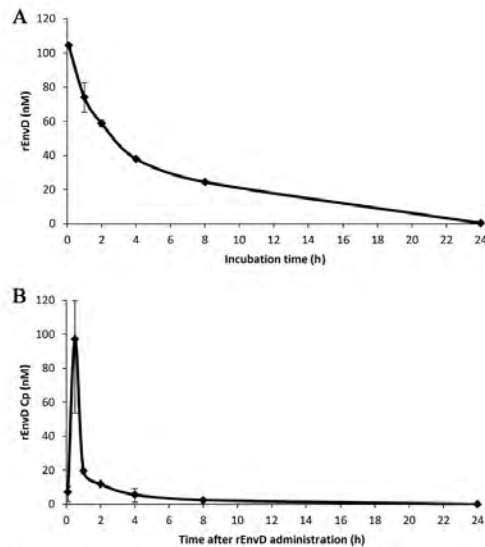


FIG 1 *In vitro* stability in serum and elimination of rEnvD from the circulation of BALB/c mice. (A) Stability of rEnvD in BALB/c mouse serum. Enzyme (100 nM) was incubated at 37°C in serum, and activity was determined by FRET assay (12). Enzyme activity in relative fluorescence units was converted to concentration of active enzyme by comparison to a standard curve. Error bars represent the range of three separate determinations; the $t_{1/2}$ in serum of rEnvD was 2.95 h (177 min). (B) rEnvD in serum obtained from mice intravenously dosed with 10 mg/kg rEnvD. Serum was obtained by terminal bleed, and enzyme activity was determined by FRET assay. Serum concentration (Cp) of rEnvD was obtained by comparison to a standard curve. Error bars represent the range of three separate determinations performed in duplicate. The half-life, $t_{1/2}$, was calculated by determination of the elimination rate constant (K_e) and transformation of data to the natural log (ln) to produce a line of best fit for each phase, with the slope equal to K_e ; $t_{1/2} = \ln(2)/K_e$. The $t_{1/2}$ was 0.22 h (13 min) for the initial alpha phase between 0.5 h and 1 h, and it was 2.71 h (163 min) for the beta phase between 2 h and 24 h.

tral circulation into the peripheral body tissues (alpha phase) followed by a gradual decrease in plasma concentration attributable to metabolism and excretion of the drug (beta phase). The AUC was determined as 118 nM · h/liter. Based on these data, we established a dosing regimen in which mice received rEnvD (0.5 to 10 mg/kg body weight) by i.v. injection 12 h, 24 h, 48 h, 72 h, 96 h, and 120 h after spore challenge.

rEnvD administration prevents inhalation anthrax in aerosol-challenged mice. Typically, all animals in the sham-treated (PBS) control groups met humane endpoints within 72 h (median time to death, 48 h), whereas all mice treated with 10 mg/kg of rEnvD survived the treatment period ($P < 0.0001$; log rank test) (Fig. 2A). Nine days after termination of treatment, 70% of rEnvD-treated mice had survived ($P < 0.0001$, compared to survival of control animals). The protective effect of rEnvD was reflected in the comparative health status of the mice: abnormal clinical signs were absent from rEnvD-treated animals during the 5-day period of enzyme administration (Fig. 2B). At 6 and 14 days postchallenge and in contrast to results in controls, bacteria were not cultured from the

blood or spleen of surviving rEnvD-treated mice from the group assigned for harvesting of tissues; sham-treated mice were found to carry a high *B. anthracis* bioburden in the blood (mean, 2.4×10^4 CFU/ml) and spleen (mean, 5.84×10^4 CFU/mg) at the time of *postmortem* examination (based on severity threshold score). High numbers of viable bacteria were also present in the lung of sham-treated animals at the same time point (mean, 1.37×10^5 CFU/mg). In comparison to levels in controls, a significant ($P = 0.006311$) reduction in the lung bioburden was noted in EnvD-treated animals 6 days after spore challenge (mean, 1.55×10^2 CFU/mg), and the bioburden was lower (mean, 2.07×10^1 CFU/mg) in the lung of surviving animals 14 days after challenge (Fig. 3).

Microscopic changes attributable to infection with *B. anthracis* were observed in the lung and spleen of all control animals. In the lung, prominent pulmonary congestion and patchy hemorrhage, expanding septal cavities, and numerous bacilli located in alveolar spaces, walls, and within vessel lumina (bacteremia) (Fig. 4A) were observed. In the spleen, numerous bacilli within the red pulp sinusoids and vascular lumina were present in the control animals (data not shown). Further, splenic white pulp contained prominent degeneration and loss of lymphocytes, characterized by nuclear fragmentation and cellular paucity. In contrast, animals receiving rEnvD and surviving until study endpoints were found to be clear of gross pathological changes, and bacilli were not visible within lung (Fig. 4B) or spleen tissue.

Experiments with 5 mg/kg rEnvD dosed over 3 days also demonstrated a high degree of protection from anthrax infection (100% survival at 3 days; 60% survival at 14 days), but 0.5 mg/kg rEnvD did not prevent the emergence of clinical symptoms and death. rEnvD administered for 5 days provided better protection than orally dosed ciprofloxacin administered by the oral route throughout the 14-day period (Fig. 2C and D).

DISCUSSION

This study provides clear evidence that prompt serial i.v. administration of small quantities of EnvD prevents the onset and progression of inhalation anthrax in a robust murine model of invasive disease. Even though the strain employed in this study is highly toxigenic, removal of the capsule during the early stages of infection appears sufficient to confound the pathogenic potential of the invading bacteria and further supports the key role of the protective PDGA capsule in anthrax pathogenesis (4, 11), highlighting the requisite nature of the capsule for *in vivo* dissemination of vegetative bacilli. The study also adds to growing evidence that prophylaxis and treatment of severe systemic infections can be realized by agents that do not kill the target bacterial population *per se* but modify the phenotype of the pathogen in a way that is beneficial to the host (16). Further, this approach has the potential to deliver exquisitely selective therapeutics that are unaffected by the presence of antibiotic resistance mechanisms.

Treatment of bacterial infections with capsule depolymerases was first explored over 80 years ago by Dubos, Avery, and colleagues at the Rockefeller Institute for Medical Research. They used an enzyme preparation from cultures of a peat soil bacterium to selectively remove the polysaccharide capsule, the pathogen's principle means of defense against immune attack, from the surface of type III pneumococci (17). Intraperitoneal administration of enzyme extracts to mice prior to challenge with type III pneumococci gave rise to type III-specific protection (18), and i.v. administration to rabbits with type III dermal infections resulted in

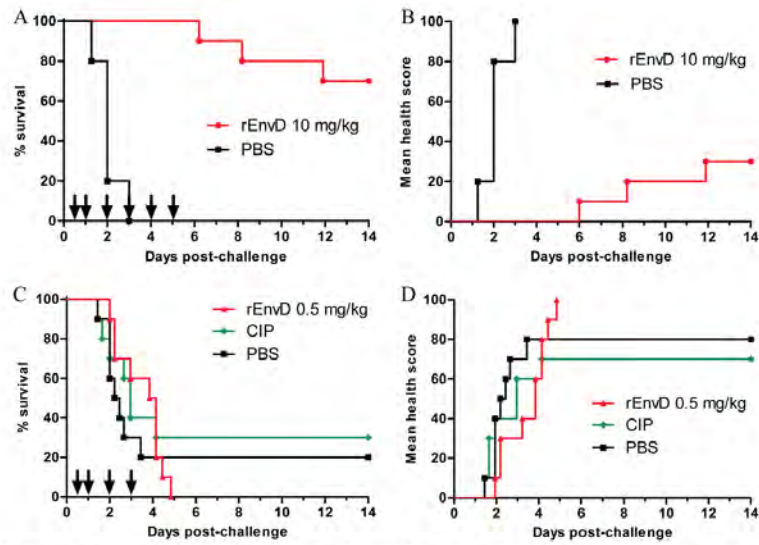


FIG 2 Impact of intravenous administration of rEnvD on inhalation anthrax in mice. Combined Kaplan-Meier survival plots (A and C) and cumulative mean clinical observation scores (B and D) for rEnvD-dosed, infected BALB/c mice. Mice were infected with *B. anthracis* Ames on day 0 by aerosol, followed by tail vein administration of either 10 mg/kg rEnvD or PBS vehicle (A and B) and of either 0.5 mg/kg rEnvD or PBS (C and D) at the times indicated by arrows. Ciprofloxacin (CIP; 118 mg/kg) was also administered orally for 14 days (C and D). Clinical observations were scored as described previously (13) and were based on severity of symptoms (ruffled fur, closed eyes, arched back, immobility, and weight loss).

early termination of the normally fatal infection (19). The enzyme also prevented dissemination, sterilized the blood, and promoted early recovery in nonhuman primates infected by the intratracheal and intrabronchial routes (20). In addition to our previous work on systemic neonatal *E. coli* infections (9, 10), capsule depolymerases have been shown to resolve potentially lethal experimental *Klebsiella pneumoniae* K1 infections in mice (21).

Recently, other attempts have been made to exploit PDGA depolymerases as antianthrax therapeutics. CapD is a γ -glutamyltranspeptidase elaborated by *B. anthracis* and catalyzes the attachment of PDGA to peptidoglycan, but it also functions as a depolymerase, effecting the release of diffusible PDGA fragments from the sur-

face of producer strains (22). CapD mediates removal of the capsule and induces macrophage uptake and neutrophil killing *in vitro* (23). Intraperitoneal coinjection of CapD and vegetative *B. anthracis* Ames bacteria afforded some protection against infection in mice, but no significant protection could be demonstrated when the enzyme was administered after challenge with Ames spores (24), almost certainly due to the labile nature of CapD (12, 20). rEnvD is a far more robust enzyme (12) and a better candidate for therapeutic development.

Current evidence suggests that although the toxin complex undoubtedly plays a vital role in anthrax pathogenesis, probably by suppression of the immune response in early stages of the disease,

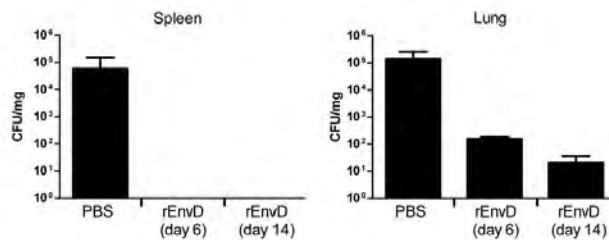


FIG 3 *B. anthracis* (CFU/mg tissue) in the spleen and lung of mice following rEnvD or PBS administration by the intravenous route ($n = 7$ to 10; values are means \pm 1 standard deviation). PBS controls were culled when the clinical score reached threshold levels as the animals were then close to death (13). Tissues were weighed and homogenized in sterile water, the homogenates were serially diluted in sterile water and plated onto Trypticase soy agar, and the plates were incubated at 37°C for 16 to 24 h.

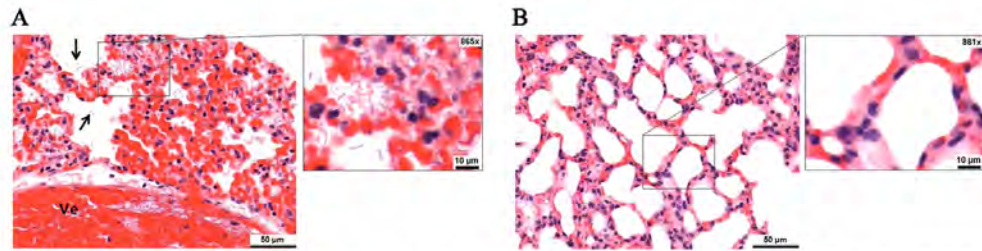


FIG 4 Pathology of lung tissue 6 days after inhalation of spores. Samples were fixed in 10% neutral buffered formalin, processed to paraffin wax, sectioned to 3 to 5 μm , stained with hematoxylin and eosin, and examined by light microscopy. Slides were randomized by a third party before microscopic examination to avoid prior knowledge of group or treatment. (A) Images from animals receiving only PBS vehicle. The region shows iatrogenic thickening of the alveolar walls due to the collapsed nature of the tissue. Arrows indicate bacilli located in alveolar spaces. Ve, vessel lumina. (B) Images from a region of inflated lung from animals receiving 10 mg/kg rEnvD over 5 days.

death occurs from overwhelming bacteremia and sepsis due to uncontrolled bacterial proliferation and release of proinflammatory mediators (25). Thus, a therapeutic window may be available if treatment is initiated before extensive bacterial division occurs in the blood. Our results support this hypothesis: depolymerase administration initiated 12 h after aerosol challenge provided significant protection against systemic anthrax and prevented bacteremia and dissemination of bacilli to the spleen. This finding concurs with that of a previous report that the capsule is essential for hematogenous bacillary spread as capsule-negative mutants did not migrate to the spleen in experimental infections (11). In the current study, deaths generally occurred following cessation of treatment. Viable bacteria were present in the lung of rEnvD-treated mice after the treatment period, and animals that subsequently succumbed to infection almost certainly died due to delayed germination of latent spores and after enzyme had been cleared from the blood circulation. *B. anthracis* spores are known to persist in the lung for extended periods. For example, latent spores have been isolated from the lung tissue of nonhuman primates months after initial exposure (26). The size of the mouse restricts the number of i.v. injections that can be given over a relatively short period of time, and this issue will be addressed using larger species, such as the rabbit. In addition, the mouse is particularly susceptible to death from systemic anthrax due to uncontrolled *in vivo* bacterial growth and a high quantitative level of bacteremia (27), factors which do not favor an anticapsule therapeutic strategy. The relative susceptibility of humans to toxemia and infection in anthrax is poorly documented; but the rabbit is used as an equivalent to human infection (27), and examination of rEnvD in this species will be an important next step.

ACKNOWLEDGMENTS

Funding was provided by a project grant GA2014-001R from the British Society for Antimicrobial Chemotherapy, Centre for Defence Enterprise contract DSTLX1000088481 from the Defence Science and Technology Laboratory, and project grant HFSE PoC-13-020 from UCL Business.

This work was supported by the National Institute for Health Research University College London Hospitals Biomedical Research Centre.

REFERENCES

- Leitenberg M, Zilinskas RA. 2012. The Soviet biological weapons program: a history. Harvard University Press, Cambridge, MA.
- Inglesby TV, O'Toole T, Henderson DA, Bartlett JG, Ascher MS, Eitzen

- Friedlander AM, Gerberding J, Hauer J, Hughes J, McDade J, Osterholm MT, Parker G, Perl TM, Russell PK, Tonat K. 2002. Anthrax as a biological weapon, 2002: updated recommendations for management. *JAMA* 287:2236–2252. <http://dx.doi.org/10.1001/jama.287.17.2236>.
- Meselson M, Guillemin J, Hugh-Jones M, Langmuir A, Popova I, Shelokov A, Yampolskaya O. 1994. The Sverdlovsk anthrax outbreak of 1979. *Science* 266:1202–1208. <http://dx.doi.org/10.1126/science.7973702>.
- Mock M, Fouet A. 2001. Anthrax. *Annu Rev Microbiol* 55:647–671. <http://dx.doi.org/10.1146/annurev.micro.55.1.647>.
- Lincoln R, Hodges DR, Klein F, Mahlandt BG, Jones WI, Jr, Haines BW, Rhian MA, Walker JS. 1965. Role of the lymphatics in the pathogenesis of anthrax. *J Infect Dis* 115:481–494. <http://dx.doi.org/10.1093/infdis/115.5.481>.
- Adalja AA, Toner E, Inglesby TV. 2015. Clinical management of potential bioterrorism-related conditions. *N Engl J Med* 372:954–962. <http://dx.doi.org/10.1056/NEJMr1409755>.
- Turnbull PCB, Sirianni NM, LeBron CI, Samaan MN, Sutton FN, Reyes AE, Peruski LF. 2004. MICs of selected antibiotics for *Bacillus anthracis*, *Bacillus cereus*, *Bacillus thuringiensis*, and *Bacillus mycoides* from a range of clinical and environmental sources as determined by the Etest. *J Clin Microbiol* 42:3626–3634. <http://dx.doi.org/10.1128/JCM.42.8.3626-3634.2004>.
- Ågren J, Finn M, Bengtsson B, Segerman B. 2014. Microevolution during an anthrax outbreak leading to clonal heterogeneity and penicillin resistance. *PLoS One* 9:e89112. <http://dx.doi.org/10.1371/journal.pone.0089112>.
- Mushtaq N, Redpath MB, Luzio JP, Taylor PW. 2004. Prevention and cure of systemic *Escherichia coli* K1 infection by modification of the bacterial phenotype. *Antimicrob Agents Chemother* 48:1503–1508. <http://dx.doi.org/10.1128/AAC.48.5.1503-1508.2004>.
- Mushtaq N, Redpath MB, Luzio JP, Taylor PW. 2005. Treatment of experimental *Escherichia coli* infection with recombinant bacteriophage-derived capsule depolymerase. *J Antimicrob Chemother* 56:160–165. <http://dx.doi.org/10.1093/jac/dki177>.
- Drysdale M, Heninger S, Hutt J, Chen Y, Lyons CR, Koehler TM. 2005. Capsule synthesis by *Bacillus anthracis* is required for dissemination in murine inhalation anthrax. *EMBO J* 24:221–227. <http://dx.doi.org/10.1038/sj.emboj.7600495>.
- Negus D, Taylor PW. 2014. A poly- γ -D-glutamic acid depolymerase that degrades the protective capsule of *Bacillus anthracis*. *Mol Microbiol* 91:1136–1147. <http://dx.doi.org/10.1111/mmi.12523>.
- Hatch GJ, Bate SR, Crook A, Jones N, Funnell SG, Vipond J. 2014. Efficacy testing of orally administered antibiotics against an inhalational *Bacillus anthracis* infection in BALB/c mice. *J Infect Dis Ther* 2:175.
- Stabler RA, Negus D, Pain A, Taylor PW. 2013. Draft genome sequences of *Pseudomonas fluorescens* BS2 and *Pseudomonas noertemamii* BS8, soil bacteria that cooperate to degrade the poly- γ -D-glutamic acid anthrax capsule. *Genome Announc* 1:e00057-12. <http://dx.doi.org/10.1128/genomeA.00057-12>.
- Shargel L, Yu ABC. 1993. Applied biopharmaceutics and pharmacokinetics, 3rd ed. Appleton and Lange, Norwalk, CT.

16. Taylor PW, Bernal P, Zelmer A. 2009. Modification of the bacterial phenotype as an approach to counter the emergence of multidrug-resistant pathogens, p 43–78. *In* Bonilla AR, Muniz KP (ed), *Antibiotic resistance: causes and risk factors, mechanisms and alternatives*. Nova Science Publishers, Hauppauge, NY.
17. Dubos R, Avery OT. 1931. Decomposition of the capsular polysaccharide of pneumococci type III by a bacterial enzyme. *J Exp Med* 54:51–71. <http://dx.doi.org/10.1084/jem.54.1.51>.
18. Avery OT, Dubos R. 1931. The protective action of a specific enzyme against type III pneumococcus infection in mice. *J Exp Med* 54:73–89. <http://dx.doi.org/10.1084/jem.54.1.73>.
19. Goodner K, Dubos R, Avery OT. 1932. The action of a specific enzyme upon the dermal infection of rabbits with type III pneumococcus. *J Exp Med* 55:393–404. <http://dx.doi.org/10.1084/jem.55.3.393>.
20. Francis T, Terrell EE, Dubos R, Avery OT. 1934. Experimental type III pneumococcus pneumonia in monkeys. II. Treatment with an enzyme which decomposes the specific capsular polysaccharide of pneumococcus type III. *J Exp Med* 59:641–667.
21. Lin TL, Hsieh PF, Huang YT, Lee WC, Tsai YT, Su PA, Pan YJ, Hsu CR, Wu MC, Wang JT. 2014. Isolation of a bacteriophage and its depolymerase specific for K1 capsule of *Klebsiella pneumoniae*: implication in typing and treatment. *J Infect Dis* 210:1734–1744. <http://dx.doi.org/10.1093/infdis/jiu332>.
22. Candela T, Fouet A. 2005. *Bacillus anthracis* CapD, belonging to the γ -glutamyltranspeptidase family, is required for the covalent anchoring of capsule to peptidoglycan. *Mol Microbiol* 57:717–726. <http://dx.doi.org/10.1111/j.1365-2958.2005.04718.x>.
23. Scorpio A, Chabot DJ, Day WA, O'Brien DK, Vietri NJ, Itoh Y, Mohamadzadeh M, Friedlander AM. 2007. Poly- γ -glutamate capsule-degrading enzyme treatment enhances phagocytosis and killing of encapsulated *Bacillus anthracis*. *Antimicrob Agents Chemother* 51:215–222. <http://dx.doi.org/10.1128/AAC.00706-06>.
24. Scorpio A, Tobery SA, Ribot WJ, Friedlander AM. 2008. Treatment of experimental anthrax with recombinant capsule depolymerase. *Antimicrob Agents Chemother* 52:1014–1020. <http://dx.doi.org/10.1128/AAC.00741-07>.
25. Coggeshall KM, Lupu F, Ballard J, Metcalf JP, James JA, Farris D, Kurosawa S. 2013. The sepsis model: an emerging hypothesis for the lethality of inhalation anthrax. *J Cell Mol Med* 17:914–920. <http://dx.doi.org/10.1111/jcmm.12075>.
26. Henderson DW, Peacock S, Belton FC. 1956. Observations on the prophylaxis of experimental pulmonary anthrax in the monkey. *J Hyg (Lond)* 54:28–36. <http://dx.doi.org/10.1017/S0022172400044272>.
27. Goossens PL. 2009. Protective antigen as a correlative marker for anthrax in animal models. *Mol Aspects Med* 30:467–480. <http://dx.doi.org/10.1016/j.mam.2009.07.005>.

Original article

TREE, J. A., HALL, G., PEARSON, G., RAYNER, E., GRAHAM, V. A., STEEDS, K., BEWLEY, K. R., HATCH, G. J., DENNIS, M., TAYLOR, I., ROBERTS, A. D., FUNNELL, S. G. & VIPOND, J. 2015. Sequence of pathogenic events in cynomolgus macaques infected with aerosolized monkeypox virus. *J Virol*, 89, 4335-44.

Impact factor: 4.324

Contributions by HATCH, G. J.

Home Office – Personal Licence holder

Development and qualification of aerosol, biocontainment and clinical parameter systems. Performance of aerosol challenge.

Study management – Study design, liaison and co-ordination with sponsors, virology, immunology, histology and in vivo teams, scheduling, reporting

Data analysis and manuscript review

Citation metrics

Google Scholar: 5 citations

Sequence of Pathogenic Events in *Cynomolgus* Macaques Infected with Aerosolized Monkeypox Virus

J. A. Tree, G. Hall, G. Pearson, E. Rayner, V. A. Graham, K. Steeds, K. R. Bewley, G. J. Hatch, M. Dennis, I. Taylor, A. D. Roberts, S. G. P. Funnell, J. Vipond

Microbiological Services, Public Health England, Porton Down, Salisbury, Wiltshire, United Kingdom

ABSTRACT

To evaluate new vaccines when human efficacy studies are not possible, the FDA's "Animal Rule" requires well-characterized models of infection. Thus, in the present study, the early pathogenic events of monkeypox infection in nonhuman primates, a surrogate for variola virus infection, were characterized. *Cynomolgus* macaques were exposed to aerosolized monkeypox virus (10^5 PFU). Clinical observations, viral loads, immune responses, and pathological changes were examined on days 2, 4, 6, 8, 10, and 12 postchallenge. Viral DNA (vDNA) was detected in the lungs on day 2 postchallenge, and viral antigen was detected, by immunostaining, in the epithelium of bronchi, bronchioles, and alveolar walls. Lesions comprised rare foci of dysplastic and sloughed cells in respiratory bronchioles. By day 4, vDNA was detected in the throat, tonsil, and spleen, and monkeypox antigen was detected in the lung, hilar and submandibular lymph nodes, spleen, and colon. Lung lesions comprised focal epithelial necrosis and inflammation. Body temperature peaked on day 6, pox lesions appeared on the skin, and lesions, with positive immunostaining, were present in the lung, tonsil, spleen, lymph nodes, and colon. By day 8, vDNA was present in 9/13 tissues. Blood concentrations of interleukin 1ra (IL-1ra), IL-6, and gamma interferon (IFN- γ) increased markedly. By day 10, circulating IgG antibody concentrations increased, and on day 12, animals showed early signs of recovery. These results define early events occurring in an inhalational macaque monkeypox infection model, supporting its use as a surrogate model for human smallpox.

IMPORTANCE

Bioterrorism poses a major threat to public health, as the deliberate release of infectious agents, such as smallpox or a related virus, monkeypox, would have catastrophic consequences. The development and testing of new medical countermeasures, e.g., vaccines, are thus priorities; however, tests for efficacy in humans cannot be performed because it would be unethical and field trials are not feasible. To overcome this, the FDA may grant marketing approval of a new product based upon the "Animal Rule," in which interventions are tested for efficacy in well-characterized animal models. Monkeypox virus infection of nonhuman primates (NHPs) presents a potential surrogate disease model for smallpox. Previously, the later stages of monkeypox infection were defined, but the early course of infection remains unstudied. Here, the early pathogenic events of inhalational monkeypox infection in NHPs were characterized, and the results support the use of this surrogate model for testing human smallpox interventions.

Since smallpox was declared as being eradicated by the World Health Organization in 1980 (1), laboratory investigations of variola virus have been restricted, leaving a significant gap in the understanding of the immune responses and pathogenesis of this infection (2). Recently, the majority of the human population has not been vaccinated; consequently, a proportion of the population lacks protective immunity (3). Concerns over the use of variola virus or monkeypox virus (a closely related orthopoxvirus) as a biological weapon remain high, as a deliberate release would have catastrophic consequences on global health (4).

The efficacy of therapeutics and vaccines against smallpox cannot be tested in phase III clinical trials in humans, as this is neither ethical nor feasible. Therefore, testing new medical countermeasures requires FDA marketing approval according to the "Animal Rule" (5). Monkeypox virus infection of nonhuman primates (NHPs) presents a potential surrogate disease model for testing intervention strategies for smallpox. Monkeypox virus is related to variola virus and causes a lethal systemic infection in primates. It can also infect humans and presents clinical symptoms similar to those of classic smallpox (6, 7).

Several studies have reported the development of an NHP model of monkeypox virus infection. A variety of challenge routes

have been used, including intrabronchial (8), intravenous (8–14), intratracheal (15, 16), intratracheal with MicroSprayer (17), and subcutaneous (18, 19). Natural infection of smallpox usually occurs as a result of close contact with an infected person, via the oropharynx or nasopharynx (20). A deliberate release of variola or monkeypox virus, however, would probably be in aerosol form for rapid dispersion over large areas (21). A limited number of studies have used the aerosol route, characterizing the pathogenic events following aerosol monkeypox virus infection (22–24). Zauha and

Received 15 October 2014 Accepted 26 January 2015

Accepted manuscript posted online 4 February 2015

Citation Tree JA, Hall G, Pearson G, Rayner E, Graham VA, Steeds K, Bewley KR, Hatch GJ, Dennis M, Taylor I, Roberts AD, Funnell SGP, Vipond J. 2015. Sequence of pathogenic events in *cynomolgus* macaques infected with aerosolized monkeypox virus. *J Virol* 89:4335–4344. doi:10.1128/JVI.03029-14.

Editor: G. McFadden

Address correspondence to J. A. Tree, julia.tree@phe.gov.uk.

Copyright © 2015, American Society for Microbiology. All Rights Reserved.

doi:10.1128/JVI.03029-14

colleagues described the systemic dissemination of the monkeypox virus in cynomolgus macaques through a monocytic-cell-associated viremia, similar to that of variola in human beings (23). More recently, two studies described the clinical progression of disease in NHPs following exposure to different doses of aerosolized monkeypox virus (22, 24). These three studies described disease progression from 8 to 17 days after exposure. Pathogenic events earlier than 8 days postinfection have not been reported.

The purpose of this study was to gain a better understanding of the early pathogenic events of monkeypox virus infection following aerosol challenge with a target dose of 10^5 PFU. This study also further characterizes the use of this challenge dose, as used previously, for testing smallpox vaccines (25). In this work, clinical signs of disease, immune cell and antibody responses, viral spread through the body, and pathological changes were examined from days 2 to 12 postchallenge.

MATERIALS AND METHODS

Experimental animals. Twenty-one captive-bred, healthy, male cynomolgus macaques (*Macaca fascicularis*) of Mauritian origin were obtained from a United Kingdom breeding colony. They weighed >2.5 kg and were >2 years of age. All animals were negative for neutralizing antibodies to orthopoxvirus prior to the start of the study. The macaques were housed as required by the United Kingdom Home Office *Code of Practice for the Housing and Care of Animals Used in Scientific Procedures* (26) and the National Committee for Refinement, Reduction, and Replacement (NC3Rs) *Guidelines on Primate Accommodation, Care, and Use* (27). When a procedure required the removal of a primate from a cage, it was sedated by intramuscular (i.m.) injection with ketamine hydrochloride (10 mg/kg of body weight) (Ketaset; Fort Dodge Animal Health Ltd., Southampton, United Kingdom). All procedures were conducted under a project license approved by the local Ethical Review Process of Public Health England, Salisbury, United Kingdom, and the United Kingdom Home Office.

Pathogenesis study. The animals were divided into seven groups of 3 animals and were exposed to aerosolized monkeypox virus on one of two separate occasions with a target dose of 1×10^5 PFU. The mean presented dose was 7.3×10^4 PFU. Animals were scheduled to be euthanized on days 2, 4, 6, 8, 10, and 12 postchallenge. Three animals were designated the reserve group and were used to replace animals that met humane endpoints earlier than their planned necropsy, thus ensuring that 3 animals were available for necropsy at each scheduled time point.

On the day of necropsy, animals were sedated and whole blood and throat swabs collected. For the latter, a flocked swab (Copan Diagnostics, California, USA) was gently stroked 6 times across the back of the throat in the tonsillar area. Viral loads were determined in the blood and throat samples by real-time PCR and plaque assay (see below). The concentration of IgG circulating in the blood was determined by enzyme-linked immunosorbent assay (ELISA; see below). The concentrations of cytokines and the phenotypes of cellular immune populations were determined by Luminex and flow cytometry, respectively (see below). At necropsy, tissues were sampled for histological examination and the determination of viral load by real-time PCR (see below).

Monkeypox virus challenge strain. Monkeypox virus, strain Zaire 79, NR-2324, was obtained from the Biodefense and Emerging Infections Research Resources Repository (BEI Resources, Virginia, USA). On the day of challenge, stocks of virus were thawed and diluted appropriately in minimum essential medium (MEM) containing Earl's salts (Sigma, Poole, United Kingdom), 2 mM L-glutamine (Sigma), and 2% (vol/vol) fetal calf serum (FCS) (Sigma).

Aerosol exposure. Animals were challenged with monkeypox virus using the AeroMP-Henderson apparatus, in which the challenge aerosol was generated using a six-jet Collision nebulizer (BGI, Waltham, MA, USA). This apparatus was designed to deliver a particle size with a mass

median diameter of 2.5 μ m and a geometric standard deviation of approximately 1.8 (28, 29). The aerosol was mixed with conditioned air in the spray tube (30) and delivered to the nose of each animal via a modified veterinary anesthesia mask. Samples of the aerosol were taken using an SKC BioSampler (SKC Ltd., Dorset, United Kingdom) and an aerodynamic particle sizer (TSI Instruments Ltd., Bucks, United Kingdom); these processes were controlled and monitored using the AeroMP management platform (Biaera Technologies LLC, Maryland, USA). To enable delivery of consistent doses to individuals, each animal was sedated and placed in a "head-out" plethysmograph (Buxco, North Carolina, USA). The aerosol was delivered simultaneously with measurement of the respired volume. A back titration of the aerosol samples taken at the time of challenge was performed to calculate the presented/inhaled dose.

ELISA. Samples of blood were collected at time points throughout the study; serum was separated and assayed for IgG antibodies to vaccinia virus using an ELISA. MaxiSorp 96-well plates (Nunc, Roskilde, Denmark) were coated overnight at 4°C with a preparation of commercially prepared psoralen/UV-inactivated, sucrose density gradient-purified vaccinia virus (Lister strain) (Autogen Bioclear United Kingdom Ltd., Wiltshire, United Kingdom) in calcium carbonate buffer at 2.5 μ g ml⁻¹. Unbound antigen was removed by washing the plates 3 times. The plates were treated with blocking buffer (phosphate-buffered saline [PBS], 5% milk powder [Sigma], 0.1% Tween 20 [Sigma]) for 1 h at room temperature with shaking. Unbound blocking solution was removed by washing 3 times with Tris-buffered saline (TBS). Fourfold serially diluted serum samples (starting at 1:50) were added to the plate for 2 h at room temperature, with shaking. Unbound antibodies were removed from the plate by washing 3 times with TBS. The plates were incubated for 2 h, with shaking, with horseradish peroxidase-labeled anti-monkey IgG (Kirkegaard and Perry Laboratories, Maryland, USA). Unbound detection antibody was removed by washing 5 times with TBS and developed using the 2,2'-azino-di-[3-ethylbenzthiazoline sulfonate (6)] (ABTS) peroxidase substrate system (Kirkegaard and Perry Laboratories). The development of the ELISA was stopped by using ABTS stop solution (Kirkegaard and Perry Laboratories). ELISA titers were calculated and compared with a vaccinia immune globulin standard (BEI Research Repository Resource, USA), which was used to convert the titer into arbitrary international units (AIU) per milliliter.

Flow cytometry. Whole blood was collected on days 2, 4, 6, 8, 10, and 12 by using heparin as the anticoagulant. Antibodies to CD3e, CD4, CD20, CD16 (BD Biosciences, Oxford, United Kingdom), and CD8a (Invitrogen, United Kingdom) conjugated to R-phycoerythrin (R-PE)-cyanine dye (Cy7), allophycocyanin (APC), PE, fluorescein isothiocyanate (FITC), and PE-Texas red (TR), respectively, were incubated with the blood for 30 min at room temperature. The red blood cells were removed from the whole blood by lysis with Uti-Lyse reagent (Dako, Cambridgeshire, United Kingdom) and decontaminated overnight with a 4% formaldehyde final concentration solution. Flow count beads (Beckman Coulter, High Wycombe, United Kingdom) were added to provide a standard to enable cell counts per microliter of blood, before being acquired on the flow cytometer. Data were collected on an FC500 flow cytometer (Beckman Coulter) and analyzed with CXP Analysis software version 2.1.

Luminex analysis of cytokines. The concentrations of cytokines were determined in serum samples using an NHP 23-plex kit (Merck Millipore, Massachusetts, USA) according to the manufacturer's instructions. Samples were acquired using a Luminex 200 system (Luminex, Austin, TX, USA), and the data were analyzed using the Xponent software, version 3.0. The concentration of each cytokine in the serum was calculated based on a comparison with the corresponding standard curve generated using purified cytokines from the kit.

Monkeypox virus plaque assay. During the course of the study, EDTA-treated blood and throat swabs were collected and frozen at -80°C . At necropsy, tissues were collected and snap-frozen in liquid nitrogen. Before being tested, tissue was thawed and homogenized in PBS with 1.8-mm ceramic beads in a Precellys24 tissue homogenizer (Ber-

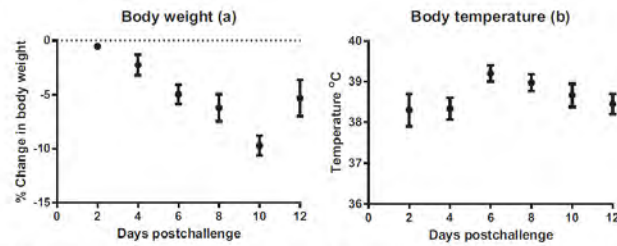


FIG 1 Clinical parameters. (a) Percentage change in body weight; (b) change in body temperature of cynomolgus macaques following aerosol challenge with monkeypox virus (mean \pm 1 SE, n = 3 to 5 macaques). Body temperature was taken upon euthanasia.

tin Technologies, Villeurbanne, France). The titers of the infectious virus in the tissues, blood, and throat swabs were determined by plaque assay. Samples were incubated in 24-well plates (Nunc; Thermo Fisher Scientific, Loughborough, United Kingdom) with Vero E6 (ATCC CRL-1586; American Type Culture Collection, USA) cell monolayers under MEM (Life Technologies, California, USA) containing 1.5% carboxymethylcellulose (Sigma), 5% (vol/vol) fetal calf serum (Life Technologies), and 25 mM HEPES buffer (Sigma). After incubation at 37°C for 72 h, they were fixed overnight with 20% (wt/vol) formalin-PBS, washed with tap water, and stained with methyl crystal violet solution (0.2% [vol/vol]) (Sigma).

Virus detection by quantitative PCR (qPCR). Tissue samples collected and snap-frozen in liquid nitrogen were defrosted and homogenized in PBS using a Precellys24 tissue homogenizer. Viral DNA was isolated from homogenates using a Qiagen tissue kit (Qiagen, Crawley, West Sussex, United Kingdom) by following the manufacturer's instructions. Blood and throat swabs were processed using a Qiagen blood DNA mini-kit (Qiagen) by following the manufacturer's instructions. Real-time PCR was performed using an Applied Biosystems 7500 Fast instrument (Life Technologies) with an in-house TaqMan assay targeted at the viral hemagglutinin (HA) gene, residues 158734 to 158798, inclusive, in the Z79 genome (GenBank accession no. HQ857562.1, strain V79-1-005).

Clinical and euthanasia observations. Clinical observations were made and scored every 4 to 6 h postchallenge. A scale was used to define disease severity (0 = none, 1 = mild, 2 = substantial, 3 = intense), based on observations that included rectal temperature, body weight, behavioral changes (depression/unresponsiveness/repetitive activity), nasal discharge, cough, dyspnea, and rash/skin swelling. In order to meet the requirement of the project license to limit suffering of animals and identify an endpoint for euthanasia, the clinical well-being of each subject was assessed using a euthanasia scoring scheme which included observations of >20% loss in body weight, convulsions, hemorrhagic rash, and persistent prostration.

Necropsy procedures. Animals were anesthetized with ketamine hydrochloride (20 mg ml⁻¹, i.m.) (Fort Dodge Animal Health Ltd.), and exsanguination was effected via cardiac puncture, followed by injection of an anesthetic overdose (Dolethal, 140 mg/kg; Vetquinol United Kingdom Ltd.) to ensure euthanasia. A necropsy was performed immediately after confirmation of death.

Pathological studies. At necropsy, abnormalities were recorded and samples were collected from lung lobes, trachea, heart, liver, kidneys, spleen, tongue, tonsil, esophagus, stomach, ileum, descending colon, lymph nodes (tracheobronchial, axillary, mesenteric, mandibular, and inguinal), adrenal gland, ovary or testis, skin (with and without lesion), and brain and placed in 10% neutral buffered formalin. Fixed tissues were processed to paraffin wax, and 5- μ m sections were cut and stained with hematoxylin and eosin (H&E). For immunohistochemistry, formalin-fixed, paraffin-embedded tissue sections were mounted on positively charged X-tra adhesive slides (Leica Biosystems, United Kingdom),

deparaffinized, and rehydrated. Immunohistochemical staining was achieved using a BOND-MAX immunostainer (Leica Microsystems, United Kingdom) and a Leica Bond Polymer Refine detection kit (Leica Biosystems, United Kingdom). A heat-induced epitope retrieval cycle with buffer ER2 (Leica Biosystems, United Kingdom) was applied for 20 min, followed by a peroxide block for 5 min (Leica Biosystems). Incubation was then performed with a mouse monoclonal antivaccinia antibody (ViroStat, USA) at a dilution of 1:1,800, followed by the post-primary antibody for 8 min (Leica Biosystems). Hematoxylin was used as the counterstain. Positive- and negative-control slides were included. Immunolabeled slides were evaluated using light microscopy.

RESULTS

Clinical signs. Clinical observations from the animals necropsied on days 2 (n = 3) and 4 (n = 3) scored 0, similar to preexposure levels. Euthanasia scores and body weights (Fig. 1a) remained similar to preexposure levels. On day 4, three animals (from other groups) began to cough. On day 6, signs of acute disease were noted that included increased weight loss, dyspnea, anorexia, and a peak in body temperature (mean, 39.2°C; n = 3 animals) (Fig. 1b). On day 8, animals showed signs of severe illness; additionally, two animals from the "reserve group" met the euthanasia criteria on day 8, thus the group size for necropsy on day 8 was n = 5 animals. Day 8 was the peak time for clinical signs; coughing was reported for 10 out of 12 animals, and the mean loss in body weight was -9.7% (Fig. 1a). By day 12, surviving animals were showing signs of recovery, with only one animal still coughing. The remaining animal from the "reserve group" was euthanized on day 12; hence, the sample size was n = 4 animals.

Enlargement of the lymph nodes (lymphadenopathy) was observed at necropsy in all animals from day 2 onward (see the detailed description in the "Pathology" section below).

The skin of the animals on days 2 and 4 were normal. Pox lesions appeared on day 6 (mean lesion count = 5, range = 0 to 16, n = 3 animals). The peak number of lesions occurred on day 8 (mean lesion count = 52, range = 0 to 189, n = 5 animals). The mean number of lesions decreased by day 10 (mean lesion count = 45, range = 17 to 70, n = 3 animals) and remained similar on day 12 (mean lesion count = 47, range = 4 to 92, n = 4 animals).

Immunophenotyping. The changes in absolute counts of different populations of immune cells, in the whole blood, are shown in Table 1. Compared to baseline levels, by day 2 postinfection, there were reductions in lymphocytes (-2×10^6 ml⁻¹), CD4⁺ T cells (-4×10^5 ml⁻¹), CD8⁺ T cells (-2×10^5 ml⁻¹), CD3⁺ T

TABLE 1 Changes in immune populations

Day	Cellular population change (cells × 10 ³ ml ⁻¹) ^a													
	Lymphocytes		CD4 ⁺ T cells		CD8 ⁺ T cells		CD3 ⁺ T cells		NK cells		B cells		Monocytes	
	Mean	±1 SE	Mean	±1 SE	Mean	±1 SE	Mean	±1 SE	Mean	±1 SE	Mean	±1 SE	Mean	±1 SE
postchallenge														
2	-1,607	606	-398	184	-160	63	-626	267	-132	40	-508	315	-141	7
4	-794	169	-64	75	-60	15	-197	84	-13	17	-278	78	75	83
6	-4,782	3,210	-851	240	-370	156	-1,397	444	-254	121	-625	170	-25	76
8	427	471	-136	142	46	131	-417	279	-60	65	-186	152	262	121
10	2,329	842	186	589	796	181	-77	1348	-66	67	-448	316	556	364
12	1,298	1,225	201	354	645	293	1,636	864	-34	84	-450	293	102	105

^a Mean absolute cell counts (cells × 10³ ml⁻¹) in different populations (+1 SE; n = 3 to 5 macaques) compared to baseline levels (average from two bleeds, taken on different days, prior to challenge) in whole blood, following challenge with aerosolized monkeypox virus.

cells ($-6 \times 10^5 \text{ ml}^{-1}$), NK cells ($-1 \times 10^5 \text{ ml}^{-1}$), B cells ($-5 \times 10^5 \text{ ml}^{-1}$), and monocytes ($-1 \times 10^5 \text{ ml}^{-1}$). By day 4, cell counts started to rise but remained below baseline levels, except for monocytes, which rose above prechallenge counts ($+7.5 \times 10^4 \text{ ml}^{-1}$) (Table 1). A second reduction in most immune cells was noted on day 6, followed by a steady rise until day 10 (Table 1). A positive increase was seen in lymphocytes (notably CD8⁺ T cells) and monocytes on days 8, 10, and 12 (CD4⁺ T cells rose above baseline from day 10 onward).

Cytokine responses. On day 2, a rise in interleukin 8 (IL-8) (increase of 567 pg ml⁻¹) was seen compared to prechallenge levels, and other biomarkers either decreased (e.g., monocyte chemoattractant protein 1 [MCP-1], IL-12/23, and IL-2) or remained unchanged (Table 2). On day 4, there were increases in the concentrations of gamma interferon (IFN- γ), IL-1ra, IL-6, IL-8, MCP-1, vascular endothelial growth factor (VEGF), IL-18, and IL-2. The concentrations of some cytokines, e.g., IFN- γ (1,322 pg ml⁻¹), IL-1ra (3,335 pg ml⁻¹), IL-6 (570 pg ml⁻¹), IL-8 (2,546 pg ml⁻¹), and MCP-1 (726 pg ml⁻¹), peaked on day 8. Small peaks in

the concentrations of other biomarkers, e.g., tumor necrosis factor alpha (TNF- α), IL-1 β , macrophage inflammatory protein 1 β (MIP-1 β), and IL-12/23, occurred on day 10. In contrast, small rises in granulocyte-macrophage colony-stimulating factor (GM-CSF) and IL-10 occurred later, by day 12 (Table 2).

Humoral immune responses. The levels of IgG serum antibodies in the blood to vaccinia virus, determined by ELISA, were increased from day 10 onward (Fig. 2).

Viral load. Viral DNA was first detected in the throat (3.4×10^4 copies ml⁻¹) on day 4. The concentration increased to 9.5×10^5 copies ml⁻¹ on day 8 and remained high until the last study day (day 12) (Fig. 3). In contrast, viral DNA (vDNA) was first detected in the blood (8.3×10^3 copies ml⁻¹) on day 8, and its concentration rose to 4.5×10^5 copies ml⁻¹ on day 10 and returned to 1.1×10^4 copies ml⁻¹ by day 12 (Fig. 3). Viral PFU were detected in throat swabs (above the limit of detection = 25 PFU ml⁻¹) from day 4 to day 12, and a peak in the infectious virus concentration was detected on day 8 (1.4×10^3 PFU ml⁻¹). No

TABLE 2 Serum cytokine profiles of cynomolgus macaques taken during the pathogenesis study

Biomarker	Change in concn of biomarker (pg ml ⁻¹) by day postchallenge ^a											
	Day 2		Day 4		Day 6		Day 8		Day 10		Day 12	
	Mean	±1 SE	Mean	±1 SE	Mean	±1 SE	Mean	±1 SE	Mean	±1 SE	Mean	±1 SE
IFN- γ	-2	1	212	55	842	250	1,322	210	380	168	32	13
IL-1ra	-2	4	52	8	313	173	3,335	3,200	18	15	21	7
IL-6	-1	0.3	43	22	213	88	570	339	70	29	17	3
TNF- α	0	0	0	0	2	2	1	1	15	11	1	1
IL-8	567	754	1,186	1,067	193	499	2,546	1,112	1,458	1,511	671	373
IL-1 β	0	0	0	0	0	0	1	1	7	6	1	1
MCP-1	-131	64	383	78	651	413	726	93	201	105	132	103
MIP-1 α	0	0	0	0	0	0	0	0	1	1	0	0
VEGF	-6	3	6	3	27	11	59	12	20	8	15	9
GM-CSF	0	0	0	0	0	0	1	0.4	1	1	7	7
MIP-1 β	-2	1	-1	0	0.3	1	2	1	13	8	3	3
IL-5	-2	1	1	1	-0.3	0.3	1	1	6	3	1	0.5
IL-13	0	0	0	0	0	0	0.2	0.2	2	2	0.3	0.3
IL-10	-1	0	-0.3	0.3	-1	0	0	0.8	3	3	4	4
IL-12/23	-22	11	-5	10	-37	8	-68	13	69	80	46	44
IL-15	-2	1	-1	0.3	3	1	0	1	2	3	-1	1
IL-17	0	0	0	0	0	0	0.2	0.2	0	0	0	0
IL-18	-4	1	4	1	2	3	6	2	3	2	2	0.4
IL-2	-18	2	16	4	17	7	26	5	6	9	9	6

^a Mean concentration (pg ml⁻¹) (+1 SE; n = 3 to 5 macaques) change in cytokine levels compared to baseline levels (average from two bleeds, taken on different days, prior to challenge) on various days following challenge with aerosolized monkeypox virus.

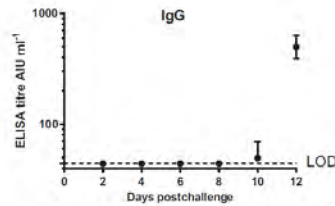


FIG 2 Serum IgG responses following challenge, measured by ELISA (mean \pm 1 SE, $n = 3$ to 5 macaques). Day 0, time of challenge with monkeypox virus. LOD, limit of detection (44.1 AIU ml^{-1}).

infectious virus (PFU) above the limit of detection was detected in the blood on any of the days tested (Table 3).

Body tissues were assayed by real-time PCR, and on day 2, positive PCR results were restricted to the lungs (2.5×10^4 to 2.7×10^4 copies mg^{-1}); by day 4, this increased to 5.1×10^5 to 2.9×10^6 copies mg^{-1} (Fig. 4). On day 4, vDNA was also detected in the spleen and tonsils. By day 6, at least seven of the 13 tissues contained vDNA. The level of vDNA in the lungs remained high (3.7×10^6 to 5.7×10^6 copies mg^{-1}), while at least approximately 1×10^5 copies mg^{-1} of vDNA were detected in the spleen, tonsil, and tongue. By day 8, 9/13 tissues were positive for vDNA, including the kidney, heart, tongue, cerebrospinal fluid, spleen, and mediastinal lymph nodes. The concentration of virus in the tonsils (6×10^6 copies mg^{-1}) exceeded that in the lungs (3×10^6 copies mg^{-1}). Two animals in the "reserve group" were euthanized on humane grounds on day 8, and there was no difference in virological data between these two animals and the scheduled three animals. By day 10, the PCR values detected in the lungs decreased to 6.8×10^5 to 1.3×10^6 copies mg^{-1} (Fig. 4), although the concentration of vDNA in the tonsil was still high at 1.8×10^7 copies mg^{-1} . A decrease in viral load was apparent in all the animals on day 12, with values down to 1.1×10^5 to 3.8×10^5 copies mg^{-1} in the lungs (Fig. 4). This was consistent with clinical observations indicating that these animals were recovering.

Pathology. Histopathological changes and results of immunostaining are summarized in Table 4. On day 2 postchallenge, histological changes were restricted to respiratory bronchioles (Fig. 5a) in the lungs of two of three animals. They comprised occasional, small foci of dysplastic and sloughed cells. In immuno-

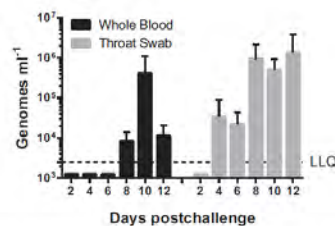


FIG 3 Mean number (± 1 SD) of viral genomes (HA gene) as determined from qPCR in the blood and throat in samples taken following challenge with aerosolized monkeypox virus. The lower limit of quantification for qPCR (LLQ) was $2,500 \text{ genomes ml}^{-1}$.

TABLE 3 Mean number of PFU of monkeypox virus in whole blood and throat swabs taken on different days postchallenge

Day postchallenge	Live virus PFU ml^{-1} (\pm SE)	
	Whole blood	Throat swab
2	<LOD ^a	25 ± 0
4	<LOD	$4.5 \times 10^2 \pm 4.3 \times 10^2$
6	<LOD	$1.9 \times 10^2 \pm 85$
8	<LOD	$1.4 \times 10^3 \pm 1.2 \times 10^3$
10	<LOD	$2.2 \times 10^2 \pm 1.9 \times 10^2$
12	<LOD	$6.4 \times 10^2 \pm 6.2 \times 10^2$

^a <LOD, less than the limit of detection (250 PFU ml^{-1}).

stained sections, monkeypox antigen was present focally in all three animals, most frequently in the bronchioles and alveoli but occasionally in the epithelium of bronchi. Positive immunostaining was not observed in any other tissue on day 2.

On day 4 postchallenge, histological abnormalities were observed in the lungs of 3 animals. They were more numerous and developed than on day 2 postchallenge, comprising foci of epithelial necrosis and inflammation. In bronchioles, focal epithelial dysplasia, epithelial necrosis, and sloughing (Fig. 5b), with infiltration by neutrophils and occasionally eosinophils, were observed. Thickening of alveolar walls was seen diffusely in one animal and focally in another; a small number of alveoli were dilated. In the tracheobronchial lymph node of 1/3 animals, scattered foci of inflammatory cells, primarily histiocytes, were detected (Fig. 5c). Pathological changes were not observed in any other organ. Monkeypox antigen was detected by immunostaining in all lung lobes in all animals, more prominently than on day 2, located in the epithelium of bronchi (Fig. 5b inset), bronchioles, and alveolar walls. In the hilar (tracheobronchial) lymph node, positive staining was located in the outer cortex adjacent to the subcapsular sinus (Fig. 5c, inset). In addition, in the absence of histological changes, a few scattered positive cells were detected in the spleen (Fig. 5d) and submandibular lymph nodes of one animal and the lamina propria of the colon of another animal.

On day 6 postchallenge, severe lesions were noted in the lungs, comprising focal necrosis of airway epithelium and neutrophil infiltration, with lower airways affected more severely than upper airways (Fig. 5e). Diffuse and focal thickening of alveolar walls by macrophages and neutrophils was common, and some alveolar dilation was present. Peribronchial edema and periarterial edema, sometimes with infiltration by macrophages and neutrophils, were seen less frequently. Vascular lesions, comprising endothelial margination of macrophages and neutrophils, were seen occasionally. Focal necrosis with neutrophil infiltration was noted in the tracheobronchial lymph node, occurring in the outer cortex and subcapsular sinuses and infrequently in the medulla. In addition, lesions were detected in all animals in the tonsil and spleen and in the trachea/larynx of one of three animals. Lesions in the tonsil comprised focal necrosis of the crypt epithelium and/or lymphoid follicles, with neutrophil infiltration. In the spleen, focal necrosis with neutrophil infiltration was noted, most frequently in periarteriolar lymphoid sheaths. Immunostaining was positive, with a distribution similar to that for the lesions described above, including the spleen (Fig. 5f). In addition, scattered, positive staining was found in the colon and axillary lymph node in 1/3 animals, in the absence of histological changes.

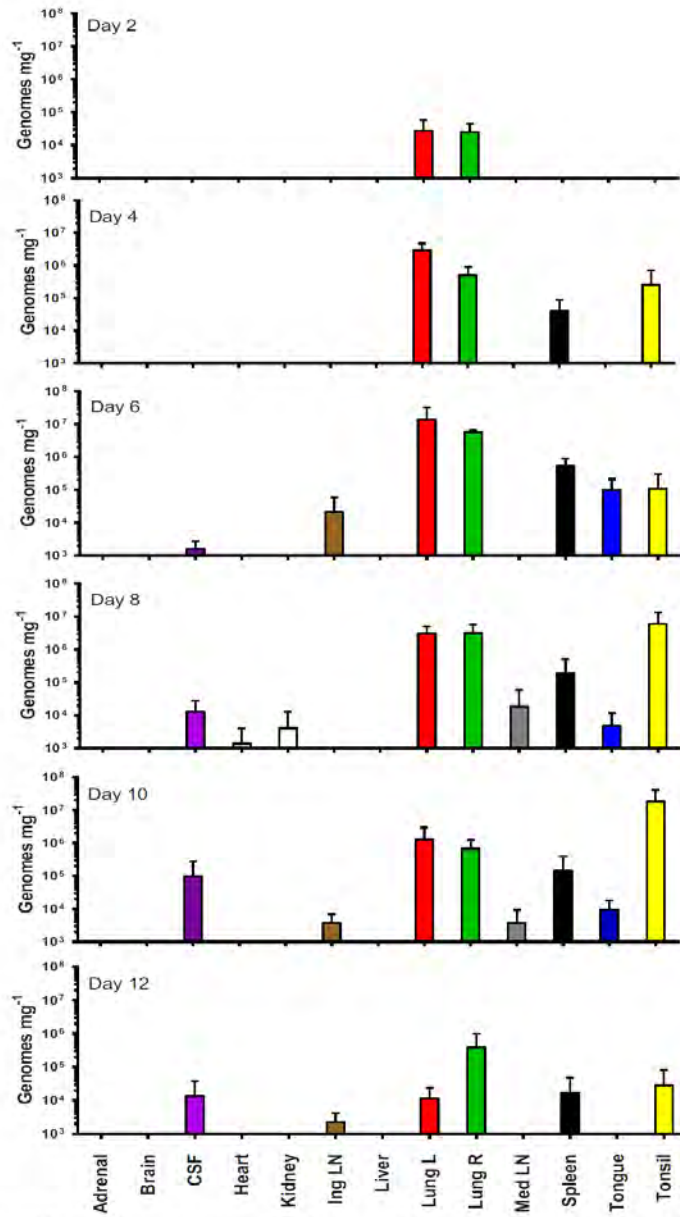


FIG 4 Viral load in tissues following challenge with monkeypox virus. The mean viral load (+1 SD), as determined by real-time PCR, in the tissues of animals taken at postmortem on different days of the study. For graphical purposes, the LLQ has been assigned 1,000 genomes mg⁻¹ due to variability in the weights of tissue recovered at necropsy.

TABLE 4 Summary of the occurrence of monkeypox-related lesions and positive immunohistochemistry results in cynomolgus macaques following challenge with monkeypox virus^a

Organ	No. of samples with positive H&E or IHC results/total no. of samples												
	Day 2		Day 4		Day 6		Day 8		Day 10		Day 12		
	H&E	IHC	H&E	IHC	H&E	IHC	H&E	IHC	H&E	IHC	H&E	IHC	
Trachea/larynx	0/3	0/3	0/3	0/3	1/3	1/3	1/5	1/5	0/3	0/3	1/4	1/4	
Lung RU	0/3	3/3	3/3	3/3	3/3	3/3	3/3	5/5	5/5	3/3	3/3	4/4	2/4
Lung RM	0/3	3/3	3/3	3/3	3/3	3/3	5/5	5/5	3/3	3/3	4/4	2/4	
Lung RL	1/3	3/3	3/3	3/3	3/3	3/3	5/5	5/5	3/3	3/3	4/4	2/4	
Lung LU	1/3	3/3	2/3	3/3	3/3	3/3	5/5	5/5	3/3	3/3	4/4	3/4	
Lung LL	2/3	3/3	3/3	3/3	3/3	3/3	5/5	5/5	3/3	3/3	4/4	3/4	
Hilar LN	0/2	0/2	1/3	2/3	3/3	3/3	4/5	4/5	1/3	2/3	2/3	1/4	
Spleen	0/3	0/3	0/3	1/3	3/3	3/3	3/5	4/5	2/3	1/3	2/4	0/4	
Tongue	0/3	0/3	0/3	0/3	0/3	0/3	2/5	2/5	0/3	0/3	0/3	0/3	
Tonsil	0/3	0/3	0/3	0/3	3/3	3/3	3/3	3/3	2/2	2/2	0/2	0/2	
Mandibular LN	0/3	0/3	0/2	1/2	2/2	2/2	2/5	3/5	1/3	1/3	0/3	0/3	
Stomach	0/3	0/3	0/3	0/3	0/3	0/3	0/5	1/5	0/3	0/3	0/3	0/3	
Ileum	0/3	0/3	0/3	0/3	0/3	0/3	0/3	0/3	0/3	0/3	0/3	0/3	
Colon	0/3	0/3	0/3	1/3	0/3	1/3	1/5	2/5	1/3	1/3	0/3	0/3	
Mesenteric LN	0/3	0/3	0/3	0/3	0/3	0/3	1/5	1/5	0/3	0/3	0/3	0/3	
Skin	0/3	0/3	0/3	0/3	0/3	0/3	1/5	1/4	0/3	0/2	1/4	1/3	
Inguinal LN	0/3	0/3	0/3	0/3	0/3	0/3	0/5	3/5	0/3	0/3	0/3	0/1	
Axillary LN	0/3	0/3	0/3	0/3	0/3	1/3	0/3	0/2	0/3	0/3	0/3	0/2	

^a Lung RU, right upper lobe; lung RM, right middle lobe; lung RL, right lower lobe; lung LU, left upper lobe; lung LL, left lower lobe; LN, lymph node; H&E, hematoxylin and eosin; IHC, immunohistochemistry (to identify monkeypox virus antigens).

From days 8 to 10 postchallenge, lesions in the lung and other tissues attributed to monkeypox infection were severe and extensive. Distribution of positive immunostaining was widespread (Table 4).

In all three animals remaining on day 12 after challenge, occasional acute lesions were observed, but there was some evidence of early resolution that comprised cuboidal, nonciliated epithelial cells. Immunostained monkeypox antigen was still present in the respiratory tract, including in the hilar lymph node, but was not observed in the remaining tissues examined (Table 4).

DISCUSSION

When human efficacy studies are neither ethical nor feasible, the FDA may grant marketing approval of a new product, such as a vaccine, based upon the Animal Rule. Well-characterized animal models, however, are a requirement of this rule. This study characterized the early stages of monkeypox infection in cynomolgus macaques, using a dose of 10^5 PFU, delivered by the aerosol route. These early events have not been previously investigated in detail. Here, special emphasis was placed on examining the virological, immunological, and pathological changes in early infection.

Previous experiments examining monkeypox disease progression have monitored the clinical signs of disease until animals have reached a humane endpoint or have died in the study. This invariably happened 6 to 9 days after challenge, depending on the dose and route of challenge. In this work, a different approach was taken; animals were divided into groups and euthanized on designated days unless individuals were observed to have reached a humane endpoint. Thus, a mix of animals was studied; some had developed severe disease at the time of euthanasia, while some developed only mild disease. This approach has allowed the detailed study of the early events following challenge that were missing from studies based on animals with severe disease (22, 23).

Few studies have examined the immune response of cynomolgus macaques following exposure to aerosolized monkeypox virus. In this work, trends in the data showed a decrease in different immune cell populations early on in the course of the infection. Larger animal group sizes, however, are needed in order to confirm this statistically. Nevertheless, this could be indicative of immunosuppression, as the immunomodulatory effect of monkeypox virus has been previously observed by others (2, 31, 32). The rises in lymphocytes, in particular CD8⁺ T cells, observed later in monkeypox infection, are likely to be the result of the host raising an adaptive immune response to the viral infection. Monocytes also increased above baseline levels on day 4 postinfection and again on days 8, 10, and 12. In this work, individual, circulating monocytes were not examined for infection with monkeypox virus; however, Zaucha and colleagues showed in their NHP studies that monocytic cells were immunopositive for poxviral antigen in a variety of organs and proposed that monkeypox virus spread initially via the lymph nodes and the mononuclear phagocytic/dendritic cell system (23).

Changes in the concentrations of circulating cytokines in the blood have been recorded in NHPs following challenge with different doses of monkeypox virus (5×10^4 to 5×10^7 PFU), via the intravenous and intrabronchial routes (8). Maximum mean peak fold changes in IFN- γ (8,028), IL-1ra (4,854), and IL-6 (3,207) were recorded on a variety of days (8). In this study, the mean peak changes in the biomarkers IFN- γ (1,322 pg ml⁻¹), IL-1ra (3,335 pg ml⁻¹), and IL-6 (570 pg ml⁻¹) occurred on day 8 postchallenge. The results of different studies are difficult to compare, because of the different ways data sets are presented and because different challenge doses and inoculation routes are used. However, it is clear IFN- γ , IL-1ra, and IL-6 play a role in the host response to monkeypox infection.

In this study, day 8 was the time when vDNA was detected in

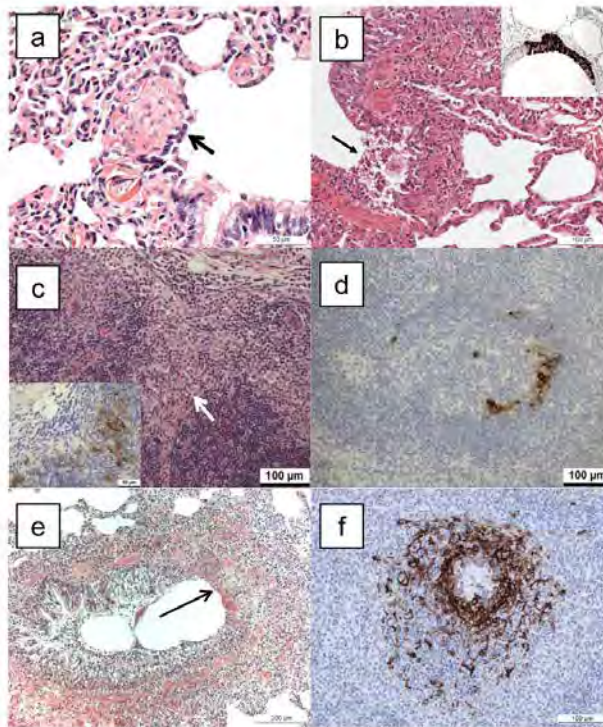


FIG 5 Histopathological changes associated with infection with monkeypox virus. (a) Lung, animal M965A, euthanized on day 2 postchallenge. Sloughing of respiratory bronchiolar epithelial cells (arrow) close to the junction with a bronchus. H&E. (b) Lung, animal M029F, euthanized on day 4 postchallenge. Focal epithelial cell necrosis (arrow), with sloughed cells and neutrophil infiltration at the junction of a bronchus and bronchiole. H&E. Inset, lung, animal I089K, euthanized on day 4 postchallenge. Focal, positive immunostaining of bronchial epithelium for monkeypox viral antigen. IHC. (c) Tracheobronchial lymph node, animal M029F, euthanized on day 4 postchallenge. Infiltration of superficial cortex by macrophages (arrow). HE. Inset, scattered, positively stained cells for monkeypox viral antigen. IHC. (d) Spleen, animal M293E, euthanized on day 4 postchallenge. Scattered, positively stained cells for monkeypox viral antigen in the white pulp. IHC. (e) Lung, animal M865B, euthanized 6 days postchallenge. Focal, bronchial epithelial necrosis (arrow). HE. (f) Spleen, animal I430G, euthanized on day 6 postchallenge. Positive immunostaining for monkeypox viral antigen in a periarterial lymphoid sheath (PALS) within the white pulp. IHC.

most tissues (9/13) and for death to most likely occur. It was also apparent that there was considerable animal-to-animal variation, and while the majority of the animals reached humane endpoints at approximately days 8 to 10, some survived the acute disease, as evidenced by the decline in the viral load in the blood and lung and tonsil tissues on day 12. The results of this experiment are similar to those reported by Nalca et al., in which, following an inhaled dose of 1.4×10^5 PFU, the mean time to death in cynomolgus macaques was 9 days (22). They also reported the peak viral load in blood (10^6 to 10^7 genomes ml^{-1}) was seen on day 10 postexposure; this was also noted on day 10 in this study (5×10^5 genomes ml^{-1}). Barnewell et al. also exposed two macaques to an aerosolized target dose of 1×10^5 PFU monkeypox virus; one died on day 8 and the other on day 9, and 2.7×10^5 to 3.6×10^5 genomes ml^{-1} were recorded in the blood on day 8 (24).

The histopathological and immunohistochemical findings in this study from animals examined on days 2, 4, and 6 postchal-

lenge confirm earlier findings (23) and have identified features of pathogenesis not reported previously, to the authors' knowledge. Zaucha and colleagues studied cynomolgus macaques exposed to an aerosol of monkeypox virus that died or were euthanized 9 to 17 days after exposure (23). They concluded that the lower airway epithelium was the principal target, and the present study supports their proposition and additionally illustrates infection and lesions in these epithelia as early as 2 days after challenge. They proposed that tonsil, mandibular nodes, and mediastinal nodes were infected early. The findings of this study support their proposition; on day 4, 2/3 hilar nodes immunostained positively and 3/3 on day 6. On day 4, one of the two mandibular lymph nodes immunostained positively, and 2/2 were positive on day 6 when 3/3 tonsils were positive. Zaucha and colleagues (23) concluded that the spleen and gastrointestinal tract became infected later, but this was not supported by the findings of this study, which recorded immunostaining in 1/3 spleens on day 4 and 3/3 on day 6.

Positive immunostaining was present in the colon of 1/3 animals on day 4. The findings from animals euthanized on days 8, 10, and 12 after challenge were consistent with those of a previous study (23).

This work describes, for the first time, the sequence of early pathological events that occur following inhalation of 10^5 PFU monkeypox virus in cynomolgus macaques. Monkeypox virus vDNA was detected in the lungs 2 days postinfection, and by day 4 the virus was detected in the throat, tonsil, and spleen. Viral antigen was also detected by immunohistochemistry in the lungs, spleen, colon, and mandibular and hilar lymph nodes on day 4. From day 6, signs of acute disease were obvious and pox lesions appeared. In 1988, Fenner and colleagues inferred, from limited available information, that the clinical manifestations of naturally acquired smallpox in humans began after an incubation period of 7 to 17 days following exposure (33). The first febrile phase lasted for 3 to 4 days, followed by the appearance of a rash. Our model partially resembles some of the features of the human condition, which helps to bridge the gap in our understanding of variola virus infection and improves our understanding of monkeypox viral disease while at the same time further characterizing this important smallpox animal model, as required by the FDA's Animal Rule.

ACKNOWLEDGMENTS

This work was funded by the National Institute of Allergy and Infectious Diseases (contact NO1-AI-30062, task orders 03 and 04).

The views in the paper are of the authors and not necessarily those of the funding body.

We thank Robert Johnson, Thames Pickett, and Helen Schiltz for reviewing the manuscript. We thank Victoria Cox (DSTL) for advice about statistical analysis. We are grateful to Susan Gray for preparing the histology samples. We appreciate the technical assistance provided by Debbie Atkinson, Gemma McLuckie, Mel Davison, and Thomas Tipton. We are also very grateful to the Biological Investigations Group at the PHE, in particular Paul Yeates and Janice Pickersgill, for conducting the animal procedures.

REFERENCES

- Breman JG, Arita I. 1980. The confirmation and maintenance of smallpox eradication. *New Engl J Med* 303:1263–1273. <http://dx.doi.org/10.1056/NEJM198011273032204>.
- Stanford MM, McFadden G, Karupiah G, Chaudhri G. 2007. Immunopathogenesis of poxvirus infections: forecasting the impending storm. *Immunol Cell Biol* 85:93–102. <http://dx.doi.org/10.1038/sj.icb.7100033>.
- von Krempelhuber A, Vollmar J, Pokorny R, Rapp P, Wulff N, Petzold B, Handley A, Mateo L, Siersbol H, Kollaritsch H, Chaplin P. 2010. A randomized, double-blind, dose-finding phase II study to evaluate immunogenicity and safety of the third generation smallpox vaccine candidate IMVAMUNE. *Vaccine* 28:1209–1216. <http://dx.doi.org/10.1016/j.vaccine.2009.11.030>.
- Chapman JL, Nichols DK, Martinez MJ, Raymond JW. 2010. Animal models of orthopoxvirus infection. *Vet Pathol* 47:852–870. <http://dx.doi.org/10.1177/0300985810378649>.
- FDA. 2002. New drug and biologics and drug products; evidence needed to demonstrate effectiveness of new drugs when human efficacy studies are not ethical or feasible. *Fed Regist* 67:37988–37998.
- Damon IK. 2011. Status of human monkeypox: clinical disease, epidemiology and research. *Vaccine* 29(Suppl 4):D54–D59. <http://dx.doi.org/10.1016/j.vaccine.2011.04.014>.
- Parker S, Buller RM. 2013. A review of experimental and natural infections of animals with monkeypox virus between 1958 and 2012. *Future Virol* 8:129–157. <http://dx.doi.org/10.2217/fvl.12.130>.
- Johnson RF, Dyall J, Ragland DR, Huzella L, Byrum R, Jett C, St Claire M, Smith AL, Paragas J, Blaney JE, Jahrling PB. 2011. Comparative analysis of monkeypox virus infection of cynomolgus macaques by the intravenous or intrabronchial inoculation route. *J Virol* 85:2112–2125. <http://dx.doi.org/10.1128/JVI.01931-10>.
- Earl PL, Americo JL, Wyatt LS, Eller LA, Whitbeck JC, Cohen GH, Eisenberg RJ, Hartmann CJ, Jackson DL, Kulesh DA, Martinez MJ, Miller DM, Mucker EM, Shamblyn JD, Zwiers SH, Huggins JW, Jahrling PB, Moss B. 2004. Immunogenicity of a highly attenuated MVA smallpox vaccine and protection against monkeypox. *Nature* 428:182–185. <http://dx.doi.org/10.1038/nature02331>.
- Earl PL, Americo JL, Wyatt LS, Espenshade O, Bassler J, Gong K, Lin S, Peters E, Rhodes L, Jr, Spano YE, Silvera PM, Moss B. 2008. Rapid protection in a monkeypox model by a single injection of a replication-deficient vaccinia virus. *Proc Natl Acad Sci U S A* 105:10889–10894. <http://dx.doi.org/10.1073/pnas.0804985105>.
- Buchman GW, Cohen ME, Xiao Y, Richardson-Harman N, Silvera P, DeTolla LJ, Davis HL, Eisenberg RJ, Cohen GH, Isaacs SN. 2010. A protein-based smallpox vaccine protects non-human primates from a lethal monkeypox virus challenge. *Vaccine* 28:6627–6636. <http://dx.doi.org/10.1016/j.vaccine.2010.07.030>.
- Hirao LA, Draghia-Akli R, Prigge JT, Yang M, Satishchandran A, Wu L, Hammarlund E, Khan AS, Babas T, Rhodes L, Silvera P, Slika M, Sardesai NY, Weiner DB. 2011. Multivalent smallpox DNA vaccine delivered by intradermal electroporation drives protective immunity in non-human primates against lethal monkeypox challenge. *J Infect Dis* 203:95–102. <http://dx.doi.org/10.1093/infdis/jiq017>.
- Huggins J, Goff A, Hensley L, Mucker E, Shamblyn J, Wlazlowski C, Johnson W, Chapman J, Larsen T, Twenhafel N, Karen K, Damon IK, Byrd CM, Bolken TC, Jordan R, Hruby D. 2009. Nonhuman primates are protected from smallpox virus or monkeypox virus challenges by the antiviral drug ST-246. *Antimicrob Agents Chemother* 53:2620–2625. <http://dx.doi.org/10.1128/AAC.00021-09>.
- Jordan R, Goff A, Frimm A, Corrado ML, Hensley LE, Byrd CM, Mucker E, Shamblyn J, Bolken TC, Wlazlowski C, Johnson W, Chapman J, Twenhafel N, Tyavanagimatt S, Amantana A, Chinsangaram J, Hruby DE, Huggins J. 2009. ST-246 antiviral efficacy in a nonhuman primate monkeypox model: determination of the minimal effective dose and human dose justification. *Antimicrob Agents Chemother* 53:1817–1822. <http://dx.doi.org/10.1128/AAC.01596-08>.
- Stittelaar KJ, van Amerongen G, Kondova I, Kuiken T, van Lavieren RF, Pistorio FH, Niesters HG, van Doornum G, van der Zeijst BA, Mateo L, Chaplin PJ, Osterhaus AD. 2005. Modified vaccinia virus Ankara protects macaques against respiratory challenge with monkeypox virus. *J Virol* 79:7845–7851. <http://dx.doi.org/10.1128/JVI.79.12.7845-7851.2005>.
- Stittelaar KJ, Neyts J, Naesens L, van Amerongen G, van Lavieren RF, Holy A, De Clercq E, Niesters HG, Fries E, Maas C, Mulder PG, van der Zeijst BA, Osterhaus AD. 2006. Antiviral treatment is more effective than smallpox vaccination upon lethal monkeypox virus infection. *Nature* 439:745–748. <http://dx.doi.org/10.1038/nature04295>.
- Goff AJ, Chapman J, Foster C, Wlazlowski C, Shamblyn J, Lin K, Kreiselmeyer N, Mucker E, Paragas J, Lawler J, Hensley L. 2011. A novel respiratory model of infection with monkeypox virus in cynomolgus macaques. *J Virol* 85:4898–4909. <http://dx.doi.org/10.1128/JVI.02525-10>.
- Saijo M, Ami Y, Suzuki Y, Nagata N, Iwata N, Hasegawa H, Iizuka I, Shiota T, Sakai K, Ogata M, Fukushi S, Mizutani T, Sata T, Kurata T, Kurane I, Morikawa S. 2009. Virulence and pathophysiology of the Congo Basin and West African strains of monkeypox virus in non-human primates. *J Gen Virol* 90:2266–2271. <http://dx.doi.org/10.1099/vir.0.010207-0>.
- Nagata N, Saijo M, Kataoka M, Ami Y, Suzuki Y, Sato Y, Iwata-Yoshikawa N, Ogata M, Kurane I, Morikawa S, Sata T, Hasegawa H. 2014. Pathogenesis of fulminant monkeypox with bacterial sepsis after experimental infection with West African monkeypox virus in a cynomolgus monkey. *Int J Clin Exp Pathol* 7:4359–4370.
- Fenner F, Henderson DA, Arita I, Jezek Z, Ladnyi ID. 1988. The epidemiology of smallpox, p 169–208. *In* Smallpox and its eradication. WHO, Geneva, Switzerland.
- Henderson DA, Inglesby TV, Bartlett JG, Ascher MS, Eitzen E, Jahrling PB, Hauer J, Layton M, McDade J, Osterholm MT, O'Toole T, Parker G, Perl T, Russell PK, Tonat K. 1999. Smallpox as a biological weapon: medical and public health management. Working Group on Civilian Biodefense. *JAMA* 281:2127–2137.
- Nalca A, Livingston VA, Garza NL, Zumbun EE, Frick OM, Chapman

- JL, Hartings JM. 2010. Experimental infection of cynomolgus macaques (*Macaca fascicularis*) with aerosolized monkeypox virus. *PLoS One* 5(9): e12880. <http://dx.doi.org/10.1371/journal.pone.0012880>.
23. Zaucha GM, Jahrling PB, Geisbert TW, Swearingen JR, Hensley L. 2001. The pathology of experimental aerosolized monkeypox virus infection in cynomolgus monkeys (*Macaca fascicularis*). *Lab Invest* 81:1581–1600. <http://dx.doi.org/10.1038/labinvest.3780373>.
 24. Barnewall RE, Fisher DA, Robertson AB, Vales PA, Knostman KA, Bigger JE. 2012. Inhalational monkeypox virus infection in cynomolgus macaques. *Front Cell Infect Microbiol* 2:117. <http://dx.doi.org/10.3389/fcimb.2012.00117>.
 25. Hatch GJ, Graham VA, Bewley KR, Tree JA, Dennis M, Taylor I, Funnell SG, Bate SR, Steeds K, Tipton T, Bean T, Hudson L, Atkinson DJ, McLuckie G, Charlwood M, Roberts AD, Vipond J. 2013. Assessment of the protective effect of Imvamune and Acam2000 vaccines against aerosolized monkeypox virus in cynomolgus macaques. *J Virol* 87:7805–7815. <http://dx.doi.org/10.1128/JVI.03481-12>.
 26. United Kingdom Home Office. 1989. Code of practice for the housing and care of animals used in scientific procedures. United Kingdom Home Office, London, United Kingdom. https://www.gov.uk/government/uploads/system/uploads/attachment_data/file/228831/0107.pdf.
 27. National Committee for Refinement, Reduction, and Replacement (NC3Rs). 2006. Guidelines on primate accommodation, care, and use. NC3Rs, London, United Kingdom.
 28. Gussman R. 1984. Note on the particle size output of Collison nebulizers. *Am Ind Hyg Assoc J* 45:B8–B12.
 29. May K. 1973. The Collison nebulizer. Description, performance and application. *J Aerosol Sci* 4:235.
 30. Druett HA. 1969. A mobile form of the Henderson apparatus. *J Hyg* 67:437–448. <http://dx.doi.org/10.1017/S0022172400041851>.
 31. Rubins KH, Hensley LE, Relman DA, Brown PO. 2011. Stunned silence: gene expression programs in human cells infected with monkeypox or vaccinia virus. *PLoS One* 6:e15615. <http://dx.doi.org/10.1371/journal.pone.0015615>.
 32. Alzhanova D, Hammarlund E, Reed J, Meermeier E, Rawlings S, Ray CA, Edwards DM, Bimber B, Legasse A, Planer S, Sprague J, Axthelm MK, Pickup DJ, Lewinsohn DM, Gold MC, Wong SW, Sacha JB, Slifka MK, Fruh K. 2014. T cell inactivation by poxviral B22 family proteins increases viral virulence. *PLoS Pathog* 10:e1004123. <http://dx.doi.org/10.1371/journal.ppat.1004123>.
 33. Fenner F, Henderson DA, Arista I, Jezek Z, Ladnyi ID. 1988. The clinical features of smallpox, p 1–68. *In* Smallpox and its eradication. WHO, Geneva, Switzerland.

Original article

FUNNELL, S. G. P., TREE, J. A., HATCH, G. J., BATE, S. R., HALL, G., PEARSON, G., RAYNER, E. L., ROBERTS, A. D. G. & VIPOND, J. 2019. Dose-dependant acute or subacute disease caused by *Burkholderia pseudomallei* strain NCTC 13392 in a BALB/c aerosol model of infection. *J Appl Microbiol*, 127, 1224-1235.

Impact factor: 2.683

Contributions by HATCH, G. J.

Home Office – Personal Licence holder

Development and qualification of aerosol, biocontainment and clinical parameter systems. Performance of aerosol challenge.



Study management – Study design, liaison and co-ordination with sponsors, bacteriology, histology and in vivo teams, scheduling, reporting

Data analysis and manuscript review

Citation metrics

Google Scholar: 2 citations

ORIGINAL ARTICLE

Dose-dependant acute or subacute disease caused by *Burkholderia pseudomallei* strain NCTC 13392 in a BALB/c aerosol model of infectionS.G.P. Funnell , J.A. Tree , G.J. Hatch, S.R. Bate, G. Hall, G. Pearson, E.L. Rayner, A.D.G. Roberts and J. Vipond

National Infection Service, Public Health England (PHE), Salisbury, Wiltshire, UK

Keywordsaerosol, BALB/c, *Burkholderia*, dose, Melioidosis, *pseudomallei*, subacute.**Correspondence**Simon G.P. Funnell, National Infection Service, Public Health England, Porton Down, Salisbury, Wiltshire, SP4 0GJ, UK.
E-mail: simon.funnell@phe.gov.uk

2019/0625: received 9 April 2019, revised 21 June 2019 and accepted 25 June 2019

This article is published with the permission of the Controller of HMSO and the Queen's Printer for Scotland.

doi:10.1111/jam.14396

Abstract

Aims: The goal of this study was to examine, for the first time, the virulence and pathogenicity of aerosolized *Burkholderia pseudomallei*, strain NCTC 13392, in BALB/c mice in order to develop an animal model for testing novel medical countermeasures (MCMs) for the treatment of human acute and subacute (a disease state between acute and chronic) melioidosis.

Methods and Results: BALB/c mice were exposed to varying doses of aerosolized bacteria. Acute disease was seen in animals exposed to a very-high dose ($\geq 10^5$ CFU per animal) and death occurred 3–4 days postchallenge (pc). Bacteria were detected in the lungs, liver, kidney and spleen. In contrast, animals exposed to a low dose (< 10 CFU per animal) survived to the end of the study (day 30 pc) but developed weight loss, a bacterial tissue burden and increasing clinical signs of infection from day 20 pc onwards, mimicking a subacute form of the disease. Pathological changes in the tissues mirrored these findings.

Conclusions: This proof of concept study has shown that *B. pseudomallei* strain NCTC 13392 is virulent and pathogenic in BALB/c mice, when delivered by aerosol. By varying the doses of aerosolized bacteria it was possible to mimic characteristics of both human acute and subacute melioidosis, at the same time, within the same study.

Significance and Impact of the Study: *Burkholderia pseudomallei*, the aetiological agent of melioidosis, causes a serious and often fatal disease in humans and animals. Novel MCMs are urgently needed for both public health and biodefense purposes. The present model provides a useful tool for the assessment and evaluation of new MCMs (e.g. therapeutics and vaccines) and offers the potential for testing new treatments for both subacute to chronic and acute melioidosis prior to human clinical trials.

Introduction

Burkholderia pseudomallei, the aetiological agent of melioidosis, causes a serious and often fatal disease in humans and animals (Titball *et al.* 2008). Despite the global widespread geographical occurrence of naturally acquired melioidosis, particularly in Southeast Asia and Northern Australia (Limmathurotsakul *et al.* 2016), there is no licensed vaccine and antibiotic therapy is

problematic because *B. pseudomallei* is intrinsically resistant to many antibiotics (Wiersinga *et al.* 2006). Concerns over the use of *B. pseudomallei* as a biological weapon has resulted in this pathogen being classified as a Tier 1 Select Agent by the United States Federal Select Agent program (<http://www.selectagents.gov/>). Novel therapeutics and vaccines, otherwise known as medical countermeasures (MCMs), are needed for both public health and biodefense purposes.

Melioidosis can affect individuals with pre-existing health conditions such as diabetes mellitus (50% of cases) (Wiersinga *et al.* 2006). The disease can present a broad range of symptoms, with both acute and chronic phases. Acute disease can be severe with symptoms including fever, weight loss, pneumonia, sepsis and death (Currie *et al.* 2000; Boruah *et al.* 2013; Cheng *et al.* 2013; Jin and Ning, 2014). Chronic infection can be less severe and may present as abscesses distributed in single or multiple sites, including the spleen, lung, liver, joints and central nervous system (Wong *et al.* 1995; Kunnathuparambil *et al.* 2013; Liang *et al.* 2016). In addition, a latent or reactivated form of disease may appear years later: the longest recorded incubation period being 62 years (Ngauy *et al.* 2005). Humans can be infected naturally with *B. pseudomallei* following bacterial inoculation, inhalation or ingestion (Peacock *et al.* 2012). The route of infection and severity of disease are linked, with inhalation associated with a more rapid disease course (Titball *et al.* 2008).

Treatment for melioidosis involves an intensive intravenous antibiotic infusion phase for a minimum of 10–14 days followed by a lengthy eradication phase of 3–6 months of oral antibiotic therapy (Pitman *et al.* 2015). Given the multidrug-resistant nature of *B. pseudomallei* to common antibiotics and the lengthy treatment regime for melioidosis, new MCMs are urgently needed. However, the protective efficacy of new therapeutics and vaccines are difficult to assess in Phase III human clinical trials because of the low incidence of naturally acquired *B. pseudomallei* in most parts of the world. It is also difficult to establish the exact route of entry of infection in human trials conducted in endemic countries. For this reason, well-characterized animal models of infection, with well-defined endpoints relevant to human disease will help evaluate the efficacy of novel MCMs for use in humans.

The mouse model of melioidosis is commonly used for prescreening the effectiveness of novel therapeutics before they are tested in larger animal models. Prior to evaluation, however, the decision about which mouse strain, the route of infection and which strain of *B. pseudomallei* to use is challenging as a variety of studies have been reported (Jeddeloh *et al.* 2003; Titball *et al.* 2008; Lever *et al.* 2009; West *et al.* 2010; Conejero *et al.* 2011; Thomas *et al.* 2012; West *et al.* 2012; Lafontaine *et al.* 2013; Massey *et al.* 2014; Welkos *et al.* 2015; Trevino *et al.* 2018). Some studies show BALB/c mice to be more sensitive to infection with *B. pseudomallei* and thus help reflect acute human infection, while C57BL/6 have been shown to be more resistant and thus mimic chronic infection (Leakey *et al.* 1998; Hoppe *et al.* 1999; Liu *et al.* 2002; Tan *et al.* 2008; Bearss *et al.* 2017; Trevino *et al.*

2018). Conversely, a chronic model of infection in BALB/c mice has been recently reported which utilizes a strain of *B. pseudomallei* 1106a, which has low virulence, delivered intraperitoneally (Amemiya *et al.* 2015). Among the reported mouse studies, a variety of delivery routes have been used (aerosol, intratracheal, intranasal, intravenous and intraperitoneal); the aerosol challenge is the most useful route, if evaluating MCMs for biodefense purposes. Choosing a representative *B. pseudomallei* challenge strain is problematic because there is a high degree of genetic and phenotypic variability among *B. pseudomallei* isolates (Ronning *et al.* 2010; Van Zandt *et al.* 2012; Sarovich *et al.* 2014; Welkos *et al.* 2015; Trevino *et al.* 2018). There is also a lack of understanding of the impact of strain variation on virulence, pathogenicity and mortality in mice; although some studies seek to further define this (Massey *et al.* 2014; Sahl *et al.* 2015). New information about novel strains adds to this body of literature, thus further characterizing the murine experimental model of melioidosis and its alignment to human disease.

The purpose of the present proof of concept study was to characterize, for the first time, the virulence and pathogenicity of *B. pseudomallei* strain NCTC 13392 (Sahl *et al.* 2013) in a BALB/c aerosol infection model. This novel murine model provides the opportunity to study subacute disease (a disease state between acute and chronic) alongside acute disease in the same experiment following exposure to different aerosolized doses of bacteria. Initially a 14-day virulence study was performed followed by a 30-day pathogenesis study; clinical score, weight, bacterial burden and histopathology are reported.

Materials and methods

Bacterial strain

Burkholderia pseudomallei strain NCTC 13392, was obtained from PHE, Culture Collections, Porton Down, Salisbury, UK. This strain was originally isolated from a septicaemic, diabetic patient with fatal melioidosis, in Khon Kaen, Thailand in 1996 at the same time as strain K96243 (Sahl *et al.* 2013). Whole genome sequencing was performed, on the isolate used in this study, using an Illumina HiSeq system.

Experimental animals

Healthy BALB/c female mice (purchased from UK Home Office accredited suppliers, Charles Rivers UK, Ltd and Envigo CRS Ltd, UK) were used, aged 10–12 weeks and weighing 18 g or more at the time of challenge. They were group housed in cages in accordance with the UK Home Office Code of Practice for the Housing and Care of

Animals Bred, Supplied or Used for Scientific Procedures (December 2014) at Advisory Committee on Dangerous Pathogens (ACDP) containment level 3 and provided with access to food and water *ad libitum*. All experimental work was conducted under the authority of a UK Home Office approved project licence that had been subject to local ethical review at PHE Porton Down by the Animal Welfare and Ethical Review Body (AWERB) as required by the *Home Office Animals (Scientific Procedures) Act 1986*. Before the start of each experiment, animals were randomly assigned to the treatment groups in order to minimize bias.

Culture conditions

Each culture of *B. pseudomallei* NCTC 13392 was prepared from a fresh vial of working stock on plates of Luria-Bertani Agar (LBA). Plates were incubated for 24–48 h at 37°C. Growth from one LBA plate was suspended in 10 ml of Luria-Bertani Broth (LBB) to yield an undiluted primary seed. The primary seed was further diluted in LBB to achieve a 100 ml culture with an optical density (OD) OD_{600} of 0.1. This was incubated with orbital shaking at 175 rev min⁻¹ for 24 h at 37°C and used in the aerosol inoculation procedures.

Aerosol procedures

The 24 h LBB broth culture of *B. pseudomallei* NCTC 13392 was diluted in phosphate-buffered saline (PBS) to achieve the target presented doses which were nominally grouped as follows: very-high dose ($\geq 10^3$ CFU per animal), high dose (10^2 to $<10^3$ CFU per animal), medium dose (10 to $<10^2$ CFU per animal) and low dose (<10 CFU per animal).

All mice were exposed to a small particle aerosol (mass medium aerodynamic diameter $\sim 1.5 \mu\text{m}$) of bacteria in an AeroMP-Henderson apparatus. The challenge aerosol was generated using a three-jet Collision Nebuliser (BGI, Inc., Waltham, MA); the aerosol was mixed with conditioned air in the spray tube and delivered to the nose of each animal through an exposure tube in which nonanaesthetized mice were held in restraint tubes. Samples of the aerosol were collected in PBS using an AGI30 glass impinger (Ace Glass, Inc., Vineland, NJ), and the mean particle size was determined with an aerodynamic particle sizer (TSI Instruments, Ltd., High Wycombe, UK). These processes were controlled and monitored from an AeroMP management platform (Biaera Technologies, Hagerstown, MD). The control animals were challenged with an aerosol produced from LBB/PBS in the same ratio as the bacterial challenge preparation. The presented dose was calculated using the results of bacterial

enumeration of aerosol samples taken throughout exposure and estimates of respired volume calculated using Guyton's formula (Guyton, 1947).

Virulence study

In order to determine the virulence of *B. pseudomallei* NCTC 13392, an initial short-term (14 day) survival study using 35 BALB/c mice was performed. Very high, high and medium doses were delivered by aerosol to three separate groups of 10 mice. Control mice ($n = 5$) were sprayed with sterile LBB/PBS broth. At 14 days postchallenge (pc), the surviving animals were killed humanely with an intraperitoneal overdose of pentobarbitone (Dolethal, Vetoquinol UK Ltd, 140 mg kg⁻¹).

Pathogenesis study

In order to determine the pathogenicity of *B. pseudomallei* NCTC 13392, a longer term (30 day) study was conducted using 60 BALB/c mice. Three aerosol doses were delivered to three groups of mice: very high ($n = 15$ animals), high ($n = 20$) and low ($n = 20$). Groups of five mice were euthanized on scheduled days. For the very-high-dose group mice, were scheduled for euthanasia on day 1 ($n = 5$), day 3 ($n = 5$) and day 4 ($n = 5$). For the high-dose group, mice were euthanized on day 3 ($n = 5$), day 10 ($n = 5$), day 20 ($n = 5$) and day 30 ($n = 5$); a similar schedule was used for the low-dose group. The control animals ($n = 5$) were sprayed with sterile LBB/PBS and euthanized on day 14. On the day of euthanasia, organs were collected for bacterial burden and histopathological examination.

Clinical and euthanasia observations

Animals were weighed at the same time of day from the day before infection until the end of the experiment, or until death or euthanasia. Animals were examined twice daily for clinical signs of disease and scores were recorded using a 'clinical observation score'. Monitoring of animals increased to at least four times daily during critical periods in the study (at times when septicaemia was likely to occur or as soon as clinical signs of septicaemia were detected). Clinical signs of disease were assigned a score based upon the following criteria: healthy, 0; ruffled fur, 2; arched back, 3; eyes shut, 3; immobile, 9; euthanasia or death in cage, 10. Clinical scores were not used to trigger euthanasia. In order to meet the requirement of the project license, three criteria for immediate euthanasia were used: (i) immobility defined as a lack of movement even after stimulus such as handling, (ii) neurological signs including repetitive or unusual movement, (iii) weight loss of more than 20% from baseline for more

than 24 h. If any animal reached any of these three euthanasia criteria, they were immediately euthanized using a UK Home Office approved Schedule 1 procedure.

Bacteriology

At necropsy, the same tissues were collected from each animal: the left lobe of the lung, the apical section of the spleen, a section from the right lateral lobe of the liver and the left section of the kidney. These tissues were frozen below -50°C . Tissue was thawed and homogenized in LBB with 1.4-mm ceramic beads in a Precellys24 tissue homogenizer (Bertin Technologies, Villeurbanne, France). Serial 10-fold dilutions of tissue homogenates were plated on LBA. Bacterial colonies were counted after incubation for 48 h at 37°C .

Pathology studies

Throughout the pathogenesis study, gross abnormalities were recorded. At necropsy, following the collection of samples for bacteriology, samples of lung, liver and kidney were collected for histopathological examination. They were placed in 10% neutral buffered formalin, processed routinely to paraffin wax and 3–5- μm sections cut and stained with haematoxylin and eosin (H and E).

Statistical analysis

The Kaplan–Meier method was used to plot the survival data from the virulence study. Differences in the number of CFUs in tissues, on different days, were determined by performing Student's *t*-tests using 95% confidence interval on \log_{10} transformed data. All combinations were tested, that is, day 10 vs day 20, day 20 vs day 30, etc.) Differences that were significant at $P < 0.05$ are reported. All analyses were done using Minitab version 16.

Results

Whole-genome sequencing

Whole-genome sequencing of the isolate used in this study was conducted by PHE for verification purposes (data not shown). The sequence showed identity (within 6–8 SNPs) with the strain supplied by PHE to Northern Arizona University, Center for Microbial Genetics and Genomics, Flagstaff, Arizona, USA who first published the genome of NCTC 13392 in 2013 (Sahl *et al.* 2013).

Virulence study

Animals exposed to the very-high dose (3.33×10^3 CFU per animal) of aerosolized *B. pseudomallei* NCTC 13392

died (10/10) within 3 days (Fig. 1). Those challenged with the high dose (7.85×10^2 CFU per animal) survived longer, but died by day 6 pc. In the group given the medium dose (6.85×10^1 CFU per animal), 9 of 10 animals survived beyond the end of the experiment at 14 days. Information gained from this virulence study was used to determine the doses for the pathogenesis study.

Pathogenesis study

Animals exposed to the very high dose (3.04×10^3 CFU per animal) of aerosolized *B. pseudomallei* NCTC 13392 where scheduled to be euthanized on days 1 ($n = 5$), 3 ($n = 5$) and 4 ($n = 5$) pc; however, some animals in the day 4 group met euthanasia criteria early, on day 3, and were thus included in the day 3 group ($n = 8$). This meant only two animals remained and they were euthanised on day 4, as planned. Those challenged with the high dose (1.11×10^2 CFU per animal) survived to the end of the study (day 30). Those animals in the low-dose group (7.69×10^0 CFU per animal) also survived to the end of the study.

Clinical signs

In the pathogenesis study, all 15 animals challenged with a very high dose of *B. pseudomallei* developed high

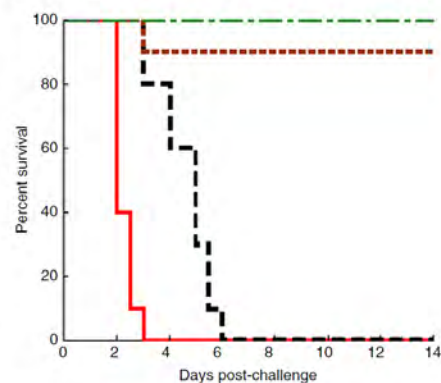


Figure 1 Virulence study: Fourteen-day survival rate of BALB/c mice infected with aerosolized *Burkholderia pseudomallei*. BALB/c mice were infected with different doses; very high (3.33×10^3 CFU per animal) (—) (solid line), high (7.85×10^2 CFU per animal) (---) (dashed line) and medium (6.85×10^1 CFU per animal) (· · ·) (dotted line) doses of *B. pseudomallei* and the 14-day survival rates of mice were plotted, using the Kaplan–Meier Method. The control group (– · –) (dash-dot-dash line). [Colour figure can be viewed at wileyonlinelibrary.com]

clinical scores (8.4) and progressed rapidly to death (Fig. 2a). Ruffled fur was present from 24 h pc, followed by lethargy with arched backs which progressed to immobility or death by 3–4 days in all the animals. Animals ($n = 20$) exposed to the high dose developed clinical signs at day 3 pc that abated slightly until day 5 when signs re-emerged and the health of animals deteriorated slowly, with ruffled fur and arched backs being common (Fig. 2a). The mean individual clinical score increased to 7 by the end of the study (day 30 pc), when the remaining animals (5/5) were killed humanely. Animals ($n = 20$) exposed to the low dose displayed few clinical signs initially (2/5 animals had ruffled fur); these abated until day 20 pc. From day 20 pc, the mean individual clinical score began to increase, reaching 3.2 on day 30 pc (5/5 animals had ruffled fur and 2/5 animals had arched backs). Animals in the control group (5/5), killed humanely on day 14 pc, remained free of clinical signs throughout the study (data not shown).

Body weight

Animals in the very-high-dose group lost up to 18% of body weight, compared to baseline levels, within 3 days following challenge (Figure 2b). Animals challenged with the high dose lost 7% of their body weight by day 3 but then regained (5%) weight quickly within 24 h, afterwards there was a slow, consistent weight loss for the next 15 days. Weight change in the low-dose group was similar to animals in the control group (Figure 2b) up to day 14. On day 20, an increase in weight (6%) was observed compared to baseline levels; however, after this animals lost 10% of their body weight by day 30 (4% lower than at the start of the experiment).

Bacteriological studies

In the very-high-dose group, of the four tissues tested, the highest mean concentration of bacteria was in the lung (2.2×10^3 CFU per mg) on day 1 (Figure 3). By days 3–4 pc this significantly ($P < 0.05$) rose to an average of 3.9×10^5 CFU per mg (9/10 animals). In the spleen, kidney and liver (10/10 animals), bacteria were present at low levels (≤ 8 CFU per mg) on day 1, increasing significantly ($P < 0.05$) by days 3–4 to means of 1.2×10^4 , 1.9×10^2 and 3.0×10^3 CFU per mg tissue respectively.

In the high-dose group, bacteria were detected in 4 of 5 animals in the lung and in 1 of 5 animals in the spleen on day 3 pc. Bacterial numbers in the spleen (5/5) increased significantly ($P < 0.001$) peaking on day 20 (average 2.5×10^4 CFU per mg), whereas bacterial counts decreased (5/5) in the lung by day 20 (≤ 1 CFU per mg). Between days 20 and 30 pc, there was a rise in bacterial counts in the lung,

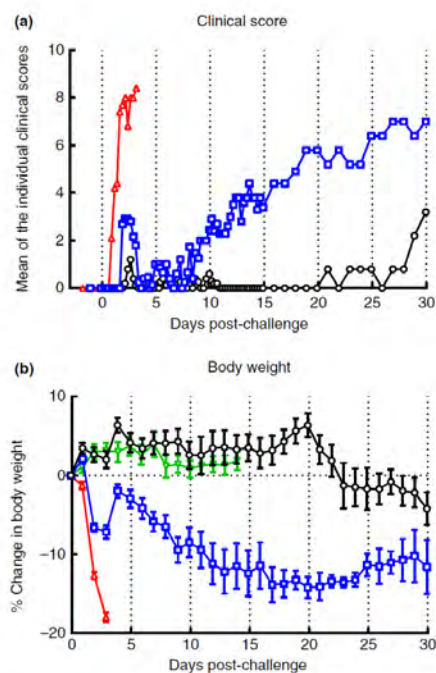


Figure 2 Pathogenesis study: Individual clinical scores and change in percentage body weight after aerosol challenge with *Burkholderia pseudomallei* or vehicle control. Bacteria were presented in an aerosol (via a Henderson apparatus using three different doses) to BALB/c mice ($n = 60$). The presented doses were: very high (3.04×10^5 CFU per animal) (\blacktriangle), high (1.11×10^5 CFU per animal) (\blacksquare) and low (7.69×10^3 CFU per animal) (\circ). Mice ($n = 20$ per dose at the start of the experiment) were monitored for clinical signs of infection and body weight changes. Results are expressed as (a) mean of the individual clinical scores (NB, control group (∇) had a zero clinical score throughout the study, data not plotted), and (b) the mean percentage (%) change in body weight compared to baseline levels, ± 1 SE. [Colour figure can be viewed at wileyonlinelibrary.com]

peaking at an average 1.9×10^3 CFU per mg. In the spleen a significant ($P < 0.05$) reduction in the mean number of bacteria was observed (mean, 9.7×10^2 CFU per mg). Throughout the course of the study there was a gradual rise in the number of bacteria in the kidney and liver; by day 30 pc these had reached mean levels of 2.7×10^2 and 4.6×10^2 CFU per mg respectively.

In the low-dose group, only 1 of 5 animals had detectable levels of bacteria in the lungs (3.9×10^3 CFU per mg) at 3 days pc and 1 of 5 animals on day 10 pc

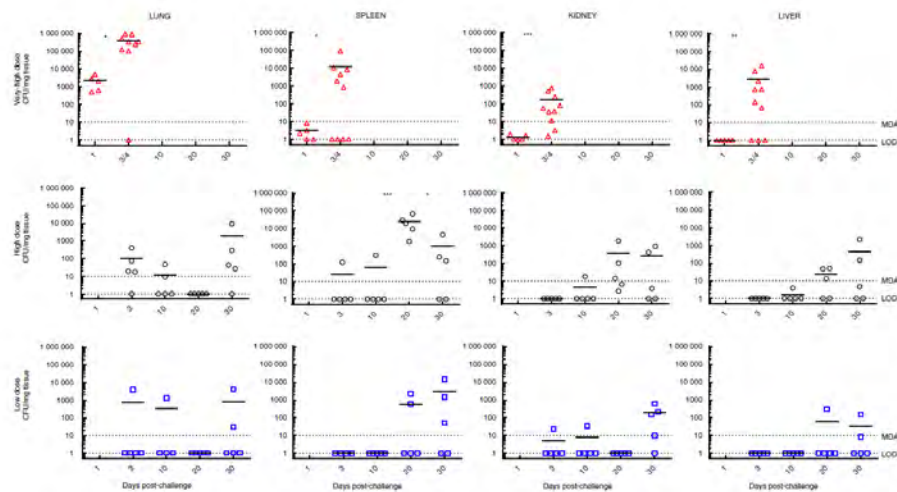


Figure 3 Pathogenesis study: Bacterial loads in the lungs, kidney, spleen and liver. Bacteria were presented in an aerosol (via a Henderson apparatus using three different doses) to BALB/c mice ($n = 60$). The presented doses were: very high (3.04×10^3 CFU per animal) (Δ); high (1.11×10^2 CFU per animal) (\square) and low (7.69×10^0 CFU per animal) (\circ). At predetermined time points postinoculation (see Materials and methods), mice ($n = 5$) were euthanized and various postmortem tissues collected. The tissues were stored frozen and subsequently thawed and homogenized so that bacterial tissue burdens could be determined. Individual results are plotted plus geometric mean, bar. For the very-high-dose group, the data for days 3 and 4 have been plotted together for graphical purposes to enable a comparison across all data sets (the study terminated on days 3/4). For the low- and high-dose groups, animals were not culled on day 1. For graphical presentation all samples that were below the limit of detection (LOD) were assigned a nominal value equivalent to the LOD (1.0 CFU per mg tissue). The minimum detectable amount varied between tissues but is shown for illustration purposes only. Significant differences between the tissue loads are indicated by asterisk * $P < 0.05$, ** $P < 0.01$ and *** $P < 0.001$, the data sets acquired on different days were compared, for example, for the very-high-dose group day 1 vs day 3/4 were compared for each tissue type. [Colour figure can be viewed at wileyonlinelibrary.com]

(1.3×10^3 CFU per mg). Bacteria were not detected on day 20 pc in 5 of 5 animals (≤ 1 CFU per mg, limit of detection) in the lungs. However, by day 30 pc, infection was re-established in the lungs of 2 of 5 animals (mean 2×10^3 CFU per mg, $n = 2$). Similarly in the kidney, bacteria (2.2×10^1 CFU per mg) were present in 1 of 5 animals on day 3 pc and in 1 of 5 animals (3.4×10^1 CFU per mg) on day 10 pc. Bacteria were not detected on day 20 pc, but again infection was re-established in 4 of 5 animals by day 30 (2.4×10^2 CFU per mg, $n = 4$). No bacteria were detected in the liver or spleen on days 3 and 10 pc; however, by day 20, bacteria were found in 2 of 5 animals (mean 1.4×10^3 CFU per mg, $n = 2$) in the spleen and in 1 of 5 animals in the liver (3×10^2 CFU per mg). By day 30 pc, 3 of 5 and 2 of 5 animals had bacteria in the spleen and liver respectively. *Burkholderia pseudomallei* were not isolated from the tissues of control animals.

Histopathology findings

The findings for all groups are summarized in Table 1. Five lesion types were seen in lung that were associated with infection with *B. pseudomallei*. These comprised: parenchymal, multifocal pyogranulomatous inflammation, with either central necrosis (A), or the lesions were non-necrotic (B); patchy, interstitial, histiocytic inflammation, variably accompanied by neutrophils (C); bronchial and bronchiolar inflammatory cell infiltrates (D); and bronchial and bronchiolar epithelial cell necrosis (E). In the spleen, multifocal, necrotizing splenitis with neutrophils \pm lymphocytes, with cellular degeneration (necrosis/apoptosis) (F), and large, well-demarcated pyogranulomatous foci (abscesses) (G), were observed. In the liver, two lesions were noted, namely random, multifocal, necrotizing hepatitis \pm neutrophils (H), and hepatocyte degeneration and focal inflammatory cell infiltrate (I).

Very-high-dose group

No animal survived beyond day 4 pc. In the lung at day 1, lesions B-E were present with varying frequency (Fig. 4a). Necrosis was not observed within pyogranulomas (A) until day 3 pc (Fig. 4b). In the spleen, changes were absent on day 1 pc. By days 3 and 4 pc, necrotizing splenitis (F) was the only lesion type observed, and present in a proportion of animals (Fig. 4c). In the liver, necrotizing hepatitis (H) was seen in a proportion of animals at each time point pc (Fig. 4d).

High-dose group

Lesions were assessed at 3, 10, 20 and 30 days pc. Lung lesions A and B, namely pyogranulomatous inflammation in the presence or absence of necrosis, were common at day 3 pc and less common subsequently (Fig. 5a). In contrast, lesions C-E were observed frequently at the later time points. In the spleen, necrotizing splenitis (F) was limited to one animal at day 20 pc. Pyogranulomas (G) were not seen at day 3 pc, but were common at days 10, 20 and 30 (Fig. 5b). In the liver, both lesion types H and I were seen frequently at all time points pc.

Low-dose group

Lesions were assessed at 3, 10, 20 and 30 dpc. In the lung, interstitial histiocytic inflammation (C) was the most frequently observed lesion type at all time points. The remaining changes were seen occasionally (Figure 5c, d). In the spleen, both splenitis (F) and pyogranulomas (G) were present at all time points. In the liver, both lesion types H and I were seen frequently at all time points pc. Histopathological changes were not detected in the kidney in any animal in any group.

Discussion

Well-characterized animal models are needed to better understand the pathogenic process of infection by aerosolized *B. pseudomallei* (Massey *et al.* 2014). Animal models are also needed to help evaluate the efficacy of novel therapeutics because Phase III human clinical trials are difficult to perform. This study reports on, for the first time, the virulence and pathogenicity of *B. pseudomallei* NCTC 13392 in BALB/c mice where both acute and subacute disease were observed following challenge with different aerosolized doses of bacteria.

Table 1 Histological features of pathogenesis study. A summary of treatment-related changes in the lung, spleen and liver on different days. Number of animals with treatment-related changes/total number of animals. No changes were observed in the kidney of any animal in any group

Organ	Lesion	Exposure dose (no. of animals with treatment-related changes/total no. of animals)											
		Very high dose			High dose			Low dose					
		Days postchallenge											
		1	3	4	—	3	10	20	30	3	10	20	30
Lung	Parenchymal, multifocal, necrotizing, pyogranulomatous inflammation	0/5	3/8	2/2	—	2/5	0/5	1/5	1/5	1/5	1/5	1/5	0/5
	Parenchymal, multifocal, pyogranulomatous inflammation	5/5	8/5	2/0	—	3/5	0/5	1/5	1/5	0/5	1/5	1/5	0/5
	Patchy, interstitial histiocytic inflammation ± neutrophils	2/5	5/8	2/2	—	3/5	2/5	5/5	4/5	2/5	2/5	3/5	4/5
	Bronchial/bronchiolar inflammatory cell exudates	4/5	7/8	2/2	—	3/5	0/5	1/5	0/5	2/5	1/5	1/5	0/5
	Bronchial/bronchiolar epithelial cell necrosis	1/5	3/8	0/2	—	0/5	0/5	1/5	0/5	2/5	1/5	1/5	0/5
		5/5	8/5	2/0	—	5/5	5/5	5/5	5/5	5/5	5/5	5/5	5/5
Spleen	Multifocal, necrotizing splenitis with neutrophils ± lymphocyte necrosis/apoptosis	0/5	2/8	2/2	—	0/5	0/5	1/5	0/5	4/5	1/5	1/5	4/5
	Large, well-demarcated pyogranulomatous foci (abscess)	0/5	0/8	0/2	—	0/5	2/5	5/5	3/5	0/5	2/5	4/5	3/5
		5/5	8/5	2/0	—	5/5	5/5	5/5	5/5	5/5	5/5	5/5	5/5
Liver	Random, multifocal, necrotizing hepatitis ± neutrophils	1/5	4/8	2/2	—	2/5	3/5	2/5	4/5	1/5	3/5	1/5	2/5
	Hepatocyte degeneration and focal inflammatory cell infiltrate	0/5	0/8	0/2	—	3/5	5/5	4/5	4/5	3/5	4/5	4/5	4/5
		5/5	8/5	2/0	—	5/5	5/5	5/5	5/5	5/5	5/5	5/5	5/5

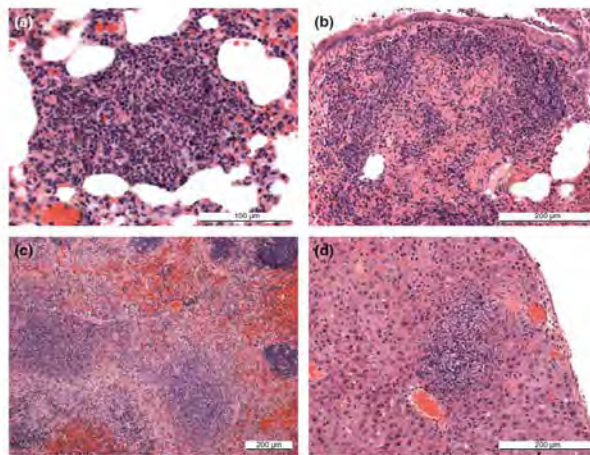


Figure 4 Pathogenesis study: Examples of lesions. (a) Lung, very-high-dose group, 1 day pc. Focal, pyogranulomatous inflammation. (b) Lung, very-high-dose group, 3–4 days pc. Focal, necrotizing, pyogranulomatous inflammation. (c) Spleen, very-high-dose group, 3–4 days pc. Multifocal, coalescing, necrotizing splenitis in the red and white pulp. (d) Liver, very-high-dose group, day 1 pc. Focal, necrotizing hepatitis (All sections stained with haematoxylin and eosin). [Colour figure can be viewed at wileyonlinelibrary.com]

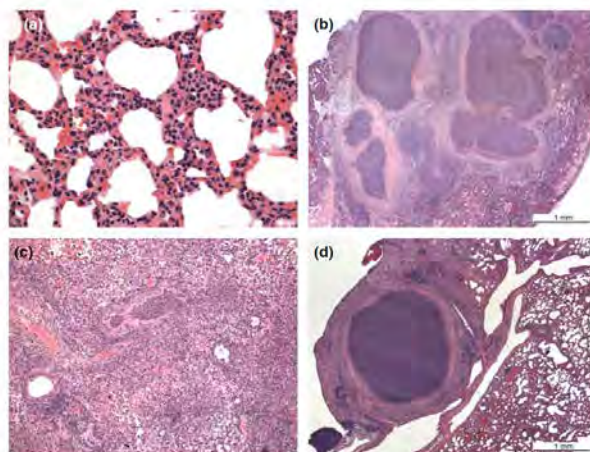


Figure 5 Pathogenesis Study: Examples of lesions. (a) Lung, high-dose group, day 10 pc. Patchy, interstitial, histiocytic cell infiltration of alveolar walls, with scattered neutrophils. (b) Spleen, high-dose group, 10 days pc. Coalescing, large, well-demarcated, pyogranulomatous foci (abscesses). (c) Lung, low-dose group, 3 days pc. Prominent, bronchial and bronchiolar inflammatory cell exudates, comprising primarily neutrophils, filling lumina (arrow), surrounded by necrotizing, pyogranulomatous inflammation. (d) Lung, low-dose group, 10 days pc. Well-demarcated, pyogranuloma (abscess) surrounded by fibrosis and inflammatory cells (All sections stained with haematoxylin and eosin). [Colour figure can be viewed at wileyonlinelibrary.com]

Acute disease was observed when BALB/c mice were challenged with a very high dose ($>10^3$ CFU per animal) of *B. pseudomallei* NCTC 13392. Animals succumbed to the disease very quickly and died within 3–4 days following exposure. Acute disease was characterized by mean high individual clinical scores of 8.4 (comprising ruffled fur, arched backs and lethargy) and weight loss (up to 18%). In people, acute disease is characterized by a range of symptoms including weight loss, fever, pneumonia, sepsis and death (Currie *et al.* 2000; Boruah *et al.* 2013; Cheng *et al.* 2013; Jin and Ning, 2014). In people, the lung is the most commonly affected organ. Changes in the lung, described in the current study, are similar to those described in human disease, where the initial presenting signs are associated with pneumonia or primary lung abscesses (White, 2003).

In addition to the lung, in humans, seeding and abscess formation can arise in any organ; the liver, spleen, skeletal muscle and prostate being common sites (White 2003). A recent fatal case of melioidosis, describes how a male suffered a fever for a week prior to death and at postmortem the lung, liver and spleen contained multiple microabscesses (<1 cm diameter) and neutrophilic infiltration with occasional giant cells (Tan *et al.* 2019), all sites were microbiological culture positive for *B. pseudomallei*. Similarly, in the present study, during acute disease, bacteria were found in the spleen, liver, kidney and the highest bacterial burden (3.9×10^5 CFU per mg) was in the lungs of mice, on days 3–4 pc. The pathological changes in the mouse lung, seen here, are similar to those described in human disease (White, 2003). Overall many of the pathogenic characteristics of *B. pseudomallei* NCTC 13392 infection in the present mouse study align with those seen in acute human disease, demonstrating that this bacterial strain, aerosolized dose and mouse model are suitable for evaluating MCMs against acute melioidosis.

The characteristics of subacute melioidosis were also observed in the present study when BALB/c mice were exposed to a low dose of NCTC 13392 (<10 CFU per animal). Here, low clinical scores (≤ 1.2) were observed initially; these subsided until day 20 pc. Afterwards clinical scores began to increase to a mean of 3.2 by day 30 pc, weight loss (4%) was also seen. This pattern of symptoms mimics human subacute/chronic infection; in humans, chronic melioidosis is characterized as a symptomatic infection that lasts >2 months; the nonspecific signs and symptoms, during the incubation period, can often hinder the diagnosis and treatment of this disease (Wiersinga *et al.* 2018). In this study, on day 10 pc, hepatic abscesses were present and hepatic degeneration and inflammation was observed, which is consistent with subacute/chronic infection. On day 30 pc, bacteria were

found in multiple sites and microscopic lesions (pyogranulomas/abscesses), attributable to *B. pseudomallei* infection, were noted in most mice. This is consistent with human subacute/chronic disease, where abscesses in different organs are seen (White, 2003). In the present proof of concept study a model for subacute human infection is described, and thus therapeutics could be prescreened to assess their effectiveness against subacute/chronic disease. The model requires further refinement and would benefit from larger animal numbers per treatment group to enable statistical significance and also a longer study duration (e.g. 60 days).

In the present pathogenesis study, BALB/c survivors exposed to the low and high dose showed clinical signs, histological features of infection and weight loss by day 30; these are clearly indicators of a subacute infection. If this study was longer in duration then these animals may have fully succumbed to the disease and died. The subacute characteristic of *B. pseudomallei* NCTC 13392 has made the accurate estimation of an LD₅₀ for this strain difficult to ascertain. Using the virulence study data (14 day duration) an estimated LD₅₀ of approximately 200 CFU could be determined; however, the data obtained from the 30-day duration pathogenesis experiment indicates that an LD₅₀ of <8 CFU should be used for NCTC 13392. The true LD₅₀, however, can only be found by performing a study with a longer observation period (e.g. 60–100 days). Other researchers have also noted a lowering of LD₅₀ values, in mice, when they compared the LD₅₀ results from 21-day and 60-day duration intraperitoneal infection studies with other strains of *B. pseudomallei* (Welkos *et al.* 2015). Recent low-dose, aerosol challenge studies comparing different clinical isolates of *B. pseudomallei* in BALB/c mice describe an LD₅₀ value of 25.1 CFU for K96243 (prototype strain), 0.99 CFU for HBPUB10134a and 0.35 CFU for MSHR5855 (Trevino *et al.* 2018). A working hypothesis is that the virulence of NCTC 13392 falls somewhere between these strains. A property of NCTC 13392 in particular, is that the LD₅₀ is likely to be inversely proportional to the study length due to its subacute characteristics, at low dose. The bacterial burden in the lungs and spleens of BALB/c mice infected with HBPUB10134a and MSHR5855 (delivered by aerosol with doses 6 CFU and 1.2 CFU respectively) is higher than mice infected with a low dose (8 CFU) of NCTC 13392 at day 10 pc, indicating that the infection caused by these other two strains, at low doses, becomes established more quickly (Trevino *et al.* 2018).

Currently most MCMs for melioidosis are evaluated in animal models for their effectiveness against acute disease; the mouse model being the most widely used (Warawa, 2010) although larger animal models have been

evaluated for instance: Rhesus macaques (Yingst, Face-mire *et al.* 2014); African Green monkeys (Yeager *et al.* 2012) and marmosets (Nelson *et al.* 2011; Nelson *et al.* 2014; Nelson *et al.* 2015). Aerosolized doses of <10 CFU per animal *B. pseudomallei* NCTC 13392 caused a lethal infection by day 3–4 in marmosets, indicating these animals are highly susceptible to this strain (Nelson *et al.* 2011; Erratum, 2013). Overall there is a need to focus on defining acute disease and developing MCMs because of the potential for *B. pseudomallei* to be used as a biological weapon (Kwon *et al.* 2018). Studies on aerosol delivery are particularly important to help characterize the natural history of inhalational exposure to *B. pseudomallei* in a deliberate-release scenario, where the inoculum is likely to be much higher than exposure from an environmental source (Gilad *et al.* 2007). Fewer MCMs are tested for their effectiveness against chronic disease and it remains unclear whether treatment recommendations for this condition remain the same as for acute melioidosis (Currie *et al.* 2000; Nandi and Tan, 2013). Chronic disease is usually a public health concern often arising from a low-dose environmental exposure in a country where this disease is endemic. There are fewer animal models for subacute/chronic melioidosis (Warawa, 2010; Conejero *et al.* 2011; Sofiler *et al.* 2012; Amemiya *et al.* 2015; Bearss *et al.* 2017).

In conclusion, the present proof of concept study has, for the first time, shown that *B. pseudomallei* NCTC 13392 is virulent and lethality is dose dependant, when delivered by aerosol to BALB/c mice; thus, this strain is suitable for use in MCM evaluation studies. Both acute and subacute melioidosis disease can also be modelled with this strain by adjusting the challenge dose. Following further refinement, this combination of mouse strain, bacterial strain and dosing regime, will provide a useful toolkit for the preliminary screening of the effectiveness of novel vaccines or therapeutics for both acute and subacute melioidosis, at the same time.

Acknowledgements

The authors gratefully acknowledge the support from the Biological Investigations Group, the BPEG Bacteriology group and the Histology department at the National Infection Service, PHE, Porton Down, United Kingdom. The authors also fully appreciate assistance with whole-genome sequencing and analysis from Professor Sharon Peacock, University of Cambridge and Dr Michael Elmore, Dr Edward Burnett and Dr Julie Russell from PHE, Porton Down. The views expressed in this paper are those of the authors and not necessarily those of the

funding body. This work was fully funded by NIAID [contract number: N01-A1-30062 Task Order C19].

Conflicts of Interest

No conflicts of interest declared.

References

- Amemiya, K., Dankmeyer, J.L., Fetterer, D.P., Worsham, P.L., Welkos, S.L. and Cote, C.K. (2015) Comparison of the early host immune response to two widely diverse virulent strains of *Burkholderia pseudomallei* that cause acute or chronic infections in BALB/c mice. *Microb Pathog* **86**, 53–63.
- Bearss, J.J., Hunter, M., Dankmeyer, J.L., Fritts, K.A., Klimko, C.P., Weaver, C.H., Shoe, J.L., Quirk, A.V. *et al.* (2017) Characterization of pathogenesis of and immune response to *Burkholderia pseudomallei* K96243 using both inhalational and intraperitoneal infection models in BALB/c and C57BL/6 mice. *PLoS ONE* **12**, e0172627.
- Boruah, D.K., Prakash, A., Bora, R. and Buragohain, L. (2013) Acute pulmonary melioidosis in a child: a case report and review of literature. *Indian J Radiol Imaging* **23**, 310–312.
- Cheng, A.C., Currie, B.J., Dance, D.A., Funnell, S.G., Limmathurotsakul, D., Simpson, A.J. and Peacock, S.J. (2013) Clinical definitions of melioidosis. *Am J Trop Med Hyg* **88**, 411–413.
- Conejero, L., Patel, N., De Reynal, M., Oberdorf, S., Prior, J., Felgner, P.L., Titball, R.W., Salguero, F.J. *et al.* (2011) Low-dose exposure of C57BL/6 mice to *Burkholderia pseudomallei* mimics chronic human melioidosis. *Am J Pathol* **179**, 270–280.
- Currie, B.J., Fisher, D.A., Anstey, N.M. and Jacups, S.P. (2000) Melioidosis: acute and chronic disease, relapse and re-activation. *Trans R Soc Trop Med Hyg* **94**, 301–304.
- Erratum (2013) Erratum. *Int J Exp Pathol* **94**, 74.
- Gilad, J., Harary, I., Dushnitsky, T., Schwartz, D. and Amsalem, Y. (2007) *Burkholderia mallei* and *Burkholderia pseudomallei* as bioterrorism agents: national aspects of emergency preparedness. *Isr Med Assoc J* **9**, 499–503.
- Guyton, A.C. (1947) Measurement of the respiratory volumes of laboratory animals. *Am J Physiol* **150**, 70–77.
- Hoppe, I., Brenneke, B., Rohde, M., Kreft, A., Haussler, S., Reganzerowski, A. and Steinmetz, I. (1999) Characterization of a murine model of melioidosis: comparison of different strains of mice. *Infect Immun* **67**, 2891–900.
- Jeddeloh, J.A., Fritz, D.L., Waag, D.M., Hartings, J.M. and Andrews, G.P. (2003) Biodefense-driven murine model of pneumonic melioidosis. *Infect Immun* **71**, 584–587.
- Jin, J.L. and Ning, Y.X. (2014) Septicemic melioidosis: a case report and literature review. *J Thorac Dis* **6**, E1–E4.

- Kunnathuparambil, S.G., Sathar, S.A., Tank, D.C., Sressh, S., Mukunda, M., Narayanan, P. and Vinayakumar, K.R. (2013) Splenic abscess due to chronic melioidosis in a patient previously misdiagnosed as tuberculosis. *Ann Gastroenterol* **26**, 77–79.
- Kwon, E.H., Reisler, R.B., Cardile, A.P., Cieslak, T.J., D'Onofrio, M.J., Hewlett, A.L., Martins, K.A., Ritchie, C. *et al.* (2018) Distinguishing respiratory features of category A/B potential bioterrorism agents from community-acquired pneumonia. *Health Secur* **16**, 224–238.
- Lafontaine, E.R., Zimmerman, S.M., Shaffer, T.L., Michel, F., Gao, X. and Hogan, R.J. (2013) Use of a safe, reproducible, and rapid aerosol delivery method to study infection by *Burkholderia pseudomallei* and *Burkholderia mallei* in mice. *PLoS ONE* **8**, e76804.
- Leakey, A.K., Ulett, G.C. and Hirst, R.G. (1998) BALB/c and C57Bl/6 mice infected with virulent *Burkholderia pseudomallei* provide contrasting animal models for the acute and chronic forms of human melioidosis. *Microb Pathog* **24**, 269–275.
- Lever, M.S., Nelson, M., Stagg, A.J., Beedham, R.J. and Simpson, A.J. (2009) Experimental acute respiratory *Burkholderia pseudomallei* infection in BALB/c mice. *Int J Exp Pathol* **90**, 16–25.
- Liang, C.C., Chen, S.Y., Chen, T.Y. and Chen, S.T. (2016) Central nervous system melioidosis mimics malignancy: a case report and literature review. *World Neurosurg* **89**, 732.e19–23.
- Limmathurotsakul, D., Golding, N., Dance, D.A., Messina, J.P., Pigott, D.M., Moyes, C.L., Rolim, D.B., Betherat, E. *et al.* (2016) Predicted global distribution of *Burkholderia pseudomallei* and burden of melioidosis. *Nat Microbiol* **1**, 15008.
- Liu, B., Koo, G.C., Yap, E.H., Chua, K.L. and Gan, Y.H. (2002) Model of differential susceptibility to mucosal *Burkholderia pseudomallei* infection. *Infect Immun* **70**, 504–511.
- Massey, S., Yeager, L.A., Blumentritt, C.A., Vijayakumar, S., Sbrana, E., Peterson, J.W., Brasel, T., Leduc, J.W. *et al.* (2014) Comparative *Burkholderia pseudomallei* natural history virulence studies using an aerosol murine model of infection. *Sci Rep* **4**, 4305.
- Nandi, T. and Tan, P. (2013) Less is more: *Burkholderia pseudomallei* and chronic melioidosis. *MBio* **4**, e00709–13.
- Nelson, M., Dean, R.E., Salguero, F.J., Taylor, C., Pearce, P.C., Simpson, A.J. and Lever, M.S. (2011) Development of an acute model of inhalational melioidosis in the common marmoset (*Callithrix jacchus*). *Int J Exp Pathol* **92**, 428–435.
- Nelson, M., Salguero, F.J., Dean, R.E., Ngugi, S.A., Smither, S.J., Atkins, T.P. and Lever, M.S. (2014) Comparative experimental subcutaneous glanders and melioidosis in the common marmoset (*Callithrix jacchus*). *Int J Exp Pathol* **95**, 378–391.
- Nelson, M., Nunez, A., Ngugi, S.A., Sinclair, A. and Atkins, T.P. (2015) Characterization of lesion formation in marmosets following inhalational challenge with different strains of *Burkholderia pseudomallei*. *Int J Exp Pathol* **96**, 414–426.
- Ngauy, V., Lemshev, Y., Sadkowski, L. and Crawford, G. (2005) Cutaneous melioidosis in a man who was taken as a prisoner of war by the Japanese during World War II. *J Clin Microbiol* **43**, 970–972.
- Peacock, S.J., Limmathurotsakul, D., Lubell, Y., Koh, G.C., White, L.J., Day, N.P. and Titball, R.W. (2012) Melioidosis vaccines: a systematic review and appraisal of the potential to exploit biodefense vaccines for public health purposes. *PLoS Negl Trop Dis* **6**, e1488.
- Pitman, M.C., Luck, T., Marshall, C.S., Anstey, N.M., Ward, L. and Currie, B.J. (2015) Intravenous therapy duration and outcomes in melioidosis: a new treatment paradigm. *PLoS Negl Trop Dis* **9**, e0003586.
- Ronning, C.M., Losada, L., Brinkac, L., Inman, J., Ulrich, R.L., Schell, M., Nierman, W.C. and Deshazer, D. (2010) Genetic and phenotypic diversity in *Burkholderia*: contributions by prophage and phage-like elements. *BMC Microbiol* **10**, 202.
- Sahl, J.W., Stone, J.K., Gelhaus, H.C., Warren, R.L., Crutwell, C.J., Funnell, S.G., Keim, P. and Tuanyok, A. (2013) Genome sequence of *Burkholderia pseudomallei* NCTC 13392. *Genome Announc* **1**, 3.
- Sahl, J.W., Allender, C.J., Colman, R.E., Califf, K.J., Schupp, J.M., Currie, B.J., Van Zandt, K.E., Gelhaus, H.C. *et al.* (2015) Genomic characterization of *Burkholderia pseudomallei* isolates selected for medical countermeasures testing: comparative genomics associated with differential virulence. *PLoS ONE* **10**, e0121052.
- Sarovich, D.S., Price, E.P., Webb, J.R., Ward, L.M., Voutsinos, M.Y., Tuanyok, A., Mayo, M., Kaestli, M. *et al.* (2014) Variable virulence factors in *Burkholderia pseudomallei* (melioidosis) associated with human disease. *PLoS ONE* **9**, e91682.
- Soffler, C., Bosco-Lauth, A.M., Aboellail, T.A., Marolf, A.J. and Bowen, R.A. (2012) Development and characterization of a caprine aerosol infection model of melioidosis. *PLoS ONE* **7**, e43207.
- Tan, G.Y., Liu, Y., Sivalingam, S.P., Sim, S.H., Wang, D., Paucod, J.C., Gauthier, Y. and Ooi, E.E. (2008) *Burkholderia pseudomallei* aerosol infection results in differential inflammatory responses in BALB/c and C57Bl/6 mice. *J Med Microbiol* **57**, 508–515.
- Tan, R.Z., Mohd Nor, F., Shadie, S. and Tan, L.J. (2019) Melioidosis mimicking military tuberculosis. *Forensic Sci Med Pathol* **15**, 151–154.
- Thomas, R.J., Davies, C., Nunez, A., Hibbs, S., Eastaugh, L., Harding, S., Jordan, J., Barnes, K. *et al.* (2012) Particle-size dependent effects in the BALB/c murine model of inhalational melioidosis. *Front Cell Infect Microbiol* **2**, 101.

- Titball, R.W., Russell, P., Cuccui, I., Easton, A., Haque, A., Atkins, T., Sarkar-Tyson, M., Harley, V. *et al.* (2008) *Burkholderia pseudomallei*: animal models of infection. *Trans R Soc Trop Med Hyg* **102**(Suppl. 1), S111–S116.
- Trevino, S.R., Klimko, C.P., Reed, M.C., Aponte-Cuadrado, M.J., Hunter, M., Shoe, J.L., Meyer, J.R., Dankmeyer, J.L. *et al.* (2018) Disease progression in mice exposed to low-doses of aerosolized clinical isolates of *Burkholderia pseudomallei*. *PLoS ONE* **13**, e0208277.
- Van Zandt, K.E., Tuanyok, A., Keim, P.S., Warren, R.L. and Gelhaus, H.C. (2012) An objective approach for *Burkholderia pseudomallei* strain selection as challenge material for medical countermeasures efficacy testing. *Front Cell Infect Microbiol* **2**, 120.
- Warawa, J.M. (2010) Evaluation of surrogate animal models of melioidosis. *Front Microbiol* **1**, 141.
- Welkos, S.L., Klimko, C.P., Kern, S.J., Bearss, J.J., Bozue, J.A., Bernhards, R.C., Trevino, S.R., Waag, D.M. *et al.* (2015) Characterization of *Burkholderia pseudomallei* strains using a murine intraperitoneal infection model and in vitro macrophage assays. *PLoS ONE* **10**, e0124667.
- West, T.E., Myers, N.D., Limmathurotsakul, D., Liggitt, H.D., Chantratrata, N., Peacock, S.J. and Skerrett, S.J. (2010) Pathogenicity of high-dose enteral inoculation of *Burkholderia pseudomallei* to mice. *Am J Trop Med Hyg* **83**, 1066–1069.
- West, T.E., Myers, N.D., Liggitt, H.D. and Skerrett, S.J. (2012) Murine pulmonary infection and inflammation induced by inhalation of *Burkholderia pseudomallei*. *Int J Exp Pathol* **93**, 421–428.
- White, N.J. (2003) Melioidosis. *Lancet* **361**, 1715–1722.
- Wiersinga, W.J., Van der Poll, T., White, N.J., Day, N.P. and Peacock, S.J. (2006) Melioidosis: insights into the pathogenicity of *Burkholderia pseudomallei*. *Nat Rev Microbiol* **4**, 272–282.
- Wiersinga, W.J., Virk, H.S., Torres, A.G., Currie, B.J., Peacock, S.J., Dance, D.A.B. and Limmathurotsakul, D. (2018) Melioidosis. *Nat Rev Dis Primers* **4**, 17107.
- Wong, K.T., Puthucheary, S.D. and Vadivelu, J. (1995) The histopathology of human melioidosis. *Histopathology* **26**, 51–55.
- Yeager, J.J., Facemire, P., Dabisch, P.A., Robinson, C.G., Nyakiti, D., Beck, K., Baker, R. and Pitt, M.L. (2012) Natural history of inhalation melioidosis in rhesus macaques (*Macaca mulatta*) and African green monkeys (*Chlorocebus aethiops*). *Infect Immun* **80**, 3332–3340.

6. Ethics Form UPR16

FORM UPR16

Research Ethics Review Checklist

Please include this completed form as an appendix to your thesis (see the Research Degrees Operational Handbook for more information)



Postgraduate Research Student (PGRS) Information		Student ID:	947572
PGRS Name:	Graham Jonathan HATCH		
Department:	Faculty of Science	First Supervisor:	Professor Graham Mills
Start Date: (or progression date for Prof Doc students)	01 February 2019		
Study Mode and Route:	Part-time <input checked="" type="checkbox"/>	MPhil <input type="checkbox"/>	MD <input type="checkbox"/>
	Full-time <input type="checkbox"/>	PhD <input checked="" type="checkbox"/>	Professional Doctorate <input type="checkbox"/>
Title of Thesis:	High Consequence Pathogens – Refinement of Aerosol Models of Disease		
Thesis Word Count: (excluding ancillary data)	9100		
<p>If you are unsure about any of the following, please contact the local representative on your Faculty Ethics Committee for advice. Please note that it is your responsibility to follow the University's Ethics Policy and any relevant University, academic or professional guidelines in the conduct of your study</p> <p>Although the Ethics Committee may have given your study a favourable opinion, the final responsibility for the ethical conduct of this work lies with the researcher(s).</p>			
UKRIO Finished Research Checklist:			
(If you would like to know more about the checklist, please see your Faculty or Departmental Ethics Committee rep or see the online version of the full checklist at: http://www.ukrio.org/what-we-do/code-of-practice-for-research/)			
a) Have all of your research and findings been reported accurately, honestly and within a reasonable time frame?	YES	<input checked="" type="checkbox"/>	
	NO	<input type="checkbox"/>	
b) Have all contributions to knowledge been acknowledged?	YES	<input checked="" type="checkbox"/>	
	NO	<input type="checkbox"/>	
c) Have you complied with all agreements relating to intellectual property, publication and authorship?	YES	<input checked="" type="checkbox"/>	
	NO	<input type="checkbox"/>	
d) Has your research data been retained in a secure and accessible form and will it remain so for the required duration?	YES	<input checked="" type="checkbox"/>	
	NO	<input type="checkbox"/>	
e) Does your research comply with all legal, ethical, and contractual requirements?	YES	<input checked="" type="checkbox"/>	
	NO	<input type="checkbox"/>	
Candidate Statement:			
I have considered the ethical dimensions of the above named research project, and have successfully obtained the necessary ethical approval(s)			
Ethical review number(s) from Faculty Ethics Committee (or from NRES/SCREC):	N/A		
If you have <i>not</i> submitted your work for ethical review, and/or you have answered 'No' to one or more of questions a) to e), please explain below why this is so:			
PhD by publication, all papers included have undergone appropriate ethical review by PHE			
Signed (PGRS):			Date: 13 January 2020